Aktivierung des Psp-Systems durch TatA-induzierten Membranstress in *Escherichia coli*

Von der Naturwissenschaftlichen Fakultät der
Gottfried Wilhelm Leibniz Universität Hannover

zur Erlangung des Grades
Doktorin der Naturwissenschaften (Dr. rer. nat.)

genehmigte Dissertation
von

Eyleen Sabine Heidrich, M. Sc.

[2019]

Referent: Prof. Dr. rer. nat. Thomas Brüser

Korrefernt: Prof. Dr. rer. nat. Kürşad Turgay

Tag der Promotion: 07.01.2019

Kurzzusammenfassung

Das *phage shock protein* (Psp)-System stellt eine bakterielle Stress-Antwort dar, die durch verschiedene Bedingungen aktiviert wird, die alle gemeinsam haben, sich negativ auf die Eigenschaften der Cytoplasmamembran auszuwirken. Obwohl die erste Psp-Komponente, PspA, bereits vor drei Jahrzehnten in *Escherichia coli* entdeckt wurde, ist es bis heute unklar, welches Stress-Signal in der Cytoplasmamembran die Psp-Antwort auslöst. Um herauszufinden, welches Stress-Signal an der Cytoplasmamembran stattfinden muss, wurde auf Grund seines einfachen Aufbaus der Membrananker der *twin-arginine translocation* (Tat)-System-Komponente TatA genutzt und als Modellinduktor der Psp-Antwort in *E. coli* etabliert. Es konnte gezeigt werden, dass die rekombinante Überproduktion des ungewöhnlich kurzen TatA-Transmembranankers zu einer Schwächung des Membranpotentials und somit der Protonenmotorischen Kraft führt. Es wurde jedoch klar, dass die Aktivierung des Psp-Systems nicht auf eine Schwächung der Protonenmotorischen Kraft durch TatA zurückzuführen ist, sondern das Psp-System wahrscheinlich durch eine durch TatA verursachte Änderung des an der Cytoplasmamembran anliegenden Krümmungsstresses induziert wird.

PspA stellt die regulatorische Schlüsselkomponente des Psp-Systems dar und wirkt möglicherweise zusätzlich als Effektor- und Sensorkomponente. PspA ist auf Grund dessen Gegenstand vieler Studien zur Stresswahrnehmung und Signalkaskade des Psp-Systems. Es ist jedoch bis heute unklar, auf welchen Mechanismus der Wechsel zwischen den verschiedenen PspA-Funktionen zurückzuführen ist. In dieser Arbeit konnte gezeigt werden, dass die C-terminale PspA-Domäne PspA(145-222), welche für die Oligomerisierung PspAs essentiell ist, ebenfalls in der Lage ist, PspF in einem *pspA*-Deletionsstamm zu inhibieren. Im Gegensatz zu PspA und zur gut charakterisierten PspA-Domäne PspA(1-144) induziert PspA(145-222) bei rekombinanter Überproduktion das Psp-System in einem *psp*-Wildtyphintergrund. Zusätzlich kann die PspF-Inhibition durch PspA(145-222) durch TatA-induzierten Membranstress reduziert werden.

Zusätzlich gelang es zu zeigen, dass die Veränderung des Krümmungstresses der Cytoplasmamembran das Psp-Systems über eine PspC-abhängige Signalkaskade aktiviert und PspA zur Stresswahrnehmung und -weiterleitung an PspF an der Cytoplasmamembran mit der C-terminalen Domäne von PspC interagieren muss. Basierend auf den in dieser Arbeit vorgestellten Daten gelang es ein integratives Modell der Wahrnehmung von TatA-induziertem Membranstress und Signalkaskade des Psp-Systems zu entwickeln.

Schlagwörter: *phage shock protein* (Psp)-System, *twin-arginine translocation* (Tat)-System, Membranstress, bakterielle Stresswahrnehmung, Signaltransduktion

Abstract

The phage shock protein (Psp) system is a bacterial stress response that is strongly induced by various conditions that all have in common to harm the cytoplasmic membrane. Even though one of the key components of the Psp system, PspA, was discovered almost three decades ago in *Escherichia coli* (*E. coli*), it is still unresolved which kind of stress signal is able to activate this unique stress response. To investigate the signal that is sensed by the Psp system, the unusual short trans-membrane anchor of the twin-arginine-translocation (Tat) system component TatA was used as a structurally simple inducer and could be established as a model inducer in *E. coli.* It could be shown, that the trans-membrane anchor of TatA harms the cytoplasmic membrane in a way that strongly affects the membrane potential und consequently the proton motive force. However, the data suggest that it is not the TatA-induced dissipation of the proton motive force that activates the Psp system but rather the effect TatA has on the curvature elastic stress of the cytoplasmic membrane.

As PspA is a key regulatory component and a potential effector and sensor component of the Psp system, PspA is in the focus of most current research in the Psp field. However, the mechanism of the switch between effector and regulatory functions of PspA is still unclear. In this study, it could be shown that the C-terminal domain of PspA, PspA(145-222), which was previously described to mediate oligomerization, also inhibits PspF activity. In contrast to full-length PspA and the well-characterized PspA domain PspA(1-144), the C-terminal domain of PspA induces the Psp system in a *psp* wild-type background. In addition, the inhibition of PspF by PspA(145-222) could be reduced by TatA-induced membrane stress, providing new insights in stress-sensing by the Psp system.

Importantly, it could be demonstrated that an alteration of membrane-stored curvature elastic stress of the cytoplasmic membrane activates the Psp system in a PspC-dependent manner. Additionally, PspA has to co-operate with the C-terminus of PspC for sensing and transduction of the stress signal to PspF at the surface of the cytoplasmic membrane.

Based on the data presented in this thesis, an integrative model of sensing and signal transmission of TatA-induced membrane stress by the Psp system could be developed.

Key words: phage shock protein (Psp) system, twin-arginine translocation (Tat) system, membrane stress, bacterial stress-sensing, signal transmission

Inhaltsverzeichnis

Abkürzungsverzeichnis

Abkürzung	Bedeutung
2-HCC	*2-helix coiled-coil*
AAA+	*ATPases associated with diverse cellular activities*
ArcA	*Aerobic respiration control protein A*
ArcB	*Aerobic respiration control sensor protein B*
ATP	Adenosintriphosphat
B. subtilis	*Bacillus subtilis*
bEBP	Engl: *bacterial enhancer binding protein,* dt.: bakterielles Aktivatorprotein
BSA	Bovines Serumalbumin
CCCP	Carbonylcyanid-m-chlorphenylhydrazon
CHAPS	3-[(3-Cholamidopropyl)dimethylammonio]-1-propansulfonat
CL	Cardiolipin
D	Durchlauf
DesK	Sensorhistidin-Kinase des DesK/R-Systems aus *Bacillus subtilis*
DesR	Antwortregulator des DesK/R-Systems aus *Bacillus subtilis*
DNA	Desoxyribonukleinsäure
DTT	Dithiothreitol
ECL	Engl.: *enhanced chemilumescence,* dt.: verstärkte Chemilumineszenz
E. coli	*Escherichia coli*
E1-E7	Elutionsfraktionen 1 - 7
FtsH	membrangebundene, ATP-abhängige Metalloprotease
GFP	Grün-fluoreszierendes Protein
HiPIP/Hip	*High potential iron-sulfur protein*
Hip-PspA(145-222)	C-terminale Domäne von PspA, originale Aminosäuresequenz von Serin^{145}-Glutamat^{222} über einen Glycin-Serin-Linker C-terminal an die mature HiPIP-Domäne fusioniert
Hip-PspC(CT)	C-terminale Domäne von PspC, originale Aminosäuresequenz von Serin^{61}-Leucin^{119} über einen Glycin-Serin-Linker C-terminal an die mature HiPIP-Domäne fusioniert
HRP	Engl.: *horseradisch peroxidase* dt.: Meerrettichperoxidase
H10	Deca-Histidin-Tag
H6	Hexa-Histidin-Tag
IHF	*integration host factor*
IM30	*Inner membrane protein 30*
kDa	Kilodalton
LacZ	β-Galaktosidase
LB	*lysogeny broth*
LepB	Signalpeptidase I aus *E. coli*
LiaH	PspA-Homolog aus *Bacillus subtilis*
M	Membranfraktion
MD	Engl.: *molecular dynamics,* dt.: molekular-dynamisch
MU	Miller Units
NMR	Engl.: *nuclear magnetic resonance*, dt.: Kernspinresonanz
PBS	Phosphatgepufferte Saline
PE	Phosphatidylethanolamin
PG	Phosphatidylglycerol

PMF	Engl: *proton-motive force*, dt.: Protonenmotorische Kraft
PMSF	Phenylmethylsulfonylfluorid
Psp	*Phage shock protein*
PspA	*Phage shock protein A*
PspA(1-24)	In der Kristallstruktur zum *coiled-coil* zurückgefalteter N-terminaler Bereich PspAs
PspA(1-144)	Strukturaufgeklärter Bereich PspAs, originale Aminosäuresequenz von Methionin^{Startcodon}-Glutamat^{144}
PspA(145-222)	C-terminale Domäne von PspA, originale Aminosäuresequenz von Alanin^{145}-Glutamat^{222}
PspB	*Phage shock protein B*
PspC	*Phage shock protein C*
PspC(CT)	C-terminale Domäne von PspC, originale Aminosäuresequenz von Serin^{61}-Leucin^{119}
PspD	*Phage shock protein D*
PspE	*Phage shock protein E*
PspF	*Phage shock protein F*
PspG	*Phage shock protein G*
pIV	Phagen-Protein IV
PVDF	Polyvinylidenfluorid
RNA	Ribonukleinsäure
SCE	Engl.: *stored curvature elastic,* dt.: anliegender Krümmungsstress
SDS	Natriumdodecylsulfat
SDS-PAGE	Natriumdodecylsulfat-Gelelektrophorese
Sec	Engl.: *secretion*, TypII-Sekretionssystem, welches ungefaltete Proteine über die Cytoplasmamembran transportiert
Tat	*twin-arginine translocation*
TatA	*twin-arginine translocation protein A*
TatA-NT-Hip	Membrananker von TatA, originale TatA-Aminosäuresequenz von Methionin^{Startcodon}-Phenylalanin^{20} über einen Glycin-Serin-Linker N-terminal an die mature Domäne von HiPIP fusioniert
TatA-NT(LA)$_6$-Hip	Membrananker von TatA, originale TatA-Aminosäuresequenz von Methionin^{Startcodon}-Phenylalanin^{20} ersetzt ab Glutamat^{8} durch repetitive Leucin-Alanin-Sequenz, N-terminal an die mature Domäne von HiPIP fusioniert
TatA-NT(9+6L)-Hip	Membrananker von TatA, originale TatA-Aminosäuresequenz von Methionin^{Startcodon}-Phenylalanin^{20} mit einer Insertion von 6 Leucinen nach Glutamat^{8} über einen Glycin-Serin-Linker N-terminal an die mature Domäne von HiPIP fusioniert
TatA-NT(STGG)$_3$-Hip	Membrananker von TatA, originale TatA-Aminosäuresequenz von Methionin^{Startcodon}-Phenylalanin^{20} ersetzt durch (Serin-Threonin-Glycin-Glycin)$_3$-Linker, N-terminal an die mature Domäne von HiPIP fusioniert
TatB	*twin-arginine translocation protein B*
TatC	*twin-arginine translocation protein C*
TatD	*twin-arginine translocation protein D*
TatE	*twin-arginine translocation protein E*
TMH	Transmembranhelix
Tris	Tris-(hydroxymethyl)-aminomethan
T3SS	Typ-III-Sekretionssystem

UAS	Engl.: *Upstream activator sequence,* dt.: dem Promotorbereich vorgeschaltete Bindestelle des Aktivatorproteins der σ^{54}-abhängigen Transkription
Vipp1	*Vesicle-inducing protein in plastids 1*, PspA-Homolog in Chloroplasten
W	Letzte Waschfraktion
Y. enterocolitica	*Yersinia enterocolitica*
YidC	Membranprotein-Insertase aus *E. coli*

Einbuchstabencode der Aminosäuren

A	Alanin	M	Methionin
C	Cystein	N	Asparagin
D	Asparaginsäure	P	Prolin
E	Glutaminsäure	Q	Glutamin
F	Phenylalanin	R	Arginin
G	Glycin	S	Serin
H	Histidin	T	Threonin
I	Isoleucin	V	Valin
K	Lysin	W	Tryptophan
L	Leucin	Y	Tyrosin

1 Einleitung

Organismen haben im Laufe der Zeit unterschiedliche Mechanismen und Stress-Antworten entwickelt, welche ihr Überleben unter verschiedenen Bedingungen sicherstellen. Der in dieser Arbeit verwendete Gram-negative Modellorganismus *Escherichia coli* besitzt als didermes Bakterium zwei Biomembranen, welche zum einen den Organismus von der Umwelt abgrenzen und zum anderen der Kompartimentierung der Zelle dienen. Die Äußere Membran umschließt die Zelle und trennt diese von ihrer Umgebung ab, ist jedoch für viele Stoffe permeabel. Auf Grund dieser Permeabilität steht das Periplasma, welches sich zwischen Cytoplasmamembran und Äußerer Membran befindet, in einem stetigen Stoffaustausch mit der Zellumgebung. Im Periplasma ist die bakterielle Zellwand, auch Mureinschicht oder Peptidoglykan genannt, lokalisiert, welche den Organismus gegen osmotische Einflüsse schützt und stabilisiert. Das Cytoplasma als Ort der Proteinbiosynthese wird von der Cytoplasmamembran umgeben (Abbildung 1). Im Gegensatz zur Äußeren Membran stellt die Cytoplasmamembran für viele Stoffe eine Permeabilitätsbarriere dar. Durch die unterschiedlichen Permeabilitäten der Cytoplasmamembran und der Äußeren Membran unterscheiden sich das Cyto- und

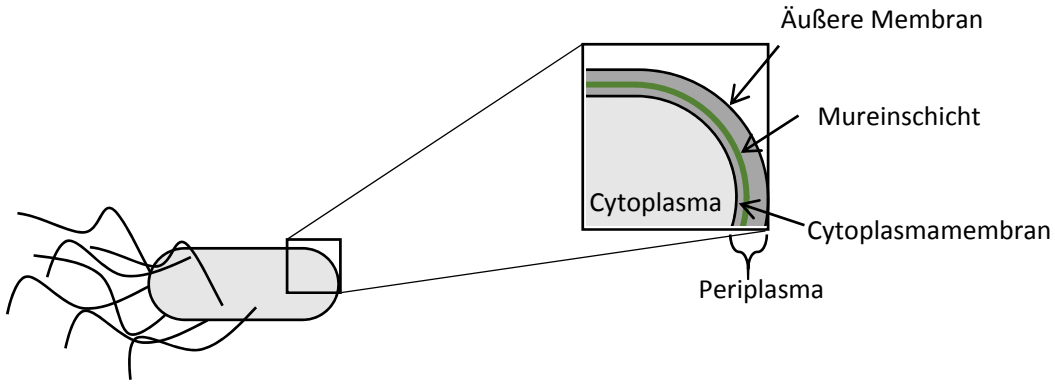

Abbildung 1 Schematischer Aufbau des Gram-negativen Organismus *E. coli* Der diderme Organismus *E. coli* besitzt eine stäbchenförmige Struktur und eine peritriche Begeißelung (links). Das Cytoplasma ist von der Cytoplasmamembran umgeben. Darauf folgt als weiteres Kompartiment das Periplasma, welches die zellwandbildende Mureinschicht enthält. Das Periplasma wird durch die Äußere Membran von der Umwelt abgegrenzt (rechts).

und Periplasma stark in ihren physikochemischen Eigenschaften, wodurch die Zelle unterschiedliche Reaktionsräume besitzt, in denen jeweils optimale Reaktionsbedingungen für überlebenswichtige Stoffwechselreaktionen vorherrschen. Durch die unterschiedliche Stoffzusammensetzung des reduktiven Cyto- und oxidativen Periplasmas und durch Transportvorgänge an der Cytoplasmamembran liegt ein Konzentrationsgefälle von Ionen an der Cytoplasmamembran an, wodurch das Membranpotential ($\Delta\psi$) entsteht. Dieses bildet zusammen mit dem an der Cytoplasmamembran anliegenden Protonengradienten (ΔpH), die protonenmotorische Kraft (PMF), die für viele essentielle Stoffwechselprozesse, wie z. B. die ATP-Synthese, die nötige Energie bereitstellt.

Die Cytoplasmamembran besteht aus Phospholipiden und Proteinen. Phospholipide sind molekular aus einem Glycerol-Molekül, welches mit zwei Fettsäuren sowie einer negativ geladenen Phosphatgruppe an einem endständigen Kohlenstoffatom verestert ist, aufgebaut. Die Phosphatgruppe kann weitere gebundene Alkylreste oder andere Gruppen besitzen, welche die Kopfgruppe der Phospholipide bilden. Auf Grund der Zusammensetzung aus hydrophoben Fettsäuren und hydrophiler Kopfgruppe handelt es sich bei Phospholipiden um amphipathische Moleküle, welche in einer wässrigen Umgebung die für Biomembranen typische Phospholipiddoppelschicht mit einem hydrophoben Kern und einer hydrophilen Oberfläche ausbilden.

Die Cytoplasmamembran von *E. coli* besteht vornehmlich aus den drei Phospholipiden Phosphatidylethanolamin (PE), Phosphatidylglycerol (PG) und Cardiolipin (CL), wobei PE mit circa 75% den Großteil der Phospholipide in der Cytoplasmamembran ausmacht [1]. PE besitzt ein an die Phosphatgruppe gebundenes Ethanolamin, dessen Aminogruppe protoniert vorliegt. Auf Grund der negativen Ladung der Phosphatgruppe und der positiven Ladung des Ethanolamins unter physiologischen Bedingungen ist PE zwitterionisch. PG und CL sind anionische Phospholipide. PG besitzt ein an die Phosphatgruppe gebundenes Glycerol, welches nicht geladen ist, wodurch PG eine negative Ladung besitzt. CL besteht aus zwei PG-Molekülen, welche über ihre Phosphatgruppen über die endständigen Kohlenstoffatome eines Glycerols miteinander verbunden sind. CL besitzt auf Grund zweier negativ geladener Phosphatgruppen zwei negative Ladungen. In *E. coli* enthält die Cytoplasmamembran bis zu 15-20% PG und zu 5-10% CL [2,3]. In der Cytoplasmamembran sind zahlreiche Proteine unterschiedlicher Funktion eingelagert bzw. peripher assoziiert.

1.1 Das *phage shock protein* (Psp)-System

Dass Mikroorganismen in der Lage sein müssen, schnell und effektiv auf eine Schädigung der Cytoplasmamembran reagieren zu können, ergibt sich aus ihrer überlebenswichtigen Funktion. Das in dieser Arbeit untersuchte *phage shock protein* (Psp)-System stellt eine bakterielle Stress-Antwort dar, die durch verschiedene Induktoren ausgelöst wird, welche gemein haben, sich negativ auf die Struktur und Stabilität der Cytoplasmamembran oder den Energiestatus der Zelle auszuwirken. Die Induktoren des Psp-Systems sind dabei zahlreich und divers und reichen von in die Cytoplasmamembran fehllokalisierten Sekretinen der Äußeren Membran bis hin zur Behandlung der Zellen mit organischen Lösungsmitteln [4–9]. Auch ein hyperosmotischer oder alkalischer Schock, Blockade von bakteriellen Proteintransportsystemen oder die Deletion der Membranprotein-Insertase YidC wurden als Auslöser der Psp-Antwort in *E. coli* beschrieben [4,10–12]. Das Psp-System ist ebenfalls während der Biofilmbildung und in persistenten Zellen induziert [13,14]. Die Induktion des Psp-Systems unter Membranstress-Bedingungen führt über eine komplexe Regulationskaskade, an welcher viele Proteine beteiligt sind, zu einer stark erhöhten Proteinbiosynthese des *phage shock protein* A (PspA), welches an der Cytoplasmamembran akkumuliert. PspA bildet dabei große netzwerkartige Strukturen aus [15], weshalb angenommen wird, dass PspA die Cytoplasmamembran bei Membranstress stabilisiert [16].

1.1.1 Die Entdeckung der Komponenten des Psp-Systems und dessen Operonstruktur in *E. coli*

PspA wurde 1989 als erste Komponente des Psp-Systems entdeckt [4]. Brissette *et al.* (1989) beobachteten im Zuge ihrer Arbeiten zur Infektion von *E. coli* mit filamentösen Phagen die Induktion der Proteinbiosynthese eines bis dato unbekannten circa 25 kDa großen Genprodukts. Ausschlaggebend für die starke Initiation der Proteinbiosynthese dieses Proteins war die Produktion des Phagen-Sekretins pIV, weshalb dieses zunächst *phage shock protein* [4] und später *phage shock protein* A, PspA, genannt wurde [17]. PspA konnte in mit f1-Phagen infizierten Zellen in der

löslichen Zellfraktion nachgewiesen werden, sedimentierte jedoch auch mit Membranen, sodass vermutet wurde, das es sich bei PspA um ein peripher-membranassoziiertes Protein handelt [4].

Kurz darauf wurden PspB, PspC, PspD und PspE als weitere Komponenten des Psp-Systems in *E. coli* identifiziert [17]. Bei PspB und PspC handelt es sich um kleine membranintegrale Proteine mit einer molekularen Masse von circa 8,8 kDa bzw. 13,5 kDa [17,16], welche direkt an der Regulation der Psp-Antwort beteiligt sind [16–18]. Für das peripher-membrangebundene PspD konnte bis heute keine eindeutige Funktion innerhalb der Regulationskaskade bestimmt werden. PspE ist eine im Periplasma lokalisierte Rhodanese, welche bei starker Überproduktion teilweise die periplasmatische Thioldisulfidoxidoreduktase DsbA des *disulfid bond formation* (Dsb)-Systems in *E. coli* ersetzen kann [19–22].

PspA ist zusammen mit *pspB, pspC, pspD* sowie *pspE* im *pspABCDE*-Operon organisiert [17], welches σ^{54}-abhängig reguliert wird, wobei *pspE* zusätzlich einen σ^{70}-abhängigen Promotor besitzt (Abbildung *2*, [18,23,24]). Zur Intitiation der σ^{54}-abhängigen Transkription werden sogenannte *bacterial enhancer binding proteins* (bEBPs) benötigt, welche an regulatorische DNA-Sequenzen, sogenannte UAS (*upstream activator sequences*)-Regionen, binden, die sich in 5‘-Richtung ausgehend vom Promotor der σ^{54}-abhängig exprimierten Gene befinden [25,26]. Stromaufwärts des *pspA*-Promotors konnten zwei solcher UAS-Regionen (UASI und UASII) identifiziert werden [23,27]. Auch die für die σ^{54}-abhängige Transkription typische Bindung des *integration host factors* (IHF) an seine Konsenssequenz, welche sich zwischen den UAS-Elementen und der σ^{54}-Bindestelle des *pspA*-Promotors befindet, konnte nachgewiesen werden (Abbildung 2, [27]).

PspF wurde mittels Transposon-Mutagenesestudien als das für die σ^{54}-abhängige Transkription des *pspABCDE*-Operons nötige bEBP kurze Zeit später identifiziert [28,29]. *PspF* wird selbst abhängig von Sigma-Faktor σ^{70} transkribiert, und ist stromaufwärts auf dem Gegenstrang zum *pspABCDE*-Operon codiert, wobei sich die entsprechenden Promotorelemente überschneiden (Abbildung 2, [28,30]).

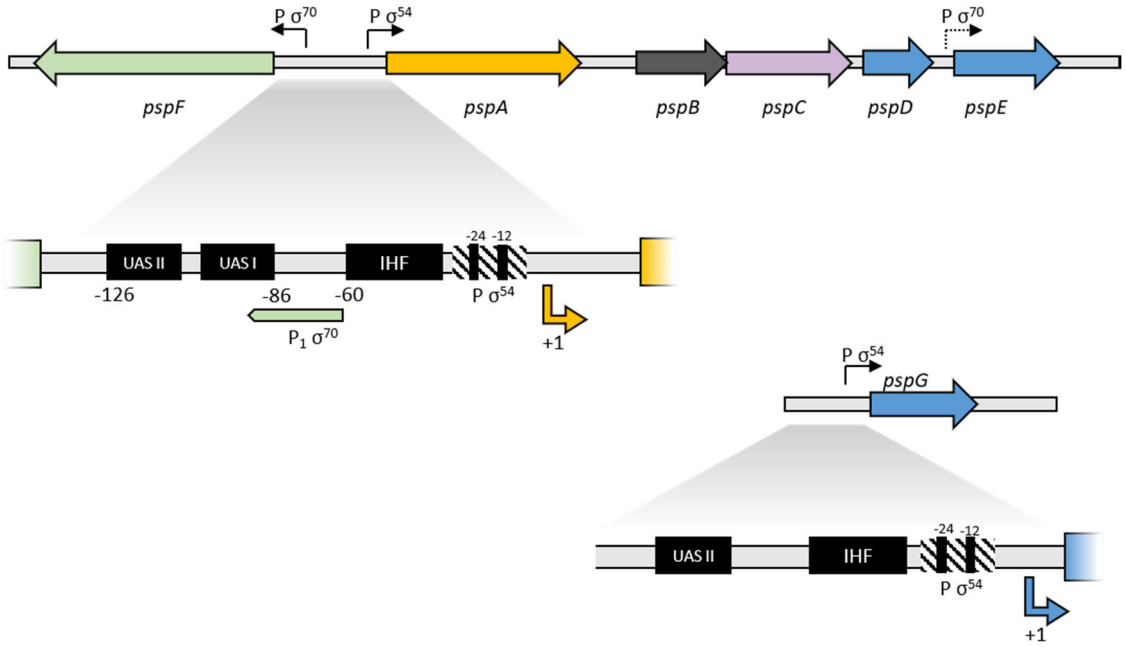

Abbildung 2 Schematische Darstellung der Operonstruktur des *pspABCDE*-Operons sowie der monocistronischen Gene *pspF* und *pspG* [18,27,6] *PspA* bildet zusammen mit *pspB*, *pspC*, *pspD* und *pspE* ein durch σ^{54}-reguliertes Operon aus. Die Transkription von *pspE* wird zusätzlich durch den Sigma-Faktor σ^{70} reguliert. *PspF* wird auf dem Gegenstrang in 5`-Richtung zum *pspABCDE*-Operon codiert. Zwischen *pspF* und *pspA* sind die für die σ^{54}-abhängige Transkription typischen Bindestellen für den *integration host factor* (IHF) sowie die Bindestellen für das für die σ^{54}-abhängige Transkription notwendige bEBP (UASI und UASII), sowie Bindestellen für den Sigma-Faktor σ^{54} lokalisiert. Die Promotorregion von *pspG* ist ähnlich zu der des *pspABCDE*-Operons aufgebaut, wobei nur eine Bindestelle für das nötige bEBP (UASII) identifiziert werden konnte.

Dies führt auf Grund der negativen Autoregulation der *pspF*-Transkription zu gleichbleibend niedrigen PspF-Leveln in der Zelle (ca. 130 Kopien) [30]. Mittels Transkriptomanalysen konnte YjbO als einzig weiteres PspF und σ^{54}-abhängig produziertes Genprodukt identifiziert werden, dessen Proteinbiosynthese ebenfalls durch die Produktion von pIV induziert wird. YjbO wurde aus diesem Grund in PspG umbenannt [6]. *PspG* bildet einen vom *pspABCDE*-Operon unabhängigen monocistronischen Genlokus, welchem ebenfalls eine regulatorische UASII-Region vorangestellt ist ([6], Abbildung 2). Bei PspG handelt es sich um ein Membranprotein unbekannter Funktion.

1.1.2 Weitere Psp-Systeme in Enterobakterien und PspA-Homologe der PspA/IM30-Proteinfamilie

Zehn Jahre nach der Entdeckung des Psp-Systems in *E. coli* wurde für das Humanpathogen *Yersinia enterocolitica (Y. enterocolitica)* ein Psp-System beschrieben, dessen Operonstruktur sowie auch die einzelnen Psp-Komponenten eine sehr große Homologie zum Psp-System aus *E. coli* aufweisen [5,31]. Das Psp-System wird in *Y. enterocolitica* durch die Produktion von zelleigenen Sekretinen des Typ-III-Sekretionssystems (T3SS), welche wichtige Virulenzfaktoren darstellen, induziert. Zudem zeigte *Y. enterocolitica* eine reduzierte Virulenz und stark eingeschränkte Viabilität im Wirtsorganismus, wenn *pspC* deletiert wurde [5,31,32], weshalb sich schon früh eine mögliche Effektorfunktion von PspC in *Y. enterocolitica* manifestiert hat. Auf Grund der Verbindung zum T3SS und der daraus resultierenden medizinischen Relevanz, stellt das Psp-System aus *Y. enterocolitica* eins der am besten charakterisierten Modell-Systeme der Psp-Antwort in Enterobakterien dar, wobei gerade die in diesem Organismus durchgeführte Untersuchungen zur Funktion von PspB und PspC weitreichende Beiträge zum heutigen Modell der durch Membranstress ausgelösten Signalkaskade des Psp-Systems leisteten [5,32–40]. Auf Grund der hohen Sequenzidentität der regulatorisch wirkenden Psp-Komponenten PspF, PspA, PspB und PspC[1] aus *Y. enterocolitica* und *E. coli* von circa 75% basieren heutige Modelle der Regulation der Psp-Antwort auf Experimentaldaten beider Systeme und werden auf den jeweils anderen Organismus angewandt. Psp-Systeme mit homologer Operonstruktur zu *Y. enterocolitica* und *E. coli* konnten ebenfalls in anderen humanpathogenen Enterobakterien nachgewiesen werden. Beispielhaft seien hier *Salmonella enterica* serovar Typhimurium, *Shigella flexneri* oder auch *Klebsiella pneumoniae* genannt [5,24,42,43].

PspA ist die am stärksten konservierte Komponente des Psp-Systems und gehört der PspA/IM30-Proteinfamilie an, deren Homologe nicht nur in Proteobakterien, sondern auch in Gram-positiven Bakterien, Archaeen, Cyanobakterien und Chloroplasten zu finden sind [8,44–47]. Die Komponenten des Lia-Systems aus *Bacillus subtilis* zeigen bei Membranstress ein ähnliches Verhalten wie Psp-Komponenten aus γ-Proteobakterien. So wird die Produktion des PspA-Homologs LiaH ebenfalls durch

[1] PspC aus *Y. enterocolitica* besitzt im Vergleich zu anderen Spezies einen um 20 Aminosäuren N-terminal verlängerten N-Terminus, dessen Deletion jedoch keine Effekte auf die Induktion des Psp-Systems zeigte [41].

Membranstress induziert [7,48]. Die Regulation des *liaIH*-Operons durch das Drei-Komponenten-System LiaFSR ist nicht identisch, zeigt aber prinzipiell Ähnlichkeit mit der Regulation der Psp-Antwort aus *E. coli* oder *Y. enterocolitica* [7,48–50]. *Bacillus subtilis* besitzt noch für ein weiteres Homolog der PspA/IM30-Familie, dieses ist jedoch nicht weiter charakterisiert [51]. Das *vesicle-inducing plastid protein* 1 (Vipp1) stellt ein gut charakterisiertes Mitglied der PspA/IM30-Familie dar, welches in Thylakoidmembranen von Chloroplasten wie auch in Cyanobakterien vorkommt [52].

1.1.3 Funktionen und Eigenschaften der Komponenten des Psp-Systems

Die Expression des *pspABCDE*-Operons bzw. von *pspG* unter Normal- und Membranstressbedingungen geschieht über ein komplexes autoregulatorisches Netzwerk, an dem die Psp-System-Komponenten PspA, PspB, PspC sowie PspF beteiligt sind und verschiedene Funktionen in Bezug auf die Wahrnehmung des Membranstresses, der Signalweiterleitung sowie der Aktivierung der Psp-Antwort unter Stressbedingungen erfüllen.

1.1.3.1 PspF als Aktivator der σ^{54}-abhängigen Transkription der psp-Gene

PspF als bEBP der σ^{54}-abhängigen Transkription des *pspABCDE*-Operons sowie von *pspG* gehört zur Gruppe der AAA+-ATPasen (*ATPases associated with a varity of cellular activites*) [53] und ist strukturell aus einer N-terminal lokalisierten AAA+-ATPase-Domäne und einer C-terminalen DNA-Bindedomäne aufgebaut [28]. PspF bildet die für ATPasen dieser Gruppe typische, homooligomere ringförmige Strukturen und ist in der Zelle nur als Hexamer aktiv, wobei die für die Initiation der σ^{54}-abhängigen Transkription notwendige Energie durch die Hydrolyse von ATP durch die ATPase-Domäne bereitgestellt wird [54–56]. Zur Initiation der σ^{54}-abhängigen Transkription des *psp*-Operons durch PspF sind mehrere Schritte nötig. Zunächst bindet σ^{54} im konservierten Promotorbereich an die entsprechenden Konsensussequenzen etwa 24 und 12 Basenpaare vor dem Transkriptionsstart von *pspA* (oder *pspG)* und bildet zusammen mit der DNA und der RNA-Polymerase den sogenannten *closed complex* (RP_C) [25,57]. Im RP_C ist der DNA-Doppelstrang nur leicht geöffnet und die RNA-Polymerase nicht in der Lage die Transkription zu

initiieren. PspF bindet nun an eine UAS-Region und die Bindung des *integration host factors* (IHF) führt zu einer Schleifenbildung der DNA, wodurch die Interaktion von PspF mit dem RP_C ermöglicht wird [29,58,59] . Durch die Hydrolyse von ATP durch die AAA+-Domäne von PspF kommt es zu einer Konformationsänderung im PspF-Hexamer welche auf σ^{54} übertragen und diesen näher zum Transkriptionsstart rücken lässt. Dabei gelingt eine ausreichende Öffnung des DNA-Doppelstrangs und der *open complex* (RP_O) wird gebildet [25,54,60–66]. Nach Ablösen von PspF beginnt die Transkription des *pspABCDE*-Operons sowie von *pspG* [6,28].

1.1.3.2 PspA – vom negativen Regulator zum Effektorprotein der Psp-Antwort

Im Unterschied zu anderen prokaryotischen bEBPs besitzt PspF keine eigene N-terminale regulatorische Domäne. PspF wird stattdessen ausschließlich *in trans* in einer negativen Feedback-Schleife durch das erste Genprodukt des *pspABCDE*-Operons, PspA, negativ reguliert [67], wobei die negative regulatorische Funktion von PspA direkt in der Bindung von PspF und der daraus resultierenden Inhibition der ATPase-Aktivität begründet liegt [68]. PspA bildet zusammen mit PspF *in vitro* einen stabilen Komplex mit einer 6:6-Stöchiometrie [69,70].

Bei PspA handelt es sich um ein Protein mit einer Länge von 222 Aminosäuren und einer *in silico* vorhergesagten *coiled-coil* Struktur, die mittels Röntgenstrukturanalyse für das PspA-Fragment PspA(1-144), welches 2/3 des Gesamtproteins umfasst, bestätigt werden konnte (Abbildung 3, [70]). PspA(1-144) bildet einen langgezogenen *coiled-coil* mit einem zurückgefalteten flexiblen N-terminalen Bereich mit einer Länge von 24 Aminosäuren. PspA(1-144) ist in der Lage, PspF *in vivo* vollständig zu inhibieren, wobei mittels Mutagenesestudien ein Bereich innerhalb der ersten *coiled-coil*-bildenden Helix identifiziert werden konnte, welcher sowohl ausschlaggebend für die PspF-Bindung als auch für die PspF-Inhibition ist [70]. Mittels *in-vitro*-Experimenten gelang es zu zeigen, dass ein Peptid, welches dem in der Röntgenstruktur flexiblen zum *coiled-coil* rückgefalteten N-terminalen Bereich von PspA entspricht, auch in der Lage ist, die ATPase-Aktivität von PspF zu inhibieren [71].

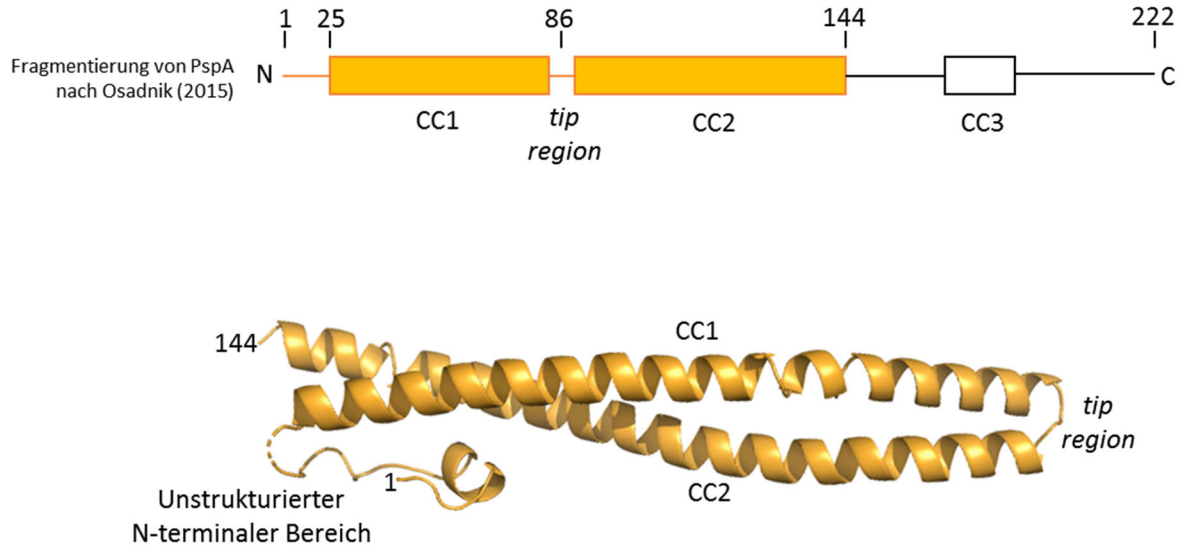

Abbildung 3 Schematischer Aufbau und Struktur PspAs oben: Domänenstruktur PspA nach Osadnik *et al. (2105)*: Für PspA werden *in silico* drei *coiled-coil*-bildende Bereiche vorhergesagt (CC1, CC2 und CC2), wobei CC1 und CC2 durch die sogenannte *tip region* miteinander verbunden sind [70]. Unten: Röntgenstruktur der PspA-Domäne PspA(1-144) (PDB: 4WHE). PspA(1-144) bildet eine langgezogene *coiled-coil*-Struktur mit einem zum *coiled-coil* zurückgefalteten vornehmlich unstrukturierten N-terminalen Bereich [70].

PspA interagiert jedoch nicht nur mit PspF, sondern akkumuliert bei Stressbedingungen sowie bei rekombinanter Überproduktion zu großen membran-assoziierten, homooligomeren und netzwerkartigen Strukturen [15,72]. Nach Behandlung mit Detergens konnte für diese Membran-assoziierten PspA-Komplexe eine neunfach symmetrische homooligomere Ringstruktur mittels Kryo-Elektronenmikroskopie nachgewiesen werden, die aus bis zu 36 PspA-Protomeren besteht [72] und einer weiteren Schädigung der Membran entgegenwirken soll [17,73,74]. Für das Erreichen dieser postulierten Effektorfunktion ist die bis heute strukturell noch nicht aufgelöste C-terminale PspA-Domäne essentiell, da PspA ohne diesen Bereich nicht in der Lage ist zu oligomerisieren [69,70]. Auch für diese PspA-Domäne wird *in silico* eine *coil*-Domäne vorgeschlagen, welche ein für Trimere typisches Sequenzmotiv enthält [70,75]. Das PspA-Homolog Vipp1 ist ebenfalls in der Lage oligomere Ringstrukturen auszubilden, welche direkt mit Membranen interagieren und ähnliche Membranbindungseigenschaften wie PspA aufweisen

[71,76–79]. Auch für LiaH konnte die Bildung von oligomeren Ringstrukturen nachgewiesen werden [50].

1.1.3.3 Die Psp-Komponenten PspB und PspC und ihre Rolle als positive Regulatoren des Psp-Systems

PspB und PspC stellen die membranständigen Komponenten des Psp-Systems dar [16]. Das kleine Membranprotein PspB besitzt einen kurzen periplasmatischen N-Terminus und eine Transmembrandomäne, auf die eine im Cytoplasma lokalisierte C-terminale Domäne folgt [16,80,17]. Für PspC wurde zunächst eine bitopische Topologie mit einer Transmembranhelix und einem im Cytoplasma lokalisierten N- und einem im Periplasma lokalisierten C-Terminus vorgeschlagen [16]. Diese Topologie wurde jedoch kurz darauf in Frage gestellt, da die C-terminale Domäne von PspC in der Lage ist, stabil mit PspA zu interagieren, welches ausschließlich im Cytoplasma oder mit der Innenseite der Cytoplasmamembran assoziiert vorliegt [4,81]. Da mittels *in-silico*-Analysen eine ähnliche Wahrscheinlichkeit für eine periplasmatische und cytoplasmatische Lokalisation der C-terminalen PspC-Domäne vorhergesagt wurde, wurde spekuliert, dass es zu einer Stress-induzierten Änderung der PspC-Konformation kommt, wobei sich der C-Terminus von PspC im uninduzierten Zustand im Peri- und im induzierten Zustand im Cytoplasma befinden sollte [81]. Auf Grund von diversen Interaktionsstudien geht man heute jedoch von einer dauerhaften cytoplasmatischen Lokalisation beider PspC-Termini und zwei ungewöhnlich kurzen Membran-durchspannenden Helices aus, welche durch ein konserviertes Glycin voneinander getrennt werden [34,35,81,82].

Bereits 1991 beschrieben Brissette *et al.* sowie Weiner *et al.* eine Abhängigkeit der durch f1-Phagen, Ethanolbehandlung oder osmotischen Schock ausgelösten Psp-Antwort von den Membrankomponenten PspB und PspC und sprachen aufgrund dessen PspB und PspC eine positive regulatorische Wirkung zu [17,18]. Auch für die Induktion des Psp-Systems durch die Überproduktion von zelleigenen Sekretinen in *Y. enterocolitica* konnte eine PspB- und PspC-Abhängigkeit zweifelsfrei gezeigt werden [39]. Auf Grund dessen, dass es sich bei PspB und PspC um die membranständigen Komponenten des Psp-Systems handelt und die Induktion der Psp-Antwort durch viele verschiedene Stressoren von der Präsenz dieser beiden Komponenten abhängt, geht

man davon aus, dass es sich bei PspB und PspC um die Sensorkomponenten des Psp-Systems handelt (z. B. [18,39,72,81,83,84]).

Die positive Regulatorfunktion von PspB und PspC zeigt sich jedoch nicht nur in der Abhängigkeit der Induktion des Psp-Systems von diesen membranständigen Psp-Komponenten. So führt die rekombinante Produktion von PspC in *E. coli* zu einer stark erhöhten Expression des *psp*-Operons und subsequent zu hohen PspA-Leveln in der Zelle [18]. Die Induzierbarkeit der Expression der *psp*-Gene durch rekombinante PspC-Level konnte sowohl in *E. coli* als auch in *Y. enterocolitica* auf die direkte Interaktion der C-terminalen PspC-Domäne mit PspA zurückgeführt werden [81]. Die rekombinante Produktion von PspB hat hingegen keinen direkten Effekt auf die Expression des *psp*-Operons. Darauf basierend wurde spekuliert, dass PspB möglicherweise katalytisch auf die für PspC beobachtete Aktivatorfunktion wirken könnte [18]. Es konnte ebenfalls gezeigt werden, dass es zu einer FtsH-abhängigen Degradation von PspC kommt, welcher PspB entgegenwirken kann, weshalb postuliert wurde, dass die Funktion von PspB möglicherweise auch in der Stabilisierung von PspC begründet liegt [85].

1.1.4 Aktuelle Modelle der Signalwahrnehmung und Regulation des Psp-Systems

Der genaue Mechanismus der Signalwahrnehmung sowie der Signalkaskade, welche unter Stressbedingungen zum Auslösen der Psp-Antwort führt, ist nach wie vor noch nicht vollständig aufgeklärt. Aktuelle Modelle der Signalwahrnehmung und -kaskade des Psp-Systems in Enterobakterien beruhen vor allem auf Lokalisations- und Interaktionsstudien zwischen den Psp-Komponenten PspF, PspA, PspB und PspC unter Normal- bzw. Membranstressbedingungen in *E. coli* und *Y. enterocolitica*, wobei auch hier die Aktivierung der Psp-Antwort auf eine Änderung der Interaktionspartner der C-terminalen PspC-Domäne zurückgeführt wird (Abbildung 4):

Im uninduzierten Zustand liegt PspA im Cytoplasma gebunden an PspF vor [72,33,83], wodurch auf Grund des negativen Feedback-Mechanismus dessen Aktivität negativ reguliert wird [67,18]. Auf Grund der basalen Aktivität des *pspA*-Promotors werden geringe Mengen an PspB und PspC auch unter nicht-induzierenden Bedingungen gebildet, welche in der Cytoplasmamembran vorliegen [33], wobei die cytoplasmatischen Domänen von PspB und PspC miteinander interagieren [35,36,41].

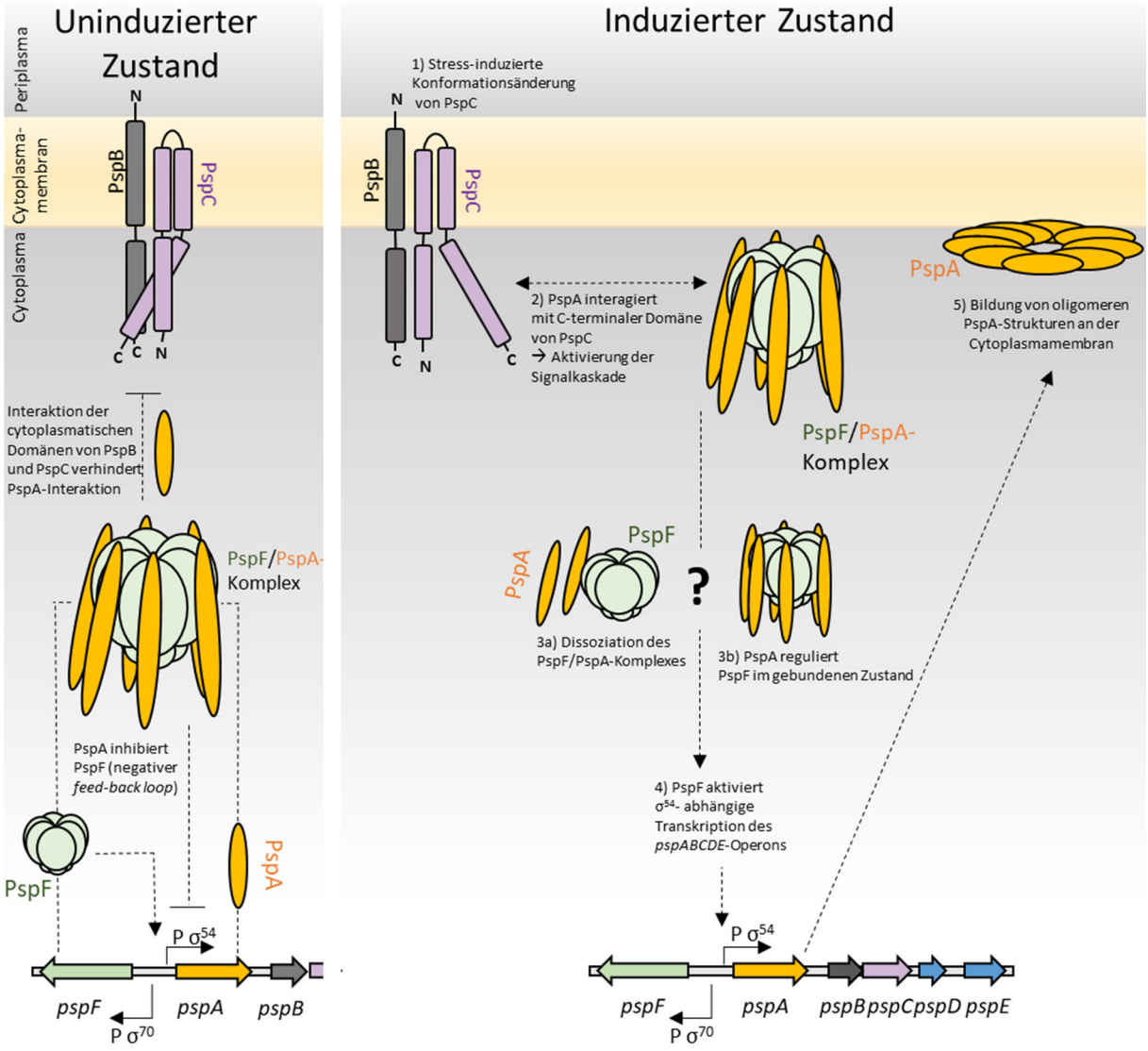

Abbildung 4 Schematische Darstellung des aktuellen Modells der Regulation der PspBC-abhängigen Psp-Antwort unter Normal- sowie Stress-Bedingungen Die Darstellung der einzelnen Komponenten ist nicht maßstabsgetreu. **Links:** PspA ist im uninduzierten Zustand des Psp-Systems an PspF gebunden und inhibiert dessen Aktivität in einem negativen Feedback-Mechanismus, wodurch die σ^{54}-abhängige abhängige Induktion des *pspABCDE*-Operons sowie von *pspG* nicht stattfinden kann. PspB und PspC liegen mobil in der Cytoplasmamembran vor, wobei die C-terminale PspC-Domäne sowohl von dessen N-terminaler als auch von der C-terminalen Domäne von PspB gebunden wird. **Rechts:** 1) Kommt es zu Psp-System induzierendem Membranstress wird dieser wahrscheinlich durch PspB und PspC wahrgenommen, was zu einer Freisetzung der C-terminalen Domäne von PspC führt, die nun mit PspA interagieren kann (2). Dies führt zu einer Aufhebung der negativen Regulation von PspF durch PspA, wobei nicht klar ist, ob PspA von PspF dissoziieren muss (3a), oder im gebundenen Zustand seine Aktivität reguliert (3b). Das aktive PspF-Hexamer bindet nun an den *pspA*- bzw. *pspG*-P romotor, wodurch die σ^{54}-abhängige Transkription initiiert wird (4). Dies führt zu großen PspA-Assemblierungen an der Innenseite der Cytoplasmamembran, für die eine Lokalisation mit PspB und PspC nachgewiesen werden konnte (5).

Bei Membranstress wurde eine Konformationsänderung von PspC beschreiben, welche zu einer Freisetzung der C-terminalen Domäne führt, welche nun in der Lage ist, PspA zu binden [33]. Es wird davon ausgegangen, dass der PspFA-Komplex in der Zelle frei diffundieren kann und ebenfalls transient an der Cytoplasmamembran vorliegt, wodurch die Interaktion von PspF-gebundenen PspA mit der C-terminalen PspC-Domäne unter induzierenden Bedingungen ermöglicht wird [33,86,87]. Die Interaktion von PspA mit dem C-Terminus von PspC führt zur Aufhebung der PspA-abhängigen Inhibition von PspF, womöglich auf Grund einer Dissoziation des PspFA-Komplexes [33,72,88]. Es konnte jedoch ebenfalls gezeigt werden, dass PspA PspF im gebundenen Zustand zu regulieren vermag, weshalb eine Dissoziation des PspFA-Komplexes zur Induktion der σ^{54}-abhängigen Transkription möglicherweise nicht notwendig ist [70]. PspF ist nun in der Lage, die σ^{54}-abhängigen Transkription des *pspABCDE*-Operons sowie die von *pspG* zu induzieren, was die Bildung von großen oligomeren PspA-Strukturen an der Cytoplasmamembran zur Folge hat [4,15,72,83], welche teilweise mit PspBC assoziiert vorliegen [33].

Schon früh wurde jedoch auch eine PspBC-unabhängige Induktion des Psp-Systems beschrieben [18]. In *E. coli* ist die durch das Phagen-Sekretin pIV induzierte Aktivierung von PspF nur unter aeroben Bedingungen PspBC-abhängig, nicht jedoch unter anaeroben Bedingungen [24]. Neueste *in-vitro*-Studien zeigen, dass PspA PspBC-unabhängig mit Membranvesikeln interagieren und die inhibitorische Wirkung von PspA auf PspF *in vitro* durch Zugabe von Membranvesikeln teilweise aufgehoben werden kann [77]. Jovanovic *et al.* (2104) postulierten bereits zuvor, dass der in der *coiled-coil* Struktur zurückgefaltete N-terminale Bereich von PspA, PspA(2-24), eine Stress-induzierte Membran-interagierende Helix ausbildet [88], die Einfluss auf die Psp-Inhibition haben könnte, wodurch PspA, gebunden im PspF/PspA-Komplex, möglicherweise direkt an der Cytoplasmamembran ein Psp-System induzierendes Signal wahrnehmen kann [87]. Kurz darauf wurde mittels Circulardichroismus-spektroskopischen Analysen von kurzen N-terminalen PspA-Peptiden gezeigt, dass das PspA-Peptid, PspA(2-24), in einer Lipidumgebung eine α-helicale Struktur annimmt, die sich in der Präsenz von negativ geladenen Phospholipiden noch verstärkte [71]. Gleichzeitig war dieses Peptid ohne Lipidzugabe in der Lage, die ATPase-Aktivität von PspF zu inhibieren, weshalb postuliert wurde, dass die Bildung einer Stress-induzierten N-terminalen amphipatischen Helix als möglicher Sensor für

Membranstress in PspA selbst in einem von PspB und PspC unabhängigen Mechanismus fungieren könnte [71].

1.1.5 Die Induktoren, das induzierende Signal und die physiologische Funktion des Psp-Systems

Allen Induktoren ist gemein, dass sie die Integrität der Cytoplasmamembran oder den Energiestatus der Zelle beeinflussen. So wurde bereits frühzeitig eine Schädigung der Cytoplasmamembran mit drauffolgender Beeinträchtigung der PMF als gemeinsames Psp-induzierendes Signal postuliert. Kleerebezem *et al*. (1996) zeigten, dass es bei Sekretinstress in einem *pspA*-Deletionsstamm zu einer Schwächung des Protonengradienten kommt [16]. Die Idee, dass die Schwächung der PMF das Psp-induzierende Signal darstellt, manifestierte sich weiter, nachdem ein starker Anstieg der PspA-Proteinbiosynthese nach Behandlung von *E. coli* mit dem Protonophor CCCP beobachtet wurde [80,89]. Jedoch zeigte sich in späteren Analysen, dass weder eine Zerstörung des Protonengradienten (ΔpH) noch des Membranpotentials ($\Delta\psi$), aus welchen sich die PMF zusammensetzt, ausreichend für eine Induktion des Psp-Systems ist [90]. Die Induktion der Psp-Antwort durch die Deletion von YidC ist ebenfalls unabhängig von einer Beeinträchtigung der PMF [91]. Es wurde daraufhin spekuliert, dass der Redoxzustand des Chinonpools der Zelle das Psp-induzierende Signal darstellen könnte und dieses durch die Sensorkinase ArcB des ArcAB-Systems zu membranständigen Psp-Komponenten weitergeleitet wird [92]. Im Gegensatz dazu zeigte eine spätere Studie, dass das ArcAB-System nicht notwendig für die Sekretin-abhängige Induktion des Psp-Systems ist und eine ArcAB-Abhängigkeit nur unter mikroanaeroben Wachstumsbedingungen besteht [93,89]. Kürzlich wurde eine Verstärkung des an der Lipiddoppelschicht anliegenden Krümmungsstresses (*membrane-stored curvature elastic* (SCE)-Stress) als vereinigendes Signal aller Psp-Induktoren vorgeschlagen [77].

Auch die physiologische Funktion des Psp-Systems in *E. coli* ist bis heute nicht vollständig aufgeklärt, was vor allem auf das Fehlen eines gemeingültigen Phänotyps der verschiedenen Induktoren in *psp*-Deletionsstämmen zurückzuführen ist. Allein Kobayashi *et al*. (2007) gelang es mittels *in-vitro*-Experimenten zu zeigen, dass als Oligomer vorliegendes PspA in der Lage ist, dem Protonenverlust von mit Ethanol behandelten Vesikeln entgegenzuwirken [73]. Es liegen bislang jedoch keine Daten

basierend auf *in-vivo*-Experimenten vor, die die beschriebene Effektorfunktion von PspA direkt in *E. coli* zeigen, stattdessen beruht die Beschreibung von PspA als mögliches Effektorprotein *in vivo* hauptsächlich auf der Untersuchung von *pspA*-Deletionsstämmen. Da diese polare Effekte auf die Transkription der im *pspABCDE*-Operon nachfolgenden Gene aufweisen können, kann ebenfalls eine Effektorfunktion von PspB und PspC in *E. coli* nicht ausgeschlossen werden (z.B. [16,94,15,24]). Interessant ist, dass PspC, jedoch nicht PspA, einen direkten Einfluss auf die Virulenz und Viabilität von *Y. enterocolitica* unter Psp-induzierenden Bedingungen zeigt [31,5,32,37]. PspB und PspC hatten zudem einen direkten Einfluss auf die Indol-induzierte Bildung von persistenten Zellen von *E. coli* [95]. Jedoch beruhen auch diese Beobachtungen ebenfalls auf Untersuchungen in *pspBC*-Deletionsstämmen, in welchen auf Grund der Regulation des Psp-Systems direkt die Menge an gebildeten PspA beeinflusst wird. Auf Grund dessen ist es bis heute völlig unklar, welche Komponente des Psp-Systems in *E. coli* eine Effektorfunktion übernimmt.

1.2 Die durch TatA ausgelöste Psp-Antwort

Ein Zusammenhang zwischen bakteriellen Sekretionssystemen und der Induktion des Psp-Systems wurde bereits vor einigen Jahren gezeigt. So führte unter anderem die Depletion der Membranprotein-Insertase YidC sowie Mutationen in Komponenten des Sec-Translokons zur Induktion des Psp-Systems [11,80]. In *E. coli* konnte eine erhöhte PspA-Proteinbiosynthese nachgewiesen werden, wenn die Tat-Translokase, welche gefaltete Proteine über die Cytoplasmamembran transportiert, durch heterolog produzierte Substrate blockierte wurde [12]. Gleichzeitig konnte rekombinant produziertes PspA dieser Blockade entgegenwirken. Ferner wurde in gleicher Studie eine Induktion des Psp-Systems durch *tat*-Deletionsmutanten beschrieben. Zusätzlich wurde gezeigt, dass die Tat-Komponente TatA das Psp-System bei rekombinanter Überproduktion abhängig von PspB und PspC induziert [94]. In gleicher Studie konnte eine PspBC-abhängige aber PspF-unabhängige Interaktion von TatA mit PspA nachgewiesen werden. Da TatA in dieser Arbeit als Modellinduktor der Psp-Antwort eingesetzt wurde, soll im Folgenden die Struktur und Funktion TatAs während der Tat-abhängigen Proteintranslokation kurz umrissen werden.

1.2.1 Das Tat-System

Das Tat-System kommt ähnlich zum Psp-System in Bakterien, Archaeen aber auch in den Thylakoidmembranen von Chloroplasten und somit auch in Eukaryoten vor [96–99]. Das Tat-System transportiert bereits im Cytoplasma gefaltete Proteine über die Cytoplasmamembran in das Periplasma, wobei Gründe für eine im Cytoplasma notwendige Proteinfaltung unter anderem die nötige Assemblierung von Kofaktoren, schnelle Faltungskinetiken oder die Bildung eines heterodimeren Proteinkomplexes, bei welchem nur eine Untereinheit das Signalpeptid besitzt, darstellen können [96,100–102].

TatA übernimmt eine entscheidende Rolle innerhalb des Tat-Transports und gehört der TatA/E/B-Proteinfamilie an, welche zusammen mit TatC die essentiellen Komponenten der Tat-Translokase in *E. coli* bilden [103,104]. TatA, TatB und TatE sind kleine Membranproteine, die sich durch eine hohe strukturelle Ähnlichkeit auszeichnen [105,98].

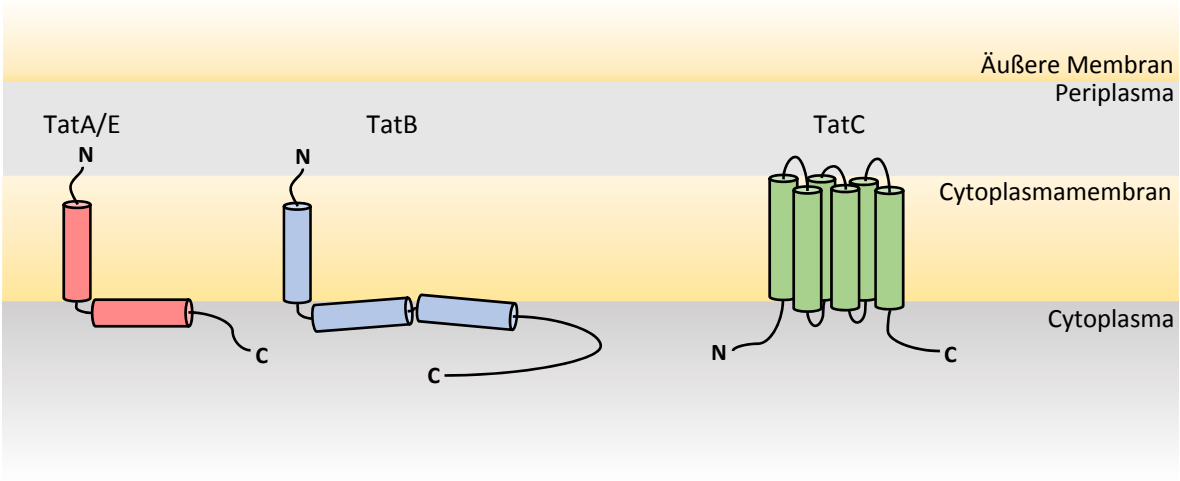

Abbildung 5 Schematischer Aufbau und Lokalisation der Tat-Komponenten in der Cytoplasmamembran von *E. coli* TatA und TatE (rot) sowie TatB (blau) besitzen einen sehr ähnlichen Aufbau mit einem im Periplasma lokalisierten N-Terminus und einer kurzen Transmembrandomäne, welche über eine kurze Linker-Region mit einer amphipathischen Helix verbunden ist. Im Vergleich zu TatA und TatE besitzt TatB einen verlängerten unstrukturieren C-terminalen bereich. TatC (grün) besitzt sechs Transmembrandomänen. N- und C-Terminus sind im Cytoplasma lokalisiert.

Bei allen drei Tat-Komponenten befindet sich der N-Terminus im Periplasma, worauf eine kurze α-helikale Transmembrandomäne folgt, die über eine flexible *hinge*-Region mit der darauffolgenden amphipathischen Helix verbunden ist. Der im Cytoplasma lokalisierte C-Terminus ist unstrukturiert und variiert je nach Tat-Komponente in seiner Länge [103,106–108]. Mittels diverser NMR-Analysen konnte die für diese Proteinfamilie postulierte Struktur bestätigt werden [109–112]. TatC ist mit einem Molekulargewicht von 28,9 kDa die größte und am stärksten konservierte Tat-Komponente [97]. Bei TatC handelt es sich um ein polytopisches Membranprotein mit sechs helikalen Transmembrandomänen und im Cytoplasma lokalisierten unstrukturierten N- und C-terminalen Bereichen [113,114].

Alle Tat-Komponenten bilden transportrelevante homo- und/oder heterooligomere Strukturen [115–121]. TatC und TatB bilden in der Cytoplasmamembran einen stabilen Komplex [115,122–126], der das Tat-Signalpeptid, welches das namensgebende Zwillingsarginin-Motiv enthält, als initialen Schritt des Transports erkennt und bindet [99,113,127–135]. TatA ist ebenfalls in der Lage direkt und unabhängig vom TatBC-Komplex mit Substraten zu interagieren, interagiert jedoch vornehmlich mit den maturen Bereichen von unprozessierten Tat-Substraten [127,136,137]. Die Bindung des Signalpeptids an den TatBC-Komplex initiiert die PMF-abhängige Assemblierung von TatA-Protomeren an den TatBC-Substrat-Komplex, wodurch der transportaktive Tat(A)BC-Komplex gebildet wird [99,138]. In einem darauffolgenden PMF- und TatA-abhängigen Schritt erfolgt die Translokation des Substrats über die Cytoplasmamembran [138]. Nach der Membranpassage des Substrats erfolgt die Prozessierung des Signalpeptids durch die membranständige Signalpeptidase I, LepB [139], die Entlassung des maturen Substrats in das Periplasma, sowie die Dissoziation von TatA vom TatBC-Komplex [99,140]. Bislang bekannte Schritte des Tat-abhängigen Transports sind schematisch in Abbildung 6 dargestellt.

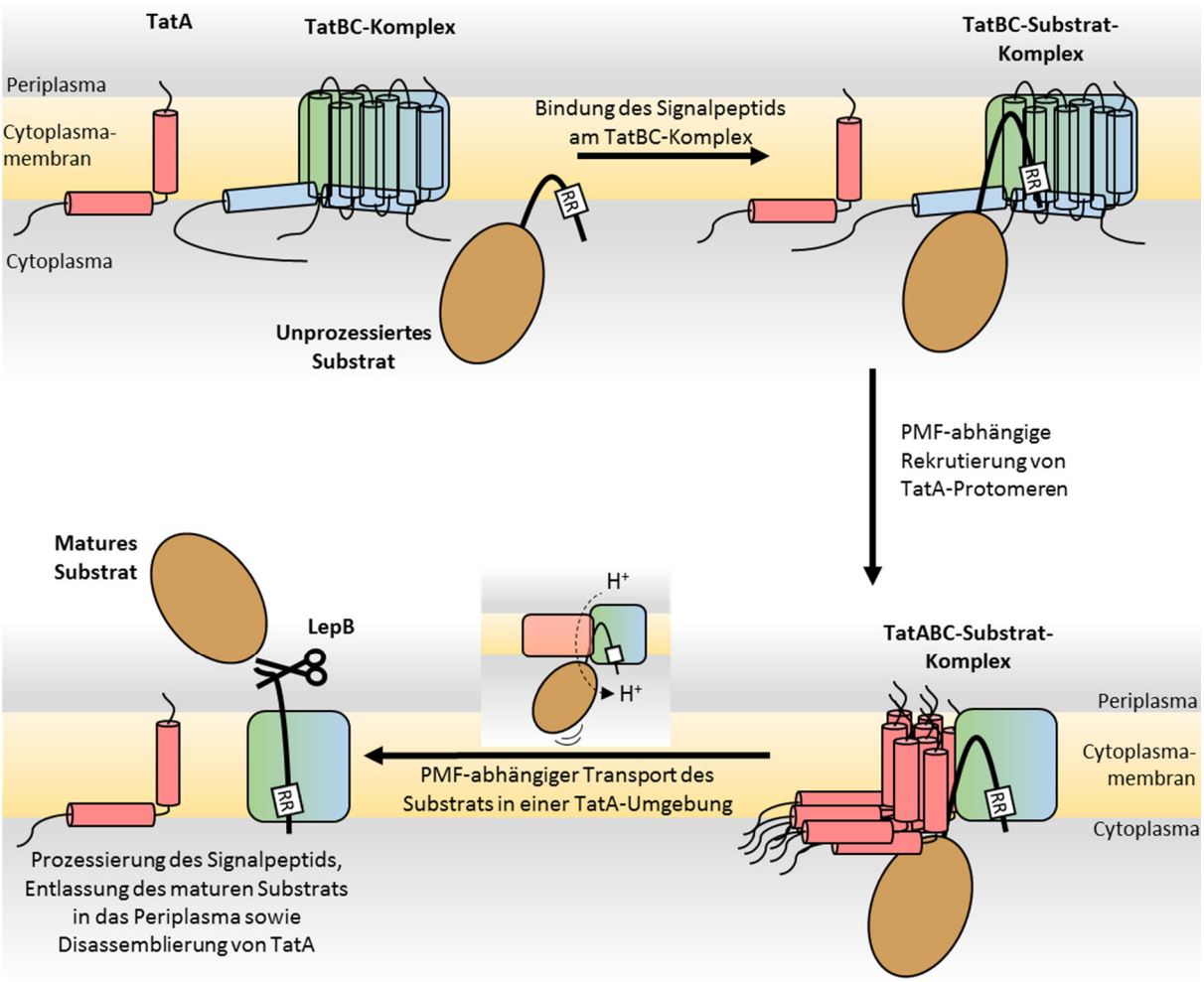

Abbildung 6 Schematische Darstellung des Mechanismus des Tat-abhängigen Transports in *E. coli* Das unprozessierte Substrat bindet mit seinem Signalpeptid an den TatBC-Komplex. In einem PMF-abhängigen Schritt wird TatA an den TatBC-Substrat-Komplex rekrutiert. Der Transport des Substrats geschieht nun PMF-abhängig in einer TatA-Umgebung, wobei das Signalpeptid am TatBC-Komplex gebunden verbleibt. Nach der Membranpassage wird das Signalpeptid an der Erkennungssequenz durch die Signalpeptidase LepB abgespalten und in das Periplasma als matures Substrat entlassen.

Der genaue mechanistische Ablauf des PMF- und TatA-abhängigen Transportschritts ist bis heute ungeklärt. Es existieren zwei konkurrierende Modelle bezüglich der Form der TatA-Assemblierungen, die direkt mit der Funktion TatAs während der Membranpassage des Substrats zusammenhängen. Rekombinant produziertes TatA bildet nach Reinigung ringförmige Strukturen unterschiedlicher Größe [116,141], weshalb eine wassergefüllte TatA-Pore vorgeschlagen wurde, die Substrat-abhängig zum TatBC-Komplex rekrutiert wird und durch welche das Substrat durch die Cytoplasmamembran transloziert werden soll [116,142,143]. Im alternativen *membrane-weakening and pulling*-Modell schwächen oligomere TatA-Assemblierungen die Cytoplasmamembran in Nähe des TatBC-Substrat-Komplexes punktuell (*weakening*) und TatC zieht durch eine Konformationsänderung das Tat-

Substrat durch die Cytoplasmamembran (*pulling*) [140]. Für beide Modelle fehlt bislang der abschließende experimentelle Beweis, jedoch ist ihnen gemein, dass der Transport in einer TatA-Umgebung im direkten Kontakt zum TatBC-Komplex und PMF-abhängig geschieht [110,140,137,144–149]. Rodriguez *et al.* (2013) lieferten kürzlich mittels *molecular dynamics* (MD)-Simulationen weitere Einblicke in die Oligomerisierung und Funktion TatAs und verbanden auf Grund ihrer *in-silico*-Analysen die Bildung einer TatA-Pore mit der im *membrane-weakening and pulling*-Modell postulierten TatA-induzierten Membranschwächung im Zuge des Proteintransports [110].

1.2.2 TatA als Modellinduktor der Psp-Antwort in *E. coli*

In Mehner *et al.* (2012) wurde bereits spekuliert, dass die Induktion des Psp-Systems durch TatA möglicherweise in der postulierten Funktion TatAs, die Cytoplasmamembran zu schwächen, begründet liegt [94]. Der ungewöhnlich kurze Membrananker von TatA konnte dabei als minimale TatA-Domäne identifiziert werden, welche sowohl das Psp-System induzierte als auch mit PspA zu interagieren vermochte [94,150]. Mittels Mutagenesestudien und Austausch ganzer Regionen im N-terminalen Bereich und im Membrananker von TatA wurde der flexible dem Periplasma hingewandte N-terminale Bereich von TatA und insbesondere Isoleucin^{6} als essentiell für die TatA-induzierte Psp-Antwort beschrieben [150]. Dieser Austausch in TatA verhinderte auch den Tat-Transport, jedoch nicht die Interaktion mit PspA. Des Weiteren wurde gezeigt, dass TatA auch dann in der Lage ist mit PspA zu interagieren, wenn es in nativen Leveln in der Cytoplasmamembran vorliegt und keine messbare Psp-Antwort auslöst. Es wurde daraufhin spekuliert, dass TatA das Psp-System nicht nur auf Grund der rekombinanter Überproduktion induziert [150]. Da keine für die PspA-Interaktion essentielle Aminosäure innerhalb TatAs identifiziert werden konnte, in gleicher Studie jedoch die nicht-ionischen Detergenzien C12E9 und N-Dodecyl-β-D-maltosid verschieden starke Einflüsse auf das Elutionsverhalten der beiden Proteine zeigten, wurde spekuliert, dass die TatA/PspA-Interaktion möglicherweise auf hydrophoben Wechselwirkungen beruht [150]. Es blieb an dieser Stelle jedoch unklar, ob ausschließlich die Interaktion zwischen PspA und TatA zu einer Induktion der PspA-Antwort führt oder ob TatA in der Lage ist ein Interaktion-unabhängiges Psp-induzierenden Signal auszulösen.

2 Zielsetzung

Ziel der im Rahmen der vorliegenden Dissertation durchgeführten Arbeiten war, die TatA-induzierte Psp-Antwort sowie die TatA/PspA-Interaktion weitergehend zu untersuchen. Durch die Anwendung verschiedener molekularbiologischer, mikroskopischer, proteinbiochemischer Methoden sowie durch *pspA*-Promotoraktivitätsstudien sollte geklärt werden, ob TatA die Psp-Antwort durch die Rekrutierung PspAs aktiviert, oder ob TatA in der Lage ist, ein definiertes Psp-induzierendes Signal in der Cytoplasmamembran auszulösen. Darauf aufbauend sollte die von TatA-ausgelöste Signalkaskade identifiziert und TatA als Modellinduktor der Psp-Antwort in *E. coli* etabliert werden.

Da die TatA/PspA-Interaktion von den membranständigen Psp-Komponenten PspB und PspC abhängig war und diese möglicherweise als Sensoren eines TatA-abhängigen Psp-System-induzierenden Signals dienen, war es Ziel, mittels Fragmentierungsstudien und anschließenden Pull-Down-Analysen zu bestimmen, ob die TatA/PspA-Interaktion von bestimmten PspB oder PspC-Domänen vermittelt wird, oder eine Abhängigkeit nur auf Grund ihrer positiven Regulatorfunktion besteht.

Auf Grund der Instabilität C-terminaler PspA-Fragmente *in vivo* sollte im Rahmen dieser Arbeit das C-terminale PspA-Fragment PspA(145-222) durch eine Proteinfusion *in vivo* stabilisiert werden. Darauf aufbauend sollte die Funktion von PspA(145-222) bezüglich der Regulation von PspF und seinen Einfluss auf die Induzierbarkeit des Psp-Systems mittels verschiedener Methoden untersucht werden. Damit einhergehend sollte untersucht werden, ob die bereits gut charakterisierte PspA-Domäne, PspA(1-144), sowie PspA(145-222) in der Lage sind, mit TatA zu interagieren, um so weitere Einblicke in die TatA-induzierte Psp-Antwort zu erhalten.

Da basierend auf *in-vitro*-Analysen postuliert wurde, dass negativ geladene Phospholipide möglicherweise ausschlaggebend für eine Signalwahrnehmung durch PspA sind und sogenannter SCE-Stress möglicherweise in einem PspBC-unabhängigen Mechanismus zu einer Induktion des Psp-Systems führt, sollte mittels Lipid-defizienten *E.-coli*-Stämmen geklärt werden, ob das Psp-System ebenfalls *in vivo* PspBC-unabhängig durch SCE-Stress induziert wird.

3 Ergebnisse

3.1 „*The TatA component of the twin-arginine translocation system locally weakens the cytoplasmic membrane of* Escherichia coli *upon protein substrate binding*"

Autoren:	Bo Hou, Eyleen S. Heidrich, Denise Mehner-Breitfeld, und Thomas Brüser
Art der Autorenschaft:	geteilte Erst-Autorenschaft mit Bo Hou
Zugehörigkeit:	Leibniz Universität Hannover, Institut für Mikrobiologie, Herrenhäuser Straße 2, 30491 Hannover
Art des Artikels:	Forschungsartikel
Beitrage:	**Bo Hou:** Planung und Durchführung der *in-vitro*-Experimente, Etablierung der spektroskopischen Messung der JC1-Färbung zusammen mit Eyleen S. Heidrich, Datenanalyse, Beiträge zum Manuskript **Eyleen S. Heidrich:** Planung und Durchführung der *in-vivo*-Experimente, JC1-Färbung und Etablierung der spektroskopischen Messung der JC1-Färbung zusammen mit Bo Hou, Datenanalyse, Zusammenstellung und Präparation der Abbildungen, Beiträge zum Manuskript **Denise Mehner-Breitfeld:** *in-vivo*-Experimente zu Beginn des Projekts **Thomas Brüser:** Planung und Koordination des Projekts, Zusammenstellung und Präparation der Abbildungen, Datenanalyse und Anfertigung des Manuskripts
Publiziert in	*Journal of Biological Chemistry*
Publiziert am	13. März 2018

This research was originally published in the Journal of Biological Chemistry.

Bo Hou, Eyleen S. Heidrich, Denise Mehner-Breitfeld, and Thomas Brüser. The TatA component of the twin-arginine translocation system locally weakens the cytoplasmic membrane of *Escherichia coli* upon protein substrate binding. J. Biol. Chem. 2018; 293(20): 7592-7605 © Bou Hou, Eyleen S. Heidrich, Denise Mehner-Breitfeld, and Thomas Brüser

Doi: 10.1074/jbc.RA118.002205

Link: http://www.jbc.org/content/293/20/7592

Wissenschaftliche Einordnung

Der genaue Mechanismus des Tat-abhängigen Transports gefalteter Proteine über die Cytoplasmamembran ist bis heute unklar. Neben dem TatBC-Komplex spielt TatA während des Transports eine entscheidende Rolle, denn erst durch die Rekrutierung TatAs an den TatBC-Substrat-Komplex erfolgt die PMF-abhängige Translokation des Substrats. Es ist jedoch nach wie vor ungeklärt, welche Aufgabe TatA in diesem entscheidenden Transportschritt übernimmt. Der stark konservierte Membrananker von TatA ist ungewöhnlich kurz und mit einer Länge von 13 Aminosäuren (Glutamat^{7}-Phenylalanin^{20}) nicht in der Lage die Cytoplasmamembran vollständig zu durchspannen. Es wurde daher bereits schon im Zuge des sogenannten *membrane weakening*-Modells des Tat-abhängigen Proteintransports postuliert, dass TatA die Cytoplasmamembran in Umgebung des TatBC-Komplexes schwächen könnte, was eine Translokation des Substrats durch TatBC in einem unbekannten Schritt möglich macht [140]. Im Artikel „*The TatA component of the twin-arginine translocation system locally weakens the cytoplasmic membrane of* Escherichia coli *upon protein substrate binding*“ konnte erstmals eine direkte Membrandestabilisierung durch den ungewöhnlich kurzen Membrananker von TatA *in vivo* und *in vitro* gezeigt werden, wobei ein starker negativer Einfluss auf des Membranpotential nachgewiesen werden konnte. Die TatA-induzierte Membrandestabilisierung wurde im Zuge der publizierten Ergebnisse erstmals mit einer Substrat-abhängigen Reorientierung TatAs in Verbindung gebracht und lieferten dabei einen entscheidenden Beitrag zum Verständnis der Funktion von TatA im Zuge des Transportmechanismus der Tat-Translokase. Die hier gezeigten Ergebnisse geben ebenfalls Hinweise auf die Ursache der Aktivierung des Psp-Systems durch die rekombinante Überproduktion von TatA.

JBC ARTICLE

The TatA component of the twin-arginine translocation system locally weakens the cytoplasmic membrane of *Escherichia coli* upon protein substrate binding

Received for publication, January 31, 2018, and in revised form, March 8, 2018 Published, Papers in Press, March 13, 2018, DOI 10.1074/jbc.RA118.002205

Bo Hou[1], **Eyleen S. Heidrich**[1], **Denise Mehner-Breitfeld, and Thomas Brüser**[2]

From the Institute of Microbiology, Leibniz Universität Hannover, Herrenhäuser Strasse 2, 30419 Hannover, Germany

Edited by Wolfgang Peti

The twin-arginine translocation (Tat) system that comprises the TatA, TatB, and TatC components transports folded proteins across energized membranes of prokaryotes and plant plastids. It is not known, however, how the transport of this protein cargo is achieved. Favored models suggest that the TatA component supports transport by weakening the membrane upon full translocon assembly. Using *Escherichia coli* as a model organism, we now demonstrate *in vivo* that the N terminus of TatA can indeed destabilize the membrane, resulting in a lowered membrane energization in growing cells. We found that in full-length TatA, this effect is counterbalanced by its amphipathic helix. Consistent with these observations, the TatA N terminus induced proton leakage *in vitro*, indicating membrane destabilization. Fluorescence quenching data revealed that substrate binding causes the TatA hinge region and the N-terminal part of the TatA amphipathic helix to move toward the membrane surface. In the presence of TatBC, substrate binding also reduced the exposure of a specific region in the amphipathic helix, indicating a participation of TatBC. Of note, the substrate-induced reorientation of the TatA amphipathic helix correlated with detectable membrane weakening. We therefore propose a two-state model in which membrane-destabilizing effects of the short TatA membrane anchor are compensated by the membrane-immersed N-terminal part of the amphipathic helix in a resting state. We conclude that substrate binding to TatABC complexes switches the position of the amphipathic helix, which locally weakens the membrane on demand to allow substrate translocation across the membrane.

The Tat[3] system serves to transport folded proteins in bacteria, archaea, plant plastids, and possibly plant mitochondria (1–4). In *Escherichia coli*, the Tat system consists of TatA, TatB, and TatC components. TatA and TatB are similar, and two-component "minimal" Tat systems exist in which TatA exerts functions of TatA and TatB (5). TatA/B components are N-terminally membrane-anchored by a very short hydrophobic transmembrane domain, which is followed by a short hinge region, an amphipathic helix (APH), and a variable C-terminal domain (6). TatC is a polytopic membrane protein with six transmembrane domains (7, 8). TatB tightly interacts with TatC (9, 10). TatA associates with these TatBC complexes and is thought to permeabilize the membrane for protein transport (11–14). TatBC complexes recognize and tightly bind the signal peptides of the cargo proteins throughout the translocation process (15, 16).

The mechanism by which this translocation is achieved must be unusual and is not understood (17). A currently favored model suggests that the N termini of multiple TatA molecules at the translocon site weaken the membrane upon substrate binding, thereby permitting a TatC-mediated pulling of the substrate through the destabilized membrane ("membrane-weakening and pulling mechanism"; see Ref. 18). Molecular dynamics simulations support this view and suggest that multiple TatA N termini can cause a local thinning of the membrane (6). However, direct experimental evidence for a thinning stress imposed by the N terminus of TatA is lacking.

Here we demonstrate that the N terminus of TatA alone can indeed destabilize the membrane. This membrane stress relates to the short length of the TatA membrane anchor. In full-length TatA, the N-terminal half of the APH immerses into the membrane and counterbalances the effects of its own N-terminal membrane anchor. Importantly, substrate association with TatA induces a reorientation of the APH and TatA and thereby destabilizes the membrane to a measurable extent. In the absence of TatBC, the same substrate-induced changes occur in the N-terminal half of the APH, but the C-terminal part of the APH is not influenced. The data suggest that local membrane destabilization is indeed part of TatABC-catalyzed transport, and substrate association triggers this destabilization on demand.

Results

A cell-growth effect of the TatA membrane anchor that is compensated by the TatA amphipathic helix

TatA is a key component of the Tat system and considered to locally weaken the membrane, thereby, in conjunction with the other Tat system components, allowing the passage of folded proteins (18, 19). TatA is anchored by its N terminus in the cytoplasmic membrane (20). The N-terminal 6 residues are in

This work was supported by DFG Grant BR2285/4-2. The authors declare that they have no conflicts of interest with the contents of this article.
This article contains Fig. S1.
[1] Both authors contributed equally to this work.
[2] To whom correspondence should be addressed. Tel.: 49-511-762-5945; Fax: 49-511-762-5287; E-mail: brueser@ifmb.uni-hannover.de.
[3] The abbreviations used are: Tat, twin-arginine translocation; APH, amphipathic helix; HiPIP, high-potential iron sulfur protein; IMV, inner membrane vesicle; NT, N-terminal domain; CCCP, carbonyl cyanide *m*-chlorophenyl hydrazone; TMR, tetramethylrhodamine; TMH, transmembrane helix; Tricine, *N*-[2-hydroxy-1,1-bis(hydroxymethyl)ethyl]glycine; YFP, yellow fluorescent protein.

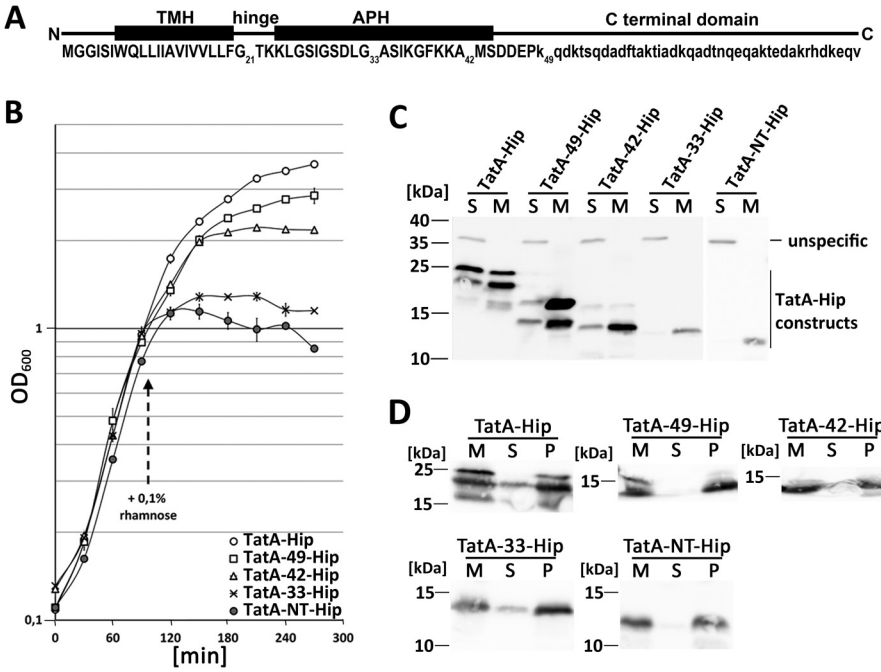

Figure 1. Inhibition of growth after production of TatA-NT-Hip. *A*, scheme of TatA, indicating the positions of the TMH, the hinge, the APH, the highly charged patch behind the APH, and the unstructured C-terminal domain. *Numbered* are positions to which the C-terminally Strep-tagged mature domain of HiPIP (experiments in Fig. 1) or only the Strep-tag (experiments in Fig. 2) have been fused to create truncated TatA variants (see "Experimental procedures"). Residues in *capital letters* have been structurally solved. *B*, growth curves of the *tatAE*-deletion strain JARV16 with recombinant rhamnose-induced production of either TatA-Hip, TatA-49-Hip, TatA-42-Hip, TatA-33-Hip, or TatA-NT-Hip. Induction of the pBW expression vectors was done with 0.1% rhamnose at the indicated time point. S.D. values (*error bars*) were calculated from three independent cultures. *C*, SDS-PAGE/Western blot analysis of subcellular fractions of the cultures analyzed in *B*. *S*, soluble fraction; *M*, membrane fraction. *unspecific*, a cross-reaction of the antibody. *D*, carbonate washes of the membrane-targeted constructs described above. *M*, membranes; *S*, supernatant after carbonate wash; *P*, pellet fraction after carbonate wash. Western blots were developed using specific HiPIP antibodies and ECL reaction.

the periplasmic surface of the membrane (6). The transmembrane helix (TMH) starts at Trp^{7}/Gln^{8} on the periplasmic side and ends at Phe^{20} on the cytoplasmic side (see Fig. S1). The hydrophobic residues Leu^{9}–Phe^{20} actually cross the lipid bilayer (21, 6). As the extremely short membrane-spanning region of TatA has been suggested to have the membrane-weakening effect, we tested whether production of the TatA membrane anchor (TatA-NT, residues 1–21) affects membrane stability. In earlier studies, we had already fused TatA-NT to a small, extremely stable soluble protein (the mature domain of the Tat substrate HiPIP from *Allochromatium vinosum*) (22), which stabilizes the peptide *in vivo* and renders it readily detectable by SDS-PAGE/Western blotting (23). In that earlier study, we had recognized that the TatA-NT-Hip construct induces the phage shock protein membrane stress response, indirectly indicating a membrane destabilization (23).

In continuation of that study, we systematically analyzed possible membrane-destabilizing effects of the TatA membrane anchor and included TatA-NT extensions to Gly^{33} (TatA-33), Ala^{42} (TatA-42), Lys^{49} (TatA-49), and full-length TatA to assess a possible influence of the adjacent amphipathic helix and further C-terminal regions (Fig. 1*A*). TatA-33 possesses the hinge region and the residues of the amphipathic helix up to the conserved flexible position Gly^{33}. TatA-42 extends the construct to Ala^{42} near the end of the amphipathic helix, and TatA-49 further includes a highly charged stretch of residues (Asp-Asp-Glu-Pro-Lys) that is proposed to be important for function (24, 25). As TatA-NT was stabilized by a fusion to HiPIP, we also fused the other constructs C-terminally to HiPIP. Their production had differential effects on growth (Fig. 1*B*). Growth readily ceased upon induction of TatA-NT-Hip production. This effect was gradually reduced in longer constructs, in the order TatA-NT-Hip > TatA-33-Hip > TatA-42-Hip > TatA-49-Hip > full-length TatA-Hip. The differential effects of the various constructs were not caused by variation of protein abundances, as the two constructs with the strongest effects were even less abundant than the others (Fig. 1*C*). The two longest constructs showed heterogeneous migration behavior that might relate to distinct stable conformations. All constructs were stably integrated into membranes, as evidenced by carbonate washes (Fig. 1*D*).

To control whether the HiPIP fusion might have had effects that influenced the outcome, we also generated all constructs without fused HiPIP, although we knew that TatA-NT alone was unstable *in vivo* (Fig. 2*A*). TatA-NT still had some inhibitory effect. The extended TatA-NT constructs showed the same order with respect to their growth-inhibitory effect as the HiPIP-fused constructs, with TatA-33 > TatA-42 > TatA-49 > TatA (Fig. 2*A*). Again, the abundance and membrane-targeting of the proteins was assessed by SDS-PAGE/Western blotting (Fig. 2*B*). As expected, TatA-NT was extremely low abundant. The three extended constructs TatA-33, TatA-42, and TatA-49 were more stable than TatA-NT. Full-length TatA was more abundant than any other construct and had to be 4-fold diluted to achieve a comparable concentration that permitted a good ECL detection of the less abundant constructs. All constructs were membrane-targeted. Membrane integration was verified by carbonate washes (Fig. 2*C*). It is known that

Control of membrane weakening by TatA

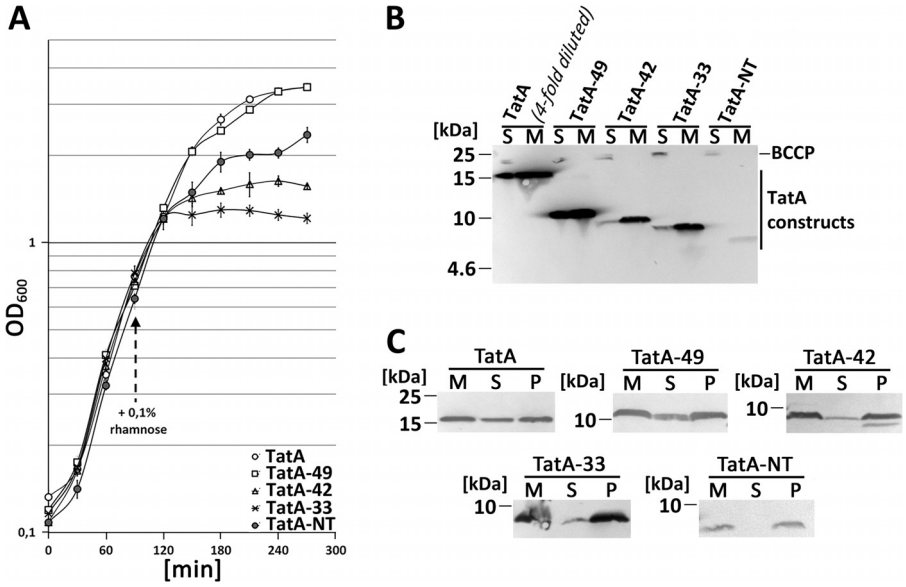

Figure 2. Effect on growth after production of TatA and truncated TatA variants without HiPIP fusion. *A*, growth curves of the *tatAE*-deletion strain JARV16 with recombinant rhamnose-induced production of either TatA, TatA-49, TatA-42, TatA-33, or TatA-NT. All constructs were Strep-tagged. Induction of the pBW expression vectors was done with 0.1% rhamnose at the indicated time point. S.D. values (*error bars*) were calculated from three independent cultures. *B*, Tricine-SDS-PAGE/Western blot analysis of fractioned cells of JARV16 producing the indicated TatA-NT variants or TatA. *S*, soluble fraction; *M*, membrane fraction. *C*, carbonate washes of TatA and the truncated TatA variants. *M*, membranes; *S*, supernatant after carbonate wash; *P*, pellet fraction after carbonate wash. Western blots were developed using Strep-Tactin-AP conjugate.

a portion of TatA can be extracted from membranes (26), and we observed this also for TatA-49. Together, the *in vivo* data indicated that the membrane anchor of TatA can strongly affect growth, and such effects are counterbalanced in full-length TatA and TatA-49. All characteristics that counterbalance the toxic effect of the TatA membrane anchor in these longer TatA constructs can be attributed to the region from Thr^{22} to Lys^{49}, which is the amphipathic helix and the adjacent charged patch.

The short length, not the sequence, of the hydrophobic TatA anchor region contributes to the growth phenotype

The above-described effect of the TatA membrane anchor raised the question whether the short membrane-spanning region in that anchor (Leu^9–Phe^{20}) was causing membrane damage. We assessed this aspect with further constructs. A TatA-NT$(STGG)_3$-Hip construct was generated in which the 12 hydrophobic residues were substituted by a $(STGG)_3$ linker. This substitution removes the hydrophobicity, which should result in a soluble protein. In addition, a TatA-NT$(LA)_6$-Hip construct was generated in which Leu^9–Phe^{20} were substituted by the artificial transmembrane domain LALALALALALA, which has been used in the past for analyses of artificial transmembrane helices (27). This construct should address questions of potential sequence specificity of observed effects. In construct TatA-NT(+6L)-Hip, we extended the hydrophobic transmembrane region by six leucine residues. This insertion was done behind the WQ motif that defines the beginning of the TMH (6). This third construct addressed the question of whether the short length of the TatA transmembrane region is responsible for the growth inhibition.

The growth was not influenced by TatA-NT$(STGG)_3$-Hip, indicating that neither the unaltered 8 residues at the extreme N terminus nor the fused HiPIP domain had any negative effect (Fig. 3*A*). The construct was stable and fully soluble and tended to dimerize (Fig. 3*B*). Apparently, the growth defects depended on membrane targeting or the sequence of the transmembrane helix. In addition, this result confirmed that the fused HiPIP domain did not cause any toxic effect. The TatA-NT$(LA)_6$-Hip construct demonstrated that the specific sequence of the membrane-spanning region was not relevant for the effect, as this construct showed the same strong effect on growth as TatA-NT-Hip (Fig. 3*A*). The TatA-NT$(LA)_6$-Hip construct exerted this strong inhibition, albeit it was much less abundant than TatA-NT-Hip (Fig. 3*B*). The membrane-targeted TatA-NT$(LA)_6$-Hip was stably membrane-integrated (Fig. 3*C*). Finally, the analysis of the TatA-NT(+6L)-Hip construct showed that the extension of the membrane-spanning hydrophobic stretch by 1½ helical turns already reduced the inhibitory effect (Fig. 3*A*), albeit the construct was more abundant than all the others (Fig. 3*B*). The membrane-targeted TatA-NT(+6L)-Hip was likewise stably membrane-integrated (Fig. 3*C*).

The energization of the cytoplasmic membrane can be compromised by the membrane anchor of TatA

The growth defect was a first experimental hint of the previously postulated membrane-destabilizing effect of the TatA membrane anchor, as membrane destabilization can diminish transmembrane ion gradients and consequently ATP synthesis, transport processes, and metabolism, ultimately resulting in growth inhibition. To address potential effects on membrane energization more directly *in vivo*, we stained cells with JC-1, a green fluorescent dye that forms red aggregates in cells with energized membranes (28). Cells containing TatA-Hip, TatA-NT-Hip, TatA-NT$(LA)_6$-Hip, and TatA-NT$(STGG)_3$-Hip were examined JC1 fluorescence microscopy. Compared with TatA-Hip and TatA-NT$(STGG)_3$-Hip, the TatA-NT-Hip and TatA-NT$(LA)_6$-Hip constructs led to a clear reduction in red JC-1 fluorescence (Fig. 4*A*). The strains containing the TatA-NT-

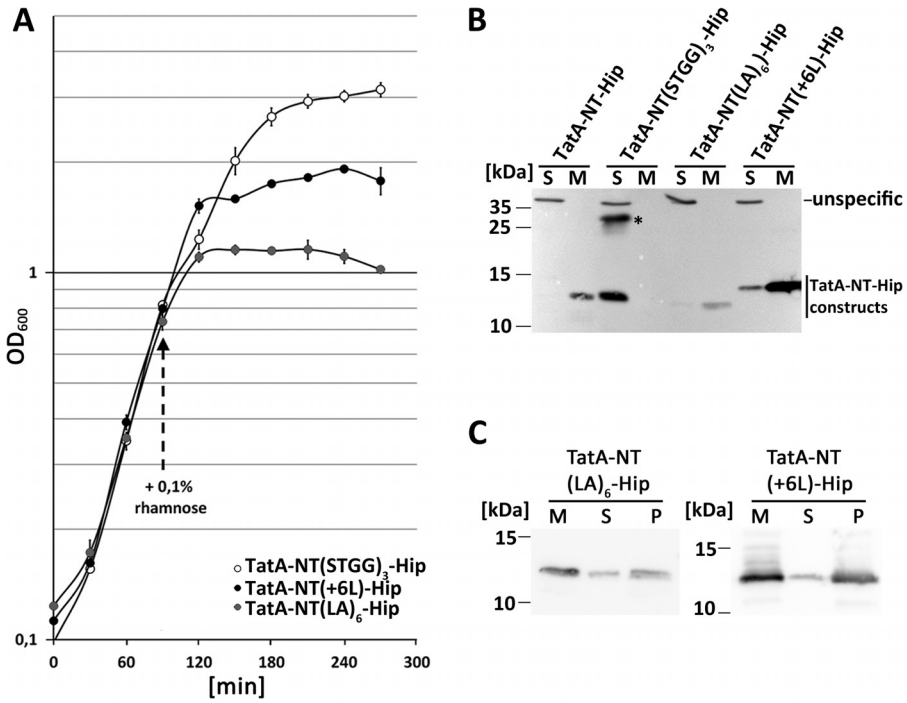

Figure 3. The short membrane anchor of TatA is responsible for the growth defect. *A*, effect on growth of recombinant TatA-NT(STGG)$_3$-Hip, TatA-NT(LA)$_6$-Hip, and TatA-NT(+6L)-Hip. All constructs were Strep-tagged. Growth curves of the *tatAE*-deletion strain JARV16 with recombinant rhamnose-induced production of indicated TatA-NT-Hip variants. pBW expression vectors were induced by the addition of 0.1% rhamnose at the indicated time point. S.D. values (*error bars*) were calculated from three independent cultures. *B*, SDS-PAGE/Western blot analysis of membrane (*M*) and soluble (*S*) fractions of JARV16 producing the indicated TatA-NT-Hip variants, using HiPIP-specific antibodies and ECL detection. *, TatA-NT(STGG)$_3$-Hip dimer. *C*, carbonate washes of membrane-targeted TatA-NT-Hip variants. Western blots were developed as described in *B*. *M*, membranes; *S*, supernatant after carbonate wash; *P*, membranes after carbonate wash.

Hip, TatA-NT(LA)$_6$-Hip, and TatA-NT(STGG)$_3$-Hip constructs all formed cell chains, which is due to the nonfunctional Tat system in these strains (29). Due to the chain formation, counting of red fluorescent cells was not feasible. Nevertheless, we achieved a quantitative measure for cell energization by determining the green/red JC1-fluorescence ratio using fluorescence spectroscopy (Fig. 4*B*). Although this method gave quite large error bars, the results demonstrated a significant de-energization by TatA-NT-Hip, and the data also agree with the microscopically observed effect of TatA-NT(LA)$_6$-Hip. As the (STGG)$_3$ substitution abolished the effects on membrane energization seen by TatA-NT-Hip, any observed reductions in membrane energization were unrelated to Tat system nonfunctionality (Fig. 4*B*).

Demonstration of proton leakage in vitro

The *in vivo* data indicated a negative influence of the TatA membrane anchor on cytoplasmic membrane energization. To overcome protein stability and growth effect issues that impeded experimental approaches *in vivo*, we decided to switch to a more defined experimental *in vitro* setup to study effects of the different TatA-NT constructs. In a first approach, we analyzed the membrane destabilization directly by acridine orange fluorescence quenching (Fig. 5). This approach monitors proton leakage as a measure for membrane destabilization. In this method, inverted cytoplasmic membrane vesicles (IMVs) are prepared and energized by the addition of ATP, which triggers the proton-pumping activity of ATP synthase (30). In the case of intact membranes, acridine orange that is present in the assay becomes protonated inside the acidified vesicles, which causes a fluorescence quenching. When the membranes show proton leakage, the proton gradient is less pronounced, resulting in a reduced acridine orange fluorescence quenching (23).

First, we used TatBC-containing vesicles in which TatA was functionally inserted by *in vitro* translation. The identical *in vitro* translation conditions were then used for all TatA-NT constructs. Note that HiPIP was not fused in these experiments, as *in vitro* translated HiPIP does not assemble its iron-sulfur cofactor and thus cannot fold. This was irrelevant, as HiPIP was not required for TatA-NT stabilization under the *in vitro* conditions (Fig. 5, *B* and *D*). After optimization of the *in vitro* translations for the individual constructs, we could obtain quantitatively comparable amounts of all constructs inserted with surface-exposed C termini in the IMVs (Fig. 5, *B* and *D*). The constructs were quantified by the fluorescence of the Strep-Tactin Chromeo 488-conjugate. All constructs were stably integrated into the membrane (Fig. 5*F*). In the acridine orange assay, full-length TatA had only a slight effect on membrane stability (Fig. 5, *A* and *E*), which has been reported before (23). Quenching efficiency was determined as the percentage of quenching relative to the fluorescence level after carbonyl cyanide *m*-chlorophenyl hydrazone (CCCP)-induced fluorescence recovery. The effect of TatA-49 was comparable with TatA. Strikingly, TatA-NT strongly reduced the proton gradient that could be generated. TatA-33 and TatA-42 also showed a strong decrease in quenching efficiency that was slightly reduced but in the same range as TatA-NT. To assess whether the short length of the hydrophobic region in the TatA membrane

Control of membrane weakening by TatA

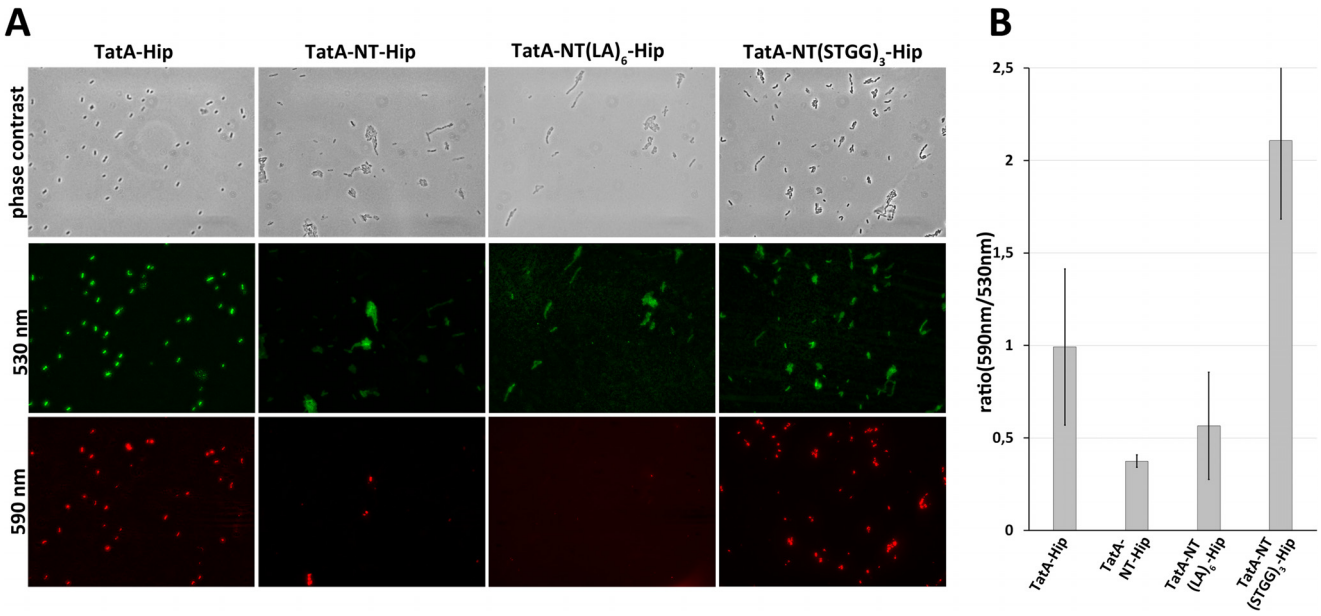

Figure 4. TatA-NT-Hip reduces the membrane potential. *A*, fluorescence microscopy of JC1 staining of JARV16 producing either TatA-Hip, TatA-NT-Hip, TatA-NT(LA)$_6$-Hip, or TatA-NT(STGG)$_3$-Hip. All constructs were Strep-tagged. Formation of red J-aggregates was strongly reduced in TatA-NT-Hip– and TatA-NT(LA)$_6$-Hip–producing cells. *B*, ratio of J-aggregates to JC1 monomers (590 nm/530 nm) of JARV16 producing the indicated TatA-NT-variant or TatA-Hip. Emission spectra were recorded with an excitation of 485 nm and emission from 500 to 650 nm. Ratios of peak maxima at 590 and 530 nm were calculated. *Error bars*, S.D.

anchor was responsible for this phenotype as it was in the *in vivo* assays, we tested also the TatA-NT(+6L) construct and found that the elongation of the hydrophobic helix by about 1.5 turns already resulted in clearly reduced membrane damage. We also checked whether the effect depended on the sequence of the TatA TMH using our TatA-NT(LA)$_6$ construct. Again in agreement with the *in vivo* data, we could observe a strong effect of the TatA-NT(LA)$_6$ on the acridine orange fluorescence quenching that was comparable with TatA-NT. We than asked the question of whether TatBC somehow contribute to the above described effects and performed the acridine orange quenching in IMVs derived from the *tat*-deficient *E. coli* strain DADE (31). As expected from the *in vivo* data, we found that TatBC did not play a role for the above described effects because the quenching efficiencies were comparable with the TatBC IMV data (Fig. 5, *C* and *E*). Again, the stable membrane insertion was confirmed (Fig. 5*F*). Together, these data demonstrate that the membrane anchor of TatA indeed can cause a TatBC-independent membrane defect that most likely relates to its very short length and not to its sequence, but in the longer TatA constructs, this defect is largely counterbalanced by the presence of the amphipathic helix and its neighboring charged region up to Lys^{49}.

A conformational switch of the APH in response to substrate binding

As full-length TatA as well as TatA-NT-49 clearly masked the membrane defects generated by its own membrane anchor, we considered a direct role of the APH in membrane stabilization during a resting state. NMR studies (32) and biochemical accessibility studies (33) already indicated that the APH of TatA can adopt a tilted orientation at the membrane surface. The APH could directly contribute to membrane thickness at the membrane-anchor sites. To address this aspect, we introduced rhodamine modifications into single-cysteine variants of TatA and checked their position relative to the membrane. Depending on the degree of exposure, the fluorescence of rhodamine can be quenched by added potassium iodide (KI). Titration of KI into the sample can be used to calculate the Stern–Vollmer constant (K_{SV}) for the individual rhodamine positions (see "Experimental procedures"). The higher this constant, the more solvent-exposed is the respective position. This method is a valuable and well-established tool to analyze protein accessibility in soluble and membrane-integral proteins (34, 35).

The positions for the rhodamine dye were chosen to address various aspects (Fig. 6*A*); position 2 faces the lumen of the IMVs and thus served as negative control. Within the TMH, we labeled positions 13, 16, 17, 18, and 19, the latter four covering a whole helical turn at the end of the hydrophobic transmembrane segment. Accessibility of this segment in any orientation to the aqueous surface in the course of substrate-induced conformational changes should thus become detectable. Dyes at positions 22, 23, 26, 27, 28, 32, 33, 34, 35, 42, and 45 cover the region from the hinge to the APH and an adjacent conserved negatively charged stretch. Position 51 served as positive control for quenching, as it is already positioned in an exposed region that is not required for functionality (25). Before carrying out the quenching experiments, we analyzed the functionality and membrane insertion of the selected single-cysteine variants in our *in vitro* translocation system with the model Tat substrate HiPIP (Fig. 6*B*). HiPIP is Tat exclusively transported due to the presence of a [4Fe-4S]$^{2+/3+}$ cluster (22). *In vitro* translated TatA completes the active translocon in TatB/TatC-containing membrane vesicles. Notably, although transport with reconstituted TatA was generally less efficient than trans-

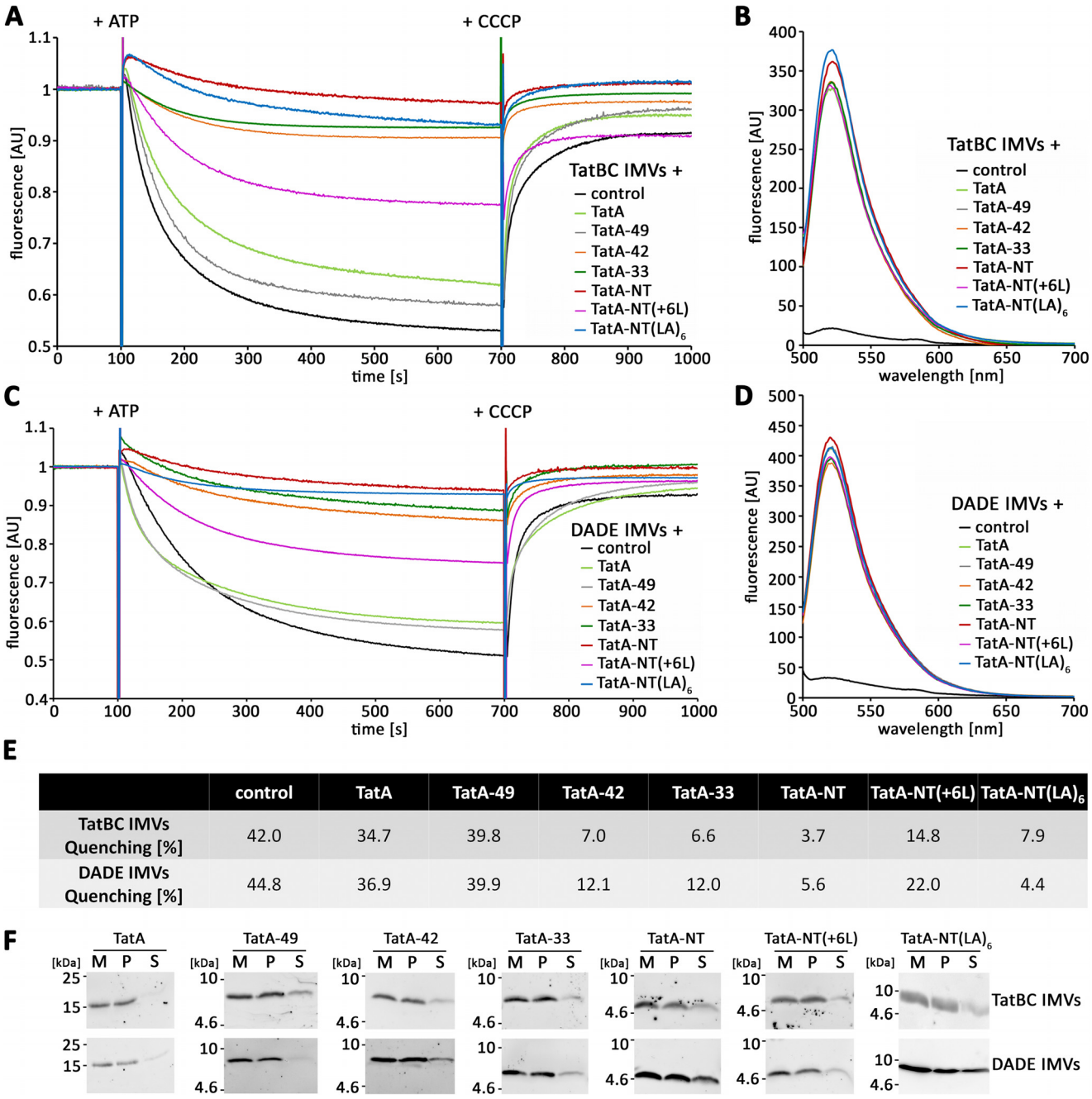

E

	control	TatA	TatA-49	TatA-42	TatA-33	TatA-NT	TatA-NT(+6L)	TatA-NT(LA)$_6$
TatBC IMVs Quenching [%]	42.0	34.7	39.8	7.0	6.6	3.7	14.8	7.9
DADE IMVs Quenching [%]	44.8	36.9	39.9	12.1	12.0	5.6	22.0	4.4

Figure 5. The short membrane anchor of TatA can cause membrane defects. *A* and *C*, acridine orange quenching of TatBC IMVs (*A*) or DADE IMVs (*C*) with the indicated reconstituted *in vitro* translated TatA variants. *B* and *D*, comparison of relative abundance of the membrane-inserted TatA constructs in the vesicles used for the quenching experiments in *A* and *C* via Strep-Tactin Chromeo 488 labeling and fluorescence spectroscopy. *E*, quantification of the data shown in the *traces below A* and *C*, as derived from the recovery of fluorescence after CCCP addition. *F*, Tricine-SDS-PAGE/Western blot analysis of carbonate washes of membrane inserted TatA variants in TatBC IMVs (*top*) or DADE IMVs (*bottom*). All constructs were Strep-tagged. Western blots were developed using Strep-Tactin-HRP and ECL detection. *M*, vesicle membranes; *P*, pellet after carbonate wash; *S*, supernatant after carbonate wash. *AU*, arbitrary units.

port with TatABC-containing membranes, most TatA single cysteine variants were active to a detectable extent and transported the model Tat substrate HiPIP. Only TatA-K23C, TatA-L32C, and TatA-G33C constructs were inactive. In agreement with this, these variants were already described to inactivate TatA function *in vivo* (37). The transport mediated by TatA-T22C was strongly affected, which similarly agrees with this *in vivo* study. For TatA-A42C, we noted transport of HiPIP *in vitro*, although we could confirm the reported block of TorA transport for that variant (37). The inability to support TorA transport may thus relate to the size or other specific properties of TorA. All cysteine variants of TatA were integrated into the membrane and thus resistant to carbonate wash treatment (Fig. 6*C*).

The KI-quenching data for these TatABC membrane vesicles with rhodamine-labeled TatA variants generated by *in vitro* translation supported the reported tilted position of the APH relative to the membrane surface (32) and indicated clear differences in solvent exposure along the APH (Fig. 6*D*, *dark columns*). In the resting state (*i.e.* in the absence of Tat substrates),

Control of membrane weakening by TatA

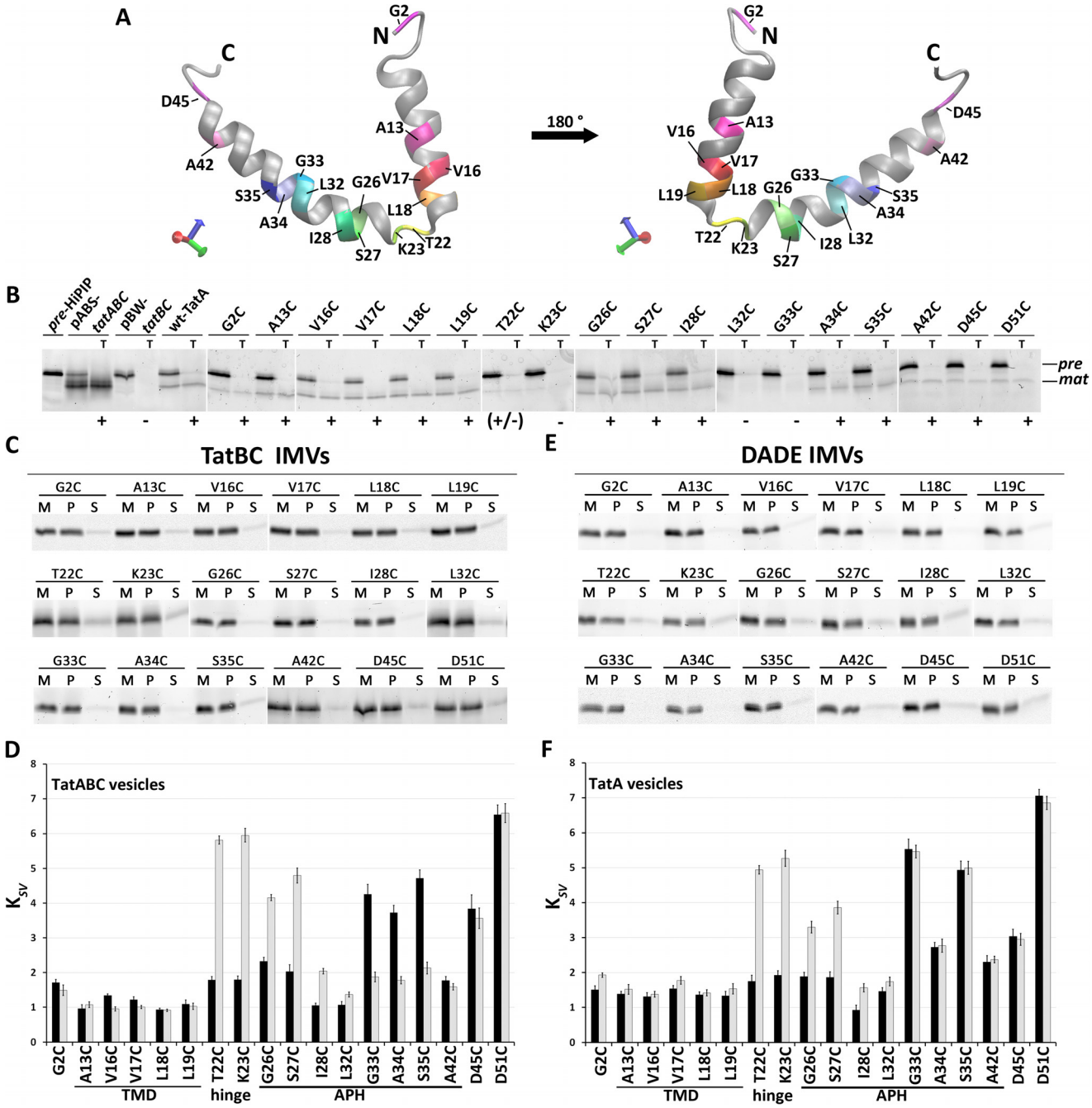

Figure 6. Quencher accessibility assays indicate a conformational switch of the APH upon substrate binding. *A*, TatA structural model (based on Protein Data Bank entry 2MN7 (21)), indicating positions of analyzed labels. Position Asp[51] was not in the structure. *B*, *in vitro* HiPIP transport assays with *in vitro* translated WT TatA and TatA variants mutated at the indicated positions. All constructs were Strep-tagged. Transport assays with IMVs generated from MC4100 pABS-*tatABC* (pABS-*tatABC*) and with IMVs lacking TatA are shown as controls. *T*, lanes with thermolysine-digested IMVs after transport. Fluorescein-labeled HiPIP was used, and fluorescence of the precursor (*pre*, at ~14 kDa) and mature (*mat*, at ~10 kDa) forms was detected after SDS-PAGE (see "Experimental procedures"). Functional (+) and nonfunctional (−) transport are indicated. *C* and *E*, analysis of carbonate washes of TatBC IMVs (*C*) or DADE IMVs (*E*) with the reconstituted rhodamine-labeled TatA constructs. Rhodamine fluorescence was detected at ~17 kDa after SDS-PAGE. *M*, membrane fraction before carbonate wash; *P* and *S*, pellet and supernatant fractions after carbonate wash. *D* and *F*, K_{SV} values at the indicated positions for TatABC IMVs, in which TatBC-containing membranes were used for TatA insertion by *in vitro* translation (*D*), or for IMVs containing no TatBC and only *in vitro* translated TatA (F). Quenching results from experiments without substrate are shown as *black columns*, and results after the addition of 2 μM HiPIP precursor are shown in *gray columns*. *Error bars*, S.D.

the APH intrudes into the membrane with its N-terminal half, as reflected by the low K_{SV} values. This N-terminal region of the APH therefore appears to contribute to the thickness of the membrane at the position of the membrane anchor, thereby counterbalancing the membrane stress of the short membrane anchor. As expected for a transmembrane domain, the positions in the TMH of the membrane anchor were highly protected, indicating little or no access of the quencher KI. Beginning with the flexible and highly conserved Gly[33] position (1), the APH was more surface-exposed with the exception of Ala[42].

We then assessed potential effects of substrate binding by adding fully folded HiPIP precursor (Fig. 6*D*, *gray columns*).

The most striking effect was a switch of the N-terminal half of the APH to a highly accessible, surface-exposed orientation. Also, the hinge region that connects the membrane-anchor with the APH moved to a surface-exposed position. In contrast, the rhodamine at positions 33, 34, and 35 became protected from quencher, and at positions 42, 45, and 51 the substrate addition had no effect. Together, the data thus indicate that the environment of the APH switches upon substrate interaction with the TatABC system. It is interesting that we did not detect any quencher accessibility to the transmembrane domain after substrate binding, although we have placed rhodamine dyes at four succeeding positions (positions 16–19) that cover a complete turn and thus all orientations of the membrane-spanning α-helix. Substrate binding thus does not seem to influence solvent accessibility of the TMH of TatA. It is also interesting that the region close to the very C terminus of the APH was not influenced by substrate binding.

Because it is known that TatA *per se* can interact with Tat substrates (26), we considered that TatA alone might already be able to make this switch. We thus carried out the same assays in the absence of other Tat components (IMVs prepared from the *tatABCD-tatE* deletion strain DADE). Again, all constructs were carbonate-resistantly membrane-integrated (Fig. 6*E*). The result was partially very similar (Fig. 6*F*); as in the case of membranes with complete TatABC systems, TatA alone showed a clear protection of the N-terminal half of the APH, suggesting a contribution to membrane thickness at the site of the TatA membrane anchor. Also as in the case of complete Tat systems, substrate binding resulted in a reorientation of the hinge and N-terminal half of the APH to a more surface-exposed position. However, in contrast to the observations in the complete TatABC system, positions 33–35 of the APH did not change their accessibility significantly when TatB and TatC were absent. It thus appears that from Gly^{33} on, there are no TatBC-independent changes in response to substrate binding, and therefore (i) there is probably flexibility at or near Gly-33, and (ii) the protection of Gly^{33}–Ser^{35} upon substrate binding to TatABC systems depends on TatBC (see "Discussion"). Interestingly, in the absence of substrate, position 34 is somewhat less exposed with TatA alone than in the presence of TatBC, which might relate to a pre-existing TatBC interaction around Ala^{34}, which is the region where we see the only TatBC effects. With respect to the method, it can be concluded that the use of single rhodamine dyes for fluorescence labeling did not interfere with a substrate-induced switch in the region from position 22 to 28, and it also permitted TatBC-dependent changes at positions 33–35.

Substrate-induced membrane destabilization by TatA

As TatA alone already showed the switch with respect to the N-terminal half of the APH, it was possible that some substrate-induced membrane weakening could be already detectable in the absence of TatBC. We thus carried out acridine orange fluorescence quenching with TatA IMVs that were either preincubated with Tat substrate precursor or mock-treated (Fig. 7). The results showed a reduced fluorescence quenching when Tat substrate was present, suggesting that indeed the above described reorientation of the APH in response to substrate

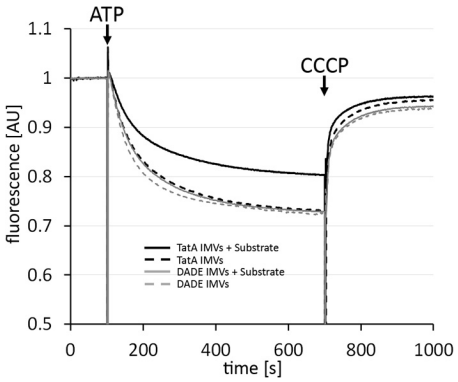

Figure 7. Substrate association with TatA alone can already affect membrane stability. Acridine orange fluorescence quenching with TatA IMVs without or with preincubation with 2 μM HiPIP precursor was performed. As control, the same experiment has been also carried out with IMVs from strain DADE (no Tat component), which demonstrates that HiPIP precursor has only a very weak effect in the absence of TatA. Time points of ATP and CCCP additions are indicated. All constructs were Strep-tagged. *AU*, arbitrary units.

interactions results in a measurable destabilization of IMVs. As it was in principle possible that Tat substrates alone already destabilized the membranes due to their reported lipid bilayer interaction (38–40), we carried out the same experiments with IMVs prepared from the Tat-deficient strain DADE. Notably, the preincubation of DADE IMVs with HiPIP precursor had no effect on the degree of fluorescence quenching in the assay, demonstrating that the effects were only due to substrate-TatA interactions and not due to a Tat-independent membrane interaction of Tat substrate.

Discussion

Substrate-induced reorientation of TatA amphipathic helices coincides with the induction of membrane defects at Tat translocation sites

We herein report a possible mechanism to induce local membrane stress on demand for Tat-dependent protein translocation. The N-terminal transmembrane domain of TatA can in principle generate membrane defects, but full-length TatA counterbalances these deleterious effects in the absence of Tat substrates. These conclusions are based on *in vivo* and *in vitro* approaches that demonstrate energization deficiencies of cells and membrane vesicles in response to the TatA constructs that are shorter than TatA-49. It thus is clear that the APH (~Lys^{24}–Met^{43}) and most likely also the highly charged adjacent region (Asp^{45}–Lys^{49}) are counterbalancing detrimental effects of the TMH. This fully agrees with the minimally required length for TatA functionality as determined by *in vivo* studies (25).

The short length of the TMH is probably the reason for the destabilization, as this domain alone can reduce membrane energization, and this effect depends on the short length (Figs. 1, 2, 4, and 5). An elongation by 1½ helical turns markedly reduces the inhibitory effect (Figs. 3 and 5). The exact sequence of the TMH is not relevant, as an artificial TMH in TatA-NT-$(LA)_6$ had the same effect (Figs. 3–5). This fits to the recent observation that the exact sequence of that region is not a determinant for function, as it can be exchanged between *E. coli* and thylakoid systems (41). Our data now experimentally show the postulated membrane weakening by the unusual TMH of TatA

(18), which was so far supported by molecular dynamics simulations (6). In this TMH, only 12 hydrophobic residues cross the lipid bilayer. Notably, a stretch of 12 hydrophobic residues, although very short, is sufficiently long for a complete membrane integration of a peptide by the Sec61 translocon in eukaryotes (42).

A membrane-weakening as the basis for Tat transport would need to be transient and local. The Tat system needs to minimize constitutive membrane stress under "resting" conditions (*i.e.* when no substrate is present to be transported). According to our data, this can be in principle achieved by the influence of the substrate-dependent orientational switch of the APH. TatA alone is able to achieve the counterbalancing of membrane weakening (Fig. 7). The N-terminal part of its APH can immerge into the lipid bilayer in the absence of substrate, and it becomes surface-exposed in response to added substrate. TatA can thus sense and respond to substrate already in the absence of TatBC.

What drives the conformational switch?

One important question is the understanding of the driving force for the reorientation of the APH in response to substrate. We have recently demonstrated that TatA can interact with Tat substrates in a signal peptide– dependent, RR-independent manner (26). In that study, also molecular dynamics simulations were carried out that indicated intensive contacts between the APH of TatA and mainly the C-domain of the signal peptide. This fully agrees with the fact that the RR motif is not recognized by TatA (26).

Molecular dynamics simulations of TatA in membranes suggest that only oligomeric TatA assemblies can destabilize the membrane (6). As we see a membrane destabilization, substrate binding therefore probably induces the conformational switch of TatA that is organized in clusters. These clusters may transiently form or pre-exist at TatBC. TatA alone can also destabilize membranes, and it is therefore likely that the known TatBC-independent TatA clusters (43) can already associate with substrate. The group of Ken Cline (12, 44, 45) demonstrated in seminal studies substrate-induced TatA-TatBC and TatA-TatA cross-links that can be explained by TatA recruitments, rearrangements, or conformational transitions. Later, a substrate-induced conformational transition of the APH that is similar to the one that we now show for the *E. coli* system had been clearly demonstrated for the thylakoid system by Aldridge *et al.* (33). The data of that study are largely consistent with our data, and in this study, it was already hypothesized that a moved APH could induce a membrane weakening. We now provide experimental evidence for such a membrane destabilization and relate this to a substrate-induced conformational change that restricts the membrane thickness to the short length of the TMH, which is probably the physiological function. As the switch of the APH conformation is a consequence of a substrate interaction, the APH itself is the most likely interaction site. An APH interaction with mature domains of Tat substrates had been for the first time experimentally demonstrated by the group of Carole Dabney-Smith (46) for the thylakoidal system. Also, in the *E. coli* system, mature domains of Tat substrates have been shown to interact with TatA (16, 47–49), and it has been demonstrated that TatA has the capacity to interact with Tat substrates in a TatBC-independent manner (26). For the thylakoid system, it has been suggested that the APH interactions relate to nonspecific passive contacts before or during the membrane passage of mature domains, as a cross-link to a position at the end of the APH (Phe^{48}) was TatB- and proton-motive force-dependent (46). In agreement with the thylakoidal system data, we also found no substrate effects at the C-terminal end of the APH in the absence of TatBC (Fig. 6*F*). The APH thus most likely binds Tat substrates around the N terminus of the APH, as evidenced by large changes in response to substrate addition in that region (Thr^{22}–Ile^{28}) in the presence as well as in the absence of TatBC (Fig. 6, *D* and *F*). Three of all analyzed positions were inactivated by their exchange to cysteine. The accessibility assays with these positions were nevertheless similar to neighboring positions, and effects were detected in response to substrate (K23C) or TatBC (G33C). Most likely, the absence of unexpected effects for these positions can be explained by the fact that the accessibility assays are end point measurements that do not monitor transport kinetics or overall functionality. If, for example, an exchange slows an important movement by 3 orders of magnitude from a millisecond to a second range, which would be a virtual block of transport, the assay would not differentiate this and recognize the movement. It also could be that the reversibility of a movement can be affected by inactivating mutations. We consider both options but favor the kinetic argumentation. The data thus can be carefully taken, and they agree with the overall conclusions.

In conclusion, we propose that the interaction of Tat substrates with the APH induces the conformational switch most likely by rearranging the APH-APH interactions in TatA clusters. Future studies will hopefully clarify this aspect.

The involvement of TatBC-independent steps in Tat transport is not unexpected

It has been believed for a long time that all Tat transport is initiated by an interaction of the signal peptide twin-arginine motif with TatBC and that TatA is recruited thereafter. This view is currently challenged by the observation that TatA has binding sites at "resting" TatBC complexes (50, 51) and that TatA can be co-purified with TatBC equally well when the substrate-binding site of TatC is inactivated (52). The initial experimental evidence for a transient recruitment of TatA to TatBC upon substrate binding to TatBC is based on cross-link data that may also have resulted from rearrangements of TatA at TatBC upon substrate binding (12, 44, 45). Other lines of evidence come from TatA that has been labeled with fluorescent protein (XFP) tags (53, 54). The problem of these approaches is that the dissociation of such TatA-XFP fusions from TatBC could be triggered by the ~26-kDa XFP tag attached to the 9.6-kDa TatA. In agreement with this, it has been observed that TatA-YFP was functionally inactive, and activity could be only re-established by co-production of nontagged TatA or TatE (54). Substrate binding might influence the affinity of TatBC for TatA, as mutations that enhance the affinity of TatBC to Tat substrates show a constitutive TatA-YFP/TatBC interaction (55). An increased affinity of TatBC for TatA could therefore compensate for XFP-tag effects. The transient recruitment of

nontagged TatA to TatBC thus remains to be shown. Based on the substrate-independent TatA/TatBC interactions, we currently favor the view that TatA and TatBC always function hand in hand and remain in close proximity.

The RR motif of Tat signal peptides can remain associated with TatC during translocation (15), and Tat substrates are contacting TatA during transport with their mature domains (26, 46, 49). TatA recognizes the transported domains to initiate the conformational switch, but TatBC recognizes the RR motif, and transport is only achieved when both activities cooperate. As TatA and TatBC act synergistically on distinct regions of the transported substrate, it is not surprising that the individual TatA/Tat substrate interaction does not require an RR recognition. It would be delusive to neglect the TatBC-independent TatA interactions; the membrane destabilization appears to rely on them.

TatBC alters the accessibility of a specific region of the APH in the presence of Tat substrate

As TatA and TatBC cooperate for Tat transport, it is important to recognize that we could detect an influence of TatBC on the accessibility of TatA regions. The main difference between the observations with TatA vesicles *versus* TatABC vesicles is related to the $Gly^{33}/Ala^{34}/Ser^{35}$ region of the APH. Whereas the accessibility of this region is essentially unaltered upon substrate interaction in the absence of TatBC, this region becomes protected upon substrate interaction in the presence of TatBC, suggestive of a TatBC "footprint" on the TatA APH that indicates a steric hindrance of solvent accessibility by a TatBC-dependent environment. This may be (i) TatBC itself, which changes conformation upon substrate binding, or it may be (ii) the substrate, which might tightly associate with this region of the TatA-APH. Both scenarios are conceivable, and a direct substrate interaction with the APH has been already demonstrated (46). Also, the substrate-induced accessibility differences that have been detected in the thylakoid system were considered to potentially indicate a steric hindrance by substrate (33). In this context, one significant difference of our data from the data reported by Aldridge *et al.* (33) may be highly important; the movement of the hinge region preceding the APH was not detected in that study. We think that this difference is caused by the much larger size of the modifying agent (methyl-$PEG_{12})_3$-PEG_4-maleimide (2360 Da) that had to be used to detect modifications by shifts in SDS-PAGE analyses. We used iodide ions (127 Da), which can access positions that are sterically inaccessible for larger molecules. It is tempting to speculate that the substrate is positioned on top of the hinge region, ready to be transported, and thereby reduces the accessibility for larger agents.

In summary, we propose the following mechanism of membrane destabilization and counterbalancing (Fig. 8). The hydrophobic region of the TatA membrane-anchor is very short and destabilizes the membrane if the N-terminal region of the APH does not immerse into the membrane and thereby elongates the membrane-spanning section. Full-length TatA controls this membrane destabilization with its APH, whose N-terminal region is able to switch its orientation in response to substrate association. This switch restricts membrane thickness to the length of the TMH, which results in a membrane destabilization on demand that can be demonstrated by substrate-induced proton leakage *in vitro*. The essential role of TatBC as translocon core and motor is not called into question by the membrane-weakening role of TatA. Future experiments will surely clarify these aspects, leading to a deeper understanding of the translocation mechanism.

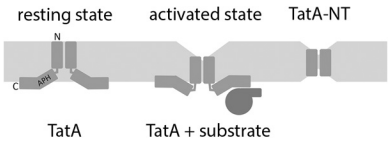

Figure 8. A model for the generation of substrate-induced membrane stress at Tat translocons. Whereas the APH of TatA contributes to membrane thickness in a resting state (*left*), substrate binding causes a conformational switch that reduces membrane thickness (*middle*). The N-terminal transmembrane domain of TatA alone (TatA-NT) destabilizes membranes by membrane thinning (*right*). See "Discussion" for details.

Experimental procedures

Strains and growth conditions

E. coli strain MC4100 and indicated derivatives thereof were used for growth experiments and *in vitro* studies, and *E. coli* XL1-blue was used for cloning. Strains were grown aerobically at 37 °C in LB medium (1% tryptone, 1% NaCl, 0.5% yeast extract) in the presence of 100 μg/ml ampicillin. For growth curves, 25-ml cultures were inoculated with OD_{600} of 0.1 and grown aerobically. The OD_{600} was determined in 30-min intervals. For induction of gene expression, 0.1% rhamnose was added after 90 min.

Genetic methods and plasmids

All constructs used in this study were Strep-tagged for their detection. Construction of pBW-*tatA-strep* and pBW-*tatA-NT-mhip-strep* were described elsewhere (23). pBW-*tatA*-33-*strep*, pBW-*tatA*-42-*strep*, and pBW-*tatA*-49-*strep* were cloned via standard methods with forward primer *tatA*-NdeI-F (5′-TCT TCT CAT ATG GGT GGT ATC AGT ATT TGG C-3′) and the corresponding reverse primer *tatA*(G33)-BamHI-R (5′-TTA AAG GAT CCA CCA AGA TCG GAA CCG ATG G-3′), *tatA*(A42)-BamHI-R (5′-TTA AAG GAT CCT GCT TTT TTA AAG CCT TTG ATC G-3′), or BamHI-*tatA*(K49)-R (5′-GAC GGA TCC CTT TGG TTC ATC ATC GCT C-3′), respectively. *mhip* fusions were cloned via BglII/BamHI, and pBW-*tatA-NT-strep* were cloned using pBW-*tatA-strep* with an additional BamHI site after G21 (23), cut with BamHI, and religated. pBW-*tatA*-NT$(STGG)_3$-*mhip-strep*, pBW-*tatA-NT*$(LA)_6$-*mhip-strep*, and pBW-*tatA*(9 + 6L)-*mhip-strep* were constructed using pBW-*tatA-NT-mhip-strep* as template and forward primers NdeI-*tatA-NT*-$(LA)_6$-*mhip*-F (5′-TAG CCA TAT GGG TGG TAT CAG TAT TTG GCA GTT AGC GCT TGC ATT GGC ACT GGC TCT CGC GCT TGC AGG CAC CAA AAA GCT CGG CTC CAT CGG-3′), NdeI-*tatA-NT*-$(STGG)_3$-*mhip*-F (5′-ATA TAC ATA TGG GTG GTA TCA GTA TTT CGA CGG GTG GGG GCA GTA CGG GTG GCG GGA GTA CGG GTG GGG GCT CCG CTC CCG CCA ATG CCG TGG CC-3′), and NdeI-*tatA-NT*(+6L)-F (5′-AAG TAC ATA TGG GTG GTA TCA GTA TTT GGC AGC TGC TCT TAC TGT TGC TGT TAT TGA TTA TTG CCG TCA TC-3′)

together with reverse primer *hip*-BamHI-R (5′-ATA TAT AGG ATC CGC CGG CCT TCA GGG TC-3′) for amplification. PCR products were cut with NdeI/BamHI and cloned in the corresponding sites of pBW-*tatA-NT-mhip-strep*, thereby exchanging the fragment. All constructs were verified via restriction analysis and sequencing.

For *in vitro* transcription and translation, the *tatA* gene or the Strep-tagged N-terminal membrane anchor–encoding sequence of TatA were cloned into pGEM-5Zf (Promega) using the forward primer *tatA*-NdeI-F (5′-TCT TCT CAT ATG GGT GGT ATC AGT ATT TGG C-3′) in combination with *tatA*-PstI-R (5′- GGA CTG CAG TTA CAC CTG CTC TTT ATC GTG-3′) and *tatA-NTstrep*-PstI-R (5′-GAC TGC AGT TAT TTT TCG AAC TGC GGG TGG CTC CAG GTG CCA AAA AGC AGT ACA AC-3′), resulting in pGEM-*tatA* or pGEM-*tatA-NTstrep*. For the construction of the pGEM-5Zf–based *in vitro* transcription system for *tatA*-NT(+6L), primers NdeI-*tatA-NT*(+6L)-F and *tatA-NTstrep*-PstI-R were combined for PCR, and the product was cloned into the corresponding sites of pGEM-5Zf. For the construction of *tatA*-33-*strep*, *tatA*-42-*strep* and *tatA*-49-*strep in vitro* transcription vectors, the corresponding pBW-*tatA*-33-*strep*, pBW-*tatA*-42-*strep* and pBW-*tatA*-49-*strep* vectors were digested with NdeI/SalI, and the fragments were cloned into the corresponding sites of pGEM-5Zf. The indicated codon mutations in *tatA* were introduced into pGEM-*tatA* by QuikChange mutagenesis (Stratagene). All constructs were confirmed by sequencing.

General biochemical methods

SDS-PAGE and subsequent Western blotting were carried out by standard procedures (56, 57). For small proteins, Schägger gels (16% T, 6 M urea) were performed as described elsewhere (58). Western blots were developed employing specific HiPIP antibodies, Strep-Tactin-AP, or Strep-Tactin-HRP conjugate as indicated according to the manufacturer's instructions (IBA, Göttingen, Germany). Images of Western blots were acquired utilizing the Intas Advanced Imager (INTAS Science Imaging Instruments GmbH, Göttingen, Germany).

For all *in vivo* experiments, Strep-tagged TatA constructs were produced using pBW22-based plasmids (23, 59). For preparation of proteins, cell fractionation experiments, and carbonate washes, 100-ml cultures of *E. coli* JARV16 were inoculated with an OD_{600} of 0.1, and pBW22-based protein production was induced after 90 min when cell densities reached an OD_{600} of ~0.6. After 3 h, cells were harvested, and cell densities were normalized to an OD_{600} of 1 before centrifugation of a 100-ml culture at 4500 × *g* for 10 min at 4 °C. Cells were resuspended in 2 ml of homogenization buffer (50 mM Tris-HCl, pH 8, 250 mM NaCl). 1 mM PMSF and DNase I were added, and cells were homogenized via French press (2 passages, 800 p.s.i.). After homogenization, cell debris was removed by centrifugation for 10 min at 20,000 × *g* at 4 °C. For cell fractionation, membranes were sedimented by ultracentrifugation at 130,000 × *g* for 30 min at 4 °C of one-half of the crude extract. Supernatant (soluble fraction) and membranes (resuspended in 1 volume of homogenization buffer) were analyzed by SDS-PAGE/Western blotting. For carbonate washes, the second half of the crude extract was used and also centrifuged at 4 °C for 30 min at 130,000 × *g*. The supernatant was carefully discarded, and crude membranes were resuspended with ice-cold 100 mM Na_2CO_3. After a second centrifugation step at 4 °C for 30 min at 130,000 × *g*, the supernatant was removed, and washed membranes were resuspended in 1 volume of 100 mM Na_2CO_3 again. All fractions were analyzed with SDS-PAGE/Western blotting. For JC1 staining, *E. coli* strain JARV16 was used. 25-ml cultures were inoculated with an OD_{600} of 0.05, and protein production was induced by adding 0.2% rhamnose directly after inoculation. When the maximum expression level was reached after 3 h, cells were harvested, and the density was normalized to 1 ml of OD_{600} = 1. After centrifugation at 3000 × *g* for 10 min, cell pellets were resuspended in 0.5 ml of TEG staining buffer (10 mM Tris-HCl, pH 7.5, 1 mM EDTA, 10 mM glucose) complemented with 0.1% (v/v) JC1 (5 mg/ml JC1 stock solution) and incubated for 30 min in the dark on a roller. Cells were sedimented again by centrifugation and washed in 2 volumes of TEG buffer without dye. After centrifugation, cells were resuspended in 1 volume of TEG buffer, and 2 μl of the cell suspension were spotted on an agar slide for fluorescence microscopy. Cells were imaged by fluorescence microscopy, using a Zeiss AxioImager M2 microscope equipped with an AxioCam MRm camera and a Zeiss ×100/numeric aperture 1.3 EC Plan-Neofluar objective. For quantification of JC1 fluorescence, 100 μl of the washed cell suspension were added to 1.4 ml of TEG buffer and transferred into a cuvette. Fluorescence emission spectra were recorded from 500 to 650 nm with an excitation at 485 nm, using the JASCO FP-6500 spectrofluorometer (Jasco International Co., Ltd., Tokyo, Japan). Spectra were analyzed, and 590 nm/530 nm ratios were calculated using JASCO Spectra Manager software.

In vitro translocation assays were carried out as described previously (60). As translocation substrate, we used a T61C variant of the HiPIP precursor, which was fluorescence-labeled by modification of the cysteine with fluorescein-5-maleimide using standard protocols for maleimide coupling (61). HiPIP precursor was refolded from inclusion bodies and purified as described previously (36). For *in vitro* transcription, the *tatA* or *tatA-NTstrep* regions in the corresponding pGEM constructs were amplified using the pGEM-recognizing primers pGEM-5-F (5′-CCC AGT CAC GAC GTT GTA AAA CG-3′) and pGEM-5-R (5′-CTT CCG GCT CGT ATG TTG TG-3′), and the purified PCR product was used as template for SP6 RNA polymerase according to the supplier's protocol (New England Biolabs). Translation was done according to standard protocols (62).

In vitro reconstitution of cysteine-labeled TatA into inverted membrane vesicles

Fluorescence-labeled TatA variants were inserted into IMVs prepared from *E. coli* strain DADE/pBW-*tatBC* (52) by employing wheat germ extract–based *in vitro* translation according to the protocol of Lin *et al.* (62), but in the presence of IMVs (A_{280} = 4) and with 600 pmol/ml tetramethylrhodamine (TMR)-cysteine-$tRNA^{Cys}$.

For preparation of TMR-cysteine-$tRNA^{Cys}$, uncharged $tRNA^{Cys}$ was partially purified from bakers' yeast tRNA (Sigma) using a Mono Q 5/50 GL (GE Healthcare) strong anion

exchanger. 5 mg of bakers' yeast tRNA dissolved in 1 ml of Buffer A (20 mM HEPES, 0.26 M NaCl) was applied on the column equilibrated with the same buffer, and tRNAs were eluted by a linear 0.26–1 M NaCl gradient over 40 ml, and 1-ml fractions were collected. The $tRNA^{Cys}$ was predominately eluted at 0.5 M NaCl with a yield of ~250 μg/ml (~10 μM). Ethanol-precipitated $tRNA^{Cys}$ was then subjected to aminoacylation with cysteine. A 2-ml aminoacylation reaction contained 250 μg of $tRNA^{Cys}$, 1 mM L-cysteine, 100 mM HEPES, pH 8.0, 10 mM $MgSO_4$, 10 mM KCl, 2 mM DTT, 4 mM ATP, 100 mM CTP, and 200 μl of *E. coli* S-100 fraction (36), and the reaction was incubated at 37 °C for 90 min. After phenolization and ethanol precipitation, the charged Cys-$tRNA^{Cys}$ was rechromatographed as before. Aminoacylation caused almost no difference on the elution of $tRNA^{Cys}$. To reduce the possibly oxidized thiol group of Cys, 10 mM DTT was added to the elution fractions. The fraction containing Cys-$tRNA^{Cys}$ was dialyzed twice against 1 liter of degassed 50 mM KH_2PO_4/K_2HPO_4, pH 7.3, 100 mM NaCl for 1 h in a cold room, and the recovered Cys-$tRNA^{Cys}$ was labeled with TMR by the addition of 1 mM TMR-5-maleimide (Sigma) for 30 min at 20 °C. Afterward, the unreacted TMR-5-maleimide was quenched by 2 mM DTT and dialyzed against Buffer A at 4 °C. The TMR-Cys-$tRNA^{Cys}$ was purified by chromatography as before, and the elution fractions containing fluorescent TMR-Cys-$tRNA^{Cys}$ were combined and ethanol-precipitated. TMR-Cys- $tRNA^{Cys}$ was stored at −80 °C.

IMVs with fluorescence-labeled TatA were applied onto a 500-μl 0.5 M sucrose cushion and sedimented for 30 min at 130,000 × *g* and 4 °C to remove soluble compounds. After washing with IMV buffer (0.25 M sucrose, 20 mM HEPES, pH 7.5, 1 mM DTT), the IMVs were suspended in 200 μl of buffer.

Rhodamine collisional fluorescence-quenching assay

To examine collisional quenching of rhodamine fluorescence at specific TatA positions, IMVs containing TMR-labeled TatA were suspended in 1.5 ml of IMV buffer to a final concentration of A_{280} = 2. TMR emission intensity was measured at λ_{ex} = 543 nM and λ_{em} = 575 nm on a JASCO FP-6500 spectrofluorometer with constant stirring. Fluorescence intensity was averaged from five successive 5-s integrations. The quencher KI was then added from a 4 M stock solution to final concentrations of 10, 20, or 40 mM, and the respective emission intensities were continually recorded. Data were analyzed using the Stern–Volmer equation, $(F_0/F) - 1 = K_{SV}$ [Q], where F_0 is the net emission intensity in the absence of quencher, [Q] is the concentration of quencher, F is the net emission intensity at [Q], and K_{SV} is the Stern–Volmer constant. A linear dependence of quenching ($(F_0/F) - 1$) on [Q] indicates direct proportionality as expected for collisional quenching. K_{SV} corresponds to the slope of a linear least-squares best fit to the data points in which the line is constrained to go through the origin.

Acridine orange fluorescence-quenching assays

Acridine orange fluorescence-quenching assays were performed on the JASCO spectrofluorometer. A 1.5-ml reaction mixture contained IMVs (A_{280} = 2) in SHM buffer (250 mM sucrose, 10 mM HEPES, pH 7.5, 5 mM $MgSO_4$), 25 mM creatine phosphate, 50 μg/ml creatine phosphate kinase, and 2 μM acridine orange. The mixture was incubated in a cuvette at 20 °C in the dark with constant stirring, and acridine orange fluorescence was measured in a time-course manner at λ_{ex} = 494 nm and λ_{em} = 540 nm. After 100 s, acridine orange quenching was induced by the addition of 1.25 mM ATP, and the measurement was continued for another 600 s. 3 μl of 5 mM CCCP was then added to the cuvette to abolish the proton gradient, and the change of the acridine orange fluorescence intensity was recorded for another 300 s.

Fluorospectrometric estimation of relative recombinant protein concentration in membranes

TatA and its variants used in acridine orange assays possess a C-terminal Strep-tag that is exposed to the outside of the IMVs. Relative amounts of membrane-targeted Strep-tagged protein could therefore be estimated by use of fluorescence-labeled Strep-Tactin. 3 μl of 0.5 mg/ml Strep-Tactin Chromeo 488 (IBA Lifesciences) was added to 50 μl of IMVs (A_{280} = 20) harboring *in vitro*–translated TatA-strep and its variants. After incubation at room temperature for 30 min with shaking, the IMVs were purified by sedimentation at 130,000 × *g* for 30 min through a 0.5 M sucrose cushion. IMVs were washed once with SHM buffer and resuspended in 1.5 ml of SHM buffer. Using an excitation wavelength at 488 nm, the relative fluorescence of IMV-bound Strep-Tactin Chromeo 488 was determined at 520 nm.

Author contributions—B. H. performed the *in vitro* assays, E. S. H. performed the *in vivo* experiments, and D. M. performed experiments in early stages of the project. All authors analyzed the data. E. S. H. and T. B. prepared figures, and T. B. conceived and coordinated the study and wrote the paper. All authors reviewed the results and approved the final version of the manuscript.

Acknowledgments—We thank Sybille Traupe and Inge Reupke for technical support.

References

1. Hou, B., and Brüser, T. (2011) The Tat-dependent protein translocation pathway. *Biomol. Concepts* **2,** 507–523 Medline
2. Natale, P., Brüser, T., and Driessen, A. J. (2008) Sec- and Tat-mediated protein secretion across the bacterial cytoplasmic membrane–distinct translocases and mechanisms. *Biochim. Biophys. Acta* **1778,** 1735–1756 CrossRef Medline
3. Palmer, T., and Berks, B. C. (2012) The twin-arginine translocation (Tat) protein export pathway. *Nat. Rev. Microbiol.* **10,** 483–496 CrossRef Medline
4. Carrie, C., Weissenberger, S., and Soll, J. (2016) Plant mitochondria contain the protein translocase subunits TatB and TatC. *J. Cell Sci.* **129,** 3935–3947 CrossRef Medline
5. Goosens, V. J., Monteferrante, C. G., and van Dijl, J. M. (2014) The Tat system of Gram-positive bacteria. *Biochim. Biophys. Acta* **1843,** 1698–1706 CrossRef Medline
6. Rodriguez, F., Rouse, S. L., Tait, C. E., Harmer, J., De Riso, A., Timmel, C. R., Sansom, M. S., Berks, B. C., and Schnell, J. R. (2013) Structural model for the protein-translocating element of the twin-arginine transport system. *Proc. Natl. Acad. Sci. U.S.A.* **110,** E1092–E1101 CrossRef Medline
7. Behrendt, J., Standar, K., Lindenstrauss, U., and Brüser, T. (2004) Topological studies on the twin-arginine translocase component TatC. *FEMS Microbiol. Lett.* **234,** 303–308 CrossRef Medline
8. Rollauer, S. E., Tarry, M. J., Graham, J. E., Jääskeläinen, M., Jäger, F., Johnson, S., Krehenbrink, M., Liu, S.-M., Lukey, M. J., Marcoux, J., McDowell,

M. A., Rodriguez, F., Roversi, P., Stansfeld, P. J., Robinson, C. V., *et al.* (2012) Structure of the TatC core of the twin-arginine protein transport system. *Nature* **492,** 210–214 CrossRef Medline
9. Bolhuis, A., Mathers, J. E., Thomas, J. D., Barrett, C. M., and Robinson, C. (2001) TatB and TatC form a functional and structural unit of the twin-arginine translocase from *Escherichia coli*. *J. Biol. Chem.* **276,** 20213–20219 CrossRef Medline
10. Richter, S., and Brüser, T. (2005) Targeting of unfolded PhoA to the TAT translocon of *Escherichia coli*. *J. Biol. Chem.* **280,** 42723–42730 CrossRef Medline
11. Cline, K., and Mori, H. (2001) Thylakoid ΔpH-dependent precursor proteins bind to a cpTatC-Hcf106 complex before Tha4-dependent transport. *J. Cell Biol.* **154,** 719–729 CrossRef Medline
12. Dabney-Smith, C., Mori, H., and Cline, K. (2006) Oligomers of Tha4 organize at the thylakoid Tat translocase during protein transport. *J. Biol. Chem.* **281,** 5476–5483 CrossRef Medline
13. Blümmel, A.-S., Haag, L. A., Eimer, E., Müller, M., and Fröbel, J. (2015) Initial assembly steps of a translocase for folded proteins. *Nat. Commun* **6,** 7234 CrossRef Medline
14. Hauer, R. S., Schlesier, R., Heilmann, K., Dittmar, J., Jakob, M., and Klösgen, R. B. (2013) Enough is enough: TatA demand during Tat-dependent protein transport. *Biochim. Biophys. Acta* **1833,** 957–965 CrossRef Medline
15. Gérard, F., and Cline, K. (2006) Efficient twin arginine translocation (Tat) pathway transport of a precursor protein covalently anchored to its initial cpTatC binding site. *J. Biol. Chem.* **281,** 6130–6135 CrossRef Medline
16. Alami, M., Lüke, I., Deitermann, S., Eisner, G., Koch, H. G., Brunner, J., and Müller, M. (2003) Differential interactions between a twin-arginine signal peptide and its translocase in *Escherichia coli*. *Mol. Cell* **12,** 937–946 CrossRef Medline
17. Keegstra, K., Werner-Washburne, M., Cline, K., and Andrews, J. (1984) The chloroplast envelope: is it homologous with the double membranes of mitochondria and Gram-negative bacteria? *J. Cell. Biochem.* **24,** 55–68 CrossRef Medline
18. Brüser, T., and Sanders, C. (2003) An alternative model of the twin arginine translocation system. *Microbiol. Res.* **158,** 7–17 CrossRef Medline
19. Cline, K. (2015) Mechanistic aspects of folded protein transport by the twin arginine translocase (Tat). *J. Biol. Chem.* **290,** 16530–16538 CrossRef Medline
20. Porcelli, I., de Leeuw, E., Wallis, R., van den Brink-van der Laan, E., de Kruijff, B., Wallace, B. A., Palmer, T., and Berks, B. C. (2002) Characterization and membrane assembly of the TatA component of the *Escherichia coli* twin-arginine protein transport system. *Biochemistry* **41,** 13690–13697 CrossRef Medline
21. Zhang, Y., Hu, Y., Li, H., and Jin, C. (2014) Structural basis for TatA oligomerization: an NMR study of *Escherichia coli* TatA dimeric structure. *PLoS One* **9,** e103157 CrossRef Medline
22. Brüser, T., Yano, T., Brune, D. C., and Daldal, F. (2003) Membrane targeting of a folded and cofactor-containing protein. *Eur. J. Biochem.* **270,** 1211–1221 CrossRef Medline
23. Mehner, D., Osadnik, H., Lünsdorf, H., and Brüser, T. (2012) The Tat system for membrane translocation of folded proteins recruits the membrane-stabilizing Psp machinery in *Escherichia coli*. *J. Biol. Chem.* **287,** 27834–27842 CrossRef Medline
24. Warren, G., Oates, J., Robinson, C., and Dixon, A. M. (2009) Contributions of the transmembrane domain and a key acidic motif to assembly and function of the TatA complex. *J. Mol. Biol.* **388,** 122–132 CrossRef Medline
25. Lee, P. A., Buchanan, G., Stanley, N. R., Berks, B. C., and Palmer, T. (2002) Truncation analysis of TatA and TatB defines the minimal functional units required for protein translocation. *J. Bacteriol.* **184,** 5871–5879 CrossRef Medline
26. Taubert, J., Hou, B., Risselada, H. J., Mehner, D., Lünsdorf, H., Grubmüller, H., and Brüser, T. (2015) TatBC-independent TatA/Tat substrate interactions contribute to transport efficiency. *PLoS One* **10,** e0119761 CrossRef Medline
27. Krishnakumar, S. S., and London, E. (2007) Effect of sequence hydrophobicity and bilayer width upon the minimum length required for the formation of transmembrane helices in membranes. *J. Mol. Biol.* **374,** 671–687 CrossRef Medline
28. Becker, L. A., Bang, I.-S., Crouch, M.-L., and Fang, F. C. (2005) Compensatory role of PspA, a member of the phage shock protein operon, in *rpoE* mutant *Salmonella enterica* serovar Typhimurium. *Mol. Microbiol.* **56,** 1004–1016 CrossRef Medline
29. Ize, B., Stanley, N. R., Buchanan, G., and Palmer, T. (2003) Role of the *Escherichia coli* Tat pathway in outer membrane integrity. *Mol. Microbiol.* **48,** 1183–1193 CrossRef Medline
30. Warnock, D. G., Reenstra, W. W., and Yee, V. J. (1982) Na^+/H^+ antiporter of brush border vesicles: studies with acridine orange uptake. *Am. J. Physiol.* **242,** F733–F739 Medline
31. Wexler, M., Sargent, F., Jack, R. L., Stanley, N. R., Bogsch, E. G., Robinson, C., Berks, B. C., and Palmer, T. (2000) TatD is a cytoplasmic protein with DNase activity: no requirement for TatD family proteins in sec-independent protein export. *J. Biol. Chem.* **275,** 16717–16722 CrossRef Medline
32. Walther, T. H., Grage, S. L., Roth, N., and Ulrich, A. S. (2010) Membrane alignment of the pore-forming component TatA(d) of the twin-arginine translocase from *Bacillus subtilis* resolved by solid-state NMR spectroscopy. *J. Am. Chem. Soc.* **132,** 15945–15956 CrossRef Medline
33. Aldridge, C., Storm, A., Cline, K., and Dabney-Smith, C. (2012) The chloroplast twin arginine transport (Tat) component, Tha4, undergoes conformational changes leading to Tat protein transport. *J. Biol. Chem.* **287,** 34752–34763 CrossRef Medline
34. Mori, H., Tsukazaki, T., Masui, R., Kuramitsu, S., Yokoyama, S., Johnson, A. E., Kimura, Y., Akiyama, Y., and Ito, K. (2003) Fluorescence resonance energy transfer analysis of protein translocase. SecYE from *Thermus thermophilus* HB8 forms a constitutive oligomer in membranes. *J. Biol. Chem.* **278,** 14257–14264 CrossRef Medline
35. Hackeng, T. M., Yegneswaran, S., Johnson, A. E., and Griffin, J. H. (2000) Conformational changes in activated protein C caused by binding of the first epidermal growth factor-like module of protein S. *Biochem. J.* **349,** 757–764 CrossRef Medline
36. Johnson, A. E., Woodward, W. R., Herbert, E., and Menninger, J. R. (1976) Ne-acetyllysine transfer ribonucleic acid: a biologically active analogue of aminoacyl transfer ribonucleic acids. *Biochemistry* **15,** 569–575 CrossRef Medline
37. Greene, N. P., Porcelli, I., Buchanan, G., Hicks, M. G., Schermann, S. M., Palmer, T., and Berks, B. C. (2007) Cysteine scanning mutagenesis and disulfide mapping studies of the TatA component of the bacterial twin arginine translocase. *J. Biol. Chem.* **282,** 23937–23945 CrossRef Medline
38. Hamsanathan, S., Anthonymuthu, T. S., Bageshwar, U. K., and Musser, S. M. (2017) A hinged signal peptide hairpin enables Tat-dependent protein translocation. *Biophys. J.* **113,** 2650–2668 CrossRef Medline
39. Shanmugham, A., Wong Fong Sang, H. W., Bollen, Y. J., and Lill, H. (2006) Membrane binding of twin arginine preproteins as an early step in translocation. *Biochemistry* **45,** 2243–2249 CrossRef Medline
40. Brehmer, T., Kerth, A., Graubner, W., Malesevic, M., Hou, B., Brüser, T., and Blume, A. (2012) Negatively charged phospholipids trigger the interaction of a bacterial Tat substrate precursor protein with lipid monolayers. *Langmuir* **28,** 3534–3541 CrossRef Medline
41. Hauer, R. S., Freudl, R., Dittmar, J., Jakob, M., and Klösgen, R. B. (2017) How to achieve Tat transport with alien TatA. *Sci. Rep.* **7,** 8808 CrossRef Medline
42. Jaud, S., Fernández-Vidal, M., Nilsson, I., Meindl-Beinker, N. M., Hübner, N. C., Tobias, D. J., von Heijne, G., and White, S. H. (2009) Insertion of short transmembrane helices by the Sec61 translocon. *Proc. Natl. Acad. Sci. U.S.A.* **106,** 11588–11593 CrossRef Medline
43. De Leeuw, E., Porcelli, I., Sargent, F., Palmer, T., and Berks, B. C. (2001) Membrane interactions and self-association of the TatA and TatB components of the twin-arginine translocation pathway. *FEBS Lett.* **506,** 143–148 CrossRef Medline
44. Mori, H., and Cline, K. (2002) A twin arginine signal peptide and the pH gradient trigger reversible assembly of the thylakoid ΔpH/Tat translocase. *J. Cell Biol.* **157,** 205–210 CrossRef Medline
45. Dabney-Smith, C., and Cline, K. (2009) Clustering of C-terminal stromal domains of Tha4 homo-oligomers during translocation by the Tat protein transport system. *Mol. Biol. Cell* **20,** 2060–2069 CrossRef Medline

46. Pal, D., Fite, K., and Dabney-Smith, C. (2013) Direct interaction between a precursor mature domain and transport component Tha4 during twin arginine transport of chloroplasts. *Plant Physiol.* **161,** 990–1001 CrossRef Medline
47. Maurer, C., Panahandeh, S., Jungkamp, A.-C., Moser, M., and Müller, M. (2010) TatB functions as an oligomeric binding site for folded Tat precursor proteins. *Mol. Biol. Cell* **21,** 4151–4161 CrossRef Medline
48. Panahandeh, S., Maurer, C., Moser, M., DeLisa, M. P., and Müller, M. (2008) Following the path of a twin-arginine precursor along the TatABC translocase of *Escherichia coli*. *J. Biol. Chem.* **283,** 33267–33275 CrossRef Medline
49. Taubert, J., and Brüser, T. (2014) Twin-arginine translocation-arresting protein regions contact TatA and TatB. *Biol. Chem.* **395,** 827–836 Medline
50. Habersetzer, J., Moore, K., Cherry, J., Buchanan, G., Stansfeld, P. J., and Palmer, T. (2017) Substrate-triggered position switching of TatA and TatB during Tat transport in *Escherichia coli*. *Open Biol.* **7,** 170091 CrossRef Medline
51. Aldridge, C., Ma, X., Gerard, F., and Cline, K. (2014) Substrate-gated docking of pore subunit Tha4 in the TatC cavity initiates Tat translocase assembly. *J. Cell Biol.* **205,** 51–65 CrossRef Medline
52. Behrendt, J., and Brüser, T. (2014) The TatBC complex of the Tat protein translocase in *Escherichia coli* and its transition to the substrate-bound TatABC complex. *Biochemistry* **53,** 2344–2354 CrossRef Medline
53. Rose, P., Fröbel, J., Graumann, P. L., and Müller, M. (2013) Substrate-dependent assembly of the Tat translocase as observed in live *Escherichia coli* cells. *PLoS One* **8,** e69488 CrossRef Medline
54. Alcock, F., Baker, M. A. B., Greene, N. P., Palmer, T., Wallace, M. I., and Berks, B. C. (2013) Live cell imaging shows reversible assembly of the TatA component of the twin-arginine protein transport system. *Proc. Natl. Acad. Sci. U.S.A.* **110,** E3650–E3659 CrossRef Medline
55. Huang, Q., Alcock, F., Kneuper, H., Deme, J. C., Rollauer, S. E., Lea, S. M., Berks, B. C., and Palmer, T. (2017) A signal sequence suppressor mutant that stabilizes an assembled state of the twin arginine translocase. *Proc. Natl. Acad. Sci. U.S.A.* **114,** E1958–E1967 CrossRef Medline
56. Towbin, H., Staehelin, T., and Gordon, J. (1979) Electrophoretic transfer of proteins from polyacrylamide gels to nitrocellulose sheets: procedure and some applications. *Proc. Natl. Acad. Sci. U.S.A.* **76,** 4350–4354 CrossRef Medline
57. Laemmli, U. K. (1970) Cleavage of structural proteins during the assembly of the head of bacteriophage T4. *Nature* **227,** 680–685 CrossRef Medline
58. Schägger, H. (2006) Tricine-SDS-PAGE. *Nat. Protoc.* **1,** 16–22 CrossRef Medline
59. Wilms, B., Hauck, A., Reuss, M., Syldatk, C., Mattes, R., Siemann, M., and Altenbuchner, J. (2001) High-cell-density fermentation for production of L-*N*-carbamoylase using an expression system based on the *Escherichia coli rhaBAD* promoter. *Biotechnol. Bioeng.* **73,** 95–103 CrossRef Medline
60. Stolle, P., Hou, B., and Brüser, T. (2016) The Tat substrate CueO is transported in an incomplete folding state. *J. Biol. Chem.* **291,** 13520–13528 CrossRef Medline
61. Kim, Y., Ho, S. O., Gassman, N. R., Korlann, Y., Landorf, E. V., Collart, F. R., and Weiss, S. (2008) Efficient site-specific labeling of proteins via cysteines. *Bioconjug. Chem.* **19,** 786–791 CrossRef Medline
62. Lin, P.-J., Jongsma, C. G., Liao, S., and Johnson, A. E. (2011) Transmembrane segments of nascent polytopic membrane proteins control cytosol/ER targeting during membrane integration. *J. Cell Biol.* **195,** 41–54 CrossRef Medline

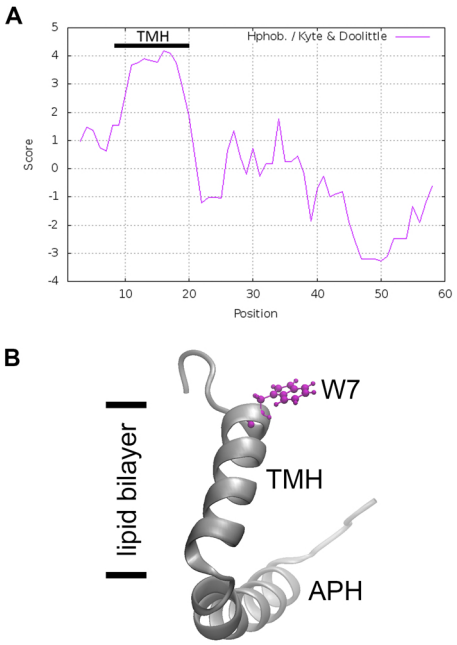

Figure S1: The TMH of TatA begins at Trp-7 (Ref 6) and therefore is very short. (A) Kyte & Doolittle hydropathy plot of $TatA_{(1-60)}$, (B) NMR structure (PDB 2MN7)

3.2 „*Evidence for a second regulatory binding site on PspF that is occupied by the C-terminal domain of PspA*"

Autoren:	Eyleen S. Heidrich und Thomas Brüser
Art der Autorenschaft:	Erst-Autorin
Zugehörigkeit:	Leibniz Universität Hannover, Institut für Mikrobiologie, Herrenhäuser Straße 2, 30419 Hannover
Art des Artikels:	Forschungsartikel
Beitrage:	**Eyleen S. Heidrich:** Konzeption und Planung der Studie zusammen mit Thomas Brüser, Planung und Durchführung aller Experimente, Datenanalyse, Präparation der Abbildungen, Anfertigung des ersten Manuskriptentwurfs **Thomas Brüser:** Konzeption und Planung der Studie zusammen mit Eyleen S. Heidrich, Datenanalyse und Fertigstellung des Manuskripts
Publiziert in	*PLoS ONE*
Publiziert am	15. Juni 2018

Wissenschaftliche Einordnung

Obwohl PspA bereits vor über drei Jahrzenten als erste Komponente des Psp-Systems in *E. coli* entdeckt wurde, bestehen bis heute viele offene Fragen über die genaue Funktionsweise dieser Psp-Komponente. Kürzlich konnte die Struktur der PspF-interagierenden und -regulierenden PspA-Domäne, PspA(1-144), gelöst werden [70]. Im Artikel *„Evidence for a second regulatory binding site on PspF that is occupied by the C-terminal domain of PspA“* konnte zum ersten Mal eine regulatorische Funktion der C-terminalen Domäne von PspA, PspA(145-222), *in vivo* gezeigt werden. Durch eine Fusion von PspA(145-222) an ein kleines, monomeres und lösliches Protein gelang es erstmals PspA(145-222) *in vivo* zu stabilisieren und seine regulatorischen Eigenschaften *in vivo* zu untersuchen, was zu einem größeren Verständnis der Funktion dieser Domäne und der regulatorischen Funktion PspAs führte.

PspA(145-222) ist in der Lage PspF in einem *pspA*-Deletionsstamm zu inhibieren, während seine Überproduktion in einem *psp*-Wildtyp-Hintergrund zu einer Induktion des Psp-Systems führt. Mittels Pull-Down- und *bacterial*-2-*hybrid*-Analysen gelang es erstmals zu zeigen, dass eine Interaktion zwischen zwei PspA-Molekülen durch die C-terminale Domäne von PspA *in vivo* vermittelt wird. Gleichzeitig konnte gezeigt werden, dass durch die rekombinante Überproduktion von TatA ausgelöster Membranstress die Inhibition von PspF durch PspA(145-222) – jedoch nicht die durch PspA(1-144) – teilweise aufhebt, was einen entscheidenden Einblick in die Stress-sensorischen Eigenschaften dieser PspA-Domäne darstellt. Des Weiteren wurde gezeigt, dass eine Fragmentierung von PspA in zwei lösliche Domänen zu einem Verlust der TatA-Interaktion führt, woraus geschlossen wurde, dass N- und C-terminale PspA-Domänen zur Membraninteraktion als auch zur Interaktion mit TatA kooperieren müssen.

PLOS ONE

RESEARCH ARTICLE

Evidence for a second regulatory binding site on PspF that is occupied by the C-terminal domain of PspA

Eyleen Sabine Heidrich, Thomas Brüser*

From the Institute of Microbiology, Leibniz Universität Hannover, Hannover, Germany

* brueser@ifmb.uni-hannover.de

OPEN ACCESS

Citation: Heidrich ES, Brüser T (2018) Evidence for a second regulatory binding site on PspF that is occupied by the C-terminal domain of PspA. PLoS ONE 13(6): e0198564. https://doi.org/10.1371/journal.pone.0198564

Editor: Eric Cascales, Centre National de la Recherche Scientifique, Aix-Marseille Université, FRANCE

Received: March 29, 2018

Accepted: May 21, 2018

Published: June 15, 2018

Data Availability Statement: All relevant data are within the paper and its Supporting Information files.

Funding: This study was funded by the Deutsche Forschungsgemeinschaft (www.dfg.de) by grant BR2285/4-2 of TB. The publication of this article was funded by the Open Access fund of Leibniz Universität Hannover. The funders had no role in study design, data collection and analysis, decision to publish, or preparation of the manuscript.

Abstract

PspA is a key component of the bacterial Psp membrane-stress response system. The biochemical and functional characterization of PspA is impeded by its oligomerization and aggregation properties. It was recently possible to solve the coiled coil structure of a completely soluble PspA fragment, PspA(1–144), that associates with the σ^{54} enhancer binding protein PspF at its W56-loop and thereby down-regulates the Psp response. We now found that the C-terminal part of PspA, PspA(145–222), also interacts with PspF and inhibits its activity in the absence of full-length PspA. Surprisingly, PspA(145–222) effects changed completely in the presence of full-length PspA, as promoter activity was triggered instead of being inhibited under this condition. PspA(145–222) thus interfered with the inhibitory effect of full-length PspA on PspF, most likely by interacting with full-length PspA that remained bound to PspF. In support of this view, a comprehensive bacterial-2-hybrid screen as well as co-purification analyses indicated a self-interaction of PspA(145–222) and an interaction with full-length PspA. This is the first direct demonstration of PspA/PspA and PspA/PspF interactions *in vivo* that are mediated by the C-terminus of PspA. The data indicate that regulatory binding sites on PspF do not only exist for the N-terminal coiled coil domain but also for the C-terminal domain of PspA. The inhibition of PspF by PspA-(145–222) was reduced upon membrane stress, whereas the inhibition of PspF by PspA(1–144) did not respond to membrane stress. We therefore propose that the C-terminal domain of PspA is crucial for the regulation of PspF in response to Psp system stimuli.

Introduction

Many proteobacteria possess the phage shock protein (Psp) system that is upregulated under various stress conditions that can harm the cytoplasmic membrane [1,2]. In *Escherichia coli* and other enterobacteria, the Psp components are encoded by the *pspABCDE* operon and the monocistronic *pspG* gene. The expression of these genes depends on σ^{54} that is regulated by the PspF component, an enhancer binding protein divergently encoded upstream of the *pspABCDE* operon [3,4]. PspF in turn is regulated by PspA, the first product of the *pspABCDE* operon [5,6]. It is believed that PspA is not only a key regulator but also a membrane-

Competing interests: The authors have declared that no competing interests exist.

stabilizing effector of the system [2,7]. Also PspB and PspC, two membrane proteins encoded within the *pspABCDE* operon, play an important role in signaling [8], and just like PspA, also PspB and PspC can have effector functions [9,10]. It is still unknown how exactly a stress signal is sensed and transmitted to PspF. Clear is that PspB and PspC interact in the membrane, and that the C-terminus of PspC in turn interacts with PspA upon a stress signal and thereby recruits PspA to the membrane [8]. The current opinion is that this membrane-recruitment leads to a dissociation of PspA from PspF, which activates PspF and thereby induces the Psp response [11]. The membrane interaction of an N-terminal amphipathic helix (AH1) of PspA is reported to be involved in stress sensing [12]. In the reported X-ray structure, this helix folds back to a coiled-coiled domain, which likely represents the resting state [13]. The interaction of this helix with membrane surfaces in response to membrane stored curvature elastic stress could be a membrane stress sensing mechanism [14,12]. Clearly, PspA is one of the key players in the regulation of the Psp response. Due to the auto-regulatory circuit, experimental approaches to study the native Psp regulatory cascade have limitations *in vivo*. Experimental work on PspA is further challenged by its tendency to aggregate and by the complexity of its numerous interactions. Fragmentation approaches proved useful to overcome some of these problems. Such approaches identified (i) determinants for PspA oligomerization in the C-terminal domain [15,5], (ii) the PspF-regulatory function of a coiled coil formed in PspA(1–144) [12,13], and (iii) the involvement of the N-terminal amphipathic helix AH1 in membrane surface interaction [16,12]. While a strong recombinant overproduction of full-length PspA leads to membrane localization of the recombinant protein and induction of the Psp system *in vivo* [17], PspA variants that lack the C-terminal region do not associate with membranes, nor do they induce the Psp response [13]. It was therefore proposed that membrane recruitment and oligomerization of PspA are linked processes that are required for the upregulation in response to membrane stress [16]. Based on these aspects, PspA has been dissected into distinct functional domains, with PspA(1–144) as the PspF interacting and regulating domain, and PspA (145–222) as the domain required for oligomerization and membrane interaction [15]. So far only negative evidence implied a role of the C terminal domain PspA(145–222) in oligomerization and membrane association [13], and its interactions have not been demonstrated. In this study, we analyzed the effects of PspA domains on the regulation of the key Psp response promoter, P_{pspA}, we determined the localization of the respective domains under non-stress and stress conditions, and addressed the interactions of the domains with other PspA-domains as well as with PspF and with a Psp response inducing protein. The data indicate a novel function of C-terminal PspA fragment PspA(145–222) in PspF regulation, which relies on PspA/PspA interactions and PspA/PspF interactions that are mediated by this domain.

Materials and methods

Strains and growth conditions

E. coli strain MC3 [18] and its derivatives were used for all fractionation and co-elution experiments, as well as for P_{pspA} promoter activity quantifications. *E. coli* strain XL1-Blue Mrf' Tet (Stratagene) was used for cloning. Cells were grown aerobically in LB medium (1% tryptone, 0.5% yeast extract, 0.5% NaCl) at 37˚C with the appropriate antibiotics (100 μg/ml ampicillin, 25 μg/ml chloramphenicol, 50 μg/ml kanamycin). 0.5 mM IPTG or 0.1% rhamnose were used to induce P_{lacZ}- or P_{rhaB}-dependent protein production at indicated time points. *E. coli* strain BTH101 (Euromedex, Souffelweyersheim, France) was used for bacterial-2-hybrid studies and 0.1% (w/v) maltose-containing MacConkey agar plates supplemented with ampicillin and kanamycin were used for screening. Cells were grown for 72 h at 30˚C.

Construction of *psp* deletion strains

The Keio-collection strains BW25113 *pspA*::*kan* and BW25113 *pspF*::*kan* [19] were used to construct the strains MC3 *pspA*::*kan* and MC3 *pspF*::*kan* by phage transduction using $P1_{vir}$ according to standard protocols [20]. After the initial selection on LB agar plates containing kanamycin (50 μg/ml), recipient clones were purified and the position of the kanamycin cassette was confirmed via colony PCR. The kanamycin cassette was removed using not nessearilypCP20-endcoded flippase according to the standard protocol of Datsenko and Wanner [21]. The loss of the kanamycin cassette was confirmed via colony PCR. For construction of the *E. coli* strain MC3 *pspFABCDE*::*kan* strain BW25113 *pspFABCDE*::*kan* was first constructed using the parental strain of the Keio-collection BW25113 [19] and the λ red recombinase system described by Datsenko and Wanner [21] using pKD4 as template and *pspF*-P1-F (CAC GCC GCA TCC GGC AAG TTG TAT TGC TCA ACT TCG GTG TAG GCT GGA GCT GCT TC) and *pspE*-P2-R (AAA ACG GCG CAT AAG CGC CGC TCA TGG TGA ATT CTT ATG GGA ATT AGC CAT GGT CC) as primer for amplification of the kanamycin cassette with flanking homologous regions that correspond to the flanking region of *pspF* and *pspE*. After transformation kanamycin-resistant clones were checked for loss of the pKD46 helper plasmid and positon of the kanamycin cassette were confirmed by colony PCR/sequencing. BW25113 *pspFABCDE*::*kan* were then used as donor for phage transduction of MC3 and the resulting kanamycin-resistant strain was checked again via PCR/sequencing.

Plasmids

The construction of pBW-*tatA*-strep and pBW-*tatA*-NT-*mhip*-strep that are derivatives of the rhamnose inducible vector pBW22 [22], has been described previously [23]. To achieve a constitutive production of the C-terminal domain of PspA, we constructed the plasmid pABS-P-tat-H10*mhip*-*pspA*(CT) which encodes an N-terminal fusion of the C-terminal region of PspA to the mature domain of HiPIP, a tightly folded 9.6 kDa protein that we used to stabilize protein fragments [23]. An N-terminal decahistidine-tag (H10) was added via amplification of *mhip* with the primers NdeI-H10-*mhip*-F (ATA TAT CAT ATG CAT CAT CAC CAC CAC CAC CAC CAC CAC CAC TCC GCT CCC GCC AAT G) and *hip*-BamHI-R (ATA TAT AGG ATC CGC CGG CCT TCA GGG TC), using the plasmid pEXH5-tac as template [24]. The PCR product was cloned in the NdeI/BamHI sites of pABS-P*tat*-*pspC*-H6 [23], resulting in pABS-P*tat*-H10*mhip*-H6. The *pspA* C-terminal region was amplified using the primers *pspA145*-BglII-F (ATA TAT AGA TCT GCA AAC TCG TCG CGC G) and *pspA*-BamHI-R (ATA TAT GGA TCC TTA TTG ATT GTC TTG CTT C). The PCR product was restricted with BglII/BamHI and cloned into the BamHI site of pABS-P*tat*-H10*mhip*-H6. pABS-P*tat*-*pspA*-H6 and pABS-P*tat*-*pspA*(1–144)-H6 were constructed using NdeI-*pspA*-F (ACA ACC ATA TGG GTA TTT TTT CTC GCT TTG C) as forward primer and *pspA*-BamHI-R or *pspA*(144)-BamHI as reverse primer, respectively, and cloned in the NdeI/BamHI sites of the above described pABS-P*tat*-*pspC*-H6. All constructs were confirmed by sequencing. Plasmids and primers used for the bacterial-2-hybrid screen are listed in S1 Table. For a fast cloning procedure, plasmids pUT18C-*pspA*(25–144)-strep and pKT25-*pspA*(25–144)-strep were constructed first, using primers XbaIgBAmHI-*pspA*(25)-F (TAT AAT CTA GAG GGA TCC CCA CAG AAA CTG GTT CG) and *pspA*(144)ggKpnIstrepTAAEcoRI-R (TTA ATG AAT TCT TAT TTT TCG AAC TGC GGG TGG CTC CAG GGT ACC CCC TGA TGA CGT AAC ATC AA TG) to amplify *pspA*(25–144) encoding PspA(25–144) with a C-terminal *Strep*-Tag. XbaI and EcoRI were used for cloning of the PCR products into pKT25 and pUT18C. Plasmids pKN-strep-T25 and pU-strep-T18 were designed by amplifying pKNT25 and pUT18 with primers NdeI-strep-BamHI-pKTN25/pUT18-F (TTA ATC ATA TGT GGA GCC ACC

CGC AGT TCG AAA AAG GAT CCA CCA TGA TTA CGC CAA G) and pKNT/pUT-NdeI-R (ATA TAC ATA TGT GTT TCC TGT GTG AAA TTG TTA TC). PCR products were cleaved with NdeI and religated. By using these plasmids, all fragments could be cloned and interchanged using the KpnI/BamHI sites.

For complementation of the minimal signaling cascade comprising PspF, PspA, PspB, and PspC, the *pspFpspABC* region was amplified using the primers PstI-strep-*pspF*-F (ATT ATC TGC AGC TAT TTT TCG AAC TGC GGG TGG CTC CAA ATC TGG TGC TTT TTC AAC) and *pspC*-BamHI-H6-PvuI-R (ATA TAT CGA TCG CTA GTG GTG GTG GTG GTG GTG GGA TCC CAG TTG ACG GAA ACG GC). The PCR product was cleaved with PstI/PvuI and ligated in the PstI/PvuI cleaved backbone of pUL-P*tat* [13] resulting in pUL-*pspF*strep-*pspABC*-H6. To construct pUL-*pspF*strep-*pspA*(1–144)*BC*-H6 the stop codon TAA was introduced at position PspA(A145) and the W56A mutation of PspF as well as the V105D mutation of PspC were introduced via QuikChange (Stratagene), using the primers listed in S2 Table. All constructs were confirmed by sequencing.

Cell fractionation

For cell fractionation experiments, cells were aerobically grown at 37 ˚C in the presence of the appropriate antibiotics. If protein production was rhamnose-dependent, rhamnose was added to a final concentration of 0.1% (v/v) and cultivation proceeded for 3 h. IPTG was added to a final concentration of 0.5 mM for detection of T25 fusion proteins in the middle of the exponential phase, and cultivation was continued for 2 h. Cells were harvested via centrifugation at 4.500 x *g* for 10 min at 4˚C. Cell densities of corresponding cultures were normalized prior to the centrifugation step. Cell pellets were suspended in 50 mM Tris HCl pH 8.0, 250 mM NaCl, and after adding DNaseI and 1 mM PMSF, cells were homogenized by ultrasonication. Cell debris was removed by centrifugation at 14.000 x *g* for 10 min at 4˚C, and membrane and soluble fractions were prepared from the supernatant by ultracentrifugation at 130,000 x *g* for 30 min at 4˚C. Fractions were analyzed by SDS-PAGE and Western blotting as described elsewhere.

Co-elution assays

To analyze interactions between Strep-tagged TatA and PspA variants, co-elution experiments were carried out as described previously [23], with the exception that cell debris was removed prior to TatA-strep purification. For co-elution assays with His-tagged proteins, cells were resuspended in 100 mM Tris-HCl pH 8.0, 150 mM NaCl, 20 mM Imidazol, and disrupted via French Press, and affinity chromatography was carried out using the Protino Ni-NTA resin (Macherey-Nagel, Düren, Germany) with the above buffer system. After loading and 6 washing steps (each 1 column volume), His-tagged proteins were eluted by increasing the imidazole concentration to 250 mM. Elution fractions were analyzed via SDS-Page and Western blotting.

β-Galactosidase assays

For the determination of the *pspA* promoter activity, LacZ assays were performed as described previously with strain MC3 and derivatives thereof [13]. All assays were done in triplicates. Some variability was observed with respect to absolute promoter activity levels between assays that were not carried out in parallel, and all data and error bars that are combined in diagrams are therefore from parallel assays. For induction of rhamnose- of IPTG-dependent expression systems, 0.1% rhamnose or 0.5 mM IPTG were added directly after inoculation, respectively. For determination of the reconstitution of the adenylate cyclase activity in BTH101, three

independent clones were picked from the MacConkey agar plates and cultivated overnight in LB medium supplemented with 0.5 mM IPTG. LacZ activities of the overnight cultures were determined as described above.

Results

PspA(1–144) and PspA(145–222) can independently inhibit the AAA+ family enhancer binding protein PspF in the absence of full-length PspA

PspA is known to have dual functions in distinct oligomerization states. It can multimerize and interact with membranes, and six PspA protomers can interact with hexameric PspF to regulate this σ^{54} activating enhancer binding protein [15]. The N-terminal domain of PspA, PspA(1–144), folds tightly to a coiled coil that is able to interact with PspF [13]. The N-terminal 22 residues of this domain fold back to the coiled-coil surface, and upon membrane surface interaction this region forms an amphipathic helix that is proposed to sense membrane stored curvature elastic stress [14,12]. The C-terminal domain, PspA(145–222), is required for oligomerization and thus likely mediates PspA-PspA interactions [15]. So far, no direct regulatory function has been attributed to the C-terminal domain. To assess the potential role of PspA (145–222) within the Psp regulatory cascade, we recombinantly produced this domain in a reporter strain that monitors the P_{pspA} promoter activity by a promoter *lacZ* reporter fusion. For comparison, we included also full-length PspA and PspA(1–144) that both are known to regulate PspF (Fig 1). To stabilize PspA(145–222) to a detectable level, we fused it to the C-terminus of HiPIP, an unrelated small globular protein that is used to stabilize fused protein fragments [23,25]. The resulting fusion protein, termed Hip-PspA(145–222), was stable and completely soluble (Fig 1B). As negative control, we also analyzed HiPIP alone in these experiments. All proteins were produced in comparable amounts (Fig 1B). As expected, recombinant full-length PspA could be detected in the soluble and the membrane fractions, whereas PspA (1-144) as well as HiPIP were only detectable in the soluble fraction (Fig 1B). We first carried out *pspA* promoter activity assays in a P_{pspA} *lacZ* reporter strain that had the chromosomal *pspA* gene deleted to avoid an interference of wt-PspA (Fig 1A). In the negative control, the strain that produced only HiPIP showed no reduction in LacZ activities, confirming that HiPIP has no influence on the regulatory cascade. In contrast, *pspA* promoter activity was almost completely downregulated by constitutive expression of full-length PspA or PspA(1–144). Full-length PspA suppressed PspF activity and thus complemented the PspA regulatory function in the mutant strain. With this expression system, PspA(1–144) silenced PspF to at least the extent of full-length PspA. To our surprise, we found a complete downregulation of PspF activity by Hip-PspA(145–222), which indicated that PspA(145–222) can silence PspF.

These findings suggested that not only the PspA(1–144) domain but also the PspA(145–222) domain can interact with PspF, and both domains contribute to its regulation.

Several regions of PspA interact with PspF and silence its transcriptional activation

Knowing that PspA(145–222) is able to silence the Psp system in a *pspA* deletion strain, we performed a comprehensive bacterial-2-hybrid (B2H) screen to identify PspA fragments that interact with PspF. In this screen, inactive adenylate cyclase fragments (T18 and T25) can reconstitute adenylate cyclase activity when they are fused to peptides that interact. The cAMP production enables a fermentation of lactose in the medium. When grown on MacConkey agar, the acidification that results from lactose fermentation causes a deep red color of colonies and their surroundings and a precipitation of bile salts in the agar. If probed protein domains

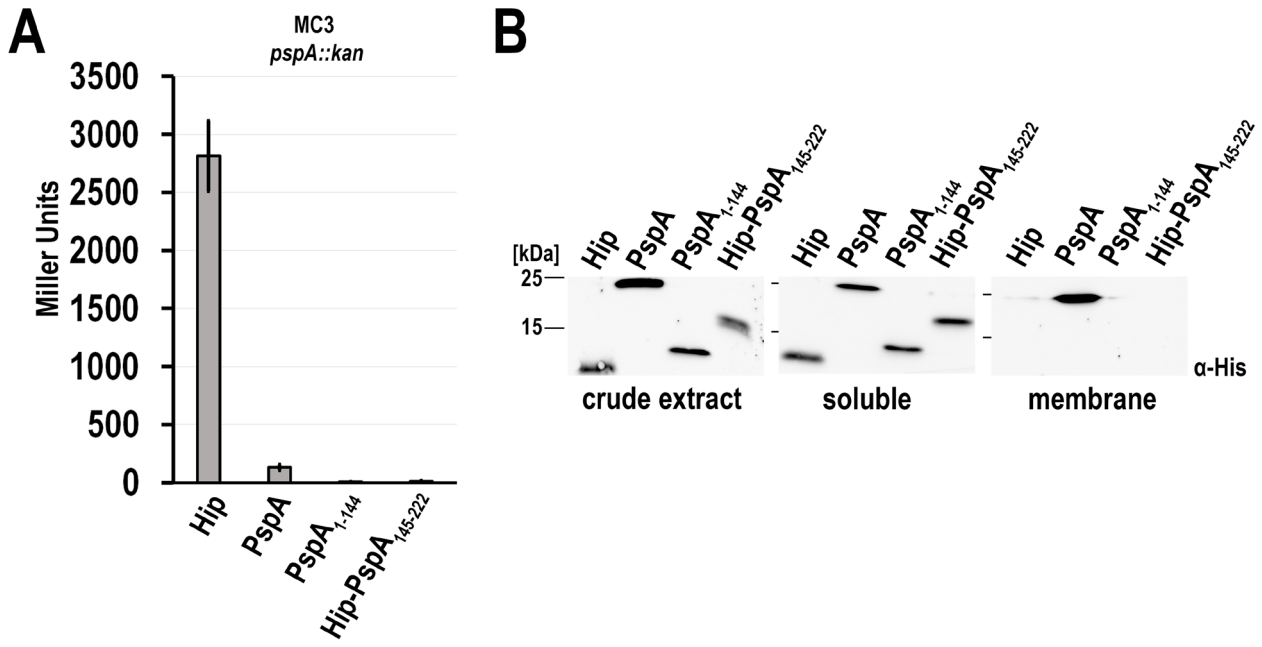

Fig 1. PspA(1–144) as well as Hip-PspA(145–222) can independently down-regulate PspF-dependent promoter activity. (A) LacZ activity assays with a *ΔpspA* reporter strain (MC3 *pspA*::*kan)*, in which the PspF regulated *pspA* promoter is fused the reporter gene *lacZ*. The strain was transformed with vectors for constitutive production of either HiPIP, PspA, PspA(1–144), or Hip-PspA(145–222). (B) Detection of the indicated hexahistdine-tagged proteins in crude extract and the soluble or membrane fractions of the strains used in (A) by SDS-PAGE/Western blotting. The optical density of all cultures was normalized pior to cell harvest. Blots were developed using specific His-Tag antibodies and ECL reaction.

https://doi.org/10.1371/journal.pone.0198564.g001

are not interacting, adenylate cyclase activity cannot be reconstituted and colonies do not metabolize the lactose of the medium, leading to small, beige colonies and a color shift to yellow that is caused by a basic pH. Based on the coiled-coil structure and further *in silico* predictions by the COILS algorithm of PspA secondary structure [26], we constructed 15 different PspA fragments that were C- or N-terminally fused to the T18 or T25 adenylate cyclase domains (Fig 2). Also PspF was fused C- or N-terminally as full-length protein to both protein domains. As only T25-fused PspF showed transcriptional activity in a Δ*pspF* reporter strain (Fig 2B), we used the functional T25-PspF and PspF-T25 constructs as bait in the B2H screen. We named the PspA fragments according to their known or predicted domain structure (Fig 2C): NT (N-terminal region) = Gly2—Pro25; HR1 (helical region 1, the first helix of the coiled coil that has been structurally solved) = Pro25—Glu85; HR2 (helical region 2, the second helix of the coiled coil that has been structurally solved) = Leu86—Gln144; HR3 (region including the predicted third helical region) = Ala-145—Ser-186; CT (C-terminal region) = Ser186—Gln222. The NT and CT regions may in principle also form helices with coiled coil tendency that are predicted by the COILS program when smaller window sizes are used (Fig 2C). The resulting names of the analyzed fragments are outlined in Table 1. We could only detect PspF/PspA fragment interactions with PspF-T25, which was also the only PspF fusion detectable by Western blotting (see Fig 2A). While the NT, HR1, HR3 and CT fragments did not exhibit any interaction with PspF-T25, the other fragments did interact (Fig 2D, 2E and 2F). The position of the T18 fusion (N- or C-terminal) was not relevant for the interactions of constructs that included the first two helical regions, i.e. the complete coiled coil domain of PspA. In contrast, the fusions to the single HR2 preferentially interacted as HR2-T18 fusion, and more clearly the HR3-T18 and especially the HR3-CT-T18 constructs interacted, whereas the N-terminal

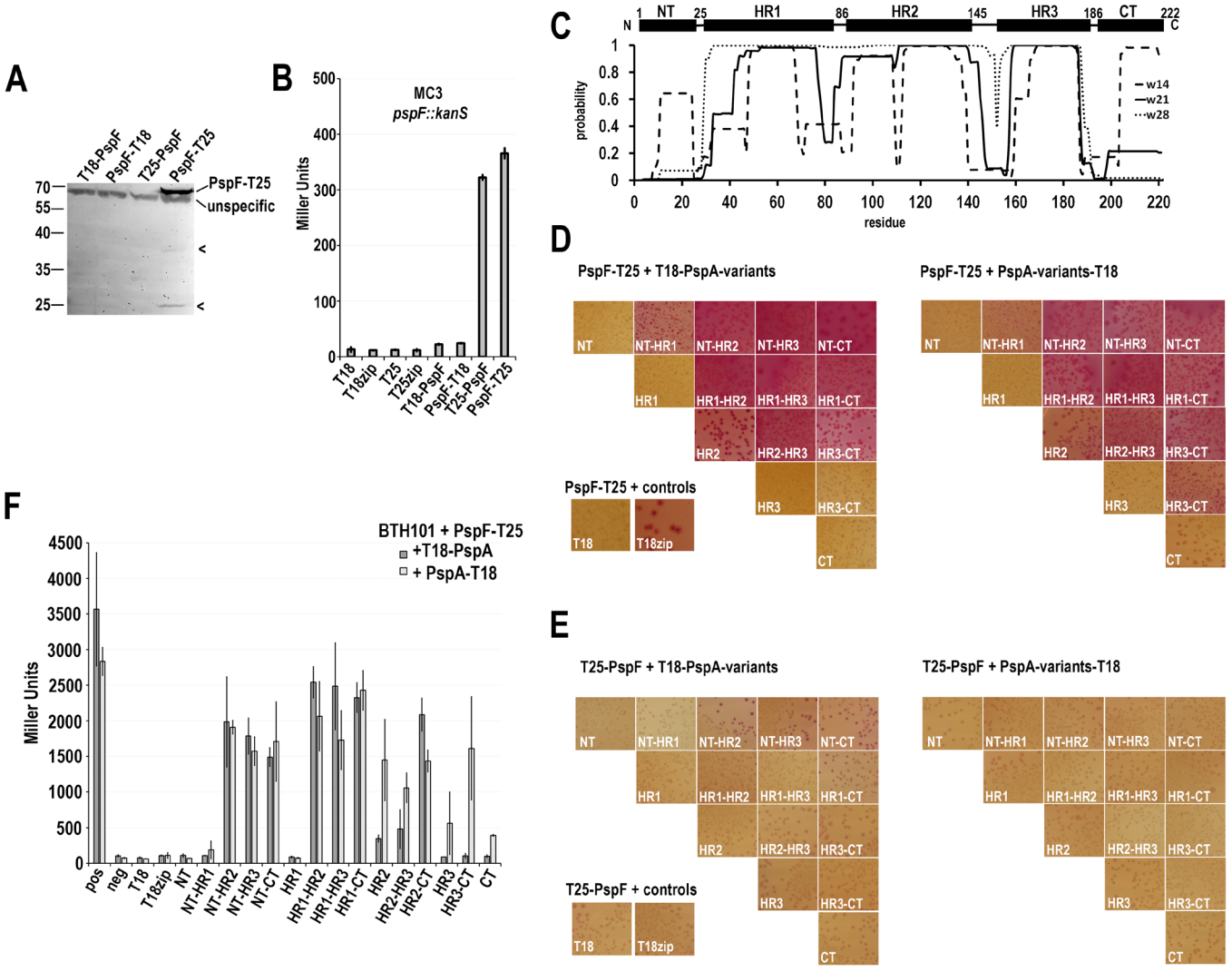

Fig 2. Not only the coiled coil domain of PspA(1–144) but also the C-terminal domain of PspA interacts with PspF. (A) SDS-PAGE/Western blot analysis of PspF fusion proteins used in the activity assay shown in (B). Western blots were developed using *Strep*-Tactin-AP conjugate (IBA) with subsequent alkaline phosphatase reaction for detection. The only detectable PspF fusion was PspF-T25. Other bands corresponded to an unspecific cross-reaction of the antibody (unspecific), and two degradation products (<). (B) LacZ activity assay of PspF fusion proteins in a reporter strain lacking PspF (*pspF*::*kanS*). Only T25 fusions of PspF were active and therefore used in the bacterial-2-hybrid screen. (C) Coils prediction of PspA using the COILS algorithm [26], and scheme including the PspA fragment start/end positions used in the B2H screen. (D/E) Bacterial-2-hybrid screen in *E. coli* strain BTH101 with PspF-T25 (D) or T25-PspF (E) in combination with the 15 indicated fragments of PspA fused N- or C-terminally to the T18 domain. Controls were performed using T18 and T18zip. (F) Quantification of LacZ activites of the B2H screen with indicated PspF-T25 and T18-PspA-variants. "pos"/"neg" indicate the positive (T18zip combined with T25zip) and negative controls as engineered by the manufacturer (T18 combined with T25, both without zipper fragment).

https://doi.org/10.1371/journal.pone.0198564.g002

Table 1. Abbreviations used for the bacterial-2-hybrid screen constructs.

Abbreviation	Start-End	Abbreviation	Start-End	Abbreviation	Start-End
NT	Gly2-Pro25	**HR1**	Pro25-Glu85	**HR2-HR3**	Leu86-Ser186
NT-HR1	Gly2-Glu85	**HR1-HR2**	Pro25-Gln144	**HR2-CT**	Leu86-Gln222
NT-HR2	Gly2-Gln144	**HR1-HR3**	Pro25-Ser186	**HR3**	Ala145-Ser186
NT-HR3	Gly2-Ser186	**HR1-CT**	Pro25-Gln222	**HR3-CT**	Ala145-Gln222
NT-CT	Gly2-Gln222	**HR2**	Leu86-Gln144	**CT**	Ser186-Gln222

https://doi.org/10.1371/journal.pone.0198564.t001

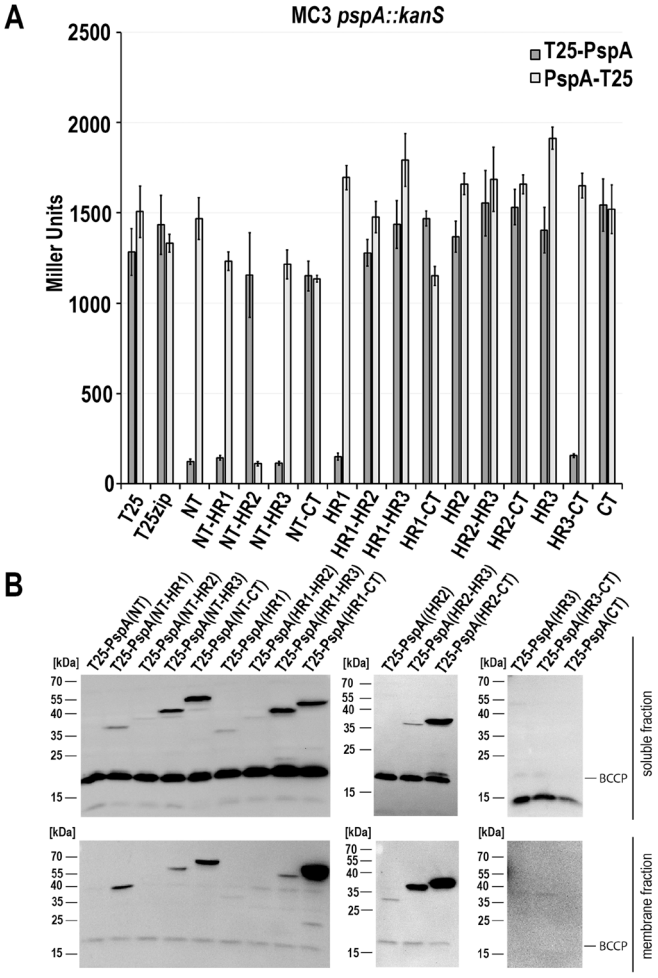

Fig 3. Not only N-terminal regions of PspA, but also Hip-PspA(145–222) inhibit PspF in a Δ*pspA* reporter strain. (A) LacZ activities of a *pspA*-deleted *pspA* promoter reporter strain (MC3 *pspA*::*kanS*) producing indicated PspA fragments N- (light grey) or C-terminally (dark grey) fused to the T25 domain. Protein production was induced by addition of 0.5 mM IPTG at the inoculation time. Inhibition of PspF activity could be observed for six fragments, namely T25-PspA(NT), T25-PspA(NT-HR1), PspA(NT-HR2)-T25, T25-PspA(NT-HR3), T25-PspA(HR1), and T25-PspA(HR3-CT). (B) Detection of T25-PspA-variants used in (A) in subcellular fractions by SDS-PAGE/Western-blotting. Among the N-terminal fusions to T25, only PspA(NT-CT)-T25 was detectable.

https://doi.org/10.1371/journal.pone.0198564.g003

fusions showed no interaction (Fig 2D and 2F). All negative controls showed very low promoter activity (Fig 2F), but the T18zip construct resulted in reddish colonies, indicating a very high sensitivity of the growth phenotype on solid media. The interaction of the HR3-CT-T18 construct suggests that the observed regulation of PspF-dependent promoter activity (Fig 1) has been caused by a direct interaction.

We then analyzed potential regulatory effects of all PspA fragments (Fig 3). As T18 fusions strongly affected growth of the promoter-*lacZ* reporter strain, we used the T25 fusions for these analyses. To ensure that an altered PspF activity only originated from an interaction of the recombinant proteins, we again used a *pspA* promoter activity reporter strain in which the chromosomal *pspA* gene was deleted. In this strain, high LacZ activities indicate that PspF activity is not affected by PspA fragments, whereas low LacZ activities indicate that PspA fragments inhibit PspF (Fig 3A). We could identify six PspA fragments that inhibited PspF activity

(NT, NT-HR1, NT-HR2, NT-HR3, HR1, and HR3-CT). It was highly relevant whether the T25 domain was fused to the N- or the C-terminus of the respective fragment: The NT, NT-HR1, NT-HR3, HR1, and HR3-CT interacted only as N-terminal fusions, whereas the NT-HR2 construct interacted only as C-terminal fusion. Despite their strong interaction with PspF, fusions to full-length PspA (= the NT-CT construct) did not inhibit PspF activity, indicating that such fusions abolish the regulatory PspA function. We then examined whether the observed effects were due to a differential abundance of PspA fragments (Fig 3B). This was not the case, as protein levels did not correlate with inhibition of PspF activity. On one hand there were non-detectable constructs that showed a strong PspF inhibition and on the other hand fusions of T25 to full length PspA were highly abundant without having an inhibitory effect on PspF. It was recently shown by the Buck group that peptides of $PspA_{1-24}$ and $PspA_{25-47}$ inhibit AAA+ ATPase activity of PspF(1–275) [12]. In agreement with this study, the strong inhibition of the promoter activity by the PspA fragments containing the corresponding NT and HR1 regions now demonstrates that these fragments can indeed downregulate the *pspA* promotor *in vivo* (Fig 3). The inhibitory effect of T25-HR3-CT on PspF activity agrees with the same effect that had been already observed with the corresponding HiPIP fusion used for the initial analysis (Fig 1).

PspA(1–144) and PspA(145–222) act differently in a PspA WT background

After having established that PspA(145–222) and PspA(1–144) both inhibited PspF in a Δ*pspA* reporter strain, we analyzed the regulatory effects in a WT *pspA* background, i.e. in a reporter strain that is not mutated in *pspA* and thus contains the wild type *pspABCDE* operon (Fig 4A). We used the unrelated HiPIP as negative control and found that, as expected, HiPIP had no influence on the *pspA* promoter activity, as the basal activity level of the *pspA* promoter was not altered by HiPIP (~100 MU). Full-length PspA and PspA(1–144) resulted in silencing of the *pspA* promoter activity, indicating that these recombinantly produced proteins inhibited PspF very efficiently. Surprisingly, Hip-PspA(145–222) did not behave like full-length PspA or PspA(1-144) in this genetic background, and instead slightly induced the Psp response about 1.5-fold. As it could have been that the production of Hip-PspA(145–222) had triggered a degradation of full-length PspA, we examined the abundances of the respective recombinant constructs in subcellular fractions and assessed also the abundance of the non-recombinant wt-PspA (Fig 4B). As expected from previous studies [23], wt-PspA was detected in the soluble and in the membrane fraction in low amounts when the Psp system was not induced. Recombinantly produced His-tagged full-length PspA was also present in both fractions, whereas the well-characterized PspA(1–144) was almost completely soluble. In agreement with the promoter activity data (Fig 4A), both constructs repressed the production of wt-PspA to a hardly detectable level. Importantly, the production of Hip-PspA(145–222) did not trigger a membrane recruitment of wt-PspA in comparison to the negative control, nor did it cause a degradation of full-length PspA. Instead, we observed slightly higher levels of wt-PspA in the soluble fraction, indicating that the increased PspA levels were not targeted to the membrane under these conditions, i.e. in the absence of membrane stress. The upregulation could be explained by an interaction of His-tagged Hip-PspA(145–222) with wt-PspA, which was already indicated by the results of the two-hybrid assays (Fig 2), and we confirmed this interaction by affinity chromatography and co-elution analyses (Fig 4C). Although a large fraction of wt-PspA was not associated with Hip-PspA(145–222), some wt-PspA clearly co-eluted with Hip-PspA(145–222), indicating that PspA(145–222) can interact with full-length PspA, which supports the view that it may modulate the effect of full-length PspA on PspF activity.

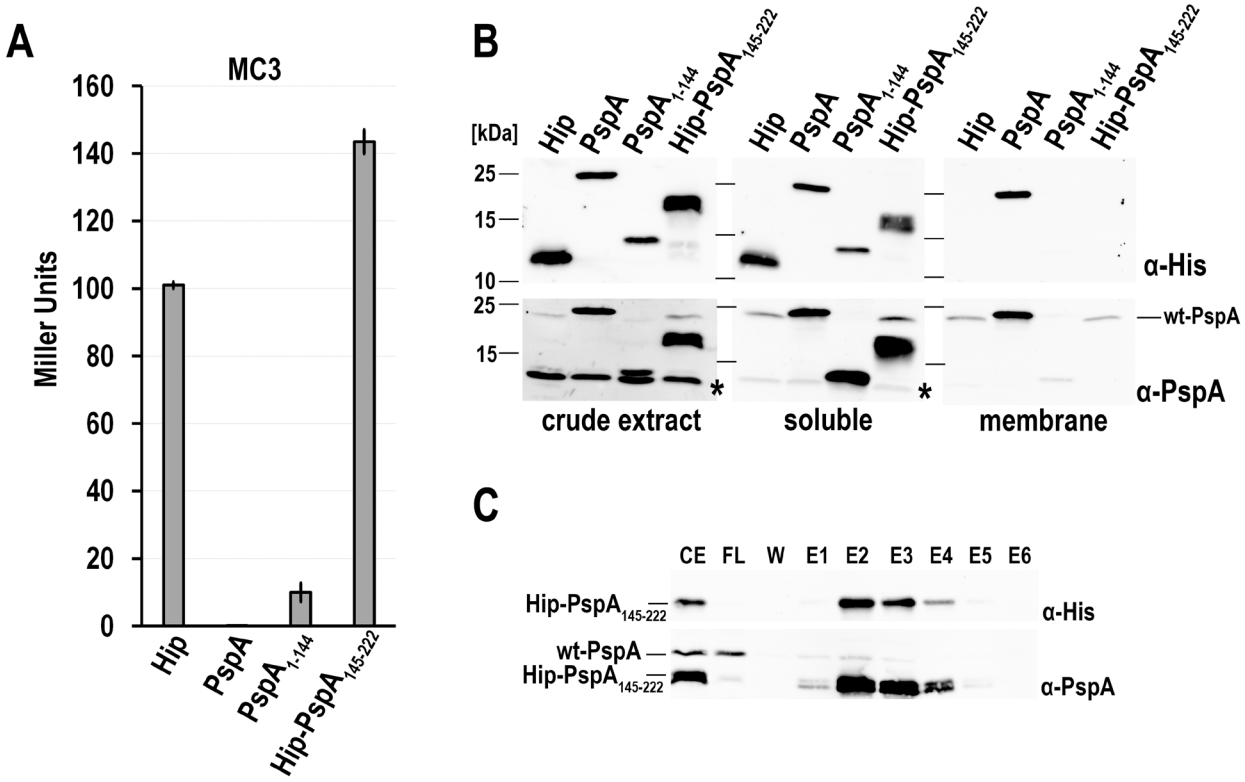

Fig 4. Hip-PspA(145–222) and PspA(1–144) have differential effects in a wild type *pspA* reporter strain. (A) LacZ activity assays of the *psp* wild-type reporter strain (MC3), constitutively producing either HiPIP, PspA, PspA(1–144), or Hip-PspA(145–222). (B) SDS-PAGE/Western blot detection of chromosomally encoded PspA (wt-PspA) and the recombinant PspA-variants used in the crude extract, soluble and membrane fractions of the strains used in (A). Blots were developed using specific antibodies recognizing the His-tag (upper panels) or PspA (lower panels, * indicates a cross-reaction of the PspA antibody). (C) Interaction of His-tagged Hip-PspA(145–222) with wt-PspA as examined by co-elution during affinity chromatography. CE = crude extract, FL = flow-through, W = last wash fraction, E1-E6 = elution fraction 1–6. Upper panel: detection of His-tagged Hip-PspA(145–222) by specific His-tag antibodies; Lower panel: detection by antibodies recognizing PspA.

https://doi.org/10.1371/journal.pone.0198564.g004

PspA(145–222) interacts with full-length PspA most likely by formation of antiparallel coiled coils

After having shown that PspA(145–222) can downregulate PspF activity as consequence of a direct interaction in the absence of full-length PspA (Figs 1–3), and after having shown that PspA(145–222) stimulates PspF activity in the presence of full-length PspA (Fig 4), we identified the region of PspA that interacts with PspA(145–222) by bacterial 2-hybrid analyses (Fig 5). We used the HR3-CT-T18 or T18-HR3-CT constructs as baits and systematically examined their interaction with all PspA fragments based on the above defined regions (NT/HR1/HR2/HR3/CT). While HR3-CT-T18 exhibited multiple interactions with full-length or truncated T25-PspA constructs (Fig 5, left panels), the T18-HR3-CT construct did not show strong interactions with any of the T25-PspA derivatives (Fig 5, right panels), indicating that an antiparallel setup (T18 fused to the C-terminus of PspA(145–222) as bait in combination with T25-fusions at the N-terminus of the prey) might be important for the interaction. N-terminal parts of PspA were not necessary for this interaction with PspA(145–222) (Fig 5, left panels). The adenylate cyclase activity could be reconstituted with HR3-CT-T18 in combination with T25 fusions to all fragments that included the HR3- or CT-regions. While the interaction with T25-HR3-CT was quite strong, the T25-HR3 or T25-CT constructs showed detectable but less

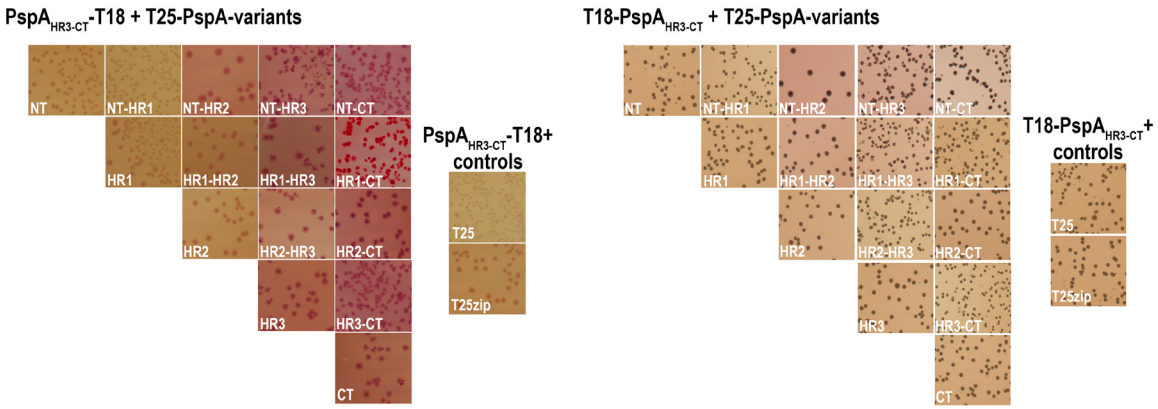

Fig 5. PspA(145–222) interacts most likely antiparallel with PspA domains. Bacterial-2-hybrid screen with HR3-CT-T18 (left side) or T18-HR3-CT (right side) and all 15 fragments of PspA as N-terminal T25 domain fusions in *E. coli* strain BTH101. Controls were performed using T25 and T25zip.

https://doi.org/10.1371/journal.pone.0198564.g005

interaction with HR3-CT-T18, suggesting that the HR3 and CT regions of PspA might interact together rather than individually with C-terminal regions of other PspA proteins. Little interaction was also obtained with the NT-HR2 fragment, which might add a level of complexity to the interactions if these weak interactions are physiologically relevant. However, the physiological function of the HR2/HR3-CT interaction has to be questioned, as the coiled coil of HR2 with HR1 is disrupted in that construct. In summary, the data support the view that PspA-PspA interactions are mediated via their C termini, and these interactions are likely antiparallel. As the C-terminal domain includes HR3, and as also the CT region might be able to form coiled coils, we suggest that this region possibly forms an antiparallel intermolecular coiled coil, which explains why the truncation of this domain results in soluble monomeric proteins [13,15].

PspA(145–222) enhances a Psp response in a *psp* WT strain

As PspA(145–222) stimulated the *pspA*-promoter activity in the presence of wt-PspA (Fig 4), we examined, whether membrane stress could induce the *pspA*-promoter activity on top of this stimulation. To induce a "complete" membrane stress Psp response involving all signaling components (i.e. PspA and the membrane components PspB and PspC), we produced the small membrane-anchored protein TatA [23]. TatA is part of the Tat translocase in *E. coli* and facilitates the translocation of folded proteins most likely by local destabilization of the lipid bilayer [25]. We thus produced TatA-*Strep* in the *pspA* promoter reporter strain in a *psp* wild type genetic background and in the presence of either PspA, PspA(1–144), or Hip-PspA(145–222), respectively. In a positive control, HiPIP was produced instead of any of the PspA constructs, which should not affect the Psp response induction by TatA. As expected, TatA induced the Psp response in the control strain (Fig 6A). In contrast, the promoter activity remained suppressed by recombinant PspA and PspA(1–144) when TatA-strep was produced, indicating that an increased abundance of these PspF-regulating proteins suppresses the Psp response. However, in the presence of Hip-PspA(145–222), which *per se* already increased the *pspA* promoter activity, TatA-*Strep* still induced a Psp response on top of this elevated level, indicating that the triggering of promoter activity by Hip-PspA(145–222) is unrelated to membrane stress and does not compromise the ability to respond to membrane stress.

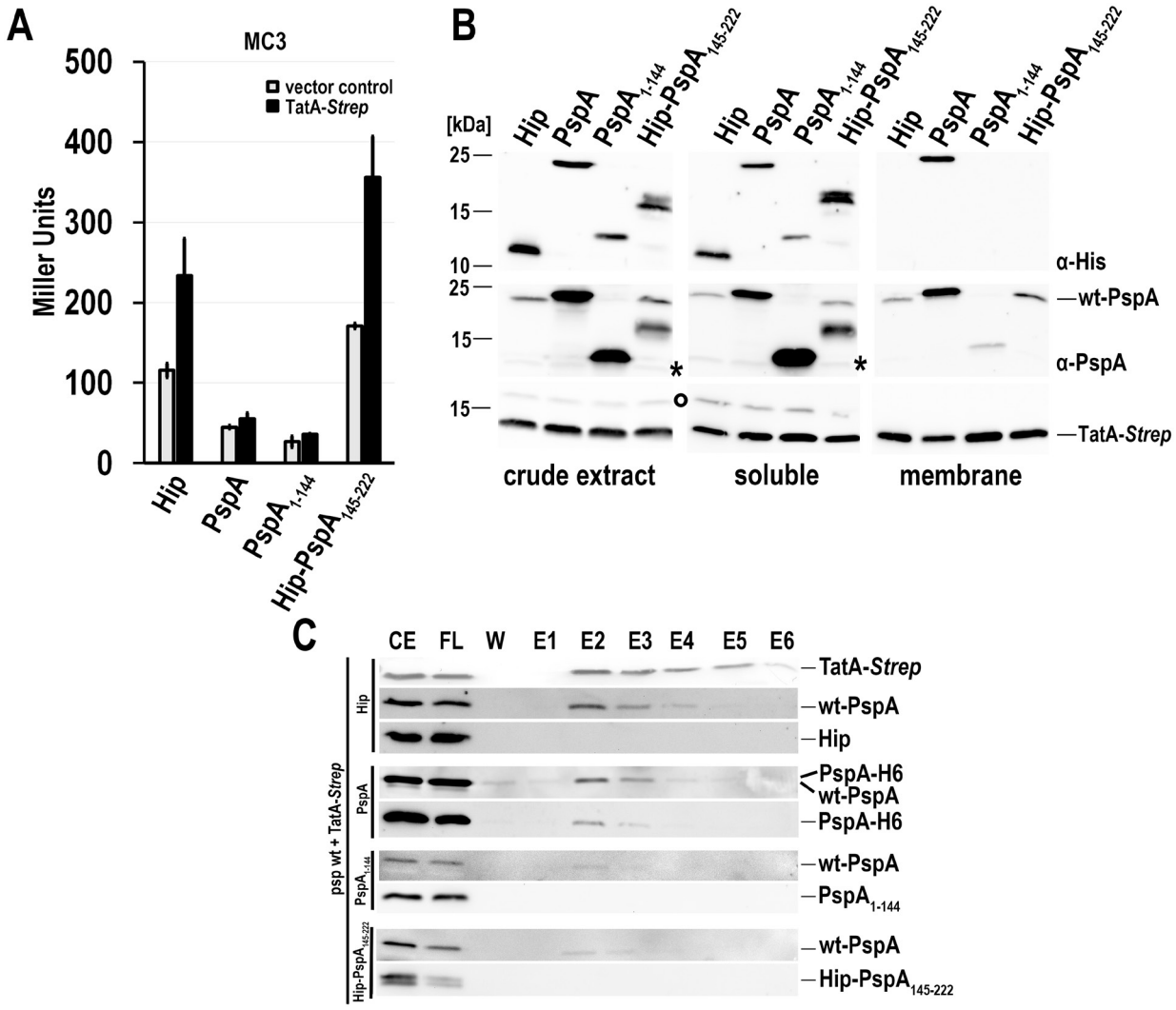

Fig 6. Inducibility of the Psp response in a *psp* wild type strain in the presence of additional recombinant PspA, PspA(1–144), or Hip-PspA (145–222). (A) LacZ activity assays of the psp wild-type reporter strain (MC3), constitutively producing either HiPIP, PspA, PspA(1–144), or Hip-PspA(145–222). Production of TatA-*Strep* was induced by 0.1% (v/v) rhamnose at the beginning of the cultivation. The strain containing the empty vector pBW22 was used as control. (B) SDS-PAGE/Western blot analysis of crude extract, soluble and membrane fractions of TatA-Strep producing strains used in (A), using for detection either specific His-antibodies (upper panels) or PspA antibodies (middle panels, * indicates a cross-reaction of the PspA antibody). TatA-Strep was detected using Strep-Tactin-HRP conjugate. "○", biotin carboxyl carrier protein, BCCP (C) Interaction of His-tagged HiPIP, PspA, PspA(1–144), and Hip-PspA(145–222) with TatA-*Strep*, as evidenced by co-elution. TatA-Strep was purified via Strep-Tactin affinity chromatography. CE = crude extract, FL = flow-through, W = last wash fraction, E1-E6 = elution fraction 1–6. All fractions were analyzed by SDS-PAGE/Western blot using Strep-Tactin-AP conjugate for detection of TatA-Strep. Specific His-tag antibodies were used for detection of his-tagged HiPIP and PspA variants. Specific PspA antibodies were used for detection of wt-PspA and PspA variants. One representative detection of TatA-strep (Blot 1) is shown on the top. Blots 2, 4, 6, 9 (counted from the top) were developed with PspA antibodies, and Blots 3, 5, 7, 9 were developed using His-tag antibodies.

https://doi.org/10.1371/journal.pone.0198564.g006

When we examined the presence of the constructs in subcellular fractions, we found that wt-PspA could not be detected when full-length PspA or PspA(1–144) was recombinantly produced, confirming that the *pspA* promoter activity remains downregulated by highly abundant PspA or PspA(1–144) under membrane stress. This agrees with the data obtained in the absence of membrane stress (Fig 4) and with the promoter activity results (Fig 6A).

Apparently, membrane stress sensing does not work when the PspF-inhibitory full-length PspA or PspA(1–144) are highly abundant.

It was shown in earlier studies that PspA interacts directly with the membrane protein TatA-*Strep*, which indicates a membrane interaction of PspA upon stress [23,25]. As TatA was *Strep*-tagged, we carried out co-elution experiments to address the question which fragments of PspA interact with TatA (Fig 6C). Notably, while full-length PspA co-eluted with TatA, neither the N- nor the C-terminal fragment of PspA could be detected in the elution fractions, possibly because these domains were not membrane-interacting (Fig 6B). The amount of full-length PspA that co-eluted with TatA-Strep appeared to be reduced in the presence of PspA (1–144) or Hip-PspA(145–222), but these domains obviously did not completely abolish the interaction of TatA-*Strep* with full-length PspA.

We then did the same experiments in a *pspA* deletion background (Fig 7). The production of HiPIP, PspA or PspA(1–144) had the same effect on LacZ activity, no matter if TatA-*Strep* was present or not, as they silenced PspF transcriptional activity in both cases to the same extent. Again, PspA(1–144) was a stronger inhibitor than full-length PspA. In contrast, when TatA-*Strep* was produced in a strain that also produced Hip-PspA(145–222), the inhibitory effect of Hip-PspA(145–222) could be partially released, as evidenced by an increase of the *pspA* promoter activity from almost 3.5 Miller Units to an average of 80 Miller Units (Fig 7A). Compared to the negative control, the observed effect was not large in terms of absolute values, but it was significant and large in terms of relative increase. This finding was very interesting, as the effect could only be observed for Hip-PspA(145–222) and not for full-length PspA and PspA(1–144). Based on this, it may be speculated that PspA(145–222) is able to interact with TatA-*Strep* when wt-PspA is missing, but this interaction could so far not be demonstrated by co-elution analyses (Fig 7C), possibly indicating that PspA(145–222) is able to sense TatA induced membrane stress without the need of a direct interaction.

PspF activity is PspC-independently upregulated in a system that lacks the C-terminal PspA domain

We then addressed the question what happens in a system producing *pspFpspA*(1–144)*BC* in a natural regulatory cascade context. A *pspFpspABCDE* deletion mutant of the *pspA* promoter reporter strain MC3 was constructed and the unaltered *pspFpspABC* genomic region as well as the same region with a translational stop at codon 145 of PspA (= *pspFpspA*(1–144)*BC*) were introduced on an pSC101-based very low copy complementation vector [13] (Fig 8). The plasmid-encoded system had a lower basal activity than wild type but was fully functional, as PspF activity could be induced by production of the membrane anchor of TatA (Fig 8A), an established trigger of the Psp response [25]. However, despite PspA(1–144) was fully soluble and more abundant than full-length PspA, PspF activity was higher in the presence of PspA(1–144) than with full-length PspA (Fig 8B). It therefore appeared that the PspA(145–222) domain was needed for keeping PspF activity down in this system. Also the higher PspC levels in the strain producing PspA(1–144) reflect the increased promoter activity (Fig 8B). Importantly, the *pspFpspA*(1–144)*BC* system was not inducible by membrane stress (Fig 8A). In line with these observations, we found that the increased promoter activity in the PspA(1–144) system did not depend on a PspA/PspC interaction (Fig 8C), which is a key interaction for signaling of membrane stress [8,27]. As the Darwin group has shown recently that a V125C mutation of PspC from *Yersinia enterocolitica* abolishes the PspC/PspA interaction [8,27], we used the corresponding mutation in the *E. coli* system, PspC(V105D), to address the importance of the PspC/PspA interaction and found that it had no influence on PspF activity (Fig 8C). In the course of another project (manuscript in preparation), we had confirmed that, like in *Y. enterocolitica*,

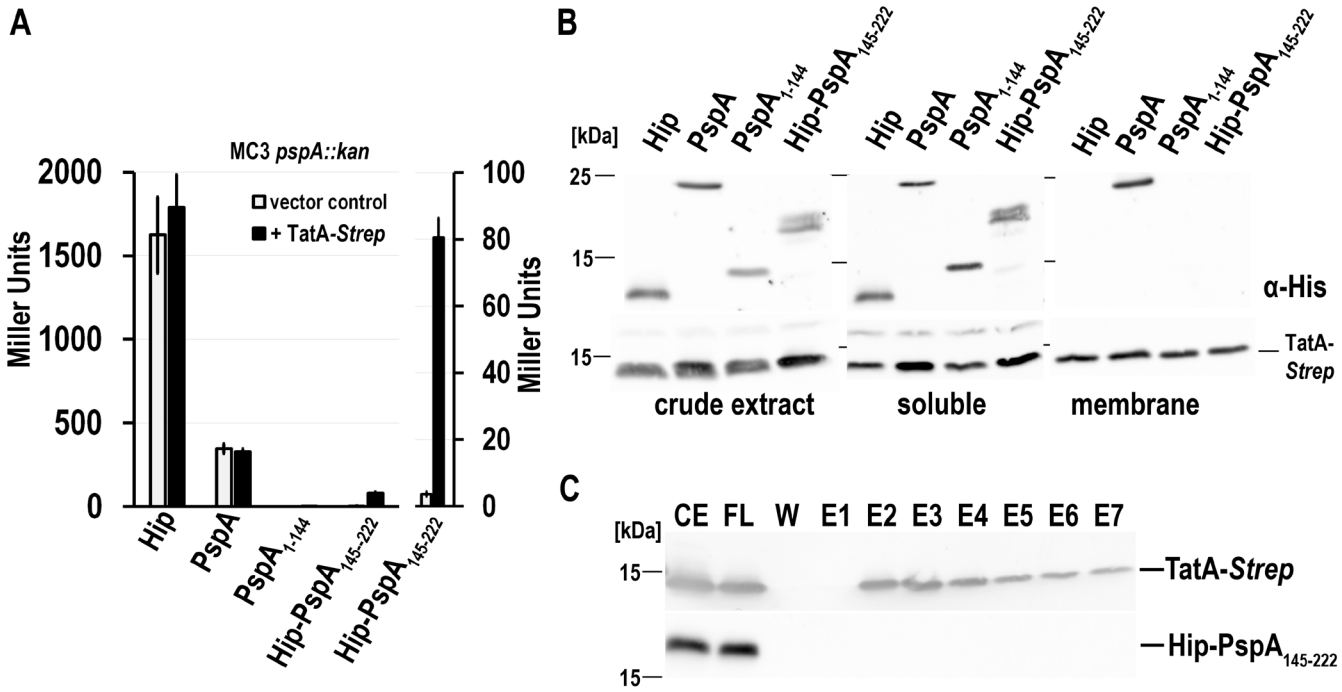

Fig 7. Examination of inducibility of the Psp response in a *pspA* deletion strain in the presence of additional recombinant PspA, PspA(1–144), or Hip-PspA (145–222). (A) LacZ activity assays of a *pspA* deletion reporter strain (MC3), constitutively producing either mature HiPIP, PspA, PspA(1–144), or Hip-PspA (145–222). Production of TatA-Strep was induced by 0.1% (v/v) rhamnose at the beginning of the cultivation. The strain containing the empty vector pBW22 was used as negative control. The graph on the right side shows a rescaled plot of the results next to it. (B) SDS-PAGE/Western blot analysis of crude extract, soluble and membrane fractions of TatA-*Strep* producing strains used in (A). Western blots were developed using His-tag (upper panels) or PspA (lower panels) specific antibodies, * indicates a cross-reaction of the PspA antibody). TatA-Strep was detected via Strep-Tactin-HRP conjugate. "○", biotin carboxyl carrier protein, BCCP. (C) Coelution analysis of Hip-PspA(145–222) with TatA-*Strep* produced in the *pspA* deletion reporter strain as described in Fig 6.

https://doi.org/10.1371/journal.pone.0198564.g007

this mutation abolished PspC dependent signal transduction also in *E. coli*. A W56A mutation in PspF that is known to abolish PspA binding to PspF [5] resulted in an induction of the Psp response, and in case of the system with full-length PspA, PspA was recruited to the membranes (Fig 8D). As expected, in the system comprising PspA(1–144) instead of full-length PspA, the PspF(W56A) mutation compromized inhibitory functions of PspA(1–144) but did not result in any detectable membrane recruitment that appears to require the PspA(145–222) domain. Protein level corresponded to the observed promoter activities and hence it can be excluded that a lowered PspA or PspA(1–144) abundance caused the observed effects (Fig 8D). Together, these data indicate (i) that the PspA(145–222) domain in full-length PspA contributes to the inhibition of PspF by PspA at physiological abundances (Fig 8A and 8D), (ii) that PspA(1–144) alone cannot respond to known triggers of the Psp response (Fig 8A), (iii) that PspA(1–144) inhibits but does not silence PspF at physiological levels (Fig 8A), (iv) that the W56A mutation in PspF reduces the inhibition by full-length PspA and PspA(1–144), and (v) that the PspA(145–222) domain is required for membrane targeting (Fig 8D).

Discussion

The C-terminal domain of PspA can regulate PspF in a stress-responsive manner

The regulatory interactions of the Psp components PspA, PspB, PspC, and PspF in response to membrane stress are in the focus of most current research that is done in the Psp field. For

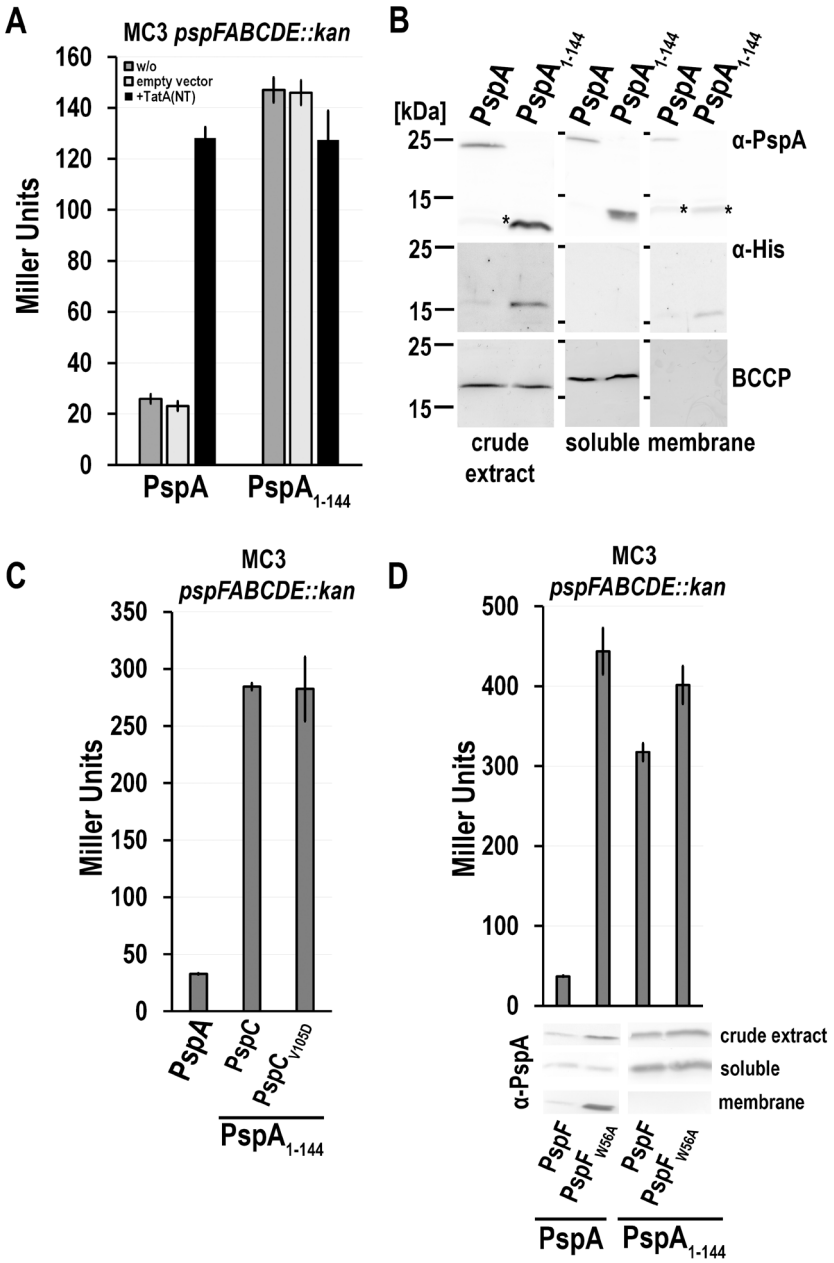

Fig 8. PspA(145–222) is necessary for keeping PspF activity at the basal level in a natively regulated Psp system. (A) LacZ activities of a *pspFABCDE* deletion P_{pspA} reporter strain MC3 *pspFABCDE*::*kan* with an in trans complemented minimal regulatory cascade using vector pUL-*pspF*strep-*pspABC*-H6 or pUL-*pspF*strep-*pspA*(1–144)BC-H6. Membrane stress was induced by rhamnose-dependent production of TatA(NT)-Hip. As negative controls, strains with the empty pBW22 vector and without the pBW22 vector (w/o) were used. (B) SDS-PAGE/Western blot analysis of crude extract, soluble and membrane fractions of the control strains (w/o) used in (A). PspA fragments were detected using PspA-specific antibodies (* = cross reaction of the PspA antibody). His-tagged PspC was detected via His-tag specific antibodies, and BCCP was detected as fractionation control with the Strep-tactin-AP conjugate. (C) LacZ activites of MC3 *pspFABCDE*::*kan* transformed with either pUL-*pspF*strep-*pspABC*-H6, pUL-*pspF*strep-*pspA*(1–144)BC-H6, or pUL-*pspF*strep-*pspA*(1–144)BC(V105D)-H6 for determination of PspC dependence of the results obtained in (B). (D) LacZ activites and detection of protein levels of MC3 *pspFABCDE*::*kan* transformed with either pUL-*pspF*strep-*pspABC*-H6, pUL-*pspF*(W56A)strep-*pspABC*-H6, pUL-*pspF*strep-*pspA*(1–144)BC-H6, pUL-*pspF*(W56A)strep-*pspA*(1–144)*BC*-H6. PspA detection in cellular fractions by SDS-PAGE/Western blot analysis, using PspA-specific antibodies.

https://doi.org/10.1371/journal.pone.0198564.g008

E. coli, it was recently shown that six PspA(1–144) domains stably associate with hexameric PspF, exhibiting a slow dissociation kinetics [13], and that PspF can be regulated by PspA and PspA(1–144) *in vivo* and *in vitro* when it is bound to it [13]. It was therefore proposed that PspA may not need to dissociate from PspF to modulate its activity in response to stress signals. The ability to respond to membrane stress was not examined so far with the complex consisting of PspF and the C-terminally truncated PspA(1–144), and it was therefore unclear whether PspA(145–222) plays an active role in the regulatory cascade *in vivo*. However, it was known that the C-terminal domain of PspA is required for PspA oligomerization [15,5,13], and based on this evidence it has been postulated that it predominantly mediates oligomerization [15]. It was also clear from experiments with PspA(1–186) that the absence of the CT region abolishes the activation of PspF by PspA in the presence of membrane vesicles [14], and this domain was reported to be capable of inhibiting PspF ATPase activity [15]. However, the C-terminal domain is quite unstable *per se* and—albeit the data with truncated constructs suggested a role in regulation—positive data demonstrating a functionality directly were missing. We compared effects of recombinantely produced PspA(1–144), Hip-PspA(145–222), in which this domain is stabilized by an N-terminally fused protein, and full-length PspA on PspF regulation in an uninduced and induced state as well as in the presence or absence of native PspA. The stabilization by HiPIP or 2-hybrid domains was crucial for obtaining the *in vivo* data with PspA(145–222). Our observation of PspF inhibition by recombinant Hip-PspA (145–222) in the absence of full-length PspA now indicates a direct regulatory function of this domain *in vivo* (Figs 1, 4, 6, 7 and 8). The PspA(145–222) domain silences the *pspA* promoter in a mode that permits a significant activation by membrane stress as induced by TatA (Fig 7). This differs from the inhibitory effect of the recombinantly produced PspA(1–144) domain, as the PspA(1–144) regulated system does not respond to membrane stress anymore (Fig 7). Even the inhibition of PspF by recombinant full-length PspA was not affected when TatA-*Strep* was over-produced, indicating that the negative regulation was dominant under these conditions. Importantly, the PspA(1–144) construct includes an N-terminal amphipathic helix (residues 2–24) that is known to sense membrane stored curvature elastic stress [12], and therefore our data now indicate that this helix alone in conjunction with the regulatory coiled coil domain does not suffice for signaling of membrane stress to PspF. In agreement with this, it was reported that in a strain lacking genome-encoded PspA the Psp system is inducible by the pIV secretin when PspA(20–222), which lacks its N-terminal helix, is produced at low levels [16], indicating that this helix cannot constitute the only pathway for PspF activation. A crucial role of the distal C-terminus of PspA for the activation of the system was already postulated based on *in vitro* results that showed a requirement of the C-terminus for PspF activation [14]. As that study used truncated PspA, it remained unclear whether the absence of the C-terminus disabled stress sensing, or whether its lack only caused a dominant inhibition by the N-terminal PspA regions that are known to inhibit PspF [15,12,13,16]. The C-terminal region that starts behind the structurally solved N-terminal coiled coil, i.e. position 145, has not been analyzed so far and C-terminal fragments included regions of this N-terminal coiled coil, which are known to have effects on their own and thus compromise the interpretability of the data. Earlier *in vitro* and *in vivo* studies convincingly showed the contribution of the C terminal domain to oligomerization of PspA, but a direct influence on PspF activity by C terminal domains of PspA could not be determined as the used PspA fragments did neither inhibit nor interact with PspF *in vivo* and *in vitro* [15,5]. Our data are therefore first direct evidence for the involvement of C terminal domain of PspA in regulation and stress-sensing, and they support the proposed role of this domain [14].

It is intriguing that neither PspA(1–144) nor PspA(145–222) interact with TatA-*Strep*, albeit a Psp system down-regulated by PspA(145–222) is able to respond to the presence of

this Psp response-inducing membrane protein. TatA-*Strep* causes this effect on PspF activity although it does not detectably interact with the PspA domains, which are not membrane associated. PspA(145–222) must be bound to the PspF hexamer to keep its activity at the observed very low level, and the activation suggests that there are transient interactions with the membrane that are below any detection limit, as the signal must be somehow transferred to PspFA. Such transient membrane interactions have been already postulated for the native PspFA complex [28,16]. It may be hypothesized that the TatA-generated stress signal induces interactions between PspA C-termini or other Psp system components that are responsible for the observed reduction of PspF inhibition. The nature of the membrane stress signal generated by TatA is so far unknown. On one hand, TatA is known to destabilize membranes, on the other hand it has been shown to interact with the Psp system [25,23]. It could be that TatA clusters can induce SCE stress, and this might be sensed by the system without direct TatA interactions [14]. As full-length PspA interacts with TatA, it is likely that this interaction can also contribute to sensing [23].

Intermolecular interactions as mediated by PspA(145–222) may explain the enhancement of PspF activity in the presence of full-length PspA

Despite a clear downregulation of PspF by PspA(1–144) and PspA(145–222) in a Δ*pspA* background, the responsiveness of the PspA(145–222) inhibited system to the membrane stressor TatA already suggested that the interactions of PspA(1–144) and PspA(145–222) with PspF have distinct functions. Strikingly, PspA(145–222) weakly induced the promoter activity in the presence of wt-PspA, whereas PspA(1–144) still silenced the promoter under these experimental conditions (Figs 1 and 4). As the C-terminus is known to mediate oligomerization of PspA, we expected that the observed upregulation was due to an induction of wt-PspA oligomerization and a concomitant membrane localization. However, although more PspA was present in the cells as consequence of the upregulation, a shift to a membrane associated state did not occur and there was rather more soluble PspA (Fig 4). The increased levels of soluble PspA in response to PspA(145–222) did not lower the transcriptional activity of PspF. This contrasts the effect of increased levels of recombinant PspA or PspA(1–144), which result in a down-regulation of the *pspA* promoter activity (Fig 4). As PspA(145–222) interacts with itself and thus also with full-length PspA (Figs 4 and 5), we propose that the interaction of PspA(145–222) with PspF-bound wt-PspA affects the interaction of this PspA domain in wt-PspA with PspF, resulting in conformational changes of PspF-bound PspA and an increased PspF activity. We do not think that PspA(145–222) can induce a dissociation of wt-PspA from PspF, as this would consequently allow excess PspA(145–222) to associate with the liberated PspF, which would inhibit its activity, considering that PspA(145–222) silences PspF in the absence of PspA (Figs 1 and 3). PspA(145–222) might interact via formations of antiparallel coiled coils, as evidenced by the two-hybrid data (Fig 5), but this is certainly speculative, and the helical structure of this PspA domain remains to be experimentally confirmed.

PspA(145–222) can mediate oligomerizations that may contribute to membrane interactions and Psp system inducibility

We noted that PspA(145–222) is completely soluble, although it can mediate PspA/PspA interactions (Figs 4 and 5). One explanation for this observation could be, that PspA can only interact with membranes when it contains its N-terminal region that can form an amphipathic helix [12]. Importantly, the monomeric PspA(1–144) is also soluble, indicating that single amphipathic helices are not stably membrane interacting *per se*. Under non-stress conditions, the monomeric PspA(1–144) proteins have their N-terminus folded back onto

the surface of the coiled coil, which is proposed to be the "parking position" of that sensor region [13]. *In vitro*, PspA(2–24) turned into a helical structure in the presence of negatively charged phospholipids and it was able to inhibit the ATPase activity of PspF [12]. The same was reported for PspA(25–47). This stretch of residues includes residues whose PspF-regulatory function has been established [13]. Although it must be noted that in these studies this fragment was taken out of its stable coiled coil environment, it appears that already the single helix of that coiled coil can regulate PspF with its known regulatory functionalities. However, only the N-terminal amphipathic helix is an obvious candidate for a region that is mediating membrane interaction. It is therefore likely that the oligomerization as mediated by the C-terminus of PspA promotes efficient membrane interactions of the N-termini that can sense stress, as multiple weak membrane interactions are additive in the oligomer, which strengthens the membrane interaction of oligomeric full-length PspA. Another contribution to this interaction will certainly be the reported binding of PspA to the C-terminus of PspC [8].

PspA(145–222) is necessary to keep PspF activity on its basal level in a native regulatory system

The Psp system and especially its upregulation currently becomes more complex than thought initially. The hypothesis that PspA and more specifically the PspA(1–144) fragment dissociates from PspF was challenged by the dissociation constant of a PspA(1–144)/PspF(1–265) complex of ~1 μM and a half-life time of the complex of ~43 minutes [13]. It has been proposed that a fast regulatory response might be possible without a dissociation of PspA from PspF. We observed that, at physiological levels, full-length PspA is much more inhibitory to PspF that the soluble PspA(1–144) domain, suggesting that the PspA(145–222) domain contributes to PspF inhibition by PspA (Fig 8), which agrees with interaction and regulation data (Figs 1–5).

Induction of the system by the N-terminal membrane anchor of TatA leads to an activation of PspF in the same range as observed for the activation by PspA(1–144). This could be a coincidence, but the reason might be that induction of the system leads to a release of the C-terminal part of PspA from its binding site on PspF. The induced state of the PspAF complex might be mimicked by the PspA(1–144)/PspF complex lacking the C-terminus of PspA. In agreement with this view would be that PspA(145–222), which alone is able to bind and silence PspF activity (Fig 1), can (i) enhance the activity of PspF in the presence of full-length PspA (Fig 4), (ii) bind to other PspA(145–222) domains (Fig 5), and (iii) respond to membrane stress (Fig 7). The mechanism by which the PspA(145–222) domain inhibits PspF is not necessarily the same as the inhibitory mechanism of the PspA(1–144) domain, which affects the ATPase activity [13]. In a nutshell, the regulation by the PspA(145–222) domain agrees with all current models of PspF regulation [16,8,13]. Future studies will hopefully clarify the exact role of the different PspA domains for signaling and activation of PspF in response to membrane stress.

Supporting information

S1 Table. Plasmids and primers used in the bacterial-2-hybrid assay.
(DOCX)

S2 Table. Primers used for QuikChange of pUL-*pspF*strep-*pspABC*-H6.
(DOCX)

Acknowledgments

We thank Nane Griem-Krey for construction of vector pABS-H10*mhip-pspA*(145–222), and Inge Reupke and Sybille Traupe for technical assistance. This work was funded by the German Research Foundation (DFG grant BR2285/4-2).

Author Contributions

Conceptualization: Eyleen Sabine Heidrich, Thomas Brüser.

Formal analysis: Eyleen Sabine Heidrich.

Funding acquisition: Thomas Brüser.

Investigation: Eyleen Sabine Heidrich.

Methodology: Eyleen Sabine Heidrich.

Project administration: Thomas Brüser.

Resources: Thomas Brüser.

Supervision: Thomas Brüser.

Writing – original draft: Eyleen Sabine Heidrich, Thomas Brüser.

Writing – review & editing: Thomas Brüser.

References

1. Flores-Kim J, Darwin AJ (2016) The phage shock protein response. Annu Rev Microbiol 70: 83–101. https://doi.org/10.1146/annurev-micro-102215-095359 PMID: 27297125
2. Joly N, Engl C, Jovanovic G, Huvet M, Toni T, Cheng X et al. (2010) Managing membrane stress: the phage shock protein (Psp) response, from molecular mechanisms to physiology. FEMS Microbiol. Rev. 34 (5): 797–827. https://doi.org/10.1111/j.1574-6976.2010.00240.x PMID: 20636484
3. Jovanovic G, Weiner L, Model P (1996) Identification, nucleotide sequence, and characterization of PspF, the transcriptional activator of the *Escherichia coli* stress-induced *psp* operon. J. Bacteriol. 178 (7): 1936–1945. PMID: 8606168
4. Dworkin J, Jovanovic G, Model P (1997) Role of upstream activation sequences and integration host factor in transcriptional activation by the constitutively active prokaryotic enhancer-binding protein PspF. J. Mol. Biol. 273 (2): 377–388. https://doi.org/10.1006/jmbi.1997.1317 PMID: 9344746
5. Elderkin S, Bordes P, Jones S, Rappas M, Buck M (2005) Molecular determinants for PspA-mediated repression of the AAA transcriptional activator PspF. J. Bacteriol. 187 (9): 3238–3248. https://doi.org/10.1128/JB.187.9.3238-3248.2005 PMID: 15838051
6. Dworkin J, Jovanovic G, Model P (2000) The PspA protein of *Escherichia coli* is a negative regulator of σ^{54}-dependent transcription. J. Bacteriol. 182 (2): 311–319. PMID: 10629175
7. Kleerebezem M, Crielaard W, Tommassen J (1996) Involvement of stress protein PspA (phage shock protein A) of *Escherichia coli* in maintenance of the protonmotive force under stress conditions. EMBO J. 15 (1): 162–171. PMID: 8598199
8. Flores-Kim J, Darwin AJ (2015) Activity of a bacterial cell envelope stress response is controlled by the interaction of a protein binding domain with different partners. J. Biol. Chem. 290 (18): 11417–11430. https://doi.org/10.1074/jbc.M114.614107 PMID: 25802329
9. Maxson ME, Darwin AJ (2006) PspB and PspC of *Yersinia enterocolitica* are dual function proteins: regulators and effectors of the phage-shock-protein response. Mol. Microbiol. 59 (5): 1610–1623. https://doi.org/10.1111/j.1365-2958.2006.05047.x PMID: 16468999
10. Horstman NK, Darwin AJ (2012) Phage shock proteins B and C prevent lethal cytoplasmic membrane permeability in *Yersinia enterocolitica*. Mol. Microbiol. 85 (3): 445–460. https://doi.org/10.1111/j.1365-2958.2012.08120.x PMID: 22646656
11. Yamaguchi S, Reid DA, Rothenberg E, Darwin AJ (2013) Changes in Psp protein binding partners, localization and behaviour upon activation of the Yersinia enterocolitica phage shock protein response. Mol. Microbiol. 87 (3): 656–671. https://doi.org/10.1111/mmi.12122 PMID: 23290031

12. McDonald C, Jovanovic G, Wallace BA, Ces O, Buck M (2017) Structure and function of PspA and Vipp1 N-terminal peptides. Insights into the membrane stress sensing and mitigation. Biochim. Biophys. Acta 1859 (1): 28–39.
13. Osadnik H, Schöpfel M, Heidrich E, Mehner D, Lilie H, Parthier C et al. (2015) PspF-binding domain PspA1-144 and the PspA·F complex: New insights into the coiled-coil-dependent regulation of AAA+ proteins. Mol. Microbiol. 98 (4): 743–759. https://doi.org/10.1111/mmi.13154 PMID: 26235546
14. McDonald C, Jovanovic G, Ces O, Buck M (2015) Membrane stored curvature elastic stress modulates recruitment of maintenance proteins PspA and Vipp1. mBio 6 (5): 15.
15. Joly N, Burrows PC, Engl C, Jovanovic G, Buck M (2009) A lower-order oligomer form of phage shock protein A (PspA) stably associates with the hexameric AAA(+) transcription activator protein PspF for negative regulation. J. Mol. Biol. 394 (4): 764–775. https://doi.org/10.1016/j.jmb.2009.09.055 PMID: 19804784
16. Jovanovic G, Mehta P, McDonald C, Davidson AC, Uzdavinys P, Ying L et al. (2014) The N-terminal amphipathic helices determine regulatory and effector functions of phage shock protein A (PspA) in *Escherichia coli*. J. Mol. Biol. 426 (7): 1498–1511. https://doi.org/10.1016/j.jmb.2013.12.016 PMID: 24361331
17. Yamaguchi S, Gueguen E, Horstman NK, Darwin AJ (2010) Membrane association of PspA depends on activation of the phage-shock-protein response in *Yersinia enterocolitica*. Mol. Microbiol. 78 (2): 429–443. PMID: 20979344
18. Bergler H, Abraham D, Aschauer H, Turnowsky F (1994) Inhibition of lipid biosynthesis induces the expression of the *pspA* gene. Microbiology 140: 1937–1944. https://doi.org/10.1099/13500872-140-8-1937 PMID: 7921245
19. Baba T, Ara T, Hasegawa M, Takai Y, Okumura Y, Baba M et al. (2006) Construction of *Escherichia coli* K-12 in-frame, single-gene knockout mutants. The Keio collection. Mol Syst Biol 2: 2006.0008. https://doi.org/10.1038/msb4100050 PMID: 16738554
20. Miller JH (1972) Experiments in molecular genetics. Cold Spring Harbor Laboratory. Cold Spring Harbor, NY
21. Datsenko KA, Wanner BL (2000) One-step inactivation of chromosomal genes in *Escherichia coli* K-12 using PCR products. Proc. Natl. Acad. Sci. U S A 97 (12): 6640–6645. https://doi.org/10.1073/pnas.120163297 PMID: 10829079
22. Wilms B, Hauck A, Reuss M, Syldatk C, Mattes R, Siemann M et al. (2001) High-cell-density fermentation for production of L-N-carbamoylase using an expression system based on the *Escherichia coli rhaBAD* promoter. Biotechnol Bioeng 73 (2): 95–103. PMID: 11255157
23. Mehner D, Osadnik H, Lünsdorf H, Brüser T (2012) The Tat system for membrane translocation of folded proteins recruits the membrane-stabilizing Psp machinery in *Escherichia coli*. J. Biol. Chem. 287 (33): 27834–27842. https://doi.org/10.1074/jbc.M112.374983 PMID: 22689583
24. Richter S, Brüser T (2005) Targeting of unfolded PhoA to the TAT translocon of *Escherichia coli*. J. Biol. Chem. 280 (52): 42723–42730. https://doi.org/10.1074/jbc.M509570200 PMID: 16263723
25. Hou B, Heidrich ES, Mehner-Breitfeld D, Brüser T (2018) The TatA component of the twin-arginine translocation system locally weakens the cytoplasmic membrane of *Escherichia coli* upon protein substrate binding. J. Biol. Chem. 293 (20): 7592–7605. https://doi.org/10.1074/jbc.RA118.002205 PMID: 29535185
26. Lupas A, van Dyke M, Stock J (1991) Predicting coiled coils from protein sequences. Science 252 (5009): 1162–1164. https://doi.org/10.1126/science.252.5009.1162 PMID: 2031185
27. Flores-Kim J, Darwin AJ (2012) Phage shock protein C (PspC) of *Yersinia enterocolitica* is a polytopic membrane protein with implications for regulation of the Psp stress response. J. Bacteriol. 194 (23): 6548–6559. https://doi.org/10.1128/JB.01250-12 PMID: 23024349
28. Mehta P, Jovanovic G, Lenn T, Bruckbauer A, Engl C, Ying L et al. (2013) Dynamics and stoichiometry of a regulated enhancer-binding protein in live *Escherichia coli* cells. Nat. Commun. 4: 1997. https://doi.org/10.1038/ncomms2997 PMID: 23764692

Supporting Information

Evidence for a second regulatory binding site on PspF that is occupied by the C-terminal domain of PspA

Eyleen S. Heidrich and Thomas Brüser

S1 Table: Plasmids and primers used in the bacterial-2-hybrid assay.

Plasmid	Primers used for cloning	Reference
pUT18	-	Euromedex
pUT18C	-	Euromedex
pUT18C-zip	-	Euromedex
pKNT25	-	Euromedex
pKT25	-	Euromedex
pKT25-zip	-	Euromedex
pKN-strep-T25 **pU-strep-T18**	**NdeI-strep-BamHI-pKTN25/pUT18-F:** TTA ATC ATA TGT GGA GCC ACC CGC AGT TCG AAA AAG GAT CCA CCA TGA TTA CGC CAA G **pKNT/pUT-NdeI-R**: ATA TAC ATA TGT GTT TCC TGT GTG AAA TTG TTA TC	This work
pUT18C-*pspA*(25-222)-strep **pKT25-*pspA*(25-222)-strep**	**XbaIgBAmHI-pspA(25)-F**: TAT AAT CTA GAG GGA TCC CCA CAG AAA CTG GTT CG ***pspA*(144)ggKpnIstrepTAAEcoRI-R**: TTA ATG AAT TCT TAT TTT TCG AAC TGC GGG TGG CTC CAG GGT ACC CCC TGA TGA CGT AAC ATC AA TG	This work
pUT18C-*pspA*(2-25)-strep **pU-strep-*pspA*(2-25)-T18** **pKT25-*pspA*(2-25)-strep** **pKN-strep-*pspA*(2-25)-T25**	**BamHI-*pspA*(2)-F**: TTT AAG GAT CCG GTA TTT TTT CTC GCT TTG CCG ***pspA*(25)ggKpnI:R**: TAT AAG GTA CCC CTG GAT CTT CCG CTT TCT CTA AC	This work
pUT18C-*pspA*(2-85)-strep **pU-strep-*pspA*(2-85)-T18** **pKT25-*pspA*(2-85)-strep** **pKN-strep-*pspA*(2-85)-T25**	**BamHI-*pspA*(2)-F:** TTT AAG GAT CCG GTA TTT TTT CTC GCT TTG CCG ***pspA*(85)ggKpnI-R**: TAT AAG GTA CCC CAT CCT CTC TCT CTT TCA GC	This work
pU-strep-*pspA*(2-144)-T18 **pKN-strep-*pspA*(2-144)-T25**	**BamHI-*pspA*(2)-F**: TTT AAG GAT CCG GTA TTT TTT CTC GCT TTG CCG ***pspA*(144)ggKpnI-R:** TTA ATG GTA CCC CCT GAT GAC GTA ACA TCA ATG	This work
pUT18C-*pspA*(2-186)-strep **pU-strep-*pspA*(2-186)-T18** **pKT25-*pspA*(2-186)-strep** **pKN-strep-*pspA*(2-186)-T25**	**BamHI-*pspA*(2)-F:** TTT AAG GAT CCG GTA TTT TTT CTC GCT TTG CCG ***pspA*(186)ggKpnI-R**: TTA TAG GTA CCC CGC TGT GGC TTT CTG CTT CCG C	This work
pUT18C-*pspA*(2-222)-strep **pU-strep-*pspA*(2-222)-T18** **pKT25-*pspA*(2-222)-strep** **pKN-strep-*pspA*(2-222)-T25**	**BamHI-*pspA*(2)-F**: TTT AAG GAT CCG GTA TTT TTT CTC GCT TTG CCG ***pspA*(222)ggKpnI-R**: AAT TTG GTA CCC CTT GAT TGT CTT GCT TCA TTT TG	This work
pUT18C-*pspA*(25-85)-strep **pU-strep-*pspA*(25-85)-T18** **pKT25-*pspA*(25-85)-strep** **pKN-strep-*pspA*(25-85)-T25**	**BamHI-*pspA*(25)-F**: TTT AAG GAT CCC CAC AGA AAC TGG TTC G ***pspA*(85)ggKpnI-R**: TAT AAG GTA CCC CAT CCT CTC TCT CTT TCA GC	This work
pUT18C-*pspA*(25-144)-strep **pU-strep-*pspA*(25-144)-T18** **pKT25-*pspA*(25-144)-strep** **pKN-strep-*pspA*(25-144)-T25**	**BamHI-*pspA*(25)-F:** TTT AAG GAT CCC CAC AGA AAC TGG TTC G ***pspA*(144)ggKpnI-R**: TTA ATG GTA CCC CCT GAT GAC GTA ACA TCA ATG	This work
pUT18C-*pspA*(25-186)-strep **pU-strep-*pspA*(25-186)-T18** **pKT25-*pspA*(25-186)-strep** **pKN-strep-*pspA*(25-186)-T25**	**BamHI-*pspA*(25)-F:** TTT AAG GAT CCC CAC AGA AAC TGG TTC G ***pspA*(186)ggKpnI-R:** TTA TAG GTA CCC CGC TGT GGC TTT CTG CTT CCG C	This work
pUT18C-*pspA*(25-222)-strep **pU-strep-*pspA*(25-222)-T18** **pKT25-*pspA*(25-222)-strep** **pKN-strep-*pspA*(25-222)-T25**	**BamHI-*pspA*(25)-F:** TTT AAG GAT CCC CAC AGA AAC TGG TTC G ***pspA*(222)ggKpnI-R**: AAT TTG GTA CCC CTT GAT TGT CTT GCT TCA TTT TG	This work

pUT18C-*pspA*(86-144)-strep **pU-strep-*pspA*(86-144)-T18** **pKT25-*pspA*(86-144)-strep** **pKN-strep-*pspA*(86-144)-T25**	**BamHI-*pspA*(86)-F:** TTT AAG GAT CCC TGG CAC GTG CAG CGT TAA TTG ***pspA*(144)ggKpnI-R**: TTA ATG GTA CCC CCT GAT GAC GTA ACA TCA ATG	This work
pUT18C-*pspA*(86-186)-strep **pU-strep-*pspA*(86-186)-T18** **pKT25-*pspA*(86-186)-strep** **pKN-strep-*pspA*(86-186)-T25**	**BamHI-*pspA*(86)-F:** TTT AAG GAT CCC TGG CAC GTG CAG CGT TAA TTG ***pspA*(186)ggKpnI-R:** TTA TAG GTA CCC CGC TGT GGC TTT CTG CTT CCG C	This work
pUT18C-*pspA*(86-222)-strep **pU-strep-*pspA*(86-222)-T18** **pKT25-*pspA*(86-222)-strep** **pKN-strep-*pspA*(86-222)-T25**	**BamHI-*pspA*(86)-F**: TTT AAG GAT CCC TGG CAC GTG CAG CGT TAA TTG ***pspA*(222)ggKpnI-R:** AAT TTG GTA CCC CTT GAT TGT CTT GCT TCA TTT TG	This work
pUT18C-*pspA*(145-186)-strep **pU-strep-*pspA*(145-186)-T18** **pKT25-*pspA*(145-186)-strep** **pKN-strep-*pspA*(145-186)-T25**	**BamHI-*pspA*(145)-F:** TTT AAG GAT CCG CGG CAA ACT CGT CGC GCG ATG ***pspA*(186)ggKpnI-R**: TTA TAG GTA CCC CGC TGT GGC TTT CTG CTT CCG C	This work
pUT18C-*pspA*(145-222)-strep **pU-strep-*pspA*(145-222)-T18** **pKT25-*pspA*(145-222)-strep** **pKN-strep-*pspA*(145-222)-T25**	**BamHI-*pspA*(145)-F**: TTT AAG GAT CCG CGG CAA ACT CGT CGC GCG ATG ***pspA*(222)ggKpnI-R**: AAT TTG GTA CCC CTT GAT TGT CTT GCT TCA TTT TG	This work
pUT18C-*pspA*(145-222)-strep **pU-strep-*pspA*(145-222)-T18** **pKT25-*pspA*(145-222)-strep** **pKN-strep-*pspA*(145-222)-T25**	**BamHI-*pspA*(145)-F**: TTT AAG GAT CCAGC TTC GGT AAA CAA AAA TCG ***pspA*(222)ggKpnI-R**: AAT TTG GTA CCC CTT GAT TGT CTT GCT TCA TTT TG	This work
pUT18C-*pspA*(186-222)-strep **pU-strep-*pspA*(186-222)-T18** **pKT25-*pspA*(186-222)-strep** **pKN-strep-*pspA*(186-222)-T25**	**BamHI-*pspA*(186)-F:** TTA AGG ATC CAG CTT CGG TAA ACA AAA ATC G ***pspA*(222)ggKpnI-R**: AAT TTG GTA CCC CTT GATT GTC TTG CTT CAT TTT G	This work
pUT18C-*pspF* strep **pU-strep-*pspF*-T18** **pKT25-*pspF*-strep** **pKN-strep-*pspF*-T25**	**BamHI-*pspF*(2)-F:** TTT AAG GAT CCG CAG AAT ACA AAG ATA ATT TAC ***pspF*(325)ggKpnI-R:** TAT AAG GTA CCC CAA TCT GGT GCT TTT TCA ACA ACG C	This work

3.3 „*Negatively charged phospholipids and PspC both contribute to membrane stress sensing by the Psp system in* Escherichia coli"

Autoren:	Eyleen S. Heidrich, Annika Schürmann und Thomas Brüser
Art der Autorenschaft:	Erst-Autorin
Zugehörigkeit:	Leibniz Universität Hannover, Institut für Mikrobiologie, Herrenhäuser Straße 2, 30419 Hannover
Art des Artikels:	Forschungsartikel
Beitrage:	**Eyleen S. Heidrich:** Konzeption und Planung der Studie zusammen mit Thomas Brüser, Planung und Durchführung aller Experimente, Datenanalyse, Präparation der Abbildungen, Anfertigung des ersten Manuskriptentwurfs **Annika Schürmann:** Durchführung der Dünnschichtchromatographie unter Aufsicht von Eyleen S. Heidrich **Thomas Brüser:** Konzeption und Planung der Studie zusammen mit Eyleen S. Heidrich, Datenanalyse und Fertigstellung des Manuskripts

Wissenschaftliche Einordnung

McDonald *et al.* (2015) postulierten basierend auf *in-vitro*-Analysen, dass eine Veränderung des an der Cytoplasmamembran anliegenden Krümmungsstresses möglicherweise das Psp-System induzierende Signal darstellen könnte [77]. Sie postulierten weiterhin, dass die Wahrnehmung von SCE-Stress durch das Psp-System in einem PspBC-unabhängigen Mechanismus erfolgt. Da die Lipid-defizienten *E.-coli*-Stämme UE54 (Δ*pgsA,* [151]) und GN10 (Δ*pssA,* [152]) im Labor vorlagen, sollte diese Hypothese *in vivo* getestet werden.

Da die Cytoplasmamembran aufgrund der *pgsA*-Deletion in UE54 vornehmlich aus PE besteht, kann in diesem Fall angenommen werden, dass erhöhter Krümmungsstress an der Cytoplasmamembran in diesem Stamm anliegt. Es zeigte sich, dass es im *E.-coli*-Stamm UE54, im Vergleich zum korrespondierenden Wildtypstamm UE53 [153], zu einer Membranrekrutierung PspAs kommt, was den Schluss zuließ, dass eine Erhöhung des SCE-Stresses tatsächlich zu einer Membranrekrutierung PspAs führt. Im Gegensatz zu der von McDonald *et al.* (2015) aufgestellten Hypothese war *in vivo* die Membraninteraktion PspAs eindeutig PspC-abhängig [77]. Interessanterweise führte zusätzlicher Membranstress, ausgelöst durch die rekombinante Produktion TatAs, in diesem Stammhintergrund nicht zu einer weiteren nachweisbaren Induktion des Psp-Systems.

Auch die erhöhte Abundanz von negativ geladenen Phospholipiden im *pssA*-Deletionsstamm führte im Gegensatz zum korrespondieren Wildtyp zu einer Membraninteraktion PspAs und zu einer Induktion des Psp-Systems.

Negatively charged phospholipids and PspC both contribute to membrane stress sensing by the Psp system in *Escherichia coli*

Eyleen S. Heidrich, Annika Schürmann, and Thomas Brüser*

From the Institute of Microbiology, Leibniz Universität Hannover, Herrenhäuser Straße 2, 30419 Hannover

*To whom correspondence should be addressed: Thomas Brüser, Institut für Mikrobiologie, Leibniz Universität Hannover, Herrenhäuser Straße 2, 30419 Hannover; brueser@ifmb.uni-hannover.de

ABSTRACT

In *Escherichia coli* and other enterobacteria, the phage shock protein (Psp) response is induced by diverse membrane stresses. The components PspA, PspB, and PspC somehow sense these different Psp stimuli. While PspB and PspC are integral membrane proteins, PspA transiently associates with membranes via lipid and/or PspC interactions, which is believed to trigger the Psp response. Here we show that, in *Escherichia coli*, the lack of cardiolipin and phosphatidylglycerol induces membrane-association of PspA. This membrane association also depended on PspC. Phosphatidylethanolamine deficiency promoted an even stronger membrane recruitment, indicating that negatively charged phospholipids indeed enhance the interaction. The data thus indicate a tight cooperation of lipid interactions and PspC for sensing of membrane stress by the Psp system *in vivo*.

KEYWORDS

Bacterial stress response, phage shock proteins, membrane interactions, phospholipids, *Escherichia coli*

ABBREVIATIONS

CL, cardiolipin; Psp, phage shock protein; SCE, stored curvature elastic; PC, phosphatidylcholine; PE, phosphatidylethanolamine; PG, phosphatidylglycerol; PS, phosphatidylserine

INTRODUCTION

Prokaryotes developed a range of stress response systems. The phage shock protein (Psp) system of *Escherichia coli* is one of these systems and its stress-related signaling is in the focus of current Psp research [1, 2]. The Psp system is stimulated by a wide range of stresses that have a negative impact on the integrity of the cytoplasmic membrane, such as infection with filamentous phages, organic solvents, osmotic shock, mislocalization of secretins, or production of membrane-destabilizing proteins [3–7]. The Psp system of *E. coli* consists of seven components, four of which are part of the regulatory cascade, namely PspA, PspB, PspC, and PspF. PspA is the most abundant component of these and homologs of PspA are believed to associate with membranes in a wide range of organisms [8]. In *E. coli*, PspA, PspB and PspC are encoded in a polycistronic operon together with PspD and PspE. The *pspABCDE* operon and the monocistronic *pspG* are σ^{54}-dependently expressed and regulated by the constitutively produced bacterial enhancer binding protein PspF [9]. PspF is an AAA+ family ATPase whose activity is regulated by PspA in a negative feed-back loop. PspF and PspA assemble to a soluble PspFA complex [10]. PspB and PspC are interacting small membrane proteins that can transmit stress signals to the PspFA complex [11, 12]. Besides interacting with PspF, PspA can also interact with the C terminus of PspC upon a stimulus. After Psp system induction, PspA becomes highly abundant in the cell and forms large associations at cytoplasmic membrane surface that possibly protect the membrane from further damage [13–15]. Although it seems clear that stress signals can be transmitted via the PspC C-terminus, it is still unresolved which component of the Psp system is actually the sensor. There is evidence that a conformational change of PspC in response to stress disrupts an interaction of the PspC C-terminus with PspB, which enables PspA interactions that trigger the response [11]. In this model, the PspFA complex is expected to be at least transiently present at membranes to receive a Psp signal transmitted by PspBC. This was supported by Mehta *et al*. who showed that the PspFA complex

transiently associates with the cytoplasmic membrane [12]. Recently, PspA/lipid interactions came into focus as membrane stored curvature elastic (SCE) stress was found to result in membrane recruitment of PspA [16], and sensing of SCE stress could integrate many different stress signals. SCE stress-dependent membrane interactions and regulatory effects were so far only addressed *in vitro* [16]. Lipid vesicle interaction of purified PspA was enhanced by SCE stress and anionic lipid content [14, 16, 17]. This interaction was initially described to be phosphatidylglycerol (PG)-dependent, as oligomeric PspA co-sediment with phosphatidylcholine (PC)-liposomes only if they contained PG [14]. Also the pathway intermediate anionic phosphatidylserine (PS), but not the abundant *E. coli* lipids phosphatidylethanolamine (PE) or cardiolipin (CL) could promote liposome association of oligomeric PspA [14]. In contrast to these results, it was later observed that PspA binds to liposomes with PE-induced SCE stress [16], and the same was found with increasing contents of anionic lipids [17, 16]. The latter was described to be due to the induction of an amphipathic helix formation of the N-terminal peptide of PspA [17]. In soluble PspA, the N-terminal helix folds back to a coiled-coil [10]. It was therefore proposed that the N-terminal peptide of PspA forms the amphipathic membrane-interacting helix in response to SCE stress, bypassing the PspBC-dependence of other Psp stimuli [17, 16]. However, these aspects have not yet been addressed *in vivo*.

Here, we show that, *in vivo*, PspA is membrane-recruited under SCE stress conditions in an *E. coli* strain lacking CL and PG, indicating that the most abundant negatively charged phospholipids are not required for an SCE-induced membrane interaction. Membrane association was absolutely PspC dependent in that strain. Membrane association was much enhanced in a PE deficient strain that contains increased levels of anionic phospholipids. Therefore, *in vivo*, PspC and lipid interactions apparently cooperate to achieve membrane association of PspA, which is important for stress sensing.

EXPERIMENTAL PROCEDURES

Strains, growth conditions and plasmids All *E. coli* strains and plasmids used in this study are listed in Table1. Strains were cultivated in LB-medium (1 % tryptone, 1 % NaCl, 0.5 % yeast extract) aerobically at 37°C, except in experiments that included strains harbouring the temperature-sensitive plasmid pMS5 (30°C). Ampicillin (100 µg/ml), chloramphenicol (25µg/ml) and kanamycin (25 µg/ml) were used for selection as needed. Strain UE54 *kan*^{S} was generated from UE54 by removal of the kanamycin resistance gene and used to create UE54 Δ*pspC* by phage transduction using the Keio collection strain BW25113 Δ*pspC* as donor [18]. The position of the kanamycin cassette was confirmed by PCR. GN10 was cured from pMS5 as described in [19].

For construction of all pBAD30 derivatives, *clsB* was removed from pBAD30-*clsB* with NdeI/HindIII cleavage, and fragments were cloned into these sites. For construction of pBAD30-*pspC*-H6, pABS-*pspC*-H6 [7] was cleaved with NdeI/HindIII to generate the *pspC-H6* insert. pBAD30-*tatA*-strep was constructed by cloning the NdeI/HindIII *tatA*-strep fragment from pBW-*tatA*-strep [7]. pBAD30-H10*mhip* was generated by amplifying *mhip* from pEXH5-tac with primers NdeI-H10-*mhip*-F (ATA TAT CAT ATG CAT CAT CAC CAC CAC CAC CAC CAC CAC CAC TCC GCT CCC GCC AAT G) and *hip*-BamHI-R (ATA TAT AGG ATC CGC CGG CCT TCA GGG TC), cleavage with NdeI/BamHI and ligation into NdeI/BamHI sites of the pABS-*pspC*-H6 backbone, resulting in pABS-H10*mhip*. pABS-*h10mhip* was then cleaved with NdeI/HindIII and H10*mhip* was ligated as the other described fragments into pBAD30.

Biochemical methods 100 ml cultures were used for cell fractionation assays. For arabinose-dependent protein production, 0.2 % arabinose was added at OD 0.5 – 0.6 and cultivation was continued for 3 hours. Cells were harvested by centrifugation at 4,500 x g for 10 min and 4°C. 100 ml with cultures, normalized to an optical density of 1, were harvested. Cell pellets were

resuspended in homogenization puffer (50 mM Tris-HCl pH 8.0, 250 mM NaCl), DNaseI and 1 mM PMSF were added, and cells were homogenized by ultrasonication on ice (micro-tip, 60% output, intensity 2-3, 3 x 30 sec pulse). Cell debris was removed by high-speed centrifugation at 20,000 x g for 10 min at 4°C. Soluble and membrane fractions were separated by ultra-centrifugation at 130,000 x *g* for 30 min at 4°C. The soluble fraction was carefully removed, and the membrane pellet was resuspended in 1 vol homogenization buffer. SDS-PAGE and Western-blotting were performed according to standard protocols [20, 21]. Antibodies specific for His-Tag, PspA or DnaK were used for ECL detections.

Lipid extraction and thin-layer chromatography

Lipid extraction was performed as described by Bligh and Dyer [22] and Ames [23] using 15 ml of cultures grown to late exponential phase. Cells were harvested by centrifugation and resuspended with 0.2 mL of 0.9 % NaCl. 0.25 ml chloroform and 0.5 ml methanol were added subsequently and vortexed vigorously. 0.95 mL chloroform and methanol were added and the suspension was mixed. For phase separation, samples were centrifuged at 500 x *g* for 5 min, the chloroform phase was transferred in a glass tube, and chloroform was evaporated overnight. Dried lipids were resolved in 100 µl chloroform and thin-layer chromatography (TLC) was performed using 30 µl of the lipid extract according to previous methods [24].

RESULTS

In a recent study, it could be shown that the N terminal peptide of PspA can form an alpha helix in the presence of anionic phospholipids [17], and it was proposed that SCE stress and the binding to anionic phospholipids triggers the upregulation of the Psp response, possibly bypassing a PspBC-dependent signaling. As the lipid interaction of PspA and its effect on the Psp regulatory cascade were so far only investigated *in vitro*, it was an open question whether SCE stress sensing can bypass PspBC also *in vivo*.

Negatively charged phospholipids enhance the membrane interaction of PspA *in vivo,* but no specific phospholipid is strictly required

In order to check *in vivo* whether PspA localization is influenced by specific phospholipids, we performed cell fractionation assays of *E. coli* strains with deletions in specific phospholipid biogenesis genes. Chosen strains were either deficient in *pgsA* and therefore lacked CL or PG (UE54), or were *pssA* deficient (GN10) and therefore did not produce PE. The *pgsA* mutant is viable due to additional deletions in *lpp* and *rcsF* that suppress lethal lipoprotein mis-targeting and stress signaling phenotypes. GN10 grows only in the presence of divalent cations ($MgCl_2$) [25]. It is propagated with a vector (pMS5) that complements *pssA in trans*, and this plasmid must be cured from the strain to do experiments in the *pssA*-deficient background [26]. A scheme of the lipid biosynthesis of the *E. coli* strain used in this study is provided in Figure 1A. For comparison, the corresponding lipid wild type strains were fractionated in parallel, which is UE53 for the *pgsA* mutant strain, and the pMS5-containing GN10 for the *pssA* knock-out strain. While PspA was predominantly detectable in the soluble fractions of the lipid wild type strains UE53 and GN10/pMS5, significant amounts of PspA fractionated with the membranes in the *pgsA* mutant strain UE54 and in the *pssA* mutant strain GN10 (Figure 1B). As PspA was soluble in UE53, we could exclude that the deletion of *lpp* and *rcsF* in strain UE53 had any effect on the Psp system. More importantly, PG and CL were not strictly required for the membrane localization of PspA, which was distributed in an approx. 1:1 ratio between the soluble and the membrane fractions in the *pgsA* mutant. In contrast, in GN10 that lacks PE, PspA expression was clearly upregulated, indicating an induction of the Psp response, and the major portion of detectable PspA was membrane localized (Figure 1B). The high abundance of negatively charged lipids in these membranes thus likely caused a membrane association of PspA, and PE itself is clearly dispensable for this membrane interaction. For all strains, lipid extraction was performed and lipid deficiency could be confirmed by thin-layer

chromatography (Figure 1C). Together, these data indicated that neither the anionic phospholipids PG and CL nor the zwitterionic PE are specifically necessary for PspA membrane interaction, but the higher abundance of negatively charged lipids in the PE deficient strain apparently promoted a membrane association of PspA. Further, the higher levels of the Psp system component PspA in GN10 indicated that PE deficiency results in increased steady state activity of PspF *in vivo*, which liklely is a result of the membrane recruitment of PspA.

The transmission of a Psp stress signal does not depend on CL or PG

We now asked the question whether the absence of specific phospholipids effects sensing of membrane stress signaling. First, we examined potential effects on transmission of a stress signal to the PspFA complex. In the signaling cascade that has been established with protein induced membrane stress, the interaction of the C-terminus of PspC is responsible for transmission of stress signals to PspA [11], which is why PspC it is a positive regulator of the Psp response [4]. We thus determined whether the inducibility of the Psp system by recombinant levels of PspC depends on the membrane lipid composition in *E. coli*. Strain UE53 and its *pgsA*-deletion mutant UE54 were therefore transformed with a pBAD30 derivative for arabinose-induced production of hexahistidine-tagged PspC. As negative control, the His-tagged mature domain of HiPIP was used, a completely soluble unrelated protein whose production does not induce the Psp response [27]. When PspC-H6 was present in the WT or in the *pgsA*-deletion mutant, the production of PspA was markedly upregulated and PspA predominantly fractionated with the membranes, indicating membrane recruitment (Figure 2). With both strains, an SDS-resistant PspA oligomer was detected in the membrane fraction (Figure 2), indicating that PspA forms its typical membrane associated oligomers. Neither PG nor CL were important for signal transmission of PspC to PspA. In contrast to the above described experiments (Figure 1B) in which cells were harvested in the late exponential phase (at an optical density at 600 nm of ~1), some membrane recruitment of PspA was detectable,

possibly due to a later harvest time point that was necessary for PspC production. An observed interaction with membranes might relate to the the known role of PspA during stationary phase [28]. Since the PE deficient mutant GN10 could not be transformed, a PE dependence on inducibility by PspC could not be examined. Nevertheless, as PspA production was enhanced in the PE deletion mutant (Figure 1), the membrane stress as generated by the lack of the usually highly abundant phospholipid PE is probably sensed.

Membrane association of PspA in the PG and CL deficient strain depends on PspC

To determine whether PspA can sense high SCE stress PspC-independently *in vivo*, we introduced a *pspC* deletion in the *pgsA* mutant strain UE54. Clearly, PspA was not anymore membrane-localized in this strain and instead was found in low abundance in the soluble fraction (Figure 3A). This indicated that membrane localization of PspA and its potential SCE stress-sensing depends on PspC *in vivo*. To check whether PspA is PspC-dependently membrane-recruited and to exclude that the observed effect was caused by polar effects of the replacement of *pspC* in the genome by the kanamycin cassette, we produced His-tagged PspC. Notably, recombinant PspC restored PspA membrane association and induced the Psp response as described before (Figure 3B). The previously found shifted SDS-resistant species of PspA in the membrane fraction that is possibly derived from membrane-associated PspA was again detected. PspC itself migrated as dimer and monomer forms in an approx. 1:1 ratio, indicating a strong PspC-PspC interaction, which agrees with previous interaction analyses [12].

Stress sensing of the Psp system may depend on negatively charged phospholipids

As signal transmission did not depend on negatively charged phospholipids, and as signal sensing was PspC-dependent in a CL/PG deficient strain, we then asked the question whether the Psp system can be induced in a CL/PG deficient strain by a Psp response-triggering protein. We used TatA as stimulus, a membrane-destabilizing protein that has been shown to interact with PspA and that induces a PspABC-dependent Psp response [7]. TatA possesses an unusual

short membrane anchor which is able to weaken to cytoplasmic membrane during transport of folded proteins by the twin-arginine translocase [29]. TatA was produced in the CL/PG mutant strain UE54 as well as in the corresponding wild type strain UE53. Only a p15A origin low-copy vector for arabinose-dependent expression worked reproducible in UE54, which must somehow relate to the lipid defects. This expression system gave not the high expression levels of *tatA* that are known to strongly induce the Psp response, but already with this system we found that PspA levels were significantly increased in the lipid wild type strain in response to TatA-*Strep* production (Figure 4, WT lanes). Membrane recruitment of PspA was obviously enhanced in the wild type strain in response to TatA-*Strep*. In contrast, PspA levels did not significantly change in a strain lacking PG and CL, and there was no clear change in PspA abundance in the membrane fraction, suggesting that negatively charged phospholipids might be involved in sensing of protein-induced membrane stress (Figure 4, PG^-/CL^- lanes). However, TatA-induced changes in abundance and membrane recruitment of PspA in the PG/CL deficient strain might have been subtle due to strain specific indirect effects.

DISCUSSION

The most abundant phospholipids in the cytoplasmic membrane of *E. coli* are phosphatidylethanolamine (PE, ~75-80 %), phosphatidylglycerol (PG, ~10-15 %), and cardiolipin (CL, ~5-10%) [26]. It is reasonable to expect that mutant strains that cannot produce either of these abundant phospholipids should experience membrane stress, which would result for example from destabilization of the subset of membrane proteins that require specific lipid interactions for stability, or simply from SCE stress that can be imposed by altered lipid compositions. Accordingly, it was not unexpected to observe a membrane recruitment of PspA to membranes that either lack the negatively charged phospholipids PG and CL or the usually most abundant phospholipid PE (Figure 1). In case of the *pgsA* mutant that lacks PG and CL under exponential growth phase conditions, the data reveal that – although these negatively

charged lipids are known to enhance membrane interactions of PspA *in vitro* [16] – they are clearly not essential for the membrane interaction (Figure 1). It is known that some other negatively charged lipids, i.e. N-acyl-PE, as well as phosphatidic acid (PA) and CDP-diacylglycerol, compensate for PG and CL deficiency in this strain [30], and it therefore can be that also the observed membrane interaction of PspA is enabled by these substitutes. However, the *pgsA* mutant strain lost its ability to respond to TatA-induced membrane destabilization, and it therefore can be concluded that PG and/or CL are highly important for the sensing of protein-induced membrane stress despite not being essential for the PspA membrane interaction. The membrane interaction of PspA was even much more triggered by the absence of PE in the *pssA* mutant strain. It must therefore be noted that the membrane interaction is likely enhanced by the highly abundant negatively charged phospholipids in the PE deficient strain, although PG/CL are not absolutely required for the interaction. This strain also showed a higher PspA abundance, indicating an increased PspF activity. The very strong membrane interaction in the PE deficient strain is in full agreement with the previous *in vitro* experiments that suggested a role of negatively charged phospholipids in membrane interaction of PspA [16, 17]. As the sensing of protein-generated membrane stress may be hampered in the absence of negatively charged phospholipids (Figure 4), it could be that the presence of abundant PG/CL in the PE deficient strain contributes to stress sensing or PspA recruitment to the membrane. The upregulation of the Psp system in that strain likely results from effects of PE depletion or increased charge density on membrane protein stability or membrane integrity. Sensing of TatA induced stress and sensing of PE deficiency may thus occur via the same mechanism. In contrast, there is no real induction of the Psp response by PG/CL deficiency (Figure 1), although some PspA is recruited to the membrane and although the not very high level of PspA is further reduced when PspC is absent (Figure 3). Most importantly, the membrane interaction in the PG/CL deficient strain completely depended on PspC, indicating that PspC can compensate partially for the absence of the negatively charged PG/CL lipids. As the PG/CL deficient strain

contains increased levels of PE and likely suffers from SCE stress, the data indicate that SCE stress alone does not really induce the Psp response, nor does SCE stress suffice to enable a membrane interaction of PspA in the absence of PspC. Therefore, our data demonstrate that PspC is not bypassed by lipid interactions of PspA *in vivo*. PspC clearly plays a crucial role for the membrane interaction of PspA, as it does – together with negatively charged phospholipids – for the sensing of membrane stress.

In summary, our data integrate the two proposed mechanisms for membrane stress sensing by the Psp system, which is the lipid interaction of PspA and the PspBC-dependent pathway. Apparently both mechanisms cooperate to achieve efficient membrane interaction of PspA and stress sensing. Future studies will surely reveal the molecular details of how these interactions are integrated to a common output of this interesting regulatory stress response pathway.

ACKNOWLEDGEMENTS

We thank Inge Reupke for technical assistance. This study was funded by grant BR2285/4-2 of the Deutsche Forschungsgemeinschaft (DFG) to TB.

REFERENCES

[1] Joly, N. et al. (2010) Managing membrane stress: the phage shock protein (Psp) response, from molecular mechanisms to physiology. FEMS Microbiol. Rev. 34, 797–827.

[2] Flores-Kim, J. and Darwin, A.J. (2016) The phage shock protein response. Annu Rev Microbiol 70, 83–101.

[3] Brissette, J.L., Weiner, L., Ripmaster, T.L. and Model, P. (1991) Characterization and sequence of the *Escherichia coli* stress-induced *psp* operon. J. Mol. Biol. 220, 35–48.

[4] Weiner, L., Brissette, J.L. and Model, P. (1991) Stress-induced expression of the *Escherichia coli* phage shock protein operon is dependent on sigma 54 and modulated by positive and negative feedback mechanisms. Genes Dev. 5, 1912–1923.

[5] Bergler, H., Abraham, D., Aschauer, H. and Turnowsky, F. (1994) Inhibition of lipid biosynthesis induces the expression of the *pspA* gene. Microbiology 140, 1937–1944.

[6] Brissette, J.L., Russel, M., Weiner Lorin and Model, P. (1990) Phage shock protein, a stress protein of *Escherichia coli*. Proc. Natl. Acad. Sci. U S A 87, 862–866.

[7] Mehner, D., Osadnik, H., Lünsdorf, H. and Brüser, T. (2012) The Tat system for membrane translocation of folded proteins recruits the membrane-stabilizing Psp machinery in *Escherichia coli*. J. Biol. Chem. 287, 27834–27842.

[8] Thurotte, A., Brüser, T., Mascher, T. and Schneider, D. (2017) Membrane chaperoning by members of the PspA/IM30 protein family. Integr. Biol. 10, e1264546.

[9] Jovanovic, G., Weiner, L. and Model, P. (1996) Identification, nucleotide sequence, and characterization of PspF, the transcriptional activator of the *Escherichia coli* stress-induced *psp* operon. J. Bacteriol. 178, 1936–1945.

[10] Osadnik, H. et al. (2015) PspF-binding domain PspA1-144 and the PspA·F complex: New insights into the coiled-coil-dependent regulation of AAA+ proteins. Mol. Microbiol. 98, 743–759.

[11] Flores-Kim, J. and Darwin, A.J. (2015) Activity of a bacterial cell envelope stress response is controlled by the interaction of a protein binding domain with different partners. J. Biol. Chem. 290, 11417–11430.

[12] Adams, H., Teertstra, W., Demmers, J., Boesten, R. and Tommassen, J. (2003) Interactions between Phage-Shock Proteins in *Escherichia coli*. J. Bacteriol. 185, 1174–1180.

[13] Standar, K., Mehner, D., Osadnik, H., Berthelmann, F., Hause, G., Lünsdorf, H. and Brüser, T. (2008) PspA can form large scaffolds in *Escherichia coli*. FEBS Letters 582, 3585–3589.

[14] Kobayashi, R., Suzuki, T. and Yoshida, M. (2007) *Escherichia coli* phage-shock protein A (PspA) binds to membrane phospholipids and repairs proton leakage of the damaged membranes. Mol. Microbiol. 66, 100–109.

[15] Hankamer, B.D., Elderkin, S.L., Buck, M. and Nield, J. (2004) Organization of the AAA(+) adaptor protein PspA is an oligomeric ring. J. Biol. Chem. 279, 8862–8866.

[16] McDonald, C., Jovanovic, G., Ces, O. and Buck, M. (2015) Membrane stored curvature elastic stress modulates recruitment of maintenance proteins PspA and Vipp1. mBio 6, 15.

[17] McDonald, C., Jovanovic, G., Wallace, B.A., Ces, O. and Buck, M. (2017) Structure and function of PspA and Vipp1 N-terminal peptides. Biochim. Biophys. Acta 1859, 28–39.

[18] Baba, T. et al. (2006) Construction of *Escherichia coli* K-12 in-frame, single-gene knockout mutants. Mol Syst Biol 2, 2006.0008.

[19] Rathmann, C., Schlösser, A.S., Schiller, J., Bogdanov, M. and Brüser, T. (2017) Tat transport in *Escherichia coli* requires zwitterionic phosphatidylethanolamine but no specific negatively charged phospholipid. FEBS Letters 591, 2848–2858.

[20] Towbin, H., Staehelin, T. and Gordon, J. (1992) Electrophoretic transfer of proteins from polyacrylamide gels to nitrocellulose sheets. Biotechnology (Reading, Mass.) 24, 145–149.

[21] Laemmli, U.K. (1970) Cleavage of structural proteins during the assembly of the head of bacteriophage T4. Nature 227, 680–685.

[22] Bligh, E.G. and Dyer, W.J. (1959) A rapid method of total lipid extraction and purification. Can. J. Biochem. Physiol. 37, 911–917.

[23] Ames, G.F. (1968) Lipids of *Salmonella typhimurium* and *Escherichia coli*. J. Bacteriol. 95, 833–843.

[24] Mozharov, A.D. (2006) Effective separation of bacterial phospholipids and neutral lipids in one dimensional thin layer chromatography. Analytical Letters 18, 609–616.

[25] Kikuchi, S., Shibuya, I. and Matsumoto, K. (2000) Viability of an *Escherichia coli pgsA* null mutant lacking detectable phosphatidylglycerol and cardiolipin. J. Bacteriol. 182, 371–376.

[26] Saha, S.K., Nishijima, S., Matsuzaki, H., Shibuya, I. and Matsumoto, K. (1996) A regulatory mechanism for the balanced synthesis of membrane phospholipid species in *Escherichia coli*. Biosci. Biotechnol. Biochem. 60, 111–116.

[27] Mehner, D. (2011) Charakterisierung und Identifizierung eines Interaktionspartners des Tat-Translokons von Escherichia coli.

[28] Weiner, L. and Model, P. (1994) Role of an *Escherichia coli* stress-response operon in stationary-phase survival. Proc. Natl. Acad. Sci. U S A 91, 2191–2195.

[29] Hou, B., Heidrich, E.S., Mehner-Breitfeld, D. and Brüser, T. (2018) The TatA component of the twin-arginine translocation system locally weakens the cytoplasmic membrane of *Escherichia coli* upon protein substrate binding. J. Biol. Chem., E-pub ahead of print.

[30] Mileykovskaya, E., Ryan, A.C., Mo, X., Lin, C.-C., Khalaf, K.I., Dowhan, W. and Garrett, T.A. (2009) Phosphatidic acid and N-acylphosphatidylethanolamine form membrane domains in *Escherichia coli* mutant lacking cardiolipin and phosphatidylglycerol. J. Biol. Chem. 284, 2990–3000.

[31] Shiba, Y., Yokoyama, Y., Aono, Y., Kiuchi, T., Kusaka, J., Matsumoto, K. and Hara, H. (2004) Activation of the Rcs signal transduction system is responsible for the thermosensitive growth defect of an *Escherichia coli* mutant lacking phosphatidylglycerol and cardiolipin. J. Bacteriol. 186, 6526–6535.

[32] Tan, B.K., Bogdanov, M., Zhao, J., Dowhan, W., Raetz, C.R.H. and Guan, Z. (2012) Discovery of a cardiolipin synthase utilizing phosphatidylethanolamine and phosphatidylglycerol as substrates. Proc. Natl. Acad. Sci. U S A 109, 16504–16509.

Table 1. Strains and plasmids unsed in this study.

Strains/Plasmids	Characteristics	Reference
JWK1299	F-, *Δ(araD-araB)567*, *ΔlacZ4787*(::rrnB-3), *λ*$^{-}$, *ΔpspC742::kan*, *rph-1*, *Δ(rhaD-rhaB)568*, *hsdR514*	[18]
UE53	MG1655 *lpp*-2 Δ*ara714 rcsF*::mini-Tn10 *cam*	[30]
UE54	MG1655 *lpp*-2 Δ*ara714 rcsF*::mini-Tn10 *cam* Δ*pgsA*::FRT-*kan*-FRT	[31]
UE54 *kan*^{S}	MG1655 *lpp*-2 Δ*ara714 rcsF*::mini-Tn10 *cam* Δ*pgsA*	[19]
UE54 Δ*pspC*	MG1655 *lpp*-2 Δ*ara714 rcsF*::mini-Tn10 *cam* Δ*pgsA* Δ*pspC*::FRT-*kan*-FRT	This work
GN10	W3110 Δ*pssA10*::cam	[26]
pMS5	Amp^{R} , *pssA*$^{+}$, derivative of pMAN035	[26]
pBAD30-*clsB*	Amp^{R} , *clsB*, derivative of pBAD30	[32]
pBAD30-H10-*mhip*	Amp^{R} ,*h10mhip*, derivative of pBAD30	This work
pBAD30-*pspC*-H6	Amp^{R} ,*pspC-h6*, derivative of pBAD30	This work
pBAD30-*tatA*-strep	Amp^{R} ,*tatA-strep*, derivative of pBAD30	This work

FIGURES

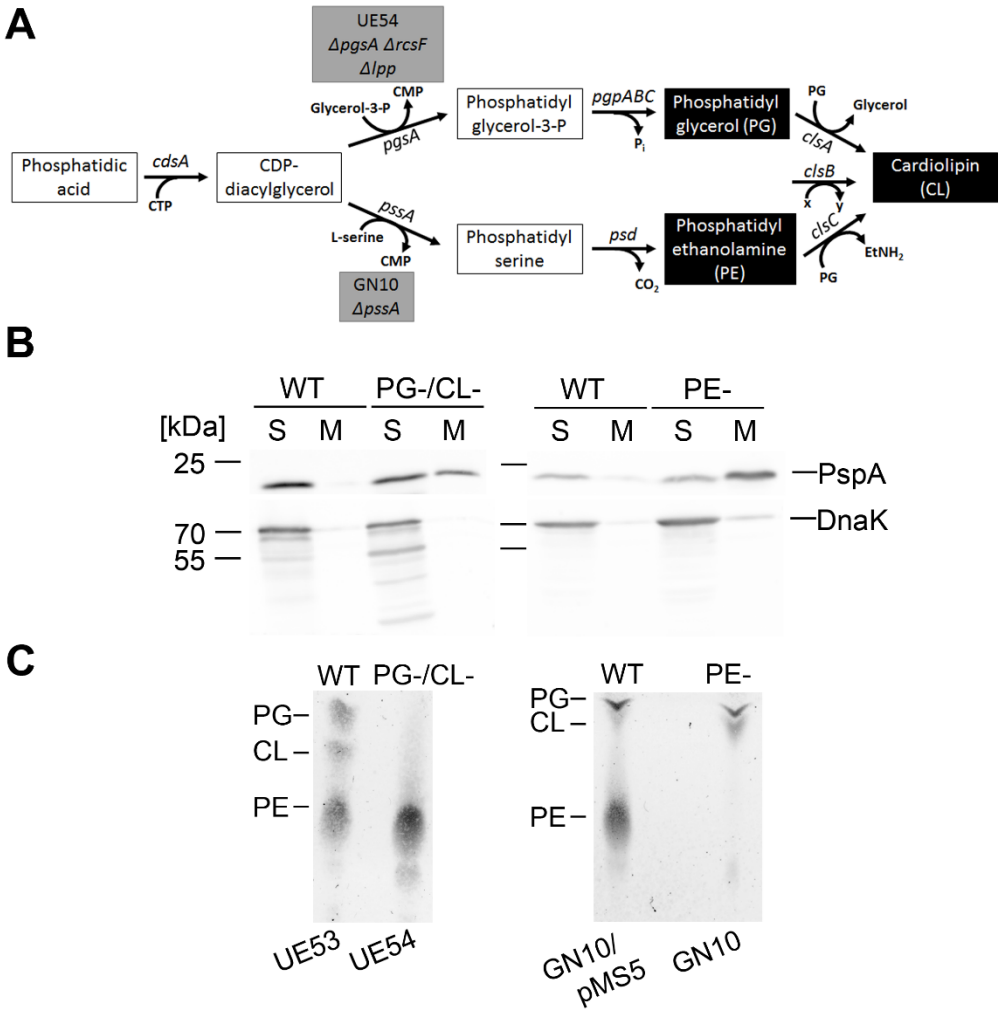

Figure 1 PspA associates with membranes in lipid deficient *E. coli* strains. (A) Scheme of the phospholipids biosynthesis pathways in *E. coli.* (B) Subcellular localization of PspA in UE54 lacking CL and PG and its corresponding parental strain UE53 (left panel), or PE in strain GN10 or its correspnding wild type strain GN10/pMS5 (right panel). Western blots were developed using specific PspA or DnaK (fractionation control) antibodies and the ECL system. (C) Thin-layer chromatography analysis of lipids from the strains used in (B).

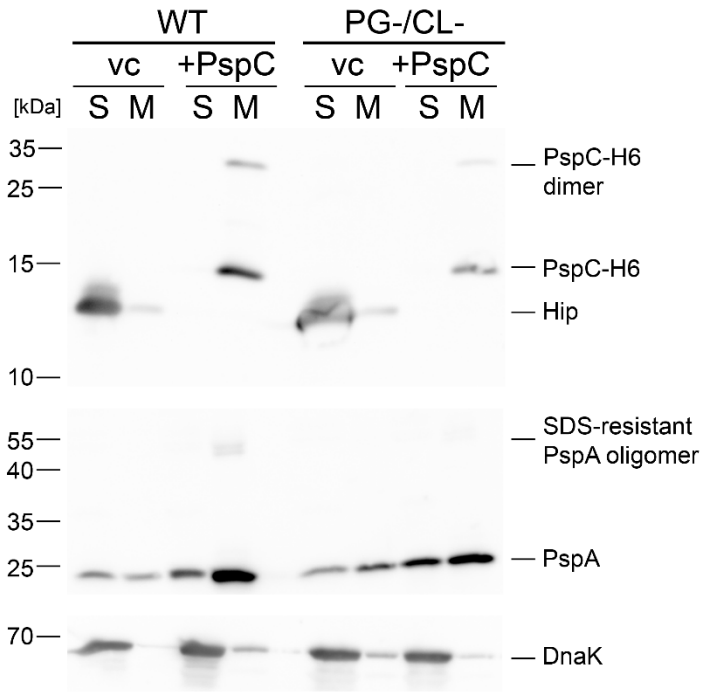

Figure 2 Signal transmission from PspC to PspA does not depend on PG/CL. Subcellular localization of PspA in UE54 lacking CL and PG, and in its corresponding parental strain UE53, producing as indicated either the His-tagged mature domain of HiPIP as vector control (vc) or His-tagged PspC (+PspC). Western blots were developed using specific His-tag, PspA or DnaK (fractionation control) antibodies and the ECL system .

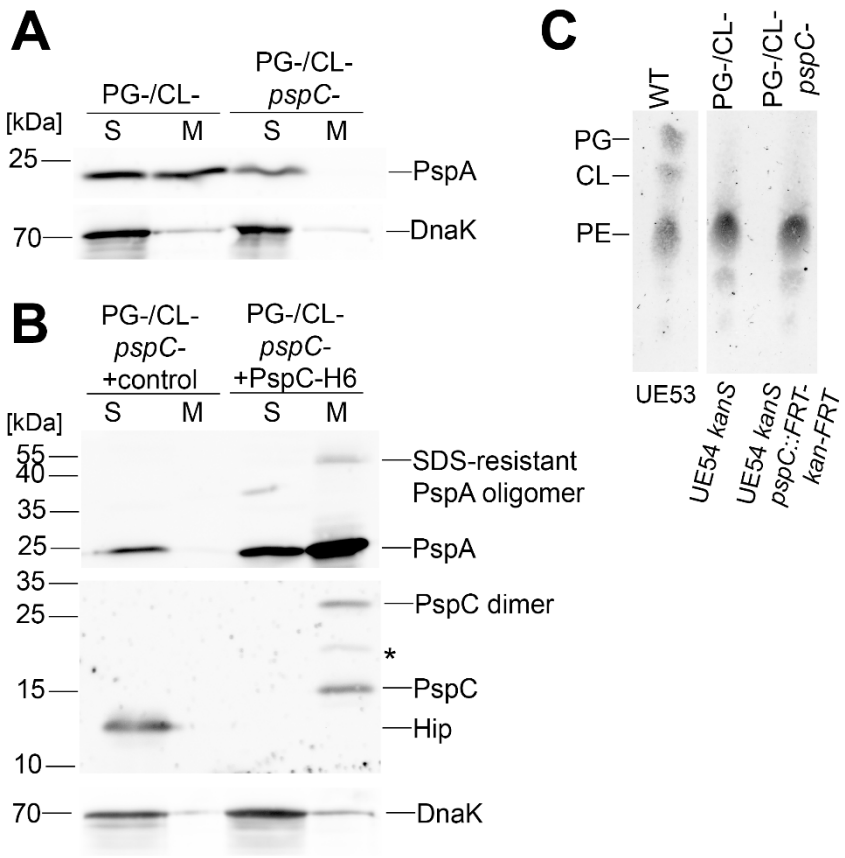

Figure 3. Constitutive levels of PspA and its membrane interaction in the PG/CL deficient strain are PspC dependent. (A) Subcellular localization of PspA in UE54 lacking CL and PG, and the effect of an additional pspC deletion in that strain. (B) Complementation of pspC deletion effects in trans. Subcellular localization of PspA in the pspC deleted derivative of UE54, producing either the His-tagged mature domain of HiPIP as control or His-tagged PspC. Western blots were developed using specific His-tag, PspA or DnaK (fractionation control) antibodies and the ECL system. (C) Thin-layer chromatography control of lipid composition of strains used in (A). UE53 is shown for comparison.

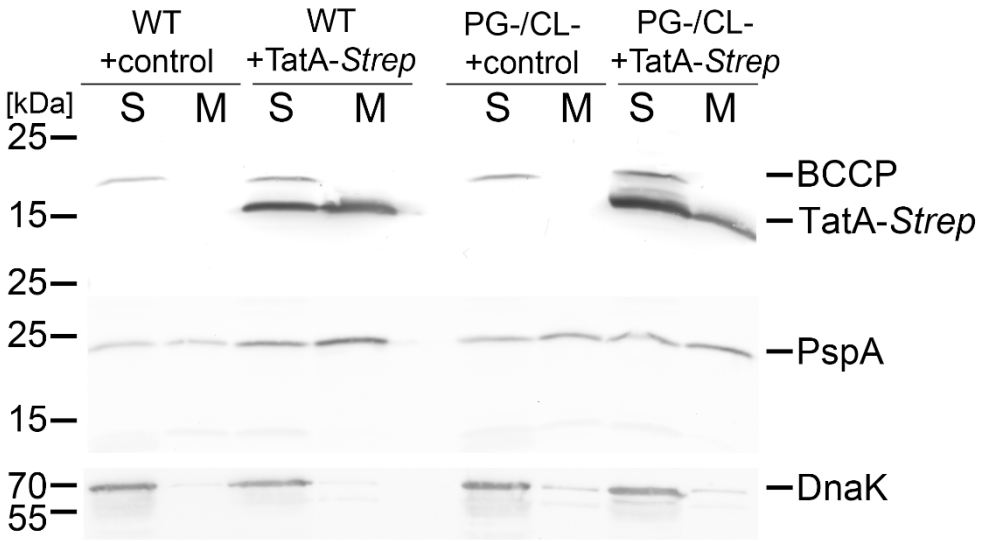

Figure 4 PspA membrane recruitment and Psp response induction by TatA-Strep is PG/CL-dependent. Subcellular localization of PspA in UE54 lacking CL and PG and its corresponding lipid wild type strain (UE53) with membrane stress as induced by production of TatA-Strep. Note the increased relative abundance of PspA in the WT strain in response to TatA-Strep, which is not observed in the PG/CL deficient strain. Western Blots were developed using specific antibodies for PspA or DnaK (fractionation control) and ECL detection.

3.4 „*Dissection of membrane stress-sensing and signal transmission by the Psp system at the cytoplasmic membrane in* Escherichia coli*”*

Autoren: Eyleen S. Heidrich und Thomas Brüser

Art der Autorenschaft: Erst-Autorin

Zugehörigkeit: Leibniz Universität Hannover, Institut für Mikrobiologie, Herrenhäuser Straße 2, 30419 Hannover

Art des Artikels: Forschungsartikel

Beitrage: **Eyleen S. Heidrich:** Konzeption und Planung der Studie zusammen mit Thomas Brüser, Planung und Durchführung aller Experimente, Datenanalyse, Präparation der Abbildungen, Fertigstellung des Manuskripts zusammen mit Thomas Brüser

Thomas Brüser: Konzeption und Planung der Studie zusammen mit Eyleen S. Heidrich, Datenanalyse und Fertigstellung des Manuskripts

Wissenschaftliche Einordnung

Die rekombinante Überproduktion der Tat-Komponente TatA führt zu einer Induktion des Psp-Systems [94]. TatA ist der einzige Induktor der Psp-Antwort in *E. coli* für welchen eine PspBC-abhängige Interaktion mit PspA nachgewiesen werden konnte [94]. Es war daher Ziel festzustellen, ob TatA das Psp-System über die gleiche Signalkaskade induziert, welche bereits für andere Induktoren identifiziert werden konnte. Des Weiteren sollte getestet werden, welche Domänen von PspB und PspC zur Induktion des Psp-Systems durch TatA und zur Interaktion von TatA mit PspA beitragen.

Es gelang im Folgenden zur Publikation vorbereiteten Artikel nachzuweisen, dass TatA das Psp-System über die gleiche Signalkaskade aktiviert, wie es bereits für Sekretine in *Y. enterocolitica* gezeigt wurde [41]. Es konnte zudem gezeigt werden, dass die Transmembrandomäne von PspC für die Wahrnehmung von durch TatA ausgelösten Membranstress nicht notwendig ist. Stattdessen stellte sich die Präsenz von PspB als entscheidend für die Signalwahrnehmung und die Membraninteraktion PspA als entscheidend für die Signalkaskade heraus.

Dissection of membrane stress sensing and signal transmission by the Psp system at the cytoplasmic membrane in *Escherichia coli*

Eyleen S. Heidrich[1] and Thomas Brüser[1,2]

[1]From the Institute of Microbiology, Leibniz Universität Hannover, Herrenhäuser Straße 2, 30419 Hannover, Germany

Running title: The TatA-induced signaling cascade of the Psp response

[2]To whom correspondence should be addressed: Thomas Brüser, Institute of Microbiology, Leibniz Universität Hannover, Herrenhäuser Straße 2, 30419 Hannover, Germany; Tel. +49 511 762 5945; Fax: +49 511 762 5287; E-mail: brueser@ifmb.uni-hannover.de

Keywords: Phage shock protein, membrane stress, signaling, protein-protein interaction, protein-membrane interaction

SUMMARY

The enterobacterial phage shock protein (Psp) response is induced by a wide range of membrane stresses to support membrane integrity. The components PspA, PspB, and PspC together regulate PspF, the activator of σ^{54}-dependent transcription of the *pspABCDE* and *pspG* genes. PspA binds PspF and inhibits its activity. The membrane proteins PspB and PspC can interact with each other and recruit PspA via the C-terminus of PspC, which is of key importance for the signaling. Here we show that the production of a soluble C-terminal domain of PspC, PspC-CT, can per se trigger the Psp response in the absence of membrane stress. Surprisingly, this signaling required PspB. Accordingly, a fraction of PspC-CT interacted with the cytoplasmic membrane in a PspB-dependent manner. When the Psp response was induced by full-length PspC, PspB was not anymore required but still clearly enhanced the induction. Therefore, the membrane localization of the C-terminal domain is most likely needed for the induction of the Psp system, and this can be mediated by PspB interactions or the PspC membrane integral domain. PspA interacted with PspC-CT at the membrane surface. The PspC-PspA interaction was required for signal transmission. Sensing of membrane stress as generated by TatA required PspB, but not the membrane-integral domain of PspC. In conclusion, our data indicate that a complex of PspA, PspB, and PspC is formed at membranes under stress conditions, in which PspB, possibly together with PspA, senses membrane stress, while the C-terminal domain of PspC needs to interact with PspA for signal transmission.

INTRODUCTION

Since almost 30 years it is known that membrane stress somehow elicits an up-regulation of a set of proteins in enteric bacteria (1–3). Initially this stress response was discovered in *Escherichia coli* in studies with non-lytic phage infections, which is why the first compound of this system was named phage shock protein A, PspA (1). Psp proteins are believed to contribute somehow to membrane integrity (4, 5). Importantly, the Psp system contributes to the virulence of pathogenic bacteria and its understanding is therefore highly relevant for medical aspects (6, 7). Current research focuses on the mechanism of membrane stress sensing and the signal transduction to the principal regulator PspF that is a AAA+ family enhancer binding protein required for σ^{54}-dependent expression of the *pspABCDE* operon and the monocistronic *pspG* (8–10). So far, it is known that the components PspA, PspB, and PspC constitute this signaling pathway (11, 12). PspA is an important negative regulator of PspF function (13). It binds PspF tightly with an N-terminal coiled coil whose structure has been solved recently (14), and with its C-terminal region (15). PspA lacks a trans-membrane domain but contains a potential N-terminal amphipathic helix that can interact with the membrane surface upon stress and otherwise is back-folded to the N-terminal coiled coil (14, 16). Recent studies have demonstrated that PspA

interacts also with a region in the C-terminus of PspC, which becomes accessible to PspA in response to a stress signal (9). This C-terminal domain is therefore a positive regulator of the Psp response (17, 18).

We aimed to use the production of the C-terminal domain of PspC alone (PspC-CT) to study the signal transduction and induction of the Psp system independent of membrane stress and sensing. To examine the sensing of membrane stress, we used the membrane destabilizing TatA protein (19). By this approach, we found that the induction of the Psp response by PspC-CT required a membrane association. Therefore, not only stress sensing but also the signal transmission to PspA requires the membrane surface. Signal transmission as triggered by PspC-CT could be further elicited by membrane stress, indicating that the membrane-integral domain of PspC is not required for stress sensing. PspB was found to be a component required for stress sensing, possibly in conjunction with PspA. This study thus increases our knowledge about the specific functions of the PspABC components in signal sensing and transmission.

RESULTS

Membrane stress generated by TatA-NT is sensed and transmitted by the same pathway that has been described for stress as induced by mis-localized secretins – The twin-arginine translocation system component TatA is a Psp-inducing and PspA-interacting protein (20). We could recently show that the unusual short N-terminal membrane anchor of TatA is able to weaken the cytoplasmic membrane of *E. coli* (19). The interaction of TatA with PspA and the induction of the Psp response by TatA are clearly PspBC dependent (20). We investigated the signal sensing and transmission cascade of the Psp system as induced by TatA further, using a reporter strain with a chromosomal P_{pspA} promoter *lacZ* fusion (21). For these assays, the genes encoding *pspABCDE* and *pspF* were deleted in that strain, and a fully functional recombinant *pspF/pspABC* system was reconstituted on a very low-copy vector (pSC101 origin) using the natural promoters. Based on studies of the Darwin and Buck groups in *Y. enterocolitica* (22) and *E. coli* (17), we selected conserved positions in PspC for mutagenesis, and the effect on Psp system inducibility was determined (Figure 1). None of the mutations in the membrane-domain of PspC affected stress-sensing, as the corresponding PspC variants still supported the Psp response. Interestingly, the G48A exchange in PspC, which was found to be important for Psp system induction by pIV secretin induced membrane stress (17), had no influence on the Psp response as induced by TatA-NT-Hip. We exchanged this glycine to valine to further reduce flexibility, and found that the Psp system could be still induced to the same level by TatA-NT-Hip (Figure 1). The uninduced steady state expression level was increased by that mutation, which likely relates to a limited orientational flexibility of the N- and C-terminal regions of PspC. The membrane integral region of PspC thus clearly played no direct role in sensing, but may be important for reducing the basal activity of the Psp system. We would like to note that an earlier studied PspC-G48A construct had no ability to induce the Psp system when overproduced alone (17), whereas our PspC-G48A construct induced the Psp response when constitutively overproduced in a Psp wild-type as well as in a *pspC* deletion P_{pspA} reporter strain, confirming that G48 is not required for Psp response induction (Supplementary Figure S1). In our screen, five mutations in the C-terminal domain (E102A, E102Q, V105D, S107P, L112D) completely abolished or strongly affected the inducibility of the Psp response by TatA-NT-Hip (Figure 1). Among these exchanges, V105D and S107P correspond to the V125D and S127P mutations that had been identified in the *Y. enterocolitica* Psp system to be important for the PspA interaction in response to phage secretin induced membrane stress (22, 9). The mutagenesis approach thus identified a region in the PspC C-terminus that is essential for the generation of a stress-induced Psp response by TatA. Several exchanges in the N-teminal domain of PspC resulted in the induction of the Psp response, which fully agrees with the view that this domain acts as negative regulator of the Psp response, most likely by recruiting the C-terminal domain of PspC. This function has been suggested by the group of Darwin based on their experiments with secretins as membrane stress inducers (23, 22). Together, the data indicate that the small membrane anchor of TatA initiates the identical Psp response signaling cascade as mis-localized secretins do.

Using the soluble isolated C-terminal domain of PspC for studying signal transmission – It is known that the production of PspC-CT induces the Psp response, indicating an involvement of this domain in signaling (17). In *E. coli*, PspC-CT constructs were so far never analyzed in the absence of PspB. The soluble PspC-CT domain should be the best artificial inducer of the Psp response as it could bind to and activate soluble PspFA complexes. For stability and detectability reasons, we fused the N-terminus of PspC-CT (residues Ser-61 to Leu-119) to the C-terminus of the N-terminally His-tagged mature domain of HiPIP (H10-Hip-PspC-CT). To examine whether the identified critical region (E102-L112D) is important for signaling or rather involved in sensing of membrane stress, we produced variants of H10-Hip-PspC-CT with the mentioned mutations and addressed whether the Psp response was induced (Figure 2). The L112D exchange could not be introduced by site-directed-mutagenesis, neither in the C terminal fragment of PspC-CT nor in the full-length protein. The non-mutated construct induced the Psp response in a Δ*pspC* background, confirming the reported signaling function of the C-terminus (9). The introduction of the individual mutations abolished this signaling, as no Psp response was induced (Figure 2A). Western blot analyses could exclude that a degradation of the mutated PspC-CT variants had caused this effect, as the all constructs were made at comparable levels, with only one exception, L112A, which was undetectable (Figure 2B). In agreement with the LacZ data, PspA production was strongly enhanced when the non-mutated C-terminus of PspC was produced, whereas PspA production was not induced by the variants carrying the mutations in PspC-CT .

To analyze the role of the PspA-PspC interaction in signaling, we carried out affinity chromatography co-elution analyses with the non-mutated or mutated PspC-CT constructs (Figure 3). The non-mutated C-terminus of PspC clearly interacted with PspA and – interestingly – also with PspB, whereas no interaction with PspA or PspB could be detected in case of PspC-CT-E102A and PspC-CT-V105D. For PspC-CT-E102Q a very weak co-elution of PspA was detectable, but obviously this interaction did not suffice to induce the Psp response, which could be later confirmed by an independent experiment (Figure 7). Importantly, PspB did not co-elute with PspC-CT-E102Q. Together, these data showed that the same region in PspC-CT that is important for signaling is also required for the interaction with PspA and PspB.

The role of the C-terminal domain of PspC as a PspA- and PspB-recruiting entity – As PspB is a second interaction partner of the soluble PspC-CT in *E. coli*, we tested the potential requirement for PspB in the PspC-CT/PspA interaction (Figure 4A). To our surprise, PspC-CT hardly pulled down any PspA with a strain that lacked PspB despite being completely soluble. As a very weak interaction might suffice to induce the Psp response, we examined whether the presence of PspB was also relevant for the Psp response induction by PspC-CT (Figure 4B). Importantly, the induction by PspC-CT was very weak in a reporter strain deleted in *pspBC*, and the presence of PspB strongly enhanced the Psp response induction by PspC-CT, indicating an important role of PspB for the signaling mediated by PspC-CT. In a strain still containing PspB and PspC, the production of PspC-CT induced the Psp response not as strong as in a strain containing only PspB (Figure 4B), which can be explained by the presence of vacant binding sites for PspC-CT in the strain lacking PspC. An explanation could be that recombinant PspC-CT saturates the PspC binding sites on the PspFA complex, and only those PspFA complexes can be activated by PspC-CT that can be recruited to the membrane via interactions with PspB.

As PspB is a membrane protein, the enhancement by PspB suggested that a membrane environment could be required for signaling. This was unexpected as PspC-CT was produced as an entirely soluble protein without its membrane domain. We thus analyzed whether PspC-CT was recruited somehow to the membrane in a PspB-dependent manner (Figure 4C). In agreement with our hypothesis, these data clearly demonstrated that indeed some soluble PspC-CT was recruited to the cytoplasmic membrane, and this membrane recruitment depended on PspB, as PspC-CT could hardly be detected in the membrane fraction in the absence of PspB. Interestingly, in a *psp* wild-type background, the membrane recruitment of PspC-CT was not as strong as in the *pspC* deletion strain, which agrees with the idea that the induction of the Psp response by PspC-CT in a wild-type

background correlates with the recruitment of PspC-CT to free binding sites at PspB (Figure 4B).

We then considered the possibility that PspB might either be required specifically for the signal transfer from PspC-CT to PspA, or that simply the membrane-attachment of PspC-CT is important, and PspB thus might have only contributed to the signaling by targeting PspC-CT to the membrane surface. We addressed this point by examining the PspB-dependence of the Psp response triggered by full-length PspC that contains its own membrane domain. First, we analyzed whether full-length PspC pulls down any PspA in the absence of PspB (Figure 4BD). The data clearly showed that the Psp response was induced by production of full-length PspC, and this induction was in principle independent from the presence of PspB, albeit PspB enhanced strongly the induction. Accordingly, PspA interacted PspB-independently with PspC (Figure 4D). In full agreement with these data, we found that only the non-mutated PspC-CT recruited PspA to the membrane, whereas membrane recruitment was fully abolished with mutated PspC-CT domains (Figure 5).

A very important additional aspect of the signaling results is that the membrane-integral domain of PspC appeared not to have any impact on signaling from PspC downstream to PspA. Previous studies had examined effects of PspC constructs that contained the original membrane-integral region (17). Our data now show that signaling and membrane recruitment both do not require the membrane-integral domain of PspC (Figures 4 and 5).

Membrane recruitment of PspC-CT is necessary for the TatA PspA interaction – As we could show that the transmembrane domain of PspC is potentially not necessary for perception of a Psp system inducing signal, we asked the question whether the transmembrane domain of PspC is necessary for the reported TatA-*Strep*/PspA interaction (20). In those experiments, co-elution of PspA with TatA-*Strep* was found to depend on PspC and PspB, and PspB and PspC were clearly co-eluting with TatA-*Strep* when produced recombinantly. To clarify this aspect, we performed again co-elution experiments with a strain lacking its genomic *pspC* copy, and produced TatA-*Strep* and PspC-CT as described above. We thereby could detect a clear interaction of PspA with TatA-*Strep* in the presence of PspC-CT, indicating that the TatA-*Strep*/PspA interaction is independent of the transmembrane domain of PspC (Figure 6). Subsequently, we checked whether the above described mutations in PspC-CT that abolish the PspA interaction influence the TatA/PspA interaction. Strikingly, no co-elution of PspA with TatA was detectable when these variants were produced together with TatA-*Strep*, demonstrating that the PspC C-terminus contributes to the TatA-PspA interaction (Figure 6). As we could show that PspC-CT is PspB-dependently membrane-recruited, we addressed the question whether this is a prerequisite for the TatA/PspA interaction. Strikingly, we could not detect a clear co-elution between TatA-*Strep* and PspA in a *pspBC* deletion mutant producing PspC-CT, indicating that the TatA-S*trep*/PspA interaction indeed depends on the membrane recruitment of PspA (Figure 7A), which is not surprising, as TatA is a membrane protein. In agreement with the above described data, the co-elution could be restored in the *pspBC* deletion mutant when full-length PspC was produced, confirming the view that membrane interaction of PspA is crucial for the direct interaction with Psp response-inducing proteins (Figure 7B, upper panels). This membrane recruitment seems to be more relevant for the TatA/PspA interaction than PspB or the trans-membrane domain of PspC. In agreement with this interpretation, we observed that recombinantly produced PspA can in principle also interact with recombinantly produced TatA-*Strep* in the absence of PspB and PspC (Figure 7B, middle panels), which most likely reflects the well-known ability of abundant PspA to interact with membranes per se (24–27). As an interaction is not direct evidence for an induction of the Psp response by TatA-*Strep*, P_{pspA} promoter activities were determined using the LacZ reporter system. Strikingly, TatA-*Strep* further induced the Psp response in a *pspC* deletion reporter strain producing PspC-CT (Figure 7C). However, TatA did not induce the Psp system further in a *pspBC* deletion reporter strain producing PspC-CT or PspC (Figure 7D), indicating that PspB is required for sensing of TatA induced membrane stress.

Identification of a region in PspA that interacts with the C terminal domain of PspC –In our efforts to characterize the PspC-PspA-related step in the signal transduction pathway, which

results in the Psp response, we screened for interactions by a bacterial two-hybrid (B2H) system. The interaction of PspC-CT with fragments covering all regions of PspA were examined by the adenylate-cyclase based B2H system, in which active adenylate cyclase (CyaA) is reconstituted from N-terminal and C-terminal domains when fused protein domains interact (28). Interactions that result in active adenylate cyclase promote the fermentation of lactose and maltose, resulting in pink color on MacConkey agar due to acid formation. As summarized in Figure 8, this screen indicated interactions between the C-terminal domain of PspC with the recently structurally characterized first coiled coil domain of PspA (14). The orientation of the fusions was highly important, as CyaA activity could only be reconstituted in a strain with the T18 domain fused N-terminally to PspC-CT. Interestingly, the first 24 residues of PspA were dispensable for the PspC interaction except for the fragment (25-222) which was obviously not able to interact with PspC for unknown reasons. However, these N-terminal residues are known to have an independent function, folding back onto the first coiled coil in a "parking position" and forming a membrane-interacting amphipathic helix under stress conditions (14, 16). The C-terminal part of PspA did not exhibit any interaction with the tested PspC domain in this initial screen. All observed interactions could be reproduced by the measurement of the LacZ activity of the tested strain in LB media. When the E102Q or V105D substitutions were introduced in the T18-PspC-CT proteins, the interaction with PspA was still detectable with the E102Q exchange and abolished by the V105D mutation, as already evidenced by the above described co-elution experiments. We now can make the conclusion that the PspC interacting domain of PspA is most likely within the 1-144 fragment of PspA.

DISCUSSION

TatA as a model inducer of the Psp system — We found that TatA induces the same signaling cascade as secretins do in *Y. enterocolitica*. Therefore, TatA can be used as a simpler model inducer of the Psp system in *E. coli.* Secretins are large oligomeric complexes that - when mistargeted to the cytoplasmic membrane - can interact with the membrane components PspB and PspC (29). TatA not only interacts with PspB and PspC, but also with PspA (20, Figure 7B). Being a constituent of a protein translocation system, TatA destabilizes membranes in response to protein substrate binding (19). The membrane anchor of TatA has an unusual short length, which is causing this destabilization (19). The oligomerization of TatA is a prerequisite for membrane destabilization (30), and most likely multiple interacting membrane anchors cause the effects that are sensed by the Psp system. TatA or TatA-NT-Hip are the only inducers of the Psp system that are shown to directly interact with PspA, and this study was conceived originally to clarify whether a specific mechanism exists that senses TatA derived membrane stress, depending on the direct Psp system interaction. As the TatA-induced Psp response depended on the PspC-PspA interaction that required the same interaction site as known for secretin induced signaling (Figures 1,3,6), and as the N-terminal domain of PspC had the same negative regulatory role (Figure 1), the mechanism of signaling to the PspFA complex appears to be the same for TatA- and secretin induced membrane stress. PspC-CT already induces the Psp response in the presence of PspB (Figures 2,4), and TatA-*Strep* was able to induce the Psp system further (Figure 7). Therefore, stress sensing as induced by TatA does not require the trans-membrane domain of PspC, and the presence of the PspC-CT does not suffice to induce the Psp response to its maximum level. As there was no quantitative difference between the Psp response as induced by recombinant full-length PspC or PspC-CT in a Δ*pspC* strain, it appears that no regions of PspC other than its C-terminal domain function as positive regulator. In full agreement with this, Flores-Kim et al. showed that the N-terminal domain of PspC negatively regulates the C-terminal domain of PspC by binding to it (23), and therefore the complex of PspB and PspC regulates the interaction of PspC with the PspFA complex.

The PspC C-terminus can only induce the Psp response in a membrane-bound state – The membrane component PspC is known to be a positive regulator of the Psp system (17, 18). We found that the C-terminal domain of PspC must be in close contact to the inner side of the cytoplasmic membrane to function as positive regulator for the activation of PspF (Figure 4). Recently it was

reported that PspC undergoes a conformational change in the course of Psp system induction, which liberates the C-terminus of PspC that otherwise interacts with the N-terminal part of PspC and PspB (23, 9). In the suggested model, the liberation of the C terminus enables PspC to interact with PspA, thereby transmitting the signal to the PspFA complex (9). We thus predicted that the soluble PspC-CT domain should be a perfect inducer independent of membrane interactions. To our surprise, this was not the case, as PspC-CT could not induce the transcriptional activity of the PspFA complex in the absence of PspB. Only PspC-CT that was membrane-recruited by PspB could induce the Psp response - possibly together with PspB, which is in full agreement with the data provided by Flores-Kim et al. (23). However, PspB was only required to associate PspC-CT with the membrane. Accordingly, when the per se membrane anchored full-length PspC was used for the induction, PspB became dispensable. It thus seems that the membrane environment of the C-terminal domain of PspC is the prerequisite for signaling to PspFA. Nevertheless, PspB strongly enhanced the Psp response induction by PspC (Figure 4B).

As there is no Psp response in a *pspBC* deletion mutant producing PspC-CT (Figure 4B), it can be assumed that PspA binds to and inhibits PspF under this condition, and PspC-CT has no effect. This changes in the presence of PspB, when some PspC-CT binds to the membrane and PspFA thus can be recruited to the membrane, resulting in an activation of PspF. It might be that some PspC-CT already interacts with PspFA in the cytoplasm, as traces of PspA were found to co-elute with PspC-CT in the absence of PspB and PspC (Figure 4A). However, in the natural case, PspB and PspC are present as full-length proteins in the membrane, and therefore PspFA must contact PspC at the membrane surface. Taken together, the data clearly indicate that the signaling to PspFA requires the interaction with the membrane surface. This agrees with the current view that PspA itself undergoes important conformational changes upon membrane interaction that may be essential for the activation of PspF (16)

Recombinant PspA can interact with TatA-Strep in the absence of PspB and PspC – As mentioned above, PspA is known to interact with the membrane-stress inducing protein TatA (20). Recently, we could show that TatA also interacts with recombinantly produced PspA that completely silenced the *psp* response (16), which was a first hint that PspB and PspC per se may not be strictly required for the TatA/PspA interaction. However, in that study, we could not exclude that very low levels of PspB and PspC were contributing to the interaction. Without overproduction, PspA requires PspB and PspC to interact with the membranes (26), and these components thereby most likely indirectly mediate the TatA/PspA interaction. Recombinantly produced PspA clearly interacted with TatA even in the absence of PspB and PspC (Figure 7B), which agrees with the observation that some recombinant PspA can associate with membranes autonomously (26, 25, 10), possibly by its N-terminal amphipathic helix (27). We thus think that PspA can in principle interact directly with stressor proteins in the membrane, albeit normally PspB and PspC enhance this interaction. In this context, it is important to recognize that PspC-CT could stimulate the interaction of PspA with TatA without becoming a detectable constituent of the association (Figure 6). Either, PspC-CT is only weakly bound and washed off during affinity purification, or it only recruites PspA to the membranes where it can interact with TatA. In conclusion, PspA seems to require PspB and PspC to associate with membranes and hence with TatA under physiological conditions, and high abundance of PspA promotes a PspBC independent membrane association that permits the TatA contact in the absence of PspB and PspC. It may be that PspB and PspC can directly interact with TatA as well, as – when recombinantly produced - these components co-eluted abundantly with TatA-*Strep* similar to PspA (Figure 7B). However, PspA was present in these strains and might have mediated this interaction.

An integrative update for the model of stress-sensing and transmission by the Psp system – We propose that the two existing models for the stress sensing and signaling by the Psp system, which attribute key functions to either PsBC or PspA (9, 23, 31), can be unified at least for the Psp response to protein-induced membrane stress: PspB is required for TatA induced membrane stress sensing and strongly enhances the transmitted signal (Figure 7). It interacts with the C-terminus of PspC,

as the isolated C-terminal domain PspC-CT is PspB-dependently recruited to the membrane (Figure 4C). The N- and C-terminal domains of PspC interact in the absence of membrane stress, and a stress signal results in accessibility of the C-terminal domain, which binds to PspA (23, 9). It is very likely that the previously reported rearrangement of interactions of the C-terminus of PspC are supported by the structure of the membrane-integral region of PspC. The central glycine residue in the middle of the transmembrane domain of PspC surely can support this flexibility, as mutation of that position results in increased steady state activity. PspC is predicted to form a coiled coil with its C-terminal domain, which includes residues that are essential for the PspA interaction, and leucine heptades even continue to the very end of PspC (Supplement Figure S2). As we identified the coiled coil domain of PspA (position 25-144) as interaction partner (Figure 8), we suggest that the C-terminus of PspA most likely can form a triple coiled coil with this domain to transduce the signal. This would require the displacement of the N-terminal PspA region (position 2-24), which is bound to the coiled coil of PspA when PspA is not membrane-interacting (14). The displacement of the N-terminal PspA region would be triggered by the reported formation of the amphipathic helix at the membrane surface (27, 16). This explains why the membrane interaction of PspA appears to be a prerequisite for the strong interaction with PspC (Figure 4C). This model, summarized in Figure 9, explains how membrane association of the amphipathic helix of PspA and the PspA/PspC interaction can be coupled processes that both must occur to achieve the stress signal transmission. Accordingly, we could detect only a very weak co-elution of PspC-CT with PspA in the absence of PspB (Figure 4A), and even if this interaction occurs in the cytoplasm, there is no induction without membrane recruitment (Figure 4BC). While it is clear that PspBC must be present for the Psp response to protein induced membrane stress *in vivo*, the membrane interaction as mediated by the amphipathic helix at the N-terminus of PspA has been shown to suffice to induce the Psp response with lipid induced membrane stress in specific *in vitro* assays (10). In fact, the PspFA regulatory complex is more conserved than the associated components PspB and PspC (32), and it is tempting to speculate that the more simple PspFA regulatory system can in principle function *per se* or in conjunction with other associated proteins as stress sensor in some systems, especially in response to stored curvature elastic membrane stress (10).

It is not clear yet what happens to the PspFA complex. The PspFA complex can potentially be found at membrane surfaces, as evidenced by Mehta et al. (31) and it can respond to the addition of phospholipids in a defined *in vitro* system without PspBC, as demonstrated by the same group some years later (10). It is therefore reasonable that the regulatory complex directly receives the inducing signal at the cytoplasmic membrane, but *in vivo* PspB and PspC-CT must be involved. It is not really clear whether or not PspA dissociates upon activation, as PspA may regulate PspF in a PspF-bound state by its first coiled coil domain (14, 16). As this coiled coil possibly interacts with PspC-CT directly (Figure 8), it is tempting to speculate that the first coiled-coil receives a signal from PspC by a direct interaction that modulates its binding to PspF. Based on our finding that an already by PspC-CT upregulated Psp system can be further induced by TatA, we believe that the PspFA complex is able to sense the Psp signal synergistically, possibly by a more efficient formation of the PspA amphipathic helix. Future studies will hopefully unravel the structure of the PspABC(F) regulatory complex at the cytoplasmic membrane, which would help to understand the molecular details of this unusual stress signaling pathway.

EXPERIMENTAL PROCEDURES

Strains and growth conditions – E. coli MC3 (21) and its derivatives were used for all fractionation and co-elution experiments. *E. coli* XL1-Blue Mrf' Tet (Stratagene) was used for cloning. Cells were grown aerobically in LB medium at 37°C with the appropriate antibiotics (100 µg/ml ampicillin, 25 µg/ml chloramphenicol, 50 µg/ml kanamycin). Bacterial-2-hybrid analyses were performed with *E. coli* BTH101 according to the manufacturer's protocol (Euromedex, France), with cultures grown at 30°C. All strains and plasmids used in this study are listed in Supplementary Table S1.

Genetic methods and plasmids – The *pspBC* double knock-out was initially introduced in the strain BW25113 with the Datsenko & Wanner

method (33) and the position of the kanamycin cassette was checked by colony PCR. The strain BW25113 *pspBC::kan* as well as the Keio-collection derived strain BW25113 *pspC::kan* were used as donor strains to construct by phage transduction with $P1_{vir}$ (34) the strains MC3 *pspC::kan* or MC3 *pspBC::kan*, respectively. After the initial selection on kanamycin (50 µg/ml) containing LB agar plates, colonies were purified two times and the position of the kanamycin cassette was confirmed via colony PCR.

To constitutively produce the C-terminal domain of PspC in a stable and detectable way, it was fused to the C-terminus of the small and tightly folded mature HiPIP (mHip, 35), and the gene was expressed using the P_{tatA} promoter. For cloning, the *pspC* C-terminal region was amplified using the primers *pspC*61-BglII-F (TAT ATA TAG ATC TTC ATT TGC GCT TGA TC) and *pspC*-BamHI-R (TAT ATA TGG ATC CTT ACA GTT GAC GGA AAC) with pABS-*Ptat-pspC*-H6 as template, restricted with BglII/BamHI and ligated into BamHI-restricted pABS-H10*mhip*-H6 (15), resulting in pABS-*Ptat*-H10*mhip-pspC(CT)*. Site specific mutations of pABS-*Ptat*-H10*mhip-pspC(CT)* and pUL-*pspF*strep-*pspABC*-H6 (15) were generated by QuikChange (Stratagene) mutagenesis. Primers are listed in Supplementary Table S2.

For bacterial-2-hybrid analysis pUT18C-*pspC*(61-119)-strep was constructed by amplifiying the *pspC* fragment with primers BamHI-*pspC*(S61)-F (AAT TAG GAT CCT CAT TTG CGC TTG ATC CAA TG) and *pspC*(119)-ggKpnI-R (TTA AAG GTA CCC CCA GTT GAC GGA AAC GGC TAC GTA ACG TG) using pABS-P*tat-pspC*-H6 as template. The PCR product was cut with KpnI/BamHI and cloned into the KpnI/BamHI restricted plasmid pUT18C-*pspA*(145-222)-strep (15). All *pspA* fragment-containing plasmids used in the bacterial-2-hybrid assays are listed in Supplementary Table S1.

Biochemical methods – For cell fractionations, cells were aerobically grown at 37°C in the presence of appropriate antibiotics. For rhamnose induction, rhamnose was added to a final concentration of 0.1 % (v/v) at an optical density of ~0.6 and cultivation was continued for at least 3 h. For cell fractionations, OD-normalized cells were harvested by centrifugation at 4500 x *g* for 10 min at 4°C. Cell pellets were suspended in 50 mM Tris-HCl pH 8.0/ 250 mM NaCl. DNaseI (~0.5 mg/ml) and 1 mM PMSF cells were added prior to cell disruption. After removal of cell debris, membrane and soluble fractions were separated by ultracentrifugation at 130,000 x *g* for 30 min at 4°C. SDS-PAGE sample buffer was immediately added after separation and samples were analysed by SDS-PAGE/Western blotting as described previously (36, 37).

For co-elution experiments TatA-*Strep* was affinity-purified as described previously (20) with the exception that purification was performed from crude cell extracts after separation of the cell debris. For co-elution assays with His-tagged proteins, cells were resuspended in 100 mM Tris-HCl pH 8.0, 150 mM NaCl, 20 mM imidazole and homogenized via French Press. Protino Ni-NTA resin (Macherey-Nagel) was used for purifications of His-tagged proteins. After 6 washing steps with homogenization buffer, bound proteins were eluted by increasing the imidazole concentration to 250 mM. Elution fractions were analyzed via SDS-PAGE/Western blotting. His-tagged proteins were detected by specific monoclonal antibodies (Qiagen). For detection of TatA-*Strep*, PspA or PspB TatA-, PspA- or PspB-specific polyclonal rabbit antibodies were used. Bound primary antibodies were detected using secondary antibodies coupled to horse raddish peroxidase or alkaline phosphatase.

PspA promoter activity was determined in *pspA* promoter *lacZ*-reporter strains by β-Galactosidase assays performed in triplicate as described in (14). LacZ activity that correlates with adenylate cyclase reconstitution in BTH101 was measured as described above with three independent clones after overnight cultivation in LB medium supplemented with 0.5 mM IPTG.

REFERENCES

1. Brissette, J. L., Russel, M., Weiner Lorin, and Model, P. (1990) Phage shock protein, a stress protein of *Escherichia coli*. *Proc. Natl. Acad. Sci. U S A* **87**, 862–866
2. Brissette, J. L., Weiner, L., Ripmaster, T. L., and Model, P. (1991) Characterization and sequence of the *Escherichia coli* stress-induced *psp* operon. *J. Mol. Biol.* **220**, 35–48
3. Weiner, L., Brissette, J. L., and Model, P. (1991) Stress-induced expression of the *Escherichia coli* phage shock protein operon is dependent on σ54 and modulated by positive and negative feedback mechanisms. *Genes Dev.* **5**, 1912–1923
4. Joly, N., Engl, C., Jovanovic, G., Huvet, M., Toni, T., Sheng, X., Stumpf, M. P. H., and Buck, M. (2010) Managing membrane stress: the phage shock protein (Psp) response, from molecular mechanisms to physiology. *FEMS Microbiol. Rev.* **34**, 797–827
5. Flores-Kim, J., and Darwin, A. J. (2016) The phage shock protein response. *Annu Rev Microbiol* **70**, 83–101
6. Flores-Kim, J., and Darwin, A. J. (2014) Regulation of bacterial virulence gene expression by cell envelope stress responses. *Virulence* **5**, 835–851
7. Wallrodt, I., Jelsbak, L., Thomsen, L. E., Brix, L., Lemire, S., Gautier, L., Nielsen, D. S., Jovanovic, G., Buck, M., and Olsen, J. E. (2014) Removal of the phage-shock protein PspB causes reduction of virulence in *Salmonella enterica* serovar Typhimurium independently of NRAMP1. *J. Med. Microbiol.* **63**, 788–795
8. Yamaguchi, S., Reid, D. A., Rothenberg, E., and Darwin, A. J. (2013) Changes in Psp protein binding partners, localization and behaviour upon activation of the *Yersinia enterocolitica* phage shock protein response. *Mol. Microbiol.* **87**, 656–671
9. Flores-Kim, J., and Darwin, A. J. (2015) Activity of a bacterial cell envelope stress response is controlled by the interaction of a protein binding domain with different partners. *J. Biol. Chem.* **290**, 11417–11430
10. McDonald, C., Jovanovic, G., Ces, O., and Buck, M. (2015) Membrane stored curvature elastic stress modulates recruitment of maintenance proteins PspA and Vipp1. *mBio* **6**, 15
11. Dworkin, J., Jovanovic, G., and Model, P. (1997) Role of upstream activation sequences and integration host factor in transcriptional activation by the constitutively active prokaryotic enhancer-binding protein PspF. *J. Mol. Biol.* **273**, 377–388
12. Jovanovic, G., Dworkin, J., and Model, P. (1997) Autogenous control of PspF, a constitutively active enhancer-binding protein of *Escherichia coli*. *J. Bacteriol.* **179**, 5232–5237
13. Dworkin, J., Jovanovic, G., and Model, P. (2000) The PspA protein of *Escherichia coli* is a negative regulator of σ^{54}-dependent transcription. *J. Bacteriol.* **182**, 311–319
14. Osadnik, H., Schöpfel, M., Heidrich, E., Mehner, D., Lilie, H., Parthier, C., Risselada, H. J., Grubmüller, H., Stubbs, M. T., and Brüser, T. (2015) PspF-binding domain PspA1-144 and the PspA·F complex: New insights into the coiled-coil-dependent regulation of AAA+ proteins. *Mol. Microbiol.* **98**, 743–759
15. Heidrich, E. S., and Brüser, T. (2018) Evidence for a second regulatory binding site on PspF that is occupied by the C-terminal domain of PspA. *PLoS One*, accepted for publication
16. McDonald, C., Jovanovic, G., Wallace, B. A., Ces, O., and Buck, M. (2017) Structure and function of PspA and Vipp1 N-terminal peptides: Insights into the membrane stress sensing and mitigation. *Biochim. Biophys. Acta* **1859**, 28–39
17. Jovanovic, G., Engl, C., Mayhew, A. J., Burrows, P. C., and Buck, M. (2010) Properties of the phage-shock-protein (Psp) regulatory complex that govern signal transduction and induction of the Psp response in *Escherichia coli*. *Microbiology* **156**, 2920–2932
18. Kleerebezem, M., Crielaard, W., and Tommassen, J. (1996) Involvement of stress protein PspA (phage shock protein A) of *Escherichia coli* in maintenance of the protonmotive force under stress conditions. *EMBO J.* **15**, 162–171

19. Hou, B., Heidrich, E. S., Mehner-Breitfeld, D., and Brüser, T. (2018) The TatA component of the twin-arginine translocation system locally weakens the cytoplasmic membrane of *Escherichia coli* upon protein substrate binding. *J. Biol. Chem.* **293**, 7592-7605
20. Mehner, D., Osadnik, H., Lünsdorf, H., and Brüser, T. (2012) The Tat system for membrane translocation of folded proteins recruits the membrane-stabilizing Psp machinery in *Escherichia coli*. *J. Biol. Chem.* **287**, 27834–27842
21. Bergler, H., Abraham, D., Aschauer, H., and Turnowsky, F. (1994) Inhibition of lipid biosynthesis induces the expression of the *pspA* gene. *Microbiology* **140**, 1937–1944
22. Gueguen, E., Savitzky, D. C., and Darwin, A. J. (2009) Analysis of the *Yersinia enterocolitica* PspBC proteins defines functional domains, essential amino acids and new roles within the phage-shock-protein response. *Mol. Microbiol.* **74**, 619–633
23. Flores-Kim, J., and Darwin, A. J. (2016) Interactions between the Cytoplasmic Domains of PspB and PspC Silence the Yersinia enterocolitica Phage Shock Protein Response. *Journal of bacteriology* **198**, 3367–3378
24. Standar, K., Mehner, D., Osadnik, H., Berthelmann, F., Hause, G., Lünsdorf, H., and Brüser, T. (2008) PspA can form large scaffolds in *Escherichia coli*. *FEBS Letters* **582**, 3585–3589
25. Kobayashi, R., Suzuki, T., and Yoshida, M. (2007) *Escherichia coli* phage-shock protein A (PspA) binds to membrane phospholipids and repairs proton leakage of the damaged membranes. *Mol. Microbiol.* **66**, 100–109
26. Yamaguchi, S., Gueguen, E., Horstman, N. K., and Darwin, A. J. (2010) Membrane association of PspA depends on activation of the phage-shock-protein response in *Yersinia enterocolitica*. *Mol. Microbiol.* **78**, 429–443
27. Jovanovic, G., Mehta, P., McDonald, C., Davidson, A. C., Uzdavinys, P., Ying, L., and Buck, M. (2014) The N-terminal amphipathic helices determine regulatory and effector functions of phage shock protein A (PspA) in *Escherichia coli*. *J. Mol. Biol.* **426**, 1498–1511
28. Karimova, G., Pidoux, J., Ullmann, A., and Ladant, D. (1998) A bacterial two-hybrid system based on a reconstituted signal transduction pathway. *Proc. Natl. Acad. Sci. U S A* **95**, 5752–5756
29. Srivastava, D., Moumene, A., Flores-Kim, J., and Darwin, A. J. (2017) Psp stress response proteins form a complex with mislocalized secretins in the *Yersinia enterocolitica* cytoplasmic membrane. *mBio* **8**
30. Rodriguez, F., Rouse, S. L., Tait, C. E., Harmer, J., Riso, A. de, Timmel, C. R., Sansom, M. S. P., Berks, B. C., and Schnell, J. R. (2013) Structural model for the protein-translocating element of the twin-arginine transport system. *Proc. Natl. Acad. Sci. U S A* **110**, 101
31. Mehta, P., Jovanovic, G., Lenn, T., Bruckbauer, A., Engl, C., Ying, L., and Buck, M. (2013) Dynamics and stoichiometry of a regulated enhancer-binding protein in live *Escherichia coli* cells. *Nat. Commun.* **4**, 1997
32. Huvet, M., Toni, T., Sheng, X., Thorne, T., Jovanovic, G., Engl, C., Buck, M., Pinney, J. W., and Stumpf, M. P. H. (2011) The evolution of the phage shock protein response system: interplay between protein function, genomic organization, and system function. *Mol. Biol. Evol.* **28**, 1141–1155
33. Datsenko, K. A., and Wanner, B. L. (2000) One-step inactivation of chromosomal genes in *Escherichia coli* K-12 using PCR products. *Proc. Natl. Acad. Sci. U S A* **97**, 6640–6645
34. Miller, J. H. (1972) *Experiments in molecular genetics,* Cold Spring Harbor Laboratory, Cold Spring Harbor NY
35. Brüser, T., Yano, T., Brune, D. C., and Daldal, F. (2003) Membrane targeting of a folded and cofactor-containing protein. *Eur. J. Biochem.* **270**, 1211–1221
36. Laemmli, U. K. (1970) Cleavage of structural proteins during the assembly of the head of bacteriophage T4. *Nature* **227**, 680–685
37. Towbin, H., Staehelin, T., and Gordon, J. (1992) Electrophoretic transfer of proteins from polyacrylamide gels to nitrocellulose sheets: Procedure and some applications. 1979. *Biotechnology (Reading, Mass.)* **24**, 145–149

ACKNOWLEDGEMENTS
We thank Inge Reupke and Sybille Traupe for technical assistance and the DFG for funding (DFG grant BR2285/4-2).

CONFLICT OF INTEREST
The authors declare that they have no conflicts of interest with the contents of this article.

AUTHOR CONTRIBUTIONS
TB and ESH conceived and designed the study. ESH did the experiments and analyzed the data together with TB. ESH prepared figures and both authors wrote the manuscript.

FIGURES

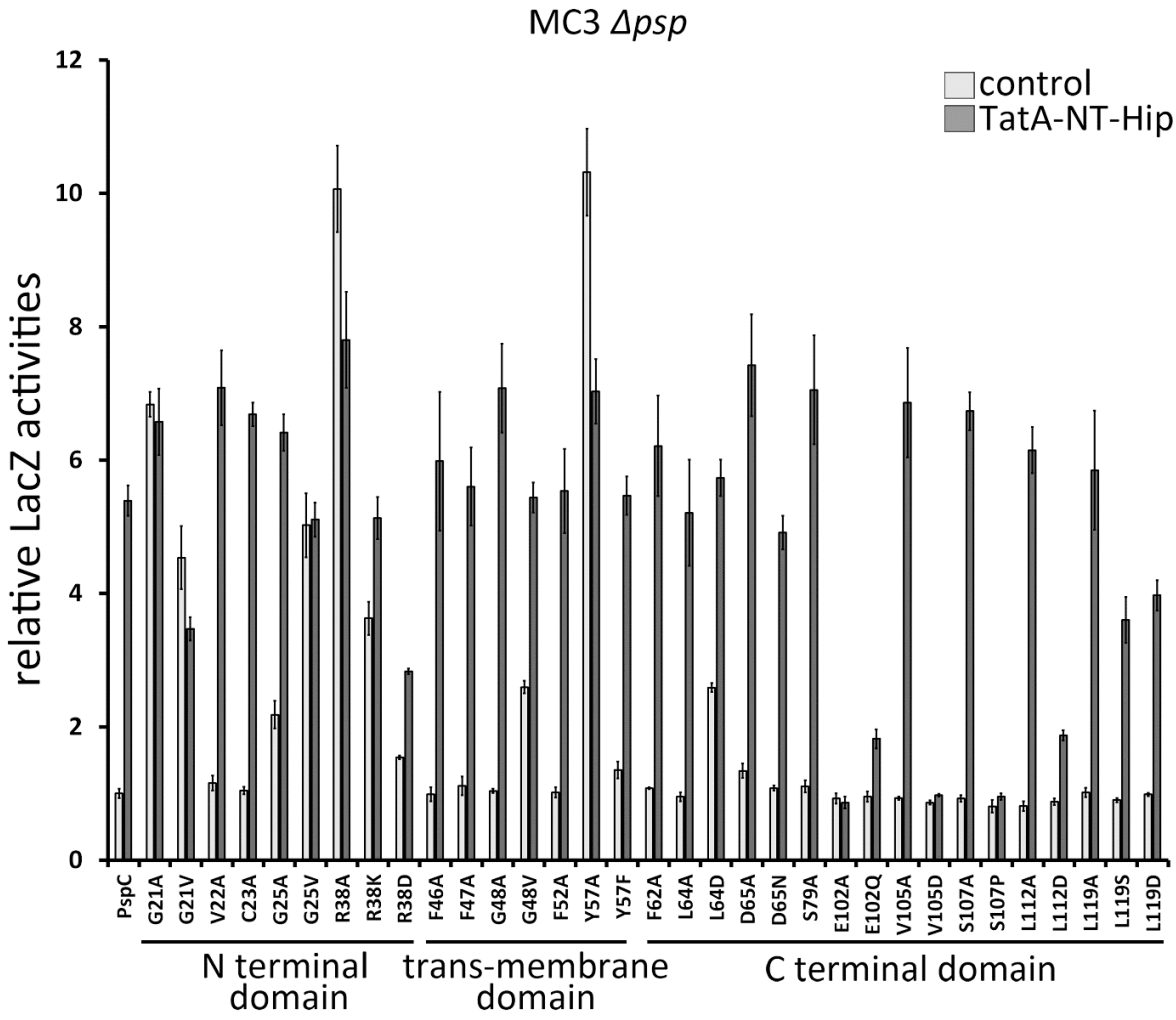

Figure 1: Effect of PspC point mutations on steady state and induced P_{pspA} expression levels. LacZ activity in the P_{pspA}-*lacZ* reporter strain MC3 Δ*pspFABCDE*, with a functionally reconstituted *pspFABC* signaling pathway (left, labeled PspC) was compared to systems with the indicated amino acid exchanges in PspC. Values were normalized to the activity of the not induced and not mutated system. Light gray, activities of the uninduced systems; dark gray, activities of the system as induced by TatA-NT-Hip.

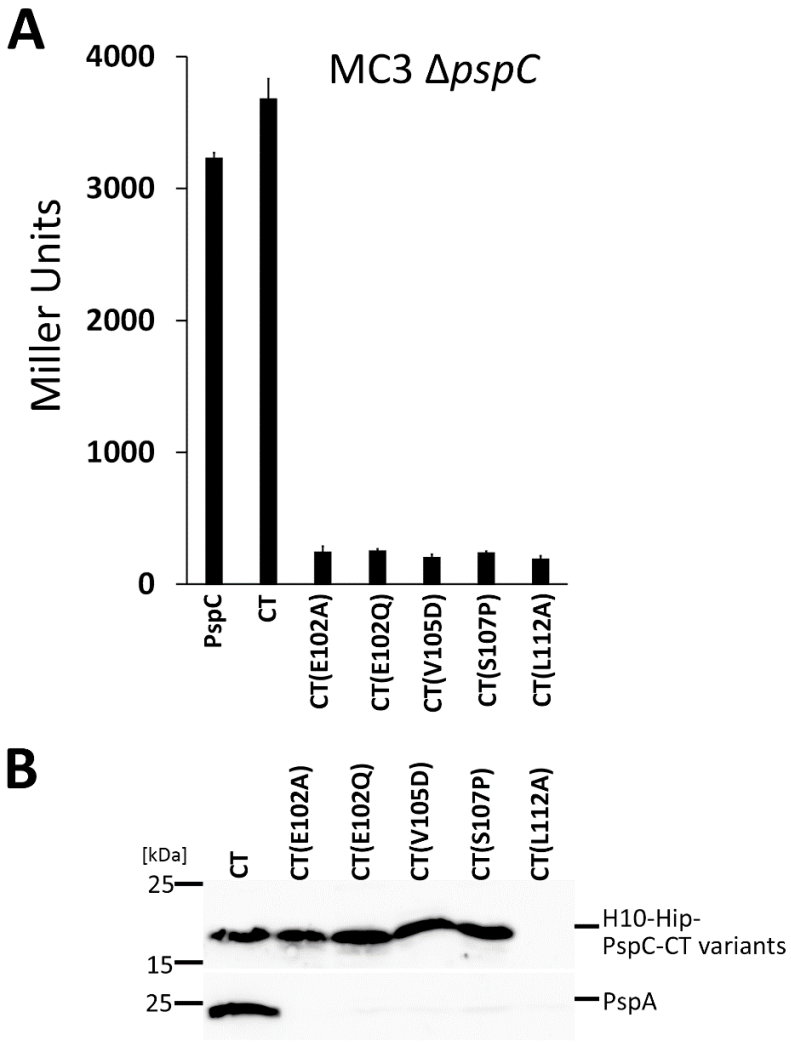

Figure 2: The C-terminus of PspC can induce the Psp response. (A) LacZ activity in the P_{pspA}-*lacZ* reporter strain MC3 deleted in *pspC*, with recombinantly produced PspC (PspC), PspC-CT (CT), or CT carrying indicated point muations that were shown to abolish the TatA-inducible Psp response. (B) SDS-PAGE/Western blot detection of His-tagged PspC-CT variants (upper blot) and PspA (lower blot), using specific antibodies against His-tags and PspA. Note that, with the exception of PspC-CT(L112A), all PspC-CT variants are produced at comparable levels, but only the unmutated protein induces the overproduction of PspA. Masses of marker proteins are indicated on the left.

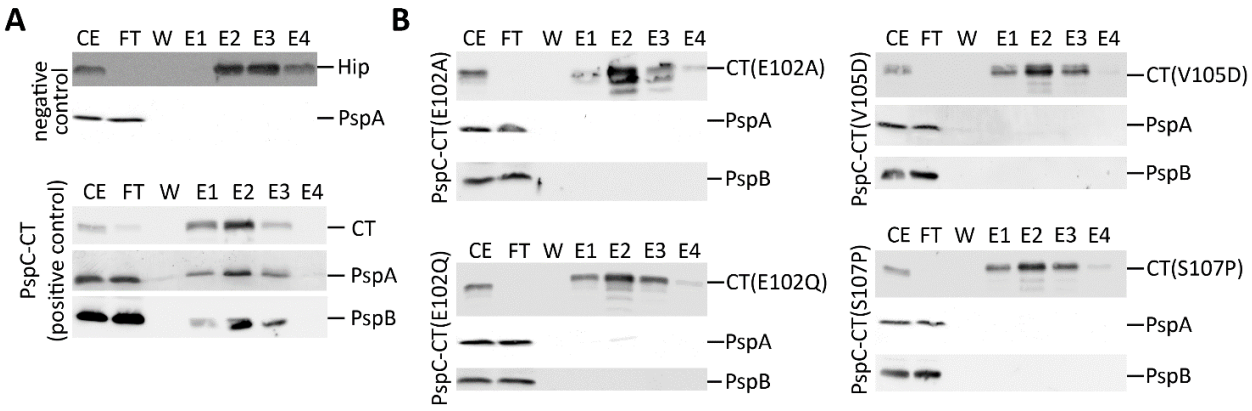

Figure 3: Analyis of the interaction of PspC-CT and its derivatives with PspA and PspB. (A) Affinity purification of His-tagged HiPIP alone (negative control) or HiPIP-fused PspC-CT (positive control), and co-elution of PspA and PspB with PspC-CT (lower blots). (B) The same analyses as in A, but with indicated point mutations in PspC-CT. Note that the mutations abolish the co-elution of PspA and PspB, and only in case of E102Q there is a faintly detectable PspA- and no PspB co-elution. CE, crude extract; FT, flow through; W, last wash fraction; E1-4, elution fractions 1-4. Apparent masses of the detected proteins: H10-HiPIP, ~12 kDa; PspA, ~23 kDa; PspB, ~11 kDa; PspC-CT variants, ~18 kDa.

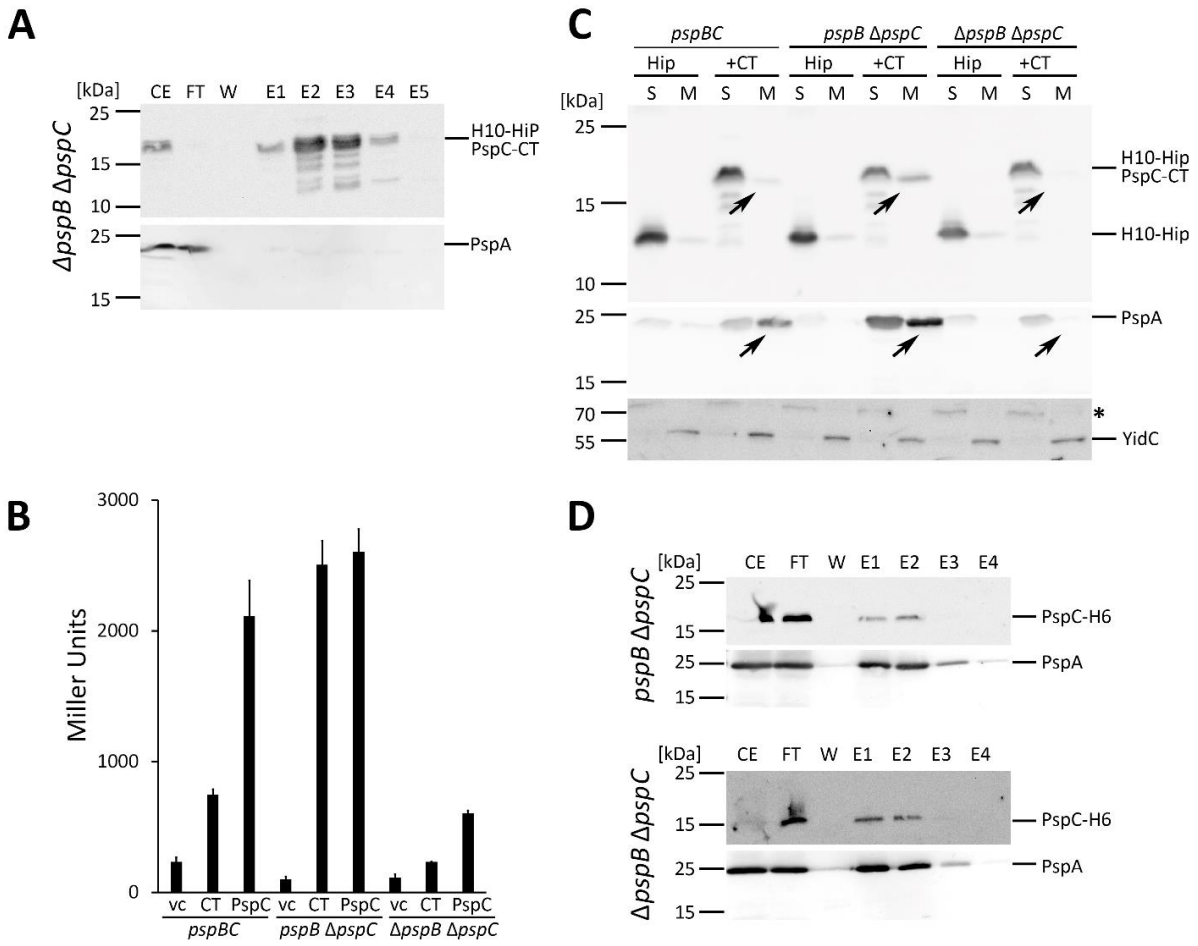

Figure 4: PspB promotes the interaction of PspC-CT with PspA. (A) Affinity purification of H10-tagged Hip-PspC-CT, and detection of Hip-PspC-CT (upper blot) and PspA (lower blot) in the fractions. Note that PspA is hardly detectable in the elution fractions. (B) LacZ activity in P_{pspA} reporter strains in the presence of an empty expression vector (vector control, vc), recombinant Hip-PspC-CT (CT), or full-length PspC, each with indicated genetic backgrounds, which were in the presence of *pspB* and *pspC* (left set of columns), in the absence of PspC (middle set of columns), or in the absence of PspB and PspC (right set of columns). (C) Detection of H10-tagged HiPIP (Hip) or Hip-PspC-CT (CT) (upper blot), and PspA (middle blot) in subcellular fractions. S, soluble fraction; M, membrane fraction. YidC was detected as membrane protein control (lower blot). The asterisk indicates a cross-reaction with a soluble protein, confirming the quality of the fractionation. Note that PspC-CT recruites most PspA to the membrane in a strain containing PspB and lacking PspC. (D) Interaction of PspA with His-tagged PspC does not require PspB. Affinity purification of His-tagged PspC, and detection of His-tagged PspC (upper blots) and PspA (lower blots) in strains lacking either PspC alone or PspC and PspB, as indicated. Fractions in A and D are labeled as described in Fig. 3. Masses of marker proteins are indicated on the left.

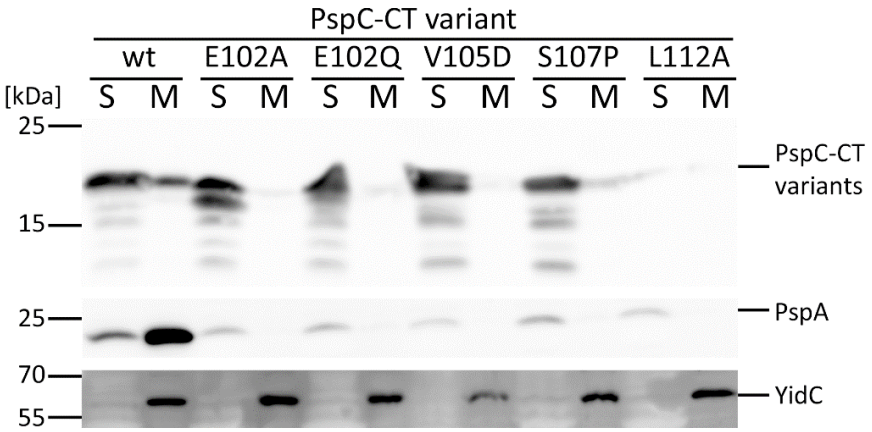

Figure 5: The residues in the C-terminus of PspC that are essential for signaling are responsible for the recruitment of PspC-CT and PspA to the cytoplasmic membrane. Soluble and membrane fractions were analyzed by SDS-PAGE/Western blotting for the presence of PspC-CT variants (upper blot) and PspA (middle blot). A YidC detection served as fractionation control (lower blot). Note the detection of wild type PspC-CT and PspA in the membrane fraction (wt lanes), whereas PspA cannot be recruited to membranes when PspC-CT carries the indicated point mutations. Masses of marker proteins are indicated on the left.

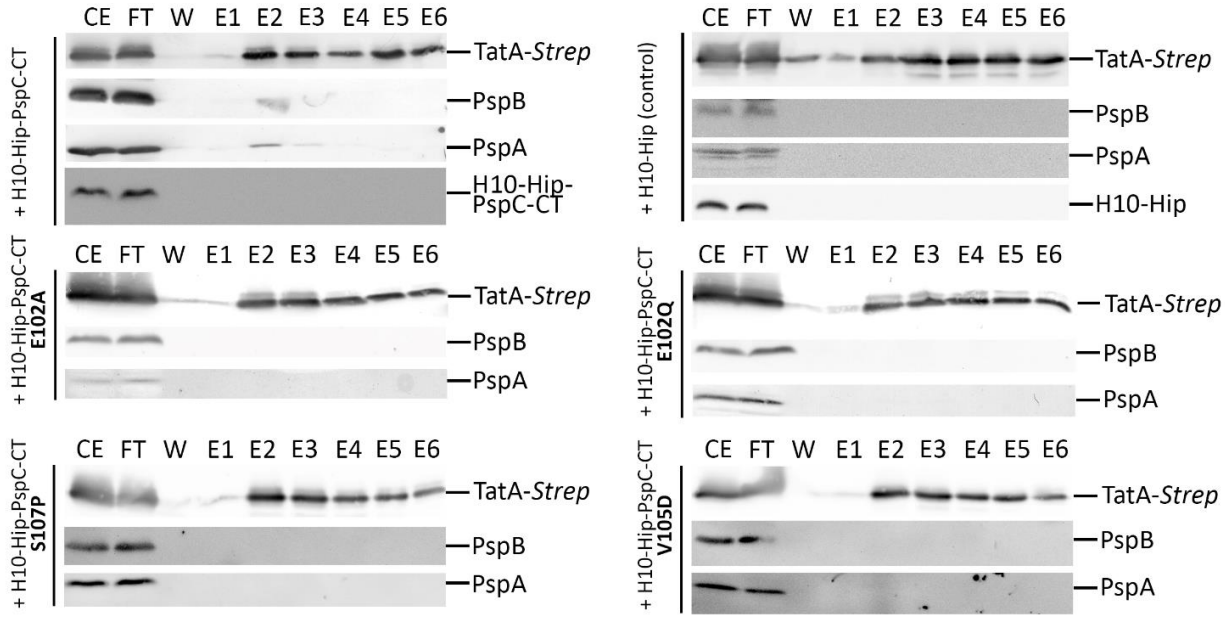

Figure 6: The residues in the C-terminus of PspC that are essential for signaling are required for the TatA interaction with PspA and PspB. Purification of Strep-tagged TatA in strains lacking PspC and producing instead the H10-Hip-PspC-CT construct without mutation in PspC-CT (upper left panels), or the same construct with mutations in PspC-CT as indicated on the left of the panels. Fractions are labeled as described in Fig. 3. Apparent masses of the detected proteins: TatA-Strep, ~14 kDa; PspB, ~11 kDa; PspA, ~23 kDa; H10-Hip-PspC-CT, ~18 kDa; H10-HiPIP, ~12 kDa.

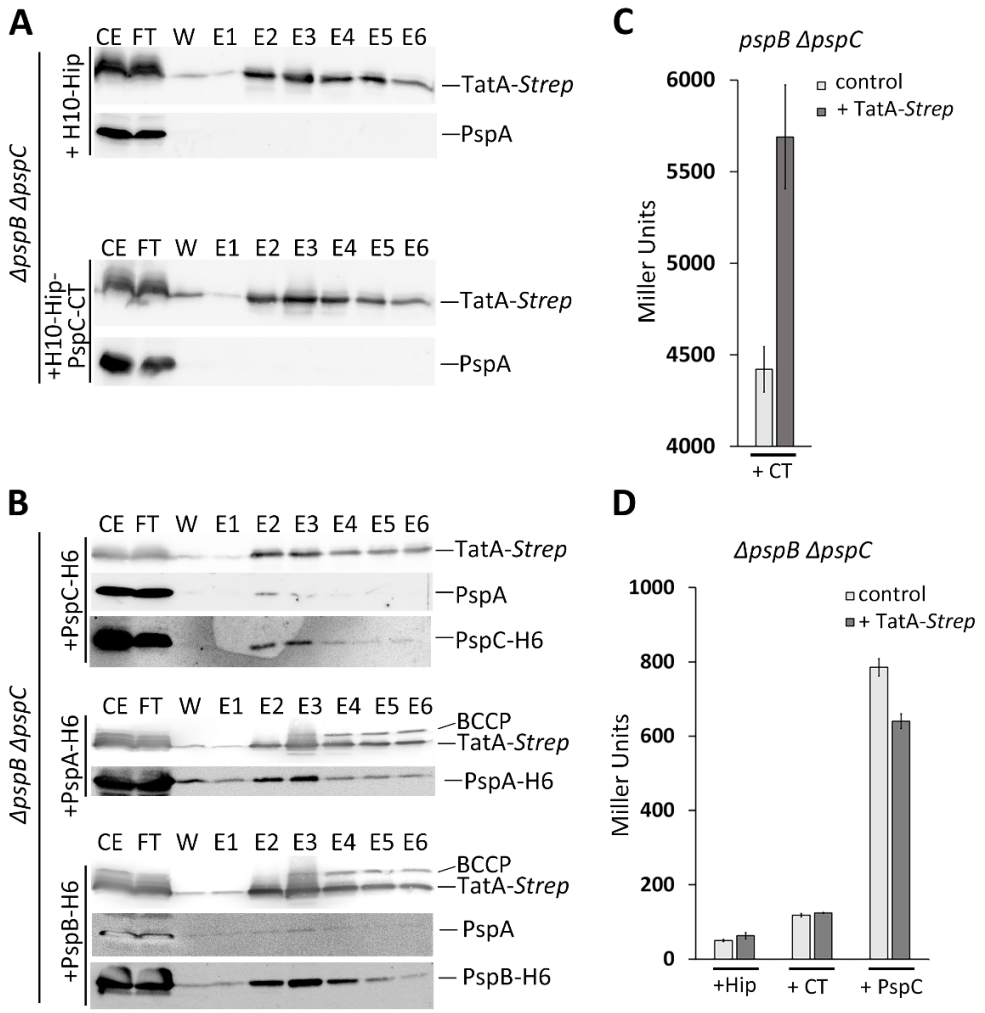

Figure 7: Requirements for the TatA interaction with Psp system components. (A) PspC-CT does not mediate the interaction of PspA with TatA in a Δ*pspBC* background. (B) Recombinantly produced PspC, PspA, or PspB can interact with TatA in a Δ*pspBC* background. (C) The trans-membrane domain of PspC is not necessary to induce a Psp response by TatA production. (D) In a strain lacking PspB, TatA cannot induce a Psp response, even in the presence of high levels of PspC-CT of PspC, which induces the Psp response per se to some extent. Fractions are labeled as described in Fig. 3. Apparent masses of the detected proteins: TatA-Strep, ~15 kDa; PspC-H6, ~16 kDa; PspB-H6, ~12 kDa; PspA, ~23 kDa; PspA-H6, ~24 kDa; H10-HiPIP, ~12 kDa; BCCP, biotin carboxyl carrier protein, ~22 kDa.

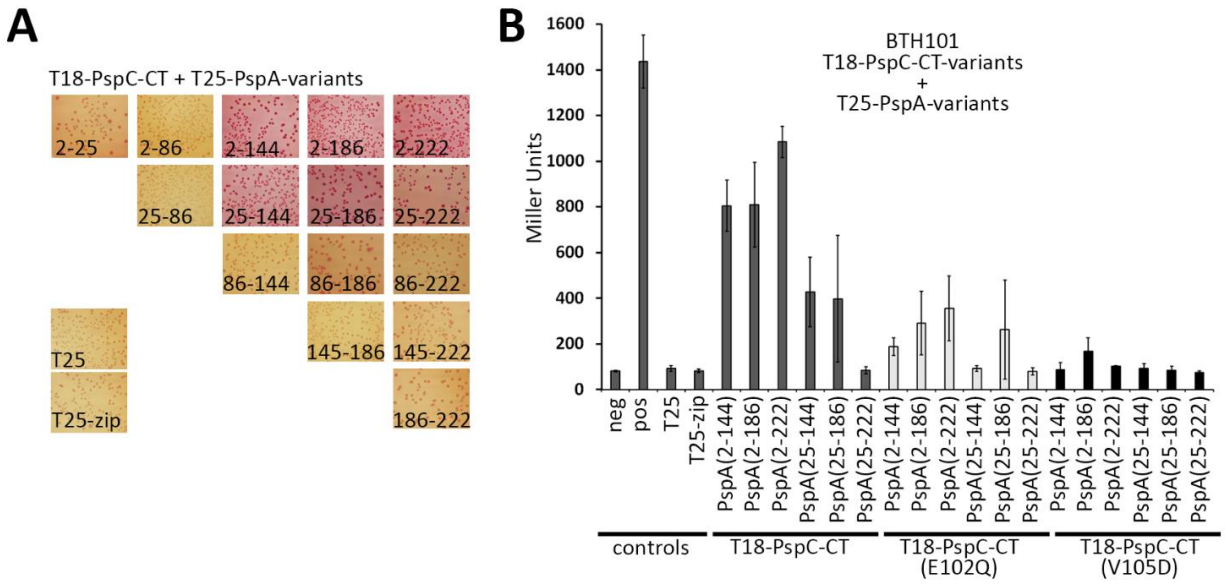

Figure 8: PspC-CT interacts with the first coiled coil domain of PspA. (A) B2H screen using T18-PspC-CT as bait and indicated PspA fragments fused to the C-terminus of the T25 domain as prey. Red colony and background color indicates an interaction. (B) Quantification of LacZ activities of the B2H strains that stained positively in A, and the analysis of potential effects of indicated mutations in PspC-CT (E102Q and V105D). The degree of LacZ activity correlates with the strength of the interaction.

The TatA-induced signaling cascade of the Psp response

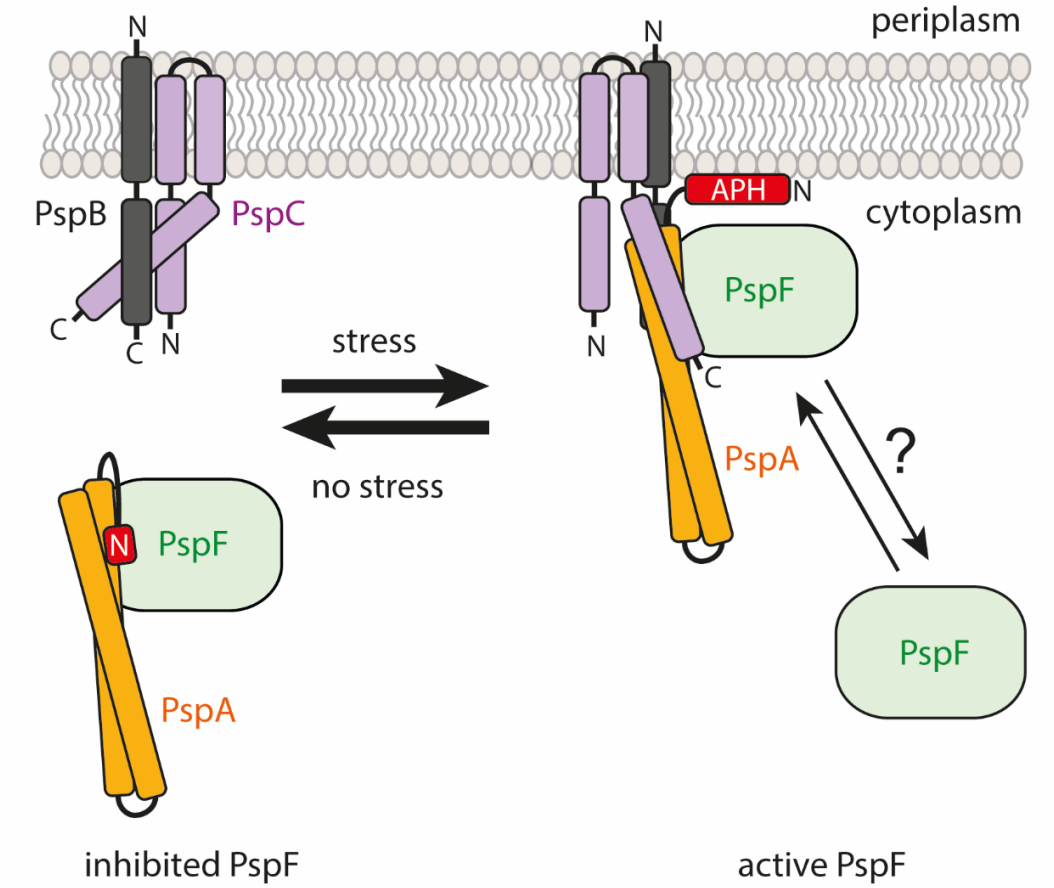

Figure 9: Coordination of the PspC/PspA interaction and the PspA amphipathic helix formation for membrane stress signal transmission in the Psp system. In the absence of stress, most PspA interacts with PspF in the cytoplasm and inhibits its activity. The N-terminus of PspA is back-folded onto the PspA coiled coil domain. The C-terminal domain of PspC is recruited by the N-terminal domain of PspC in a way that suppresses contacts with PspA. Upon membrane stress, PspA forms with its N-terminus (red) an amphipathic helix (red, APH), thereby allowing the C-terminal domain of PspC to interact with PspA, resulting in signal transduction. Whether PspF dissociates from PspA to induce the system is not clear yet. Note that we did not include the C-terminal domain of PspA in this scheme, which also interacts with PspF, for clarity reasons.

SUPPORTING INFORMATION

Dissection of membrane stress sensing and signal transmission by the Psp system at the cytoplasmic membrane in *Escherichia coli*

Eyleen S. Heidrich[1] and Thomas Brüser[1,2]

[1]From the Institute of Microbiology, Leibniz Universität Hannover, Herrenhäuser Straße 2, 30419 Hannover, Germany

Running title: The TatA-induced signaling cascade of the Psp response

[2]To whom correspondence should be addressed: Thomas Brüser, Institute of Microbiology, Leibniz Universität Hannover, Herrenhäuser Straße 2, 30419 Hannover, Germany; Tel. +49 511 762 5945; Fax: +49 511 762 5287; E-mail: brueser@ifmb.uni-hannover.de

Table S1: Strains and plasmids used in this study

Strains and Plasmids	**used for**	**Reference**
XL1	cloning	Stratagene
BW25113	strain construction	(1)
BW25113 *pspC*::*kan*	strain construction	(1)
BW25113 *pspBC*::*kan*	strain construction	This work
MC3	P_{pspA} activity reporter strain, co-elution analysis	(2)
MC3 *pspC*::*kan*	P_{pspA} activity reporter strain, co-elution analysis	(3)
MC3 *pspBC*::*kan*	P_{pspA} activity reporter strain, co-elution analysis	This work
BTH101	B2H analysis	Euromedex
MC3 *pspFABCDE*::*kan*	P_{pspA} activity activity assays, PspC mutagenesis screen	(4)
pABS-*pspC*-H6	P_{pspA} activity activity assays, co-elution analysis	(3)
pABS-H10*mhip*-H6	P_{pspA} activity activity assays, co-elution analysis	(4)
pABS-H10*mhip*-*pspC*(CT) and indicated derivatives theirof	P_{pspA} activity activity assays, co-elution analysis	This work
pBW-*tatA*-strep	P_{pspA} activity activity assays, co-elution analysis	(3)
pBW-*tatA*-NT-*mat*-*hip*-strep	P_{pspA} activity activity assays, PspC mutagenesis screen	(3)
pUL-*pspF*strep-*pspABC*-H6 and indicated derivatives theirof	P_{pspA} activity activity assays, PspC mutagenesis screen	(4)
pUT18	B2H analysis	Euromedex
pUT18C	B2H analysis	Euromedex
pUT18C-zip	B2H analysis	Euromedex
pKNT25	B2H analysis	Euromedex
pKT25	B2H analysis	Euromedex
pKT25-zip	B2H analysis	Euromedex
pKT25-*pspA*(2-25)-strep pKN-strep-*pspA*(2-25)-T25	B2H analysis	(4)
pKT25-*pspA*(2-85)-strep pKN-strep-*pspA*(2-85)-T25	B2H analysis	(4)
pKT25-*pspA*(2-144)-strep pKN-strep-*pspA*(2-144)-T25	B2H analysis	(4)
pKT25-*pspA*(2-186)-strep pKN-strep-*pspA*(2-186)-T25	B2H analysis	(4)
pKT25-*pspA*(2-222)-strep pKN-strep-*pspA*(2-222)-T25	B2H analysis	(4)
pKT25-*pspA*(25-85)-strep pKN-strep-*pspA*(25-85)-T25	B2H analysis	(4)
pKT25-*pspA*(25-144)-strep pKN-strep-*pspA*(25-144)-T25	B2H analysis	(4)
pKT25-*pspA*(25-186)-strep pKN-strep-*pspA*(25-186)-T25	B2H analysis	(4)
pKT25-*pspA*(25-222)-strep pKN-strep-*pspA*(25-222)-T25	B2H analysis	(4)
pKT25-*pspA*(86-144)-strep pKN-strep-*pspA*(86-144)-T25	B2H analysis	(4)
pKT25-*pspA*(86-186)-strep pKN-strep-*pspA*(86-186)-T25	B2H analysis	(4)
pKT25-*pspA*(86-222)-strep pKN-strep-*pspA*(86-222)-T25	B2H analysis	(4)
pKT25-*pspA*(145-186)-strep pKN-strep-*pspA*(145-186)-T25	B2H analysis	(4)
pKT25-*pspA*(145-222)-strep pKN-strep-*pspA*(145-222)-T25	B2H analysis	(4)

pKT25-*pspA*(186-222)-strep pKN-strep-*pspA*(186-222)-T25	B2H analysis	(4)
pUT18C-*pspC*(61-119)-strep	B2H analysis	This work

Table S2: Primers used for mutagenesis of PspC

Substitution in PspC	**Primer**	**Sequence**
G21A	PspC(G21A)-F	5' CATGGTCCGCGCGGTCTGCGCCGGG 3'
	PspC(G21A)-F	5' CCCGGCGCAGACCGCGCGGACCATG 3'
G21V	PspC(G21V)-F	5' CATGGTCCGCGTGGTCTGCGCCGGG 3'
	PspC(G21V)-R	5' CCCGGCGCAGACCACGCGGACCATG 3'
V22A	PspC(V22A)-F	5' CATGGTCCGCGGCGCGTGCGCCGGGATTG 3'
	PspC(V22A)-R	5' CAATCCCGGCGCACGCGCCGCGGACCATG 3'
C23A	PspC(C23A)-F	5' CATGGTCCGCGGCGTCGCGGCCGGGATTGCCAAC 3'
	PspC(C23A)-R	5' GTTGGCAATCCCGGCCGCGACGCCGCGGACCATG 3'
G25A	PspC(G25A)-F	5’ CCGCGGCGTCTGCGCCGCGATTGCCAACTATTTTG 3’
	PspC(G25A)-R	5’ CAAAATAGTTGGCAATCGCGGCGCAGACGCCGCGG 3’
G25V	PspC(G25V)-F	5' CGCGGCGTCTGCGCCGTGATTGCCAACTATTTTG 3'
	PspC(G25V)-R	5' CAAAATAGTTGGCAATCACGGCGCAGACGCCGCG 3'
R38A	PspC(R38A)-F	5' CGGTAAAACTGGTGGCGATCCTGGTGGTGCTG 3'
	PspC(R38A)-R	5' CAGCACCACCAGGATCGCCACCAGTTTTACCG 3'
R38K	PspC(R38K)-F	5' GTACCGGTAAAACTGGTGAAAATCCTGGTGGTGCTGTC 3'
	PspC(R38K)-R	5' GACAGCACCACCAGGATTTTCACCAGTTTTACCGGTAC 3'
R38D	PspC(R38D)-F	5' CCGGTAAAACTGGTGGATATCCTGGTGGTGC 3'
	PspC(R38D)-R	5' GCACCACCAGGATATCCACCAGTTTTACCGG 3'
F46A	PspC(F46A)-F	5' CCTGGTGGTGCTGTCGATTGCGTTCGGTCTGGCGCTGTTTAC 3'
	PspC(F46A)-R	5' GTAAACAGCGCCAGACCGAACGCAATCGACAGCACCACCAGG 3'
F47A	PspC(F47A)-F	5' GGTGGTGCTGTCGATTTTCGCGGGTCTGGCGCTGTTTACC 3'
	PspC(F47A)-R	5' GGTAAACAGCGCCAGACCCGCGAAAATCGACAGCACCACC 3'
G48A	PspC(G48A)-F	5' GTCGATTTTCTTCGCGCTGGCGCTGTTTACC 3'
	PspC(G48A)-R	5' GGTAAACAGCGCCAGCGCGAAGAAAATCGAC 3'
G48V	PspC(G48V)-F	5' GTCGATTTTCTTCGTGCTGGCGCTGTTTACC 3'
	PspC(G48V)-R	5' GGTAAACAGCGCCAGCACGAAGAAAATCGAC 3'
F52A	PspC(F52A)-F	5' CTTCGGTCTGGCGCTGGCGACCCTGGTTGCTTAC 3'
	PspC(F52A)-R	5' GTAAGCAACCAGGGTCGCCAGCGCCAGACCGAAG 3'
Y57A	PspC(Y57A)-F	5' CTGTTTACCCTGGTTGCTGCGATCATTTTGTCATTTGCG 3'
	PspC(Y57A)-R	5' CGCAAATGACAAAATGATCGCAGCAACCAGGGTAAACAG 3'
Y57F	PspC(Y57F)-F	5' CTGTTTACCCTGGTTGCTTTTATCATTTTGTCATTTGCGC 3'
	PspC(Y57F)-R	5' GCGCAAATGACAAAATGATAAAAGCAACCAGGGTAAACAG '
F62A	PspC(F62A)-F	5' GTTGCTTACATCATTTTGTCAGCGGCGCTTGATCCAATGCCGGAC 3'
	PspC(F62A)-R	5' GTCCGGCATTGGATCAAGCGCCGCTGACAAAATGATGTAAGCAAC 3'
L64A	PspC(L64A)-F	5'-GTTGTCCGGCATTGGATCAGCCGCAAATGACAAAATGATG-3'
	PspC(L64A)-R	5'-CATCATTTTGTCATTTGCGGCTGATCCAATGCCGGACAAC-3'
L64D	PspC(L64D)-F	5'-GTTGTCCGGCATTGGATCATCCGCAAATGACAAAATGATG-3'
	PspC(L64D)-R	5'-CATCATTTTGTCATTTGCGGATGATCCAATGCCGGACAAC-3'
D65A	PspC(D65A)-F	5' GTCATTTGCGCTTGCGCCAATGCCGGACAAC 3'
	PspC(D65A)-R	5' GTTGTCCGGCATTGGCGCAAGCGCAAATGAC 3'
D65N	PspC(D65N)-F	5' CATTTTGTCATTTGCGCTTAATCCAATGCCGGACAACATG 3'
	PspC(D65N)-R	5' CATGTTGTCCGGCATTGGATTAAGCGCAAATGACAAAATG 3'
S79A	PspC(S79A)-F	5'-TTCGCTGCTGGCAGGTAGCTGCTCACCAAAGG-3'

	PspC(S79A)-R	5'-CCTTTGGTGAGCAGCTACCTGCCAGCAGCGAA-3'
E102A	PspC(E102A)-F	5' GTTTACGCGAGATGGCGCGTTATGTCACTTC 3'
	PspC(E102A)-R	5' GAAGTGACATAACGCGCCATCTCGCGTAAAC 3'
E102Q	PspC(E102Q)-F	5' GCGTTTACGCGAGATGCAGCGTTATGTCACTTCCG 3'
	PspC(E102Q)-R	5' CGGAAGTGACATAACGCTGCATCTCGCGTAAACGC 3'
V105A	PspC(V105A)-F	5' GAGATGGAACGTTATGCGACTTCCGATACTTTCAC 3'
	PspC(V105A)-R	5' GTGAAAGTATCGGAAGTCGCATAACGTTCCATCTC 3'
V105D	PspC(V105D)-F	5' CGAGATGGAACGTTATGATACTTCCGATACTTTCACG
	PspC(V105D)-R	5' CGTGAAAGTATCGGAAGTATCATAACGTTCCATCTCG
S107A	PspC(S107A)-F	5' GATGGAACGTTATGTCACTGCGGATACTTTCACGTTACGTAG 3'
	PspC(S107A)-R	5' CTACGTAACGTGAAAGTATCCGCAGTGACATAACGTTCCATC 3'
S107P	PspC(S107P)-F	5' GATGGAACGTTATGTCACTCCGGATACTTTCACGTTACGTAG 3'
	PspC(S107P)-R	5' CTACGTAACGTGAAAGTATCCGGAGTGACATAACGTTCCATC 3'
L112A	PspC(L112A)-F	5' CTTCCGATACTTTCACGGCGCGTAGCCGTTTCCGTC 3'
	PspC(L112A)-R	5' GACGGAAACGGCTACGCGCCGTGAAAGTATCGGAAG 3'
L112D	PspC(L112D)-F	5' CTTCCGATACTTTCACGGATCGTAGCCGTTTCCGTC 3'
	PspC(L112D)-R	5' GACGGAAACGGCTACGATCCGTGAAAGTATCGGAAG 3'
L119A	PspC(L119A)-F	5' CCGTTTCCGTCAAGCGGGATCCCATCATC 3'
	PspC(L119A)-R	5' GATGATGGGATCCCGCTTGACGGAAACGG 3'
L119S	PspC(L119S)-F	5' GTAGCCGTTTCCGTCAAAGCGGATCCCATCATCATC 3'
	PspC(L119S)-R	5' GATGATGATGGGATCCGCTTTGACGGAAACGGCTAC 3'
L119D	PspC(L119D)-F	5' GTAGCCGTTTCCGTCAAGATGGATCCCATCATCATC 3'
	PspC(L119D)-R	5' GATGATGATGGGATCCATCTTGACGGAAACGGCTAC 3'

Figures

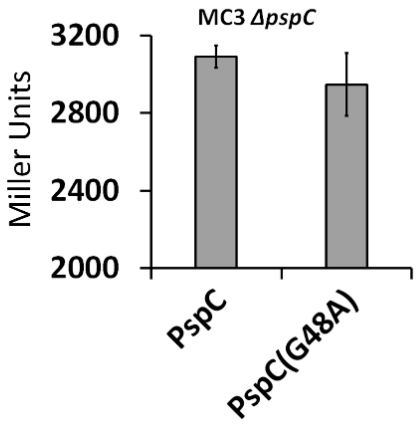

Figure S1: Substitution of Gly-48 by Ala had no influence on the Psp system induction by PspC in a *pspC* deletion mutant.

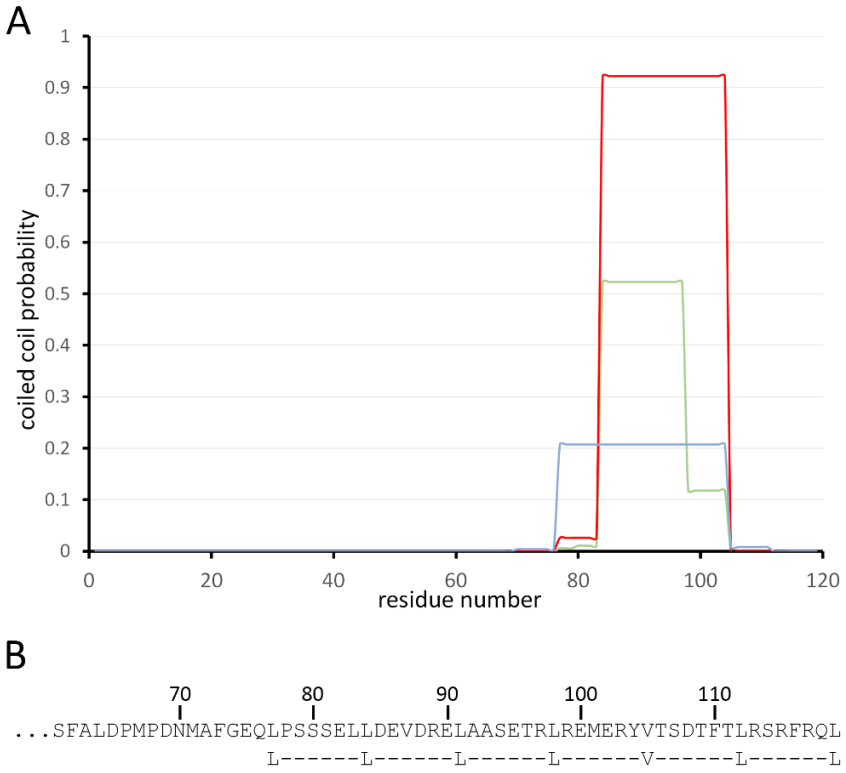

Figure S2: Prediction of coiled coil probability for PspC. (A) The probability to form a coiled coil was predicted using the program COILS (5). The window size for the sequence scan was 14 (green), 21 (red), and 28 (blue). A coiled coil of intermediate size is likely formed from position L84 to Y104. (B) A leucine heptad repeat continues behind Y104 up to the very C-terminus of PspC if V105 is tolerated.

References

1. Baba, T., Ara, T., Hasegawa, M., Takai, Y., Okumura, Y., Baba, M., Datsenko, K. A., Tomita, M., Wanner, B. L., and Mori, H. (2006) Construction of *Escherichia coli* K-12 in-frame, single-gene knockout mutants: The Keio collection. *Mol Syst Biol* **2**, 2006.0008
2. Bergler, H., Abraham, D., Aschauer, H., and Turnowsky, F. (1994) Inhibition of lipid biosynthesis induces the expression of the *pspA* gene. *Microbiology* **140**, 1937–1944
3. Mehner, D., Osadnik, H., Lünsdorf, H., and Brüser, T. (2012) The Tat system for membrane translocation of folded proteins recruits the membrane-stabilizing Psp machinery in *Escherichia coli*. *J. Biol. Chem.* **287**, 27834–27842
4. Heidrich, E. S., and Brüser, T. (2018) Evidence for a second regulatory binding site on PspF that is occupied by the C-terminal domain of PspA. *PLoS One*, accepted for publication
5. Lupas, A., van Dyke, M., and Stock, J. (1991) Predicting coiled coils from protein sequences. *Science* **252**, 1162–1164

3.5 Weitere Untersuchungen zur Induktion des Psp-Systems durch den ungewöhnlich kurzen Membrananker von TatA

Bereits einleitend wurde beschrieben, dass durch die rekombinante Überproduktion des ungewöhnlich kurzen TatA-Membranankers, welcher zur Stabilisierung N-terminal an die mature Domäne des kleinen, vollkommen löslichen Tat-Substrats HiPIP fusioniert wurde, die Psp-Antwort induziert wird [150,94]. In Abschnitt 3.1 konnte gezeigt werden, dass die rekombinante Überproduktion dieses Fusionsproteins, fortfolgend TatA-NT-Hip genannt, zu einer Inhibition des Zellwachstums führte. Dies konnte auf eine Destabilisierung der Cytoplasmamembran durch den TatA-Membrananker zurückgeführt werden. Die durch TatA-NT-Hip ausgelösten Effekte auf Zellwachstum, das Membranpotential sowie auf die PMF waren dabei unabhängig von der Sequenz des hydrophoben Bereichs des TatA-Membranankers und konnten durch die Verlängerung des hydrophoben Bereichs um sechs Leucine in ihrer Stärke reduziert werden (vgl. Abschnitt 3.1.2). Auf Grund dieser Beobachtungen lag es nahe zu untersuchen, ob die Induktion des Psp-Systems durch TatA-NT-Hip in Zusammenhang mit den oben beschriebenen Effekten steht.

3.5.1 Länge und Sequenz des hydrophoben Bereichs des TatA-Membranankers sind für die Induktion des Psp-Systems nicht ausschlaggebend

Um festzustellen, ob die Induktion des Psp-Systems direkt von der Sequenz und Länge des hydrophoben Bereichs des TatA-Membranankers abhängt, wurde untersucht, ob die verschiedenen Varianten des TatA-Membranankers TatA-NT$(LA)_6$-Hip, TatA-NT$(STGG)_3$-Hip sowie TatA-NT(9+6L)-Hip das Psp-System unterschiedlich stark induzieren. Dazu wurde der P_{pspA}-Reporterstamm MC3, welcher eine chromosomale P_{pspA}-*lacZ*-Fusion besitzt [154], genutzt. Durch die Bestimmung der Aktivität der β-Galaktosidase konnte auf die Aktivierung der Expression des *psp*-Operons und somit des Psp-Systems durch die rekombinante Produktion der verschiedenen Varianten des TatA-Membranankers geschlossen werden [155]. Die Induktion der Expression des *psp*-Operons durch rekombinant produziertes TatA konnte bereits durch Mehner *et al*. (2012) gezeigt werden [94], weshalb die Produktion von TatA als Positivkontrolle in den hier durchgeführten Analysen der *pspA*-Promotoraktivität eingesetzt wurde. Als Negativkontrolle diente der durch den

entsprechenden Leervektor transformierte Reporterstamm. Die rekombinante Produktion von TatA sowie die rekombinante Produktion derjeniger TatA-NT-Hip-Varianten, für welche eine Membranintergration in Abschnitt 3.2.2 nachgewiesen werden konnte, führte in allen Fällen zu einer verstärkten Aktivität des *pspA*-Promotors im Vergleich zur Negativkontrolle (Abbildung 7). Die Produktion von TatA-NT-Hip führte im Vergleich zur Produktion von TatA zu einer deutlich stärken Induktion der *pspA*-Promotoraktivität. Ähnliche Effekte wurden bereits in der von Denise Mehner angefertigten Dissertation beobachtetet, in welcher die Analyse der Induktion der *pspA*-Expression jedoch auf der Bestimmung von PspA-Proteinleveln beruhte [150]. Beide experimentelle Ansätze lieferten das gleiche Ergebnis: Sowohl Proteinlevel von PspA als auch die Aktivität des *pspA*-Promotors werden durch TatA-NT-Hip im Vergleich zu TatA erhöht.

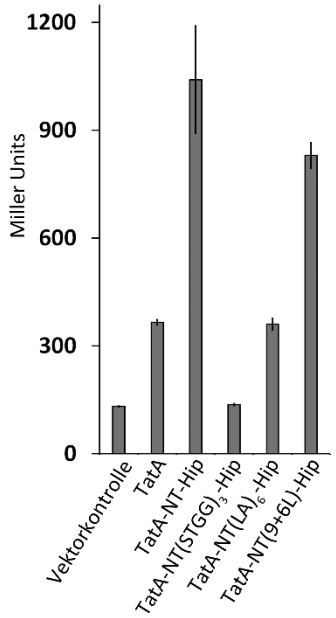

Abbildung 7 Der TatA-Membrananker induziert die Aktivität des *pspA*-Promotors unabhängig von der Sequenz und Länge seines hydrophoben Bereichs Die Bestimmung der β-Galaktosidaseaktivität des P_{pspA}-Reporterstammes MC3, welcher entweder den Leervektor pBW22 (Vektorkontrolle), pBW-*tatA*-strep (TatA), pBW-*tatA-NT-mat-hip*-strep (TatA-NT-Hip), pBW-*tatA-NT(STGG)$_3$-mat-hip*-strep (TatA-NT(STGG)$_3$-Hip), pBW-*tatA-NT(LA)$_6$-mat-hip*-strep (TatA-NT(LA)$_6$-Hip) oder pBW-*tatA-NT(9+6L)-mat-hip*-strep (TatA-NT(9+6L)-Hip) enthielt. Die Bestimmung erfolgte in technischen Triplikaten. Zur rekombinanten Produktion von TatA, TatA-NT-Hip, TatA-NT(STGG)$_3$-Hip, TatA-NT(LA)$_6$-Hip und TatA-NT(9+6L)-Hip wurde zum Zeitpunkt der Inokulation final 0,1% (w/v) Rhamnose hinzufügt. Die Bestimmung der β-Galaktosidaseaktivität erfolgte nach dreistündiger Kultivierung wie in Abschnitt 3.2.2 beschrieben. Die rekombinante pBW-abhängigen Produktion von TatA, TatA-NT-Hip, TatA-NT(LA)$_6$-Hip und TatA-NT(9+6L)-Hip führte zu einer unterschiedlich starken Induktion der *pspA*-Promotoraktivität. Die rekombinante Produktion von TatA-NT(STGG)$_3$-Hip führte nicht zu einer Induktion des *pspA*-Promotors im Vergleich zur Vektorkontrolle (pBW22-Leervektor).

Die Produktion von TatA-NT(STGG)$_3$-Hip beeinflusste die Aktivität des *pspA*-Promotors nicht. Dies wurde erwartet, da für TatA-NT(STGG)$_3$-Hip keine Membraninteraktion in den in Abschnitt 3.1 durchgeführten Experimenten festgestellt werden konnte, noch die rekombinante Produktion dieses Fragments einen Einfluss auf das Zellwachstum oder auf das Membranpotential besaß. In der Dissertation von Denise Mehner wurde zudem ein sehr ähnliches HiPIP-Konstrukt mit einem N-terminalen flexiblen (STGGG)$_3$-Linker untersucht, welches ebenfalls vollkommen löslich vorlag und dessen Produktion ebenfalls nicht zu erhöhten PspA-Leveln in der Zellen führte [150]. Die rekombinante Produktion von TatA-NT(LA)$_6$-Hip führte zu einer deutlich schwächeren Induktion der Aktivität des *pspA*-Promotors als die rekombinante Produktion von Tat-NT-Hip, während TatA-NT(9+6L)-Hip den *pspA*-Promotor ähnlich stark induzierte wie Tat-NT-Hip (Abbildung 7).

3.5.2 Die Interaktion des TatA-Membranankers mit PspA hängt wahrscheinlich von der Sequenz des hydrophoben Bereichs TatAs ab

Es wurde bereits gezeigt, dass TatA direkt mit PspA interagieren kann und diese Interaktion durch den TatA-Membrananker vermittelt wird [94]. Es sollte deshalb geklärt werden, ob auch hier die Sequenz und Länge des hydrophoben Bereichs des Membranankers ausschlaggebend für die Interaktion mit PspA ist. Dazu wurden die verschiedenen TatA-NT-Hip-Varianten mittels *Strep*-Tactin-Affinitätschromatographie, wie in Mehner *et al.* (2012) beschrieben, direkt aus der Membranfraktion ohne vorangegangene Solubilisierung angereichert und auf ihre Fähigkeit mit PspA

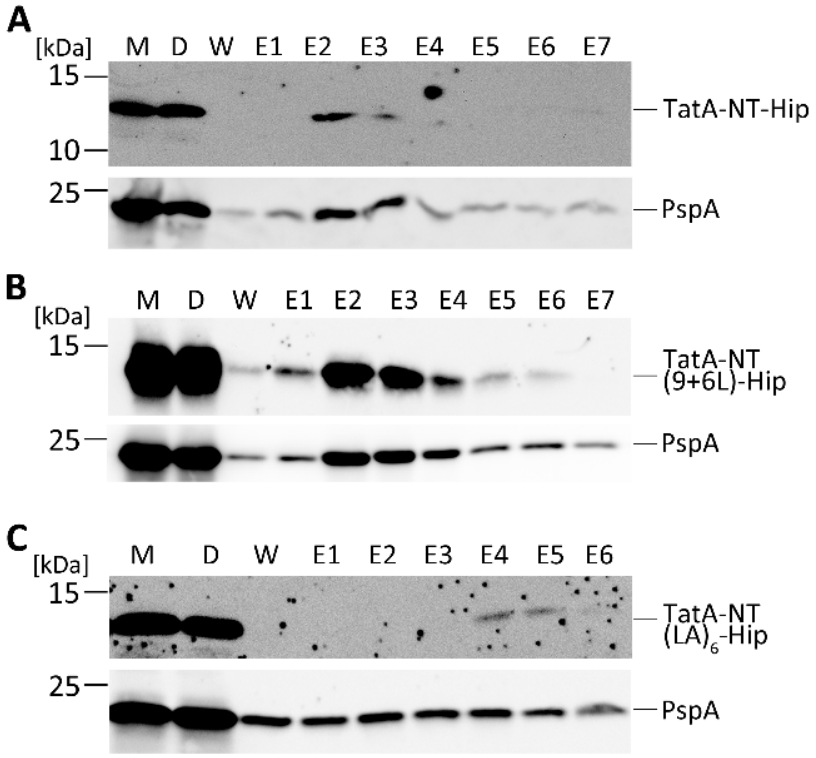

Abbildung 8: **Analyse der Interaktion von PspA mit TatA-NT-Hip, TatA-NT(9+6L)-Hip und TatA-NT(LA)$_6$-Hip** SDS-PAGE/Western-Blot-Analyse der affinitätschromatischen Anreicherung von A) TatA-NT-Hip, B) TatA-NT(9+6L)-Hip, C) TatA-NT(LA)$_6$-Hip, rekombinant produziert im *E.-coli*-Stamm JARV16 mittels Strep-Tactin®-Affinitätschromatographie. Es wurden 15%igen SDS-Polyacrylamid-Gele verwendet. Das aufgetragene Probenvolumen betrug jeweils 10 µl. Die Detektion der verschiedenen TatA-NT-Hip-Varianten erfolgte mittels spezifischer HiPIP-Antikörper (jeweils oberer Blot). Zur Detektion von PspA wurden spezifische PspA-Antikörper verwendet (jeweils unterer Blot). Die Detektion der Proteinbanden erfolgte mittels ECL-Reaktion. Das apparente Molekulargewicht der Markerproteine ist links angegeben. **M** = Membranfraktion, **D** = Durchlauf, **W** = letzte Waschfraktion, **E1-E7** = Elutionsfraktionen 1 bis 7.

interagieren zu können getestet [94]. Da PspA auch dann zusammen mit TatA von der Säule eluierte, wenn dieses in nativen Leveln in der Zelle vorhanden war und ebenfalls mit TatE interagierte, wurde der *tatAE*-defiziente *E.-coli*-Stamm JARV16 zur Proteinproduktion verwendet [94,150]. Die rekombinante Produktion von TatA-NT-Hip fungierte auch hier als Positivkontrolle und die Interaktion mit PspA wurde erfolgreich reproduziert (Abbildung 8A). PspA elutiere klar mit affinitätschromatographisch angereichertem TatA-NT(9+6L)-Hip (Abbildung 8B), jedoch nicht eindeutig mit TatA-NT$(LA)_6$-Hip (Abbildung 8C). Um TatA-NT$(LA)_6$-Hip in den Elutionfraktionen detektieren zu können, musste das zur Zellanzucht eingesetzte Kulturvolumen verdoppelt werden. Das Elutionsprofil von TatA-NT$(LA)_6$-Hip entsprach jedoch nicht dem typischen Elutionsprofil einer *Strep*-Tactin-Affinitätssäule und eluierte erst in den Fraktionen vier bis sechs. Da sowohl in der Wasch- als auch in allen Elutionsfraktionen PspA vergleichbar stark nachgewiesen wurde, kann hier nicht von einer eindeutigen Interaktion von PspA mit TatA-NT$(LA)_6$-Hip gesprochen werden. Daher lässt sich an dieser Stelle zusammenfassen, dass die Interaktion des TatA-Membranankers mit PspA von der Sequenz des hydrophoben Bereichs jedoch nicht von seiner Länge abhängt.

3.5.3 Material und Methoden

Die in diesem Abschnitt aufgeführten Methoden, Stämme und Plasmide beziehen ausschließlich auf die in Abschnitt 3.5 durchgeführten Experimente.

3.5.1.1 Verwendete Stämme und Plasmide

In den in Abschnitt 3.5 gezeigten Experimenten wurden die *E.-coli*-Stämme MC3 [154] und JARV16 [98] genutzt. Als Plasmide wurden pBW22 [156], pBW-*tatA*-strep [94], pBW-*tatA*-*NT*-*mat*-*hip*-strep [94], pBW-*tatA*-*NT*$(LA)_6$-*mat*-*hip*-strep (Abschnitt 3.1), pBW-*tatA*-*NT*$(STGG)_3$-*mat*-*hip*-strep (Abschnitt 3.1) und pBW-*tatA*-*NT*(9+6L)-*mat*-*hip*-strep (Abschnitt 3.1) eingesetzt.

3.5.1.2 Medien und Zusätze

Die Zellanzucht als Suspensionskultur erfolgte stets aerob und schüttelnd (180 U/min) bei 37°C in sterilem *lysogeny broth* (LB-) Medium (1 % Trypton (w/v), 1 % NaCl (w/v), 0,5 % Hefeextrakt (w/v) in H_2O_{bidest}) in den benötigten Volumina (5 ml, 100 ml oder 250 ml). Sollte die Kultivierung auf festem LB-Medium erfolgen, wurden final 1,5% (w/v) Europäischer Agar hinzufügt. Zur Sterilisation wurden alle Medien vor ihrer

Verwendung autoklaviert. Wenn nötig, wurde dem Medium nach Abkühlen zur Selektion Ampicillin mit einer Endkonzentration von 100 µg/ml hinzugegeben.

Von hitzelabilen Substanzen wurden zunächst Stammlösungen erstellt (Ampicillin: 100 mg/ml in H_2O_{bidest}, Rhamnose: 20 % (w/v) in H_2O_{bidest}, Glucose: 20 % (w/v) in H_2O_{bidest}) und steril filtriert (Rotilabo-Spritzenfilter, PVDF, 0,22 µm, Roth, Karlsruhe). Antibiotika-Stammlösungen wurden bei -20°C gelagert.

3.5.1.3 Bestimmung der β-Galaktosidase-Aktivität

Zur Bestimmung der β-Galaktosidase-Aktivität wurde stets der *E.-coli*-Stamm MC3, welcher zuvor mit verschiedenen Derivaten des Plasmids pBW22 transformiert wurde, eingesetzt. Die Bestimmung in drei technischen Replikaten. Dazu wurde pro Stamm dreimal 5 ml Ampicillin-haltiges LB-Medium mit 100 µl einer über Nacht gewachsenen Kultur inokuliert. Zur Induktion der Genexpression wurden zum Zeitpunkt der Inokulation final 0,1% (v/v) Rhamnose hinzugeben. Die Kultivierung erfolgte aerob und schüttelnd bei 37°C für drei Stunden. Die Bestimmung der β-Galaktosidase-Aktivität wurde wie in Osadnik *et al.* (2015) und Abschnitt 3.2 beschrieben durchgeführt [155,70].

3.5.1.4 Rekombinante Produktion, Präparation und affinitätschromatographische Anreicherung der verschiedenen TatA-NT-Hip-Varianten

Zur Proteinproduktion wurde der *E.-coli*-Stamm JARV16, welcher zuvor mit den für die verschiedenen TatA-NT-Hip codierenden Plasmiden nach der Methode von Chung *et al*. (1989) transformiert wurde [157], genutzt. Dazu wurde die Kultivierung aerob in Schikanekolben in Ampicillin-haltigen LB-Medium für drei Stunden schüttelnd bei 37°C durchgeführt. Die Kulturen wurden 4%-ig mit einer über Nacht gewachsenen Kultur inokuliert und das Zellwachstum über die Bestimmung der optischen Dichte (OD_{600nm}) im Photometer (Biochrom Libra S11 UV/Vis Spectrophotometer, Biochrom, Berlin) überwacht. Bei Erreichen einer OD_{600nm} von 0,6 wurden zur Induktion der Genexpression final 0,1 % Rhamnose hinzugegeben und die Kultivierung für drei Stunden fortgesetzt. Mittels eines Zentrifugationsschritts bei 4500 x g für 10 min bei 4°C wurden die Zellen sedimentiert und anschließend der Überstand verworfen. Das Zellpellet wurde in 3 ml Aufschlusspuffer (50 mM Tris-HCl pH 8, 250 mM NaCl) resuspendiert. Darauffolgend wurden eine Spatelspitze DNaseI und final 1 mM PMSF hinzugegeben. Der Zellaufschluss erfolgte in zwei Passagen à 620 kPa in der *French Pressure Cell Press mini* (Simoamico®, SCM Instruments Inc.). Nach Entfernung der

Zelltrümmer mittels eines Zentrifugationsschritts (4500 x g, 10 min, 4°C), erfolgte die Präparation der Membranfraktion. Dazu wurde nach der Abtrennung der Zelltrümmer der Überstand in eine Ultrazentrifugationsgefäß überführt. Es folgte ein weiterer Zentrifugationsschritt für 30 min bei 170 000 x g und 4 °C (Sorvall *Discovery M120SE*, Thermo Scientific). Nach Entfernen des Überstandes wurden die sedimentierten Membranen in 3 ml Aufschlusspuffer resuspendiert.

Da alle TatA-NT-Hip-Varianten einen C-terminal fusionierten Strep-tag® (IBA, Göttingen) besaßen wurde zur Anreicherung eine Strep-Tactin®-Affinitäts-chromatographie wie in Mehner *et al.* (2012) beschrieben durchgeführt [94]. Alle weiter zu analysierenden Fraktionen wurden aufgefangen und sofort mit 1:2 mit SDS-PAGE-Probenpuffer (80 mM Tris-HCl pH 8,8, 20 % (v/v) Glycerin, 4 % (w/v) SDS, 20 mM DTT, 0,024 % (w/v) Bromphenol-blau) versetzt und 10 min bei 95 °C aufgekocht.

3.5.1.5 SDS-PAGE, semi-dry *Western Blot und Proteindetektion*

Die nach der affinitätschromatischen Reinigung erhaltenen SDS-Proben wurde mittels SDS-PAGE und Western-Blot mit anschließendem Proteinnachweis mittels Immunpräzipitation analysiert.

Die SDS-PAGE wurde nach Laemmli *et al*. (1970) durchgeführt [158]. Es wurden jeweils 10 µl einer Probe auf das Gel appliziert. Als Größenstandard wurden 3 µl des Proteinmarkers *PageRuler Prestained Protein Ladder* (Fermentas) verwendet. Darauffolgend wurden die Proteine mittels eines *semi-dry* Western-Blots (Biometra Fastblot B33/B34 oder B43/44, Biometra) auf eine Nitrocellulosemembran (Amersham Protran 0.45 NC Nitrocellulose, GE Healthcare) nach Herstellerangaben, angelehnt an Towbin *et al.* (1979) [159], übertragen. Um eine unspezifische Bindungen von Antikörpern zu vermeiden, wurde die Nitrozellulosemembran nach Durchführung des Western Blots über Nacht in Magermilchlösung (5 % (w/v) Magermilchpulver in PBS (13,7 mM NaCl, 3 mM KCl, 4 mM Na_2HPO_4, 2 mM KH_2PO_4, pH 7,4)) inkubiert.

Zur Immunpräzipitation wurden die Nitrocellulosemembranen dreimal in PBS gewaschen. Darauf folgte eine Inkubation mit spezifischen polyklonalen Primärantikörpern gegen HiPIP (0,02% (v/v) Antikörperlösung, 0,5 % (w/v) BSA, 0,02 % (w/v) Azid in 1 x PBS-Puffer; Antigen: HiPIP,Typ: IgG (Kaninchen), [160]) oder PspA (0,01% (v/v) Antikörperlösung, 0,5 % (w/v) BSA, 0,02 % (w/v) Azid in 1 x PBS-Puffer; Antigen: PspA, Typ: IgG (Kaninchen)) für eine Stunde bei Raumtemperatur.

Nach dreimaligem Waschen in PBS erfolgte die Inkubation mit dem Sekundärantikörper, welcher mit der *horseradish peroxidase* (HRP) konjugiert war (Anti-Kanin-HRP, Roth, Karlsruhe) für eine Stunde nach Herstellerangaben. Die Detektion erfolgte über *enhanced chemiluminescence* (ECL)-Reaktion mit Luminol und Coumarinsäure als Substrat nach Ogata *et al.* (1983) [161]. Zur Detektion der Chemilumineszenz wurde der Intas Advanced Imager (INTAS Science, Imaging Instruments GmbH) verwendet.

4 Abschließende Diskussion und Ausblick

Die in Abschnitt 3 vorgestellten Ergebnisse lieferten tiefere Einblicke in die Funktionen der einzelnen Komponenten des Psp-Systems. In der folgenden Diskussion werden die in Abschnitt 3 präsentierten Ergebnisse rekapituliert und publikationsübergreifend in die bestehenden Modelle der Stresswahrnehmung und Signalkaskade des Psp-Systems eingeordnet. Dadurch kann ein Modell der Stresswahrnehmung und Signalkaskade der durch TatA-induzierten Psp-Antwort entwickelt werden, welches die Funktionen von PspB und PspC als Sensoren und Aktivatoren der Psp-Antwort mit der direkten Sensorfunktion von PspA vereint.

4.1 Die TatA-induzierte Psp-Antwort – Ein integratives Modell der PspABC-abhängigen Signalwahrnehmung und –kaskade

Die Integration der verschiedenen Modelle der Stresswahrnehmung und Signalkaskade der durch TatA induzierten Psp-Antwort gelingt auf Grund folgender Schlussfolgerungen, welche basierend auf der in Abschnitt 3 gezeigten Ergebnisse getroffen werden können:

I) Die Interaktion zwischen PspA und PspC führt nur an der Cytoplasmamembran zu einer Aktivierung von PspF (Abschnitt 3.4).

II) Die PspA-Domäne PspA(145-222) trägt entscheidend zur PspF-Inhibition bei, wobei im Gegensatz zu anderen PspA-Domänen, die PspA(145-222)-abhängige Inhibition von PspF durch TatA-induzierten Membranstress aufgehoben werden kann (Abschnitt 3.2).

III) TatA-induzierter Membranstress führt nur dann zu einer Induktion des Psp-Systems, wenn PspB in der Zelle vorhanden ist (Abschnitt 3.4).

Vereint man nun das bereits in Abschnitt 3.4 vorgeschlagene Modell mit den regulatorischen und sensorischen Funktionen der in Abschnitt 3.2 untersuchten PspA-Domäne PspA(145-222) könnte sich die Wahrnehmung von TatA-induziertem Membranstress durch das Psp-System folgendermaßen darstellen (Abbildung 9):

Im uninduzierten Zustand werden auf Grund der basalen Aktivität des *pspA*-Promotors neben PspA auch geringe Mengen an PspB und PspC gebildet. PspB und PspC bilden, wie vorgeschlagen, einen Komplex in der Cytoplasmamembran, in welchem die cytoplasmatischen Domänen PspBs und PspCs miteinander interagieren, wodurch

eine Interaktion der C-terminalen Domäne von PspC mit PspA verhindert wird [35,36,72]. PspA und PspF bilden einen stabilen Komplex im Cytoplasma, in welchem die PspF-Aktivität durch das synergistische Zusammenwirken der verschiedenen PspA-Domänen PspA(1-24), dem *coiled-coil*, sowie der C-terminalen PspA-Domäne PspA(145-222) inhibiert wird (vgl. Abschnitt 3.2 und Abschnitt 3.4). Der PspF/PspA-Komplex ist im Cytoplasma mobil und befindet sich dadurch in einem transienten Kontakt mit der Cytoplasmamembran [87]. Da kein induzierendes Signal an der Cytoplasmamembran anliegt, finden keine strukturellen Veränderungen von PspB, PspC oder PspA statt, welche zu einer Aktvierung PspFs führen könnten und der PspF/PspA-Komplex dissoziiert von der Cytoplasmamembran.

Liegt nun Membranstress an der Cytoplasmamembran an, wird dieser sowohl durch PspB und PspC als auch durch PspA wahrgenommen. Zum einen kommt es zu einer stabilen strukturellen Veränderung PspAs an der Cytoplasmamembran. Dabei kommt es zur Ausbildung der amphipathischen Helix am N-Terminus PspAs (vgl. Abschnitt 3.4, Abbildung 9) und gleichzeitig, wie in Abschnitt 3.2 vorgeschlagen, zu einer Oligomerisierung der C-terminalen PspA-Domänen, wodurch diese ihre PspF-inhibitorische Wirkung verlieren. Die *coiled-coil*-Domäne PspAs verbleibt am PspF-Hexamer gebunden. Trotz des Verlustes der inhibitorischen Wirkung der N- und C-terminalen PspA-Domänen, welcher sicherlich mit den strukturellen Veränderungen einhergeht, scheint dies *in vivo* nicht für eine messbare Induktion des Psp-Systems durch TatA auszureichend zu sein. Daher muss ebenfalls eine Aktivierung der PspF-Aktivität ausgehend von der Stresswahrnehmung und –weiterleitung durch PspC und PspB erfolgen. Membranstress führt im folgenden Schritt zu einer Veränderung der Interaktion der cytoplasmatischen Domänen von PspB und PspC. Die C-terminale Domäne von PspC kann nun zusammen mit PspB, wie in Abschnitt 3.4 bereits diskutiert, mit der *coiled-coil*-Domäne PspAs interagieren, wodurch deren inhibitorische Wirkung auf die PspF-Aktivität aufgehoben wird. Wie sich das Zusammenspiel der PspF-regulatorisch wirkenden PspA-Domänen nun mechanistisch in Bezug auf die Inhibition und Aktivierung PspFs darstellt, lässt sich auf Grund der heutigen Datenlage nicht ableiten. Es ist jedoch auf Grund dessen, dass erhöhte Level an PspA im Zuge der Psp-Antwort nicht zu einer erneuten sofortigen Inhibition PspFs führen, wahrscheinlich, dass wie von Osadnik *et al.* (2015) vorgeschlagen, PspA PspF im gebundenen Zustand regulieren muss [70].

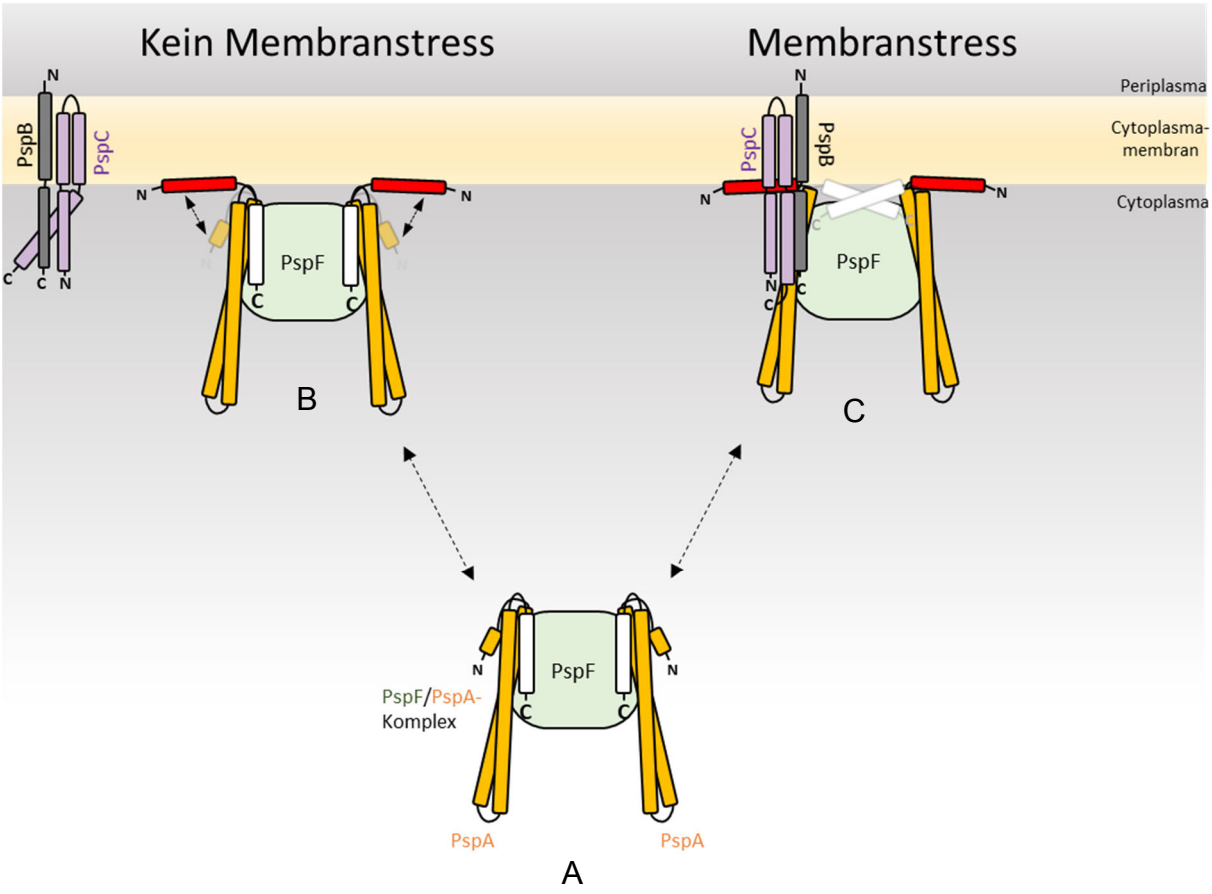

Abbildung 9 Schematische Darstellung des integrativen Modells des Zusammenwirkens von PspB, PspC und dem PspF/PspA-Komplex an der Cytoplasmamembran von *E. coli* unter Normal- und Stressbedingungen A) Das PspF-Hexamer (grün) wird im Cytoplasma durch die zwei PspA-Domänen (gelb), PspA(1-24) und PspA(25-144), sowie der C-terminalen PspA-Domäne (145-222) (weiß) inhibiert. Für eine bessere Übersichtlichkeit wurde auf die Darstellung der einzelnen PspF-Protomere sowie der DNA-Bindedomäne von PspF verzichtet und nur zwei PspA-Moleküle pro PspF-Hexamer dargestellt. B) Der PspF/PspA-Komplex ist in der Zelle mobil und diffundiert zur Cytoplasmamembran, wobei es womöglich auch ohne Membranstress zu einer Lipid-induzierten Änderung der Konformation der PspA-Domäne PspA(1-24) kommt, wodurch diese nicht länger mit PspF, sondern als amphipathische Helix (rot) mit der Cytoplasmamembran interagiert. Liegt kein Membranstress an der Cytoplasmamembran an, interagieren die cytoplasmatischen Domänen von PspB (grau) und PspC (violett), sodass die C-terminale Domäne von PspC nicht mit PspA interagieren kann und der PspF/PspA-Komplex dissoziiert von der Cytoplasmamembran. C) Kommt es zu Membranstress wird dieser von PspB und PspC wahrgenommen, worauf es zu einer Änderung der PspB-PspC-Interaktion kommt. Die C-terminalen Domäne von PspC ist auf Grund dessen nun in der Lage mit der *coiled-coil*-Struktur der PspA-Domäne PspA(25-144) zu interagieren. Gleichzeitig kommt es neben der Lipid-induzierten Ausbildung der amphipathischen Helix (rot) zu einem Verlust der PspF-Inhibition durch PspA(145-222), wobei zwei oder mehrere PspA(145-222)-Domänen miteinander interagieren (hier beispielhaft weiß schattiert dargestellt) und PspF liegt nun aktiviert in der Zelle vor.

Im Folgenden werden die in dieser Arbeit erhaltenen Ergebnisse, welche entscheidend zur Entwicklung des hier vorgeschlagenen Modells zur Aktivierung des Psp-Systems durch TatA-induzierten Membranstress betrugen, eingehender betrachtet.

4.1.1 Die Membraninteraktion PspAs ist für die Signalkaskade des Psp-Systems essentiell

Es wurde in Abschnitt 3.4 eindeutig klar, dass die Membraninteraktion PspAs eine entscheidende Rolle für die PspC-PspA-Interaktion und somit für die PspBC-abhängige Aktivierung der Psp-Antwort spielt. Bereits in Abschnitt 3.4 wurde diskutiert, dass die Abhängigkeit der PspC-PspA-Interaktion auf einer für die Signalkaskade notwendigen Konformationsänderung PspAs beruht, welche auf die Ausbildung einer Membran-assoziierten Helix des in der in der Kristallstruktur zum *coiled-coil* zurückgefalteten N-terminalen Bereichs PspAs, PspA(1-24), zurückzuführen ist. In Einklang mit McDonald *et al.* (2017) und Jovanovic *et al.* (2014) wurde in Abschnitt 3.4 vorgeschlagen, dass die Strukturveränderung dieses PspA-Bereichs durch Membranstress induziert wird und PspA(1-24) die Sensordomäne innerhalb PspAs darstellt [71,88]. Es ist jedoch ebenso denkbar, dass die strukturelle Veränderung von PspA(1-24) nicht nur bei Membranstress geschieht, sondern immer, wie in Abbildung 9 bereits angedeutet, wenn sich der PspF/PspA-Komplex in der Lipidumgebung der Cytoplasmamembran befindet, wodurch die Bindestelle der C-terminalen Domäne PspCs an der *coiled-coil*-Domäne PspAs freigegeben wird. Dies würde erklären, warum es auch ohne Membranstress nur dann zu einer starken Aktivierung von PspF kommt, wenn die C-terminale PspC-Domäne rekombinant in der Zelle produziert und zusammen mit PspA an die Membran rekrutiert wurde (Abschnitt 3.4, Abbildung 4).

Neben der sterischen Hinderung wären auch andere Mechanismen denkbar, welche die Abhängigkeit der Signalkaskade des Psp-Systems von der Membraninteraktion PspAs erklären könnten. So konnte in der von McDonald *et al.* (2017) publizierten Studie nicht nur gezeigt werden, dass PspA(1-24) in einer Lipidumgebung eine helikale Struktur ausbildet, sondern auch, dass PspA(1-24) als unstrukturiertes in Lösung vorliegendes Peptid in der Lage ist, die ATPase-Aktivität PspFs zu inhibieren [71]. Dass PspA(1-24) mit PspF interagieren und dessen Funktion als bEBP inhibiert, konnte in den hier durchgeführten Arbeiten *in vivo* mittels *bacterial-2-hybrid*-Analysen und *pspA*-Promotoraktivitätsstudien in einem *pspA*-Deletionsstamm bestätigt werden (Abschnitt 3.2, Abbildungen 2D, 2F und 3A). So wäre es ebenfalls möglich, dass die Interaktion der C-terminalen Domäne von PspC mit der *coiled-coil*-Domäne PspAs allein nicht ausreicht, um die inhibitorische Wirkung auf PspF aufzuheben, sondern die Änderung der Struktur von PspA(1-24) eine Konformationsänderung innerhalb PspAs darstellt, welche zum Verlust der PspF-inhibitorischen Wirkung von PspA(1-24) führt

und zur Aktivierung von PspF zusätzlich im Rahmen der Signalkaskade erforderlich ist.

4.1.2 PspA(145-222) als PspF-regulatorisch wirkende PspA-Domäne

Es wurde in dieser Arbeit jedoch auch klar, dass die Induktion des Psp-Systems durch TatA-induzierten Membranstress nicht nur von den im vorherigen Abschnitt beschriebenen Schritten abhängt, sondern, dass die C-terminale PspA-Domäne PspA(145-222) ebenfalls eine entscheidende Rolle sowohl in Bezug auf die Inhibition von PspF als auch in der Aktivierung der Psp-Antwort bei TatA-induziertem Membranstress spielt:

So führte die Deletion der C-terminalen Domäne von PspA in einem natürlich regulierten System zu einer Induktion der *pspA*-Promotoraktivität. Dies zeigte, dass die in Bezug auf ihre PspF-inhibitorischen Eigenschaften sehr gut charakterisierte PspA-Domäne PspA(1-144) in einem natürlich regulierten System nicht ausreicht, um PspF in dem Maße inhibieren zu können, wie es für PspA der Fall ist (Abschnitt 3.2, Abbildung 8, [70]). Auch Brissette *et al*. beobachteten bereits 1991, dass eine Deletion ausgehend vom 3‘-Ende des *pspABCDE*-Operons, welche sowohl *pspBCDE* sowie das 3‘-Ende von *pspA* umfasste, zu einer Induktion der Proteinbiosynthese einer verkürzten PspA-Variante, hier PspA(1-178), führte [17]. Schon damals wurde spekuliert, ohne PspF und die σ^{54}-abhängige Regulation der Expression des *pspABCDE*-Operons zu kennen, dass es sich bei dem deletierten Abschnitt um einen Bereich innerhalb des *pspABCDE*-Operons handelt, welcher repressorisch auf dessen Transkription wirkt. Der direkte Nachweis der PspF-Inhibition durch die C-terminale PspA-Domäne gelang hier erstmals durch die Konstruktion eines Fusionsproteins, in welchem PspA(145-222) C-terminal an die mature Domäne des kleinen, globulären Tat-Substrats HiPIP fusioniert wurde und so ein *in vivo* stabiles Fusionsprotein in der Zelle synthetisiert werden konnte, welches zudem vollkommen löslich war (Abschnitt 3.2, Abbildung 1). Warum es jedoch erst im Rahmen dieser Arbeit, und nicht in früheren Studien gelang, die regulatorischen Eigenschaften der C-terminalen PspA-Domäne nachzuweisen, kann auf verschiedene Ursachen zurückgeführt werden. Zum einen könnte dies in der Wahl der untersuchten PspA-Fragmente begründet sein. So wurden auf Grund von Strukturvorhersagen für Interaktionsanalysen vor der Aufklärung der *coiled-coil*-Struktur der PspA-Domäne PspA(1-144) häufig PspA-

Fragmente eingesetzt, in welchen die Helices des *coiled-coil*s unterbrochen wurden [162,69]. Dies könnte sowohl zu Proteininstabilität, als auch zu einer Fehlfaltung und/oder Aggregation der untersuchten PspA-Fragmente geführt haben. Des Weiteren wurden für *in-vitro*-Interaktionsanalysen PspA-Fragmente ausschließlich aus der nicht-löslichen Fraktion mit Hilfe des Detergens CHAPS gereinigt [68,69,162]. Es ist daher möglich, dass die Zugabe des Detergens nicht ausreichend war, um Proteinaggregate aufzulösen und die getesteten Fragmente nicht in ihrer nativen Konformation vorlagen, was eine Interaktion mit PspF und dessen Inhibition verhinderte.

Dass PspA(1-144) bei rekombinanter Überproduktion als starker PspF-Inhibitor wirkt, jedoch in einem natürlich regulierten System nicht in der Lage ist, die PspF-Aktivität zu inhibieren, war zunächst überraschend, spricht jedoch prinzipiell nicht gegen die von Osadnik *et al*. (2015) beschriebene regulatorische Funktion dieser PspA-Domäne [70]. Die im Vergleich zu PspA erhöhten Mengen an PspA(1-144) im Cytoplasma scheinen jedoch in Rahmen der natürlichen Regulationskaskade nicht ausreichend zu sein, um die PspF-Aktivität in dem Maße zu inhibieren, wie es bei rekombinanter Überproduktion der Fall ist (Abschnitt 3.2, Abbildung 8). Dies lässt den Schluss zu, dass in einem natürlich regulierten System eine Erhöhung der Abundanz dieser PspA-Domäne nicht zu einer Verstärkung ihrer inhibitorischen Wirkung führt und unterstützt die Hypothese, dass der PspF/PspA-Komplex ebenfalls *in vivo* ständig als gesättigter Komplex in der Zelle vorliegt, da im gegenteiligen Fall eine Inhibition von PspF zu erwarten gewesen wäre. Ob PspA(145-222) nun ebenfalls inhibitorisch auf die ATPase-Aktivität wirken kann, wie es für PspA(1-144) gezeigt wurde [70], oder ob die Inhibition der Transkriptionsaktivität PspFs durch PspA(145-222) auf einem völlig anderen Mechanismus beruht, müssen zukünftige Untersuchungen zeigen.

PspA(145-222) trägt jedoch nicht nur zur Inhibition PspFs bei, sondern ebenfalls zur Aktivierung des Psp-Systems bei Membranstress. So konnte keine Aktivierung des Psp-Systems durch TatA-induzierten Membranstress beobachtet werden, wenn die C-terminale PspA-Domäne fehlte (Abschnitt 3.2, Abbildung 7 und 8). Im Gegenzug war nur ein durch PspA(145-222) inhibiertes Psp-System durch TatA ausgelösten Membranstress induzierbar (Abschnitt 3.2, Abbildung 7). Zusätzlich konnten auch Yamaguchi *et al.* (2010) in *Y. enterocolitica* eine Aminosäure in der C-terminalen Domäne von PspA identifizieren, deren Substitution zu einem Verlust der Induzierbarkeit des Psp-System durch das kleine Membranprotein YE0566 führte [83]. Da PspA ohne die C-terminale Domäne weder in der Lage ist zu oligomerisieren, noch

mit Membranen zu interagieren [70] und die TatA-abhängige Aktivierung des Psp-Systems ohne diese PspA-Domäne nicht stattfindet, wurde in Abschnitt 3.2 vorgeschlagen, dass Membranstress die Oligomerisierung der C-terminalen Domänen von PspF-gebundenen PspA-Protomeren direkt auslöst, wodurch diese ihre PspF-inhibitorische Wirkung verlieren. Dies stellt in dem in Abbildung 9 vorgeschlagenen Modell, neben der Strukturveränderung von PspA(1-24) und der Interaktion der *coiled-coil*-Domäne mit der C-terminalen Domäne von PspC, einen maßgeblichen Schritt in der Stresswahrnehmung durch das Psp-System und in der Aufhebung der PspF-Inhibition dar.

Auch McDonald *et al*. (2015) beobachteten in *in-vitro*-Studien, dass C-terminale Bereiche PspAs, in diesem Fall PspA(187-222), eine entscheidende Funktion in der Aufhebung der PspF-inhibitorischen Wirkung PspAs besitzen. Sie zeigten, dass die Inhibition von PspF durch PspA *in vitro* aufgehoben werden kann, wenn einem Reaktionsansatz, in welchem PspF und PspA in einem Komplex vorliegen, Membranvesikel hinzugeben wurden [77]. Eine Aktivierung PspFs durch die Zugabe von Lipiden gelang jedoch nicht, wenn PspF durch das PspA-Fragment PspA(1-186) inhibiert wurde. Sie schlossen daraus, dass zum einen die Regulatorfunktion von PspA durch Lipide direkt beeinflusst wird und zum anderen, dass PspA(187-222) wichtig für die Aufhebung der inhibitorischen Wirkung PspAs ist. In dieser Studie wurde jedoch nicht nur untersucht, ob es auch bei einer Verkürzung PspAs zu einer Aufhebung der inhibitorischen Wirkung durch Membranvesikel kommt, sondern auch wie sich verschiedene Lipidzusammensetzungen der Membranvesikel auf die Stärke der Aufhebung der negativen Regulatorfunktion PspAs auswirken [77]. Es gelang zu zeigen, dass die PspF-Aktivität mit einem Anstieg des SCE-Stresses der Membranvesikel zunahm, was in der Umkehrung heißt, dass die Fähigkeit PspAs PspF inhibieren zu können mit Zunahme des SCE-Stresses abnahm. Die Autoren schlossen daraus, dass eine Zunahme des an der Cytoplasmamembran anliegenden SCE-Stresses zu einer PspBC-unabhängigen Induktion der Psp-Antwort führt, welche allein auf strukturelle Veränderungen PspAs zurückzuführen ist. Wie später eingehender diskutiert, ist es ebenfalls sehr wahrscheinlich, dass auch die rekombinante Produktion von TatA punktuell den SCE-Stress der Cytoplasmamembran erhöht.

4.1.3 PspB ist für die Wahrnehmung von Membranstress in einem artifiziell induzierten Psp-System entscheidend

Eine weitere entscheidende Beobachtung im Rahmen dieser Arbeit war, dass die rekombinante Produktion von TatA nur dann zu einer zusätzlichen Aktivierung eines bereits artifiziell induzierten Psp-Systems führte, wenn PspB in der Zelle vorhanden war (Abschnitt 3.4, Abbildung 7D). Dies zeigte, dass PspB eine entscheidende Rolle in der Signalwahrnehmung und -kaskade des Psp-Systems spielen muss und PspB möglicherweise den primären Sensor innerhalb des PspBC-Komplexes darstellt. Die Abhängigkeit der Psp-Antwort von PspB ist in der Vergangenheit schon häufig beobachtet worden, es ist jedoch völlig unklar auf welchen Mechanismus diese zurückzuführen ist [18,39,81]. Generell erscheinen die Beschreibungen der Funktion PspBs im Kontext der Stresswahrnehmung und Signalkaskade des Psp-Systems widersprüchlich: Zum einen ist PspB nötig zur Induktion der Psp-Antwort bei Membranstress [18], zum anderen wurde mittels diverser Interaktionsstudien gezeigt, dass die C-terminalen Domänen von PspB und PspC im uninduzierten Zustand des Psp-Systems interagieren, jedoch im Zuge von Membranstress dissoziieren, wodurch eine Signalweiterleitung an PspA erst ermöglicht werden soll [35,36,72]. Da in vorhergegangenen Studien keine direkte Interaktion zwischen PspB und PspA nachgewiesen werden konnte [81,84], stellt sich die Frage, wie sich die in Abschnitt 3.4 gemachten Beobachtungen über die PspB-Abhängigkeit der Induktion des Psp-Systems durch Membranstress einordnen lassen.

Sowohl in *E. coli* als auch in *Y. enterocolitica* konnte gezeigt werden, dass PspB dem FtsH-abhängigen Abbau von PspC entgegenwirkt. Aufgrund dessen wurde postuliert, dass PspB PspC womöglich in einem Komplex stabilisieren kann [85]. Dies könnte die reduzierte Induktion durch PspC in einem *pspBC*-Deletionsstamm im Vergleich zu einem Wildtypstamm erklären (Abschnitt 3.4, Abbildung 4B), jedoch nicht die positive regulatorische Funktion von PspB im Zuge der Psp-Antwort. Im Gegensatz zu einer von Jovanovic *et al.* (2010) durchgeführten Studie war in den hier durchgeführten Arbeiten die Interaktion der C-terminalen PspC-Domäne mit PspA nicht PspB abhängig (Abschnitt 3.4, Abbildung 4A, [81]). Ein weiterer Unterschied zur von Jovanovic *et al*. (2010) durchgeführten Studie ist, dass dort beschrieben wurde, dass für die artifizielle Induktion des Psp-Systems die C-terminale Domäne von PspC zusammen mit PspB in stöchiometrischen Mengen produziert werden muss. Auch dies war hier nicht der Fall, was den Schluss zulässt, dass wie von Weiner *et al.* bereits

1991 postuliert, zur initialen Induktion des Psp-Systems nur katalytische Mengen an PspB notwendig sind [18].

Besonders interessant ist in diesem Zusammenhang die Beobachtung, dass PspA zusammen mit TatA eluierte, wenn TatA affinitätschromatographisch aus einem *pspBC*-Deletionsstamm angereichert wurde, welcher PspB rekombinant produzierte. PspB konnte in diesem Fall ebenfalls in den Elutionsfraktionen nachgewiesen werden (Abschnitt 3.4, Abbildung 7B). Da die TatA-PspA-Interaktion in einem natürlich regulierten System eindeutig von PspB und PspC abhängig war [94], wäre es möglich, dass durch die rekombinante Überproduktion von PspB eine Interaktion von TatA und PspA beobachtet wurde, welche in einem natürlich regulierten System nur transient stattfindet und somit mit der gewählten Methodik nicht nachweisbar war. PspB selbst muss daher, unabhängig von PspC, einen direkten Einfluss auf PspA besitzen, sodass PspA unabhängig von PspC mit TatA interagieren konnte. Dies verstärkt nochmal die Annahme, dass sich Membranstress direkt auf PspB und dessen Struktur und Eigenschaften auswirkt. So wäre es denkbar, dass Membranstress zu einer Änderung der Eigenschaften der Transmembrandomäne PspBs führt, welche sich auf dessen cytoplasmatische Domäne überträgt. Dies könnte eine durch Stress induzierte und katalytisch wirkende Interaktion der C-terminalen PspB-Domäne mit PspA erlauben, welche ausschlaggend für die Induktion des Psp-Systems ist und hier auf Grund der starken Überproduktion PspBs beobachtet werden konnte. Eine weitere Hypothese wäre, dass in einem natürlich regulierten Psp-System PspB nicht direkt mit PspA interagiert, sondern eine räumliche Nähe zwischen PspB und PspA über die C-terminale PspC-Domäne erreicht wird. So könnte PspB die Bindung der C-terminalen Domäne von PspC an die *coiled-coil*-Struktur PspAs stabilisieren oder ausschließlich bei Membranstress in einer Weise verändern, dass es zu einer Aufhebung der PspF-Inhibition kommt (Abschnitt 3.4, Abbildung 7). Unterstützt wird diese Annahme durch Untersuchungen von Adams *et al.* (2003), welche zeigten, dass eine PspB-PspA-Interaktion von PspC abhängig ist [84]. Interessant ist in diesem Zusammenhang auch, dass sowohl für die cytoplasmatische Domäne PspBs als auch für den C-terminale PspC-Domäne mit sehr hohen Wahrscheinlichkeiten *coiled-coil*-Strukturen vorhergesagt werden (Abschnitt 3.4 und [84]). Dies würde bedeuten, dass es unter Stressbindungen zu einer Interaktion von vier *coiled-coil*-bildenden Helices und PspF kommt. Es ist in diesem Zusammenhang vorstellbar, dass die *coiled-coil*-bildenden Helices von PspB und PspC den PspF-regulierenden *coiled-coil* PspAs durch dessen

Bindung strukturell in einer Weise verändern, dass dieser seine Eigenschaft verliert, PspF inhibieren zu können.

Zusätzlich wird auf Grund der in Abschnitt 3.4 gemachten Beobachtungen in Frage gestellt, dass Membranstress durch die Transmembrandomäne von PspC wahrgenommen werden kann. So konnte gezeigt werden, dass die rekombinante Produktion von TatA in einem *pspC*-Deletionsstamm, in welchem das Psp-System artifiziell durch die C-terminale PspC-Domäne induziert wurde, zu einer weiteren Steigerung der Aktivität des *pspA*-Promotors um circa 1000 MU führte (Abschnitt 3.4, Abbildung 7C). Des Weiteren zeigten in einem natürlich regulierten Psp-System Aminosäuresubstitutionen innerhalb der Transmembrandomäne von PspC keinen Einfluss auf die Induzierbarkeit der Psp-Antwort durch Membranstress (Abschnitt 3.4, Abbildung 1). Zudem führte TatA-induzierter Membranstress nicht zu einer stärkeren Aktivität PspFs, wenn TatA in einem *pspBC*-Deletionsstamm rekombinant produziert wurde, welcher ebenfalls PspC rekombinant produzierte (Abschnitt 3.4, Abbildung 7D), was nochmals die Funktion von PspB als Sensorkomponente des Psp-Systems unterstützt. Dennoch ist es vorstellbar, dass PspB und PspC in einem Komplex zusammenwirken, wobei womöglich PspB die primäre Sensorkomponente darstellt und zusammen mit PspC die inhibitorische Wirkung von PspA auf PspF reguliert.

An dieser Stelle lässt sich zusammenfassen, dass die Regulation des bEBP PspFs durch PspA im Zuge der Psp-Antwort auf einem sehr viel komplexeren Mechanismus zurückzuführen ist als zunächst angenommen. Während anfänglich davon ausgegangen wurde, dass die Aktivierung PspFs bei Membranstress allein auf der Dissoziation PspAs bei Membranstress beruht, scheint es heute eher wahrscheinlich, dass dieses Modell zu trivial ist, um die Regulation des Psp-Systems und das Verhalten der verschiedenen Komponenten unter Normal- als auch Stressbedingungen zu erklären. So konnte das von Osadnik *et al.* (2015) vorgeschlagene Modell der Modulation der PspF-Aktivität durch PspA unter Stressbedingungen mit weiteren Daten untermauert und weiterentwickelt werden. Schlussendlich ist die Aufklärung der Struktur des PspF/PspA-Komplexes nötig, um zu verstehen, wie die Regulation der ATPase-Aktivität als auch der Transkriptionsaktivität PspFs durch die einzelnen PspA-Domänen unter verschiedenen Bedingungen geschieht.

Es wurde ebenfalls klar, dass PspA, PspB und PspC im Zuge der Stresswahrnehmung und Signalkaskade an der Cytoplasmamembran zusammenwirken müssen, und die Interaktion zwischen der C-terminalen Domäne von PspC und PspA allein nicht ausreichend für das Auslösen der Signalkaskade des Psp-Systems ist.

4.2 SCE-Stress als Auslöser der Psp-Antwort

4.2.1 SCE-Stress führt *in vivo* zu einer verstärkten Membranassoziation von PspA

Dass SCE-Stress das induzierende Signal der Psp-Antwort darstellt, ist ein sehr attraktives Modell, welches prinzipiell auf alle Induktoren des Psp-Systems angewandt werden kann. Es war jedoch zu Beginn dieser Arbeit völlig unklar, ob erhöhter SCE-Stress der Cytoplasmamembran *in vivo* zu einer Aktivierung des Psp-Systems führt und dies, wie von McDonald *et al.* (2015) postuliert, über eine von PspB und PspC unabhängige Regulationskaskade geschieht, in welcher PspA den alleinigen Sensor und Regulator des Psp-Systems darstellt [77]. In dieser Arbeit gelang es erstmals *in vivo* zu zeigen, dass es zu einer verstärkten Membranassoziation von PspA kommt, wenn die negativ geladenen Phospholipide PG und CL nicht in der Cytoplasmamembran vorhanden sind (Abschnitt 3.3). Dazu wurde der *E.-coli*-Stamm UE54 genutzt, welcher eine *pgsA*-Deletion besitzt, wodurch dieser die negativ geladenen Phospholipide PG und CL nicht mehr synthetisieren kann [151]. Aus diesem Grund besteht die Cytoplasmamembran in UE54 vornehmlich aus PE. PE liegt auf Grund seines molekularen Aufbaus in wässriger Umgebung bevorzugt in der inversen hexagonalen Phase vor und bildet keine lamellaren Strukturen aus [163]. SCE-Stress ist *in vivo* bislang nicht messbar, es kann dennoch angenommen werden, dass es in UE54, dessen Cytoplasmamembran vornehmlich aus PE besteht, im Vergleich zum hier verwendeten korrespondieren Lipidwildtypstamm UE53 zu erhöhtem an der Cytoplasmamembran anliegenden SCE-Stress kommt [153,164,165]. In Übereinstimmung mit den von McDonald *et al.* (2015) publizierten Daten [77], konnte in diesem *pgsA*-Deletionsstamm eine verstärkte Membranassoziation von PspA im Vergleich zum Wildtypstamm UE53 nachgewiesen werden (Abschnitt 3.3, Abbildung 1). Dies bestätigt die im *in-vitro*-System beobachtete erhöhte Membranaffinität von PspA unter SCE-Stress-Bedingungen und die Annahme, dass eine Veränderung des an der Cytoplasmamembran anliegenden SCE-

Stresses ein Signal darstellt, welches die Psp-Antwort auslösen könnte. Ob SCE-Stress unter den hier getesteten Bedingungen zu einer verstärkten *pspA*-Expression führt, oder lediglich ein Teil des in der Zelle vorliegenden PspAs an die Membran rekrutiert wurde, lässt sich jedoch mittels der hier gewählten Methodik nur schwer bestimmen und sollte in zukünftigen Analysen z.B. mittels quantitativer PCR oder anderer Methoden, welche direkten Aufschluss über die Aktivität des *pspA*-Promotors geben können, überprüft werden.

4.2.2 Die verstärkte Membranassoziation von PspA bei SCE-Stress ist *in vivo* PspC-abhängig

Um erste Hinweise zu erhalten, ob SCE-Stress auch *in vivo,* wie in *in-vitro*-Analysen gezeigt, zu einer PspBC-unabhängigen Aktivierung des Psp-Systems führt, wurde zusätzlich zur *pgsA*-Deletion *pspC* in UE54 deletiert. Die Deletion von *pspC* führte zu stark reduzierten PspA-Leveln in der Zelle, welche ausschließlich in der löslichen Fraktion detektierbar waren (Abschnitt 3.3, Abbildung 3). Dies zeigte, dass sowohl die Membranassoziation von PspA, sowie eine mögliche Aktivierung der Expression des *psp*-Operons in einem *pgsA*-Deletionsstamm von PspC abhängig sein muss. Dies lässt den Schluss zu, dass die Psp-Antwort *in vivo* auch unter SCE-Stressbedingungen über eine PspBC-abhängigen Signalkaskade aktiviert wird und nicht, wie von McDonald *et al.* (2015) basierend auf *in-vitro*-Analysen postuliert, in einem von PspBC-unabhängigen Mechanismus [77].

4.2.3 Eine erhöhte Abundanz der negativ geladenen Phospholipide PG und CL führen zur Membranassoziation von PspA und zur Induktion der *pspA*-Expression

Um die im vorherigen Abschnitt geäußerte Vermutung experimentell zu untermauern und um einen ersten Eindruck zu erlangen, in wie weit sich die Abundanz negativ geladener Phospholipide in der Cytoplasmamembran von *E. coli* auf das Psp-System auswirkt, wurde ebenfalls untersucht, ob es zu einer Veränderung der Lokalisation und Menge PspAs in der Zelle kommt, wenn erhöhte Mengen an negativ geladenen Phospholipiden in der Cytoplasmamembran vorhanden sind (Abschnitt 3.3, Abbildung 1). Zur Durchführung wurde der *E.-coli*-Stamm GN10 genutzt, welcher auf Grund einer

pssA-Deletion nicht mehr in der Lage ist, PE zu synthetisieren und somit die Cytoplasmamembran hauptsächlich aus den negativ geladenen Phospholipiden PG und CL aufgebaut ist [152]. Es konnte beobachtet werden, dass in diesem *pssA*-defizienten *E.-coli*-Stamm im Vergleich zum korrespondierenden Wildtyp mehr PspA vorhanden ist und PspA vornehmlich mit Membranen sedimentierte (Abschnitt 3.3, Abbildung 1). Jedoch kann auch hier nur indirekt über die Proteinmenge auf eine erhöhte PspF-Aktivität geschlossen werden. Auf Grund der signifikanten Änderung der Menge und Lokalisation von PspA kann jedoch angenommen werden, dass es in GN10 zu einer Aktivierung der Psp-Antwort kommt. Die Cytoplasmamembran in GN10 besteht wie bereits beschrieben hauptsächlich aus PG und CL, welche in wässriger Lösung bevorzugt lamellare Strukturen ausbilden [163]. Die Lebensfähigkeit des PE-defizienten *E.-coli*-Stammes GN10 hängt von der Präsenz divalenter Kationen ab [166]. Dies wird dadurch begründet, dass CL in einem *pssA*-Deletionsstamm durch die Zugabe von erhöhten Mengen divalenter Kationen eine konische Struktur annimmt und so die nicht-lamellaren Eigenschaften von PE übernimmt, welche entscheidend für die Lebensfähigkeit der Zelle sind [163,166–170]. Es ist daher naheliegend, dass es im Vergleich zum korrespondierenden Wildtyp zu einer Verstärkung des an der Cytoplasmamembran anliegenden SCE-Stresses kommt, was die Induktion der Psp-Antwort in diesem Stamm erklären könnte. Es ist ebenfalls vorstellbar, dass die erhöhte Präsenz von negativ geladenen Phospholipiden in GN10, wie von McDonald *et al.* (2017) beschrieben [71], die helikale Struktur von PspA(1-24) an der Cytoplasmembran stabilisiert und so die Psp-Antwort verstärkt wird.

4.3 Das durch TatA ausgelöste Psp-System-induzierende Signal – Eine Näherung

Ein weiteres Ziel dieser Arbeit war, das durch den Membrananker von TatA in der Cytoplasmamembran verursachte Signal, welches zu einer Psp-Antwort führt, näher zu charakterisieren und TatA als Modellinduktor der Psp-Antwort in *E. coli* zu etablieren. Auf Grund seines simplen Aufbaus stellte der TatA-Membrananker einen experimentell leicht zugänglichen Induktor der Psp-Antwort in *E. coli* dar. Der N-terminale Bereich von TatA ist stark konserviert und wird vom sogenannten WQ-Motiv, welches das für den Transport essentielle Glutamin an Position acht enthält [120] und der sogenannten *hinge*-Region auf eine Länge von 13 Aminosäuren begrenzt, und ist daher nicht in der Lage, eine Membran normaler Dicke vollständig zu durchspannen[2]. Schon im Vorfeld dieser Arbeit gelang es *in vitro* zu zeigen, dass die rekombinante Produktion von TatA mit einer Destabilisierung der Cytoplasmamembran von *E. coli* einhergeht, welche eine Schwächung des an der Membran anliegenden Protonengradienten von invertierten Membranvesikeln zur Folge hatte [94]. Basierend auf MD-Simulationen wurde eine Verdünnung der Cytoplasmamembran durch die Assemblierung von TatA-Protomeren bei Substratbindung vorhergesagt. Es wurde daher spekuliert, dass die Verdünnung und die daraus resultierende Schwächung der Cytoplasmamembran und der PMF durch die rekombinante Produktion von TatA der Grund für die Induktion des Psp-Systems sein könnte.

4.3.1 Die durch die verschiedenen TatA-NT-Hip-Varianten erhöhte *pspA*-Promotoraktivität korreliert nicht mit der Schwächung der PMF

Da die rekombinante Überproduktion des TatA-Membranankers ausreichte, um die Psp-Antwort zu induzieren und dieser ebenfalls in der Lage war mit PspA interagieren zu können, wurden dessen Membran-destabilisierende Eigenschaften weitergehend charakterisiert (Abschnitt 3.1). Es gelang in dem in Abschnitt 3.1 vorgestellten Artikel erstmals eine direkte Membrandestabilisierung durch den ungewöhnlich kurzen Membrananker von TatA *in vivo* und *in vitro* zu zeigen. Der beobachtete Effekt auf das Membranpotential war unabhängig von der Sequenz des TatA-Membranankers und

[2] Für membrandurchspannende α-Helices konnte eine durchschnittliche Länge von circa 18 Aminosäuren mittels bioinformatischen Analysen ermittelt werden [171].

konnte teilweise durch die Verlängerung des hydrophoben Bereichs um sechs Leucine aufgehoben werden.

Um herauszufinden, ob die durch die Membrandestabilisierung ausgelöste Schwächung der PMF durch die TatA-NT-Hip-Varianten den durch TatA ausgelösten „Membranstress“ darstellt, welcher zu einer Induktion der Psp-Antwort führt, wurden die entsprechenden TatA-NT-Hip-Varianten auf ihre Fähigkeit hin getestet, die Aktivität des *pspA*-Promotors zu verstärken (Abschnitt 3.5). Prinzipiell führte die rekombinante Überproduktion aller membranständiger TatA-NT-Hip-Varianten zu einer Erhöhung der *pspA*-Promotoraktivität. Wäre die Schwächung der PMF das durch die verschiedenen TatA-NT-Hip-Varianten ausgelöste Signal, welches zu einer Psp-Antwort in *E. coli* führt, hätte erwartet werden können, dass die Aktivität des *pspA*-Promotors tendenziell mit der Schwächung der PMF durch die verschiedenen TatA-NT-Hip-Varianten übereinstimmt. Dies war jedoch nur für TatA und TatA-NT-Hip der Fall, während für die TatA-NT-Hip-Varianten TatA-NT$(LA)_6$-Hip und TatA-NT(9+6L)-Hip der genau gegensätzliche Effekt beobachtet werden konnte (Tabelle 1).

Tabelle 1 Zusammenfassung der Effekte von TatA und der verschiedenen TatA-NT-Hip-Varianten auf die PMF und das Psp-System

TatA-NT-Variante	Effekt auf PMF	Stärke der Psp-Antwort
TatA	+	+
TatA-NT-Hip	+++	+++
TatA-NT$(LA)_6$-Hip	+++	+
TatA-NT(9+6L)-Hip	+	+++

Dies lässt den Schluss zu, dass die von Engl *et al.* (2011) sowie von Wang *et al.* (2010) gemachten Beobachtungen, dass die Schwächung der PMF nicht ausschlaggebend ist, um die Psp-Antwort auszulösen [90,91] auch für TatA und dessen Derivate gilt. Dies trägt neben den in Abschnitt 3.4 gezeigten Daten zu einer Etablierung TatAs als Modellinduktor des Psp-Systems bei, zeigt jedoch, dass die Induktion der *pspA*-Promotoraktivität durch TatA bzw. durch die hier getesteten verschiedenen TatA-NT-Hip-Varianten auf andere in der Cytoplasmamembran ausgelöste Signale zurückgeführt werden muss.

4.3.2 Hat die Interaktion von TatA mit PspA einen Einfluss auf die Induktion der Psp-Antwort?

Bei TatA bzw. TatA-NT-Hip handelt es sich um besondere Induktoren der Psp-Antwort in *E. coli*, da sie die einzig bekannten Induktoren der Psp-Antwort darstellen, für welche eine Interaktion mit PspA nachgewiesen werden konnte [94]. Es wurde deshalb bereits im Vorfeld dieser Arbeit spekuliert, dass die Psp-Antwort möglicherweise zusätzlich zur ausgelösten Membrandestabilisierung durch die direkte Rekrutierung von PspA an TatA bzw. TatA-NT-Hip in einem durch PspB und PspC vermittelten Mechanismus induziert werden könnte [94,150]. Betrachtet man die Effekte der TatA-NT-Hip-Varianten TatA-NT-Hip, TatA-NT$(LA)_6$-Hip und TatA-NT(9+6L)-Hip könnte ein Zusammenhang zwischen der Interaktion und Induktion bestehen. Die rekombinante Produktion von TatA-NT-Hip und TatA-NT(9+6L)-Hip führte zu einer vergleichbar starken Erhöhung der *pspA*-Promotoraktivität und PspA zeigte ein korrespondierendes Elutionsverhalten zu diesen TatA-NT-Hip-Varianten in der Affinitätschromatographie (Abschnitt 3.5). PspA zeigte indes kein zu TatA-NT$(LA)_6$-Hip vergleichbares Elutionsprofil, wenn TatA-NT$(LA)_6$-Hip affinitätschromatographisch angereichert wurde, was möglicherweise ein weiterer Grund für die reduzierte Stärke der Induktion des Psp-Systems durch TatA-NT$(LA)_6$-Hip im Vergleich zu TatA-NT-Hip sein könnte.

Ein Vergleich der Induktion des Psp-Systems durch die direkte Interaktion von Induktoren mit PspA gestaltet sich jedoch als schwierig, da für keinen weiteren Induktor eine direkte Interaktion mit PspA bislang gezeigt werden konnte. Einzig für das Sekretin YsaC aus *Y. enterocolitica* wurde eine Interaktion mit den membranständigen Komponenten des Psp-Systems PspB und PspC nachgewiesen [40]. Ein Nachweis der PspA-Interaktion gelang jedoch auf Grund des experimentellen Aufbaus nicht.

4.3.2.1 PspB und PspC vermitteln die Interaktion zwischen TatA und PspA nur indirekt

Da die Interaktion von TatA und PspA möglicherweise direkt zur Induktion des Psp-Systems beträgt und eine einzigartige Eigenschaft TatAs in Bezug auf die Aktivierung des Psp-Systems darstellen könnte, war es Ziel dieser Arbeit, diese eingehender zu untersuchen. Bereits Mehner *et al*. (2012) wiesen nach, dass die Interaktion zwischen PspA und TatA abhängig von PspB und PspC ist [94]. Da es sich sowohl bei TatA als

auch bei PspB und PspC um Membranproteine handelt und bekannt war, dass PspC direkt mit PspA interagieren kann, wurde spekuliert, dass die Interaktion von TatA mit PspA über eine Interaktion der Transmembranbereiche von TatA und PspBC vermittelt wird [94]. Dies konnte im Zuge dieser Arbeit nicht bestätigt werden (Abschnitt 3.4). Stattdessen zeigte sich, dass die Abhängigkeit der TatA/PspA-Interaktion von PspB und PspC in der Vermittlung einer stabilen Membranassoziation von PspA bestand und die einzelnen Transmembrandomänen nicht spezifisch notwendig für die TatA/PspA-Interaktion sind.

4.3.2.2 Die Interaktion zwischen TatA und PspA hängt von der Kooperation N- und C-terminaler PspA-Domänen ab

Da die Interaktion von TatA nur indirekt von PspB und PspC vermittelt wurde, war es Ziel, die TatA-interagierende Domäne innerhalb PspAs zu bestimmen (Abschnitt 3.2). Dazu wurde PspA in die PspA-Domänen PspA(1-144) und PspA(145-222) geteilt. Jedoch konnte weder für PspA(1-144) noch für PspA(145-222) eine Interaktion mit TatA nachgewiesen werden (Abschnitt 3.2, Abbildung 6). Dies wurde darauf zurückgeführt, dass es bei PspA(1-144) und PspA(145-222) um vollkommen lösliche Proteinfragmente handelte, welche offensichtlich *per se* nicht in der Lage sind, mit der Cytoplasmamembran zu interagieren. Auch in vorangegangenen Studien wurde beobachtet, dass N- und C-terminale PspA-Domänen in Bezug auf die Membraninteraktion und -assoziation PspAs zusammenwirken müssen [71,77,88,75]. In Osadnik *et al.* (2015) wurde eindeutig gezeigt, dass die hier untersuchte PspA-Domäne PspA(145-222) nötig für die Oligomerisierung und Membraninteraktion von PspA ist [70]. Es lässt sich daher an dieser Stelle zusammenfassen, dass auch in Bezug auf die TatA-Interaktion beide PspA-Domänen *in vivo* kooperieren müssen, was direkt mit der Fähigkeit PspAs in oligomeren Strukturen mit Membranen zu interagieren in Zusammenhang steht.

Da PspA ebenfalls auf Grund von rekombinanter Überproduktion auch ohne Membranstress mit Membranen assoziiert vorliegt [83], warf dies die Frage auf, ob TatA und PspA wirklich direkt miteinander interagieren oder PspA nur deshalb ein zu TatA korrespondierendes Elutionsprofil aufwies, weil es in der Lage ist in oligomeren Strukturen mit Membranvesikeln zu interagieren, welche bei der affinitätschromatographischen Anreicherung TatAs ohne vorhergegangene Solubilisierung ebenfalls

retardiert wurden. Es konnte jedoch bereits gezeigt werden, dass die TatA-PspA-Interaktion nicht von der Komplexbildung beider Proteine abhängt [150], was ausschlaggebend für die Membraninteraktion PspAs ist. Interessant ist jedoch, dass es nicht gelang, die Interaktion von TatA und PspA *in vitro* zu rekonstituieren, wenn beide Proteine zuvor getrennt voneinander gereinigt wurden (unpublizierte Daten, Denise Mehner-Breitfeld). Es wäre daher möglich, dass die Bildung der N-terminalen amphipathischen Helix von PspA, welche von der Präsenz von Lipiden abhängig ist [71], sowie die Fähigkeit zur Oligomerisierung notwendige Determinanten der Interaktion von PspA mit TatA darstellen. In zukünftigen Studien könnte deshalb untersucht werden, ob die TatA-PspA-Interaktion *in vitro* rekonstituierbar ist, wenn dem Reaktionsansatz Lipide hinzugegeben wurden. Dies könnte auch zur endgültigen Klärung beitragen, ob es sich bei dem nachgewiesenen korrespondieren Elutionsverhalten von PspA und TatA um eine „echte“ Interaktion beider Proteine handelt, welche zur Induktion des Psp-System beiträgt, oder ob PspA nur aus dem Grund in den Elutionsfraktionen der TatA-Anreichung detektierbar war, weil es nach Induktion des Psp-Systems oder durch rekombinante Überproduktion mit Membranvesikeln interagierte.

4.4.3 Ist SCE-Stress das durch den TatA-Membrananker ausgelöste Psp-Antwort-induzierende Signal?

Wie bereits in den vorhergegangenen Abschnitten diskutiert, ist es möglich, dass eine Veränderung des an der Cytoplasmamembran anliegenden SCE-Stresses das Psp-Antwort auslösende Signal darstellen kann. Dieses Modell kann auch auf TatA und die hier getesteten Varianten des TatA-Membranankers angewendet werden. Die Dicke der Cytoplasmamembran in Umgebung eines membranintegralen Proteins wird direkt von der Länge der hydrophoben Bereiche des Proteins bestimmt. So kommt es zu einer Verdickung der Cytoplasmamembran, wenn der hydrophobe Bereich des Proteins den Durchmesser der Membran übersteigt und dementsprechend zu einer Membranverdünnung, wenn die Länge des hydrophoben Bereichs nicht ausreichend für die Durchspannung der Cytoplasmamembran ist [172]. Auf diese Weise wird der biophysikalisch ungünstige Kontakt sowohl zwischen hydrophilen Bereichen des Proteins mit dem hydrophoben Kern der Cytoplasmamembran als auch zwischen hydrophoben Bereichen des Proteins mit der hydrophilen Umgebung der

Cytoplasmamembran auf ein Minimum reduziert. Als entscheidend für die beschriebene Membranverdünnung durch ein zu kurzes hydrophobes Peptid wurde das Vorhandensein von Tryptophanen an den Enden der hydrophoben Bereiche beschrieben [173]. Auch TatA besitzt ein solches Tryptophan im stark konservierten und für den Transport essentiellen WQ-Motiv [120], welches den hydrophoben Bereich des TatA-Membranankers zum Periplasma hin begrenzt. Bei dem hier verwendeten TatA-NT-Hip-Konstrukt wurde zudem ein globuläres Protein mit nur einem sehr kurzen Glycin-Serin-Linker an das C-terminale Ende des hydrophoben Bereichs fusioniert, was ein tiefes Eintauchen des Membranankers von TatA in die Membran verhindert. Es ist daher sehr wahrscheinlich, dass es durch das hier verwendete TatA-NT-Hip-Konstrukt zu einer ständigen starken Verdünnung der Cytoplasmamembran kommt, was zu einer Verstärkung des an der Cytoplasmamembran anliegenden Krümmungsstresses zur Folge hat. Auch die Stärke der Oligomerisierung von TatA-Protomoren könnte direkt einen Einfluss auf den Krümmungsstress der Cytoplasmamembran haben, da durch Einlagerung großer oligomerer Strukturen in die Cytoplasmamembran ein verstärkter lateraler Druck auf die Lipiddoppelschicht ausgeübt wird, welcher ebenfalls zu einer Verstärkung des SCE-Stresses und einer Veränderung der Membrankrümmung führen könnte (Abbildung 10). Mittels MD-Simulationen und Crosslinking-Studien wurde gezeigt, dass die Interaktion zwischen

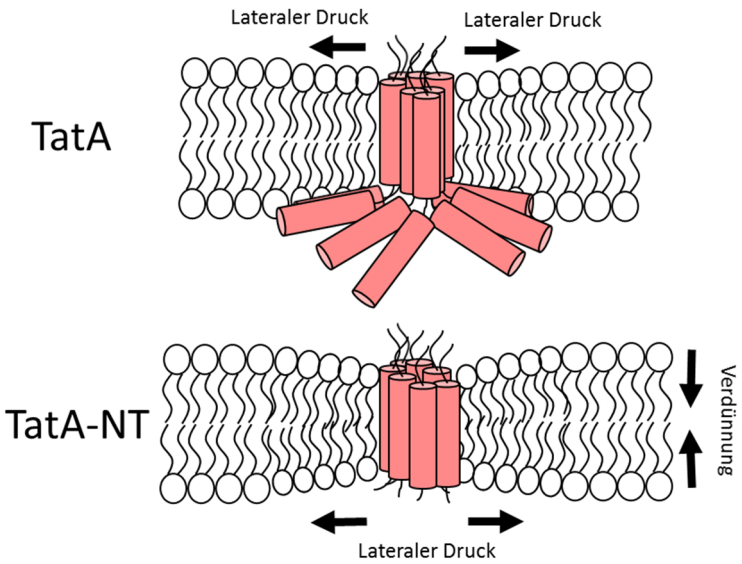

Abbildung 10 Schematische Darstellung der Effekte von TatA und TatA-NT auf die Cytoplasmamembran von *E. coli* oben: große TatA-Assemblierungen führen zu verstärktem lateralem Druck in der Cytoplasmamembran. **unten:** TatA-NT-Assemblierungen führen zusätzlich zu einer punktuellen Verdünnung der Cytoplasmamembran, was eine zusätzliche Verstärkung des Effekts auf den an der Cytoplasmamembran anliegenden Krümmungsstress im Vergleich zu TatA darstellt.

TatA-Protomeren unter anderem durch die Membrandomäne TatAs vermittelt wird [110,120,121]. Durch den Austausch der hydrophoben Region des Membranankers gegen eine repetitive Leucin-Alanin-Sequenz könnte die Interaktion der Membrandomänen gestört sein, was eine schwächere Oligomerisierung zur Folge hätte, was zu einer Verringerung des Membranstresses im Vergleich zu TatA-NT-Hip führen würde, obwohl sich die Konstrukte in ihrer Länge entsprechen. Zudem war dieses Konstrukt von allen getesteten das instabilste, was ebenfalls erklären könnte, warum TatA-NT$(LA)_6$-Hipdas Psp-System weniger stark aktivierte als TatA-NT-Hip. TatA-NT(9+6L)-Hip hingegen war *in vivo* stabiler als TatA-NT$(LA)_6$-Hip und TatA-NT-Hip, was erklären könnte, warum dieses Konstrukt die Psp-Antwort stärker induzierte als TatA-NT$(LA)_6$-Hip, obwohl TatA-NT(9+6L)-Hip einen weniger starken Effekt auf die Stabilität der Cytoplasmamembran zeigte. Zusätzlich könnte sich die Verlängerung des hydrophoben Bereiches in diesem Konstrukt durch jeweils sechs Leucine positiv auf den Oligomerisierungsgrad auswirken, was ebenfalls zu einer Erhöhung des SCE-Stresses an der Cytoplasmamembran führen würde.

Wie bereits von Flores-Kim & Darwin (2016) diskutiert, sind prinzipiell alle Induktoren des Psp-Systems auf verschiedene Art und Weise in der Lage, zu einer Verstärkung des an der Cytoplasmamembran anliegenden SCE-Stresses zu führen [174]. So könnte auch die Induktion des Psp-Systems durch große in die Cytoplasmamembran fehllokalisierte multimere Sekretine zu einer punktuellen Verstärkung des Krümmungsstresses in der Cytoplasmamembran führen. Für Ethanol-behandelte Zellen wurde eine reduzierte Elastizität der Cytoplasmamembran beschrieben [175], was ebenfalls eine Verstärkung des SCE-Stresses zur Folge hat. Auch die von Bergler *et al.* (1994) beschriebene Induktion des Psp-Systems durch die Inhibition der Lipidbiosynthese [154] und die Induktion des Psp-Systems durch die Depletion von YidC [91], welche die Fehlfaltung und Mislokalisation vieler Membranproteine zur Folge hat, könnten zu einer Verstärkung des Krümmungsstresses der Cytoplasmamembran führen, um einige Beispiele an dieser Stelle zu nennen. Die im Rahmen dieser Arbeit nachgewiesene PspC-Abhängigkeit der Induktion des Psp-Systems durch SCE-Stress *in vivo* (Abschnitt 3.3), gibt einen deutlichen Hinweis darauf, dass die durch TatA und dessen Membrananker ausgelöste Veränderung des SCE-Stresses der Cytoplasmamembran das Signal darstellen kann, welches die Psp-Antwort auslöst.

Dass sich SCE-Stress nicht nur wie von McDonald *et al.* (2105) vorgeschlagen auf PspA auswirkt [77], sondern ebenfalls Einflüsse auf die Konformation von PspB und PspC haben kann, ist ebenfalls sehr wahrscheinlich und fügt sich leicht in das in Abschnitt 4.1 vorgeschlagene Modell ein. So ist es durchaus vorstellbar, dass eine Veränderung des Krümmungsstresses und der Elastizität der Cytoplasmamembran direkt auf die membranintegralen Domänen von PspB und PspC wirken kann und zu einem strukturellen Rearrangement der cytoplasmatischen Domänen von PspB und PspC führt. Ein sehr passendes und prominentes Beispiel mit einigen Analogien zu PspB und PspC stellt in diesem Fall die Thermosensor-Histidinkinase DesK aus *B. subtilis* dar. DesK wirkt als Sensorkinase des DesKR-Zweikomponentensystems zusammen mit dem Antwortregulator DesR [176]. DesK besitzt eine membranintegrale Sensordomäne, welche aus fünf antiparallel verlaufenden Transmembranhelices (TMH1-TMH5) besteht, wobei TMH5 eine Verlängerung der helikalen Struktur in das Cytoplasma hinein besitzt, welche den membranintegralen Bereich DesKs mit der cytoplasmatischen Kinasedomäne verbindet. Zudem bildet DesK die für Sensorkinasen typischen homodimeren Strukturen, wobei die im Cytoplasma verlängerte Helixstruktur zweier TMH5 eine *coiled-coil* Struktur ausbilden (2-*helix coiled-coil* (2-HCC)) [176–178]. Die membranintegralen Helices DesKs sind in der Lage, die Dicke und Fluidität der Cytoplasmamembran wahrzunehmen und wirken so als Kältesensor. In Bezug auf das Psp-System ist besonders interessant, dass die sensorische Funktion DesKs auf eine aus Teilen der TMH1 und TMH5 bestehende „chimäre“ Transmembranhelix (*minimal sensor* (MS)-DesK) zurückgeführt werden kann [177,179]. Eine Verdickung und Verringerung der Elastizität der Cytoplasmamembran als Signal führt zu einer Veränderung der Interaktion zweier chimärer Transmembranhelices, wodurch die *2*-HCC-Struktur destabilisiert wird und die Kinasefunktion der cytoplasmatischen Domänen eines DesK-Homodimers erreicht und stabilisiert wird [180,178]. Dies ist insbesondere auch unter dem Aspekt interessant, dass sich in TMH1 und TMH5 sowie in der chimären Transmembranhelix von MS-DesK Proline befinden, für welche basierend auf MD-Simulationen eine wichtige Funktion in der Signalwahrnehmung und –weiterleitung beschrieben wurde [180]. Auch in der Transmembranhelix von PspB liegen Proline vor, welchen einen ähnlichen Abstand wie in den Transmembranbereichen DesKs oder MS-DesKs aufweisen. Es wäre daher möglich, dass die Plastizität der Proline in der Transmembranhelix PspB ebenfalls eine wichtige Rolle während der

Signalwahrnehmung und -weiterleitung von SCE-Stress des Psp-Systems spielen, wie es für DesK postuliert wurde.

In zukünftigen Untersuchungen zur Stresswahrnehmung und Signalkaskade des Psp-Systems sollte daher PspB und speziell dessen Transmembrandomäne im Fokus stehen.

5 Literaturverzeichnis

1. Cronan JE (1968) Phospholipid alterations during growth of *Escherichia coli*. J. Bacteriol. 95 (6): 2054–2061.
2. Kanemasa Y, Akamatsu Y, Nojima S (1967) Composition and turnover of the phospholipids in *Escherichia coli*. Biochim. Biophys. Acta 144 (2): 382–390.
3. Kanfer J, Kennedy EP (1963) Metabolism and Function of Bacterial Lipids. I. Metabolism of Phospholipids in *Escherichia coli* B. J. Biol. Chem. 238: 2919–2922.
4. Brissette JL, Russel M, Weiner Lorin, Model P (1990) Phage shock protein, a stress protein of *Escherichia coli*. Proc. Natl. Acad. Sci. U S A 87: 862–866.
5. Darwin AJ, Miller VL (2001) The *psp* locus of *Yersinia enterocolitica* is required for virulence and for growth *in vitro* when the Ysc type III secretion system is produced. Mol. Microbiol. 39 (2): 429–444.
6. Lloyd LJ, Jones S, Jovanovic G, Gyaneshwar P, Rolfe MD et al. (2004) Identification of a new member of the phage shock protein response in *Escherichia coli*, the phage shock protein G (PspG). J. Biol. Chem. 279 (53): 55707–55714.
7. Mascher T, Zimmer SL, Smith T-A, Helmann JD (2004) Antibiotic-inducible promoter regulated by the cell envelope stress-sensing two-component system LiaRS of *Bacillus subtilis*. Antimicrob. Agents Chemother. 48 (8): 2888–2896.
8. Vrancken K, Keersmaeker S de, Geukens N, Lammertyn E, Anné J et al. (2007) *PspA* overexpression in *Streptomyces lividans* improves both Sec- and Tat-dependent protein secretion. Appl. Microbiol. Biotechnol. 73 (5): 1150–1157.
9. Vrancken K, van Mellaert L, Anné J (2008) Characterization of the *Streptomyces lividans* PspA response. J. Bacteriol. 190 (10): 3475–3481.
10. Weiner L, Model P (1994) Role of an *Escherichia coli* stress-response operon in stationary-phase survival. Proc. Natl. Acad. Sci. U S A 91: 2191–2195.
11. van der Laan M, Urbanus ML, Hagen-Jongman CM ten, Nouwen N, Oudega B et al. (2003) A conserved function of YidC in the biogenesis of respiratory chain complexes. Proc. Natl. Acad. Sci. U S A 100 (10): 5801–5806.
12. DeLisa MP, Lee P, Palmer T, Georgiou G (2004) Phage shock protein PspA of *Escherichia coli* relieves saturation of protein export via the Tat pathway. J. Bacteriol. 186 (2): 366–373.
13. Beloin C, Valle J, Latour-Lambert P, Faure P, Kzreminski M et al. (2004) Global impact of mature biofilm lifestyle on *Escherichia coli* K-12 gene expression. Mol. Microbiol. 51 (3): 659–674.

14. Keren I, Shah D, Spoering A, Kaldalu N, Lewis K (2004) Specialized persister cells and the mechanism of multidrug tolerance in *Escherichia coli*. J. Bacteriol. 186 (24): 8172–8180.
15. Standar K, Mehner D, Osadnik H, Berthelmann F, Hause G et al. (2008) PspA can form large scaffolds in *Escherichia coli*. FEBS Lett. 582 (25-26): 3585–3589.
16. Kleerebezem M, Crielaard W, Tommassen J (1996) Involvement of stress protein PspA (phage shock protein A) of *Escherichia coli* in maintenance of the protonmotive force under stress conditions. EMBO J. 15 (1): 162–171.
17. Brissette JL, Weiner L, Ripmaster TL, Model P (1991) Characterization and Sequence of the *Escherichia coli S*tress-induced Psp operon. J. Mol. Biol. 220 (1): 35–48.
18. Weiner L, Brissette JL, Model P (1991) Stress-induced expression of the *Escherichia coli* phage shock protein operon is dependent on σ^{54} and modulated by positive and negative feedback mechanisms. Genes Dev. 5 (10): 1912–1923.
19. Adams H, Teertstra W, Koster M, Tommassen J (2002) PspE (phage-shock protein E) of *Escherichia coli* is a rhodanese. FEBS Lett. 518 (1-3): 173–176.
20. Li H, Yang F, Kang X, Xia B, Jin C (2008) Solution structures and backbone dynamics of *Escherichia coli* rhodanese PspE in its sulfur-free and persulfide-intermediate forms: implications for the catalytic mechanism of rhodanese. Biochemistry 47 (15): 4377–4385.
21. Ito K, Inaba K (2008) The disulfide bond formation (Dsb) system. Curr. Opin. Struct. Biol. 18 (4): 450–458.
22. Chng S-S, Dutton RJ, Denoncin K, Vertommen D, Collet J-F et al. (2012) Overexpression of the rhodanese PspE, a single cysteine-containing protein, restores disulphide bond formation to an *Escherichia coli* strain lacking DsbA. Mol. Microbiol. 85 (5): 996–1006.
23. Weiner L, Brissette JL, Ramani N, Model P (1995) Analysis of the proteins and cisacting elements regulating the stress-induced phage shock protein operon. Nucleic Acids Res. 23 (11): 2030–2036.
24. Huvet M, Toni T, Sheng X, Thorne T, Jovanovic G et al. (2011) The Evolution of the Phage Shock Protein Response System. Interplay between Protein Function, Genomic Organization, and System Function. Mol. Biol. Evol. 28 (3): 1141–1155.
25. Popham D, Szeto D, Keener J, Kustu S (1989) Function of a bacterial activator protein that binds to transcriptional enhancers. Science 243 (4891): 629–635.

26. Wedel A, Kustu S (1995) The bacterial enhancer-binding protein NTRC is a molecular machine. ATP hydrolysis is coupled to transcriptional activation. Genes Dev. 9 (16): 2042–2052.
27. Dworkin J, Jovanovic G, Model P (1997) Role of upstream activation sequences and integration host factor in transcriptional activation by the constitutively active prokaryotic enhancer-binding protein PspF. J. Mol. Biol. 273 (2): 377–388.
28. Jovanovic G, Weiner L, Model P (1996) Identification, Nucleotide Sequence, and Characterization of PspF, the Transcriptional activator of the *Escherichia coli S*tress-Induced *psp* Operon. J. Bacteriol. 178 (7): 1936–1945.
29. Jovanovic G, Model P (1997) PspF and IHF bind co-operatively in the *psp* promoter-regulatory region of *Escherichia coli*. Mol. Microbiol. 25 (03): 473–481.
30. Jovanovic G, Dworkin J, Model P (1997) Autogenous Control of PspF, Constitutively Active Enhancer-Binding Protein of *Escherichia coli*. J. Bacteriol. 179 (16): 5232–5237.
31. Darwin AJ, Miller VL (1999) Identification of *Yersinia enterocolitica* genes affecting survival in an animal host using signature-tagged transposon mutagenesis. Mol. Microbiol. 32 (1): 51–62.
32. Horstman NK, Darwin AJ (2012) Phage shock proteins B and C prevent lethal cytoplasmic membrane permeability in *Yersinia enterocolitica*. Mol. Microbiol. 85 (3): 445–460.
33. Yamaguchi S, Reid DA, Rothenberg E, Darwin AJ (2013) Changes in Psp protein binding partners, localization and behaviour upon activation of the *Yersinia enterocolitica* phage shock protein response. Mol. Microbiol. 87 (3): 656–671.
34. Flores-Kim J, Darwin AJ (2012) Phage Shock Protein C (PspC) of *Yersinia enterocolitica* Is a Polytopic Membrane Protein with Implications for Regulation of the Psp Stress Response. J. Bacteriol. 194 (23): 6548–6559.
35. Flores-Kim J, Darwin AJ (2015) Activity of a Bacterial Cell Envelope Stress Response Is Controlled by the Interaction of a Protein Binding Domain with Different Partners. J. Biol. Chem. 290 (18): 11417–11430.
36. Flores-Kim J, Darwin AJ (2016) Interactions between the Cytoplasmic Domains of PspB and PspC Silence the *Yersinia enterocolitica* Phage Shock Protein Response. J. Bacteriol. 198 (24): 3367–3378.
37. Flores-Kim J, Darwin AJ (2012) Links between type III secretion and extracytoplasmic stress responses in *Yersinia*. Front. Cell. Infect. Microbiol. 2: 125.

38. Flores-Kim J, Darwin AJ (2014) Regulation of bacterial virulence gene expression by cell envelope stress responses. Virulence 5 (8): 835–851.
39. Maxson ME, Darwin AJ (2006) PspB and PspC of *Yersinia enterocolitica* are dual function proteins: regulators and effectors of the phage-shock-protein response. Mol. Microbiol. 59 (5): 1610–1623.
40. Srivastava D, Moumene A, Flores-Kim J, Darwin AJ (2017) Psp Stress Response Proteins Form a Complex with Mislocalized Secretins in the *Yersinia enterocolitica* Cytoplasmic Membrane. mBio 8 :e01088-17
41. Gueguen E, Savitzky DC, Darwin AJ (2009) Analysis of the *Yersinia enterocolitica* PspBC proteins defines functional domains, essential amino acids and new roles within the phage-shock-protein response. Mol. Microbiol. 74 (3): 619–633.
42. Darwin AJ (2013) Stress relief during host infection: The phage shock protein response supports bacterial virulence in various ways. PLoS Pathog. 9 (7): e1003388.
43. Wallrodt I, Jelsbak L, Thomsen LE, Brix L, Lemire S et al. (2014) Removal of the phage-shock protein PspB causes reduction of virulence in *Salmonella enterica* serovar *Typhimurium* independently of NRAMP1. J. Med. Microbiol. 63 (Pt 6): 788–795.
44. Bidle KA, Kirkland PA, Nannen JL, Maupin-Furlow JA (2008) Proteomic analysis of *Haloferax volcanii* reveals salinity-mediated regulation of the stress response protein PspA. Microbiology 154 (Pt 5): 1436–1443.
45. Liu C, Willmund F, Golecki JR, Cacace S, Hess B et al. (2007) The chloroplast HSP70B-CDJ2-CGE1 chaperones catalyse assembly and disassembly of VIPP1 oligomers in Chlamydomonas. Plant J. 50 (2): 265–277.
46. Vothknecht UC, Otters S, Hennig R, Schneider D (2012) Vipp1: a very important protein in plastids?! J. Exp. Bot. 63 (4): 1699–1712.
47. Datta P, Ravi J, Guerrini V, Chauhan R, Neiditch MB et al. (2015) The Psp system of *Mycobacterium tuberculosis* integrates envelope stress-sensing and envelope-preserving functions. Mol. Microbiol. 97 (3): 408–422.
48. Mascher T, Helmann JD, Unden G (2006) Stimulus Perception in Bacterial Signal-Transducing Histidine Kinases. Microbiol. Mol. Biol. Rev. 70 (4): 910–938.
49. Domínguez-Escobar J, Wolf D, Fritz G, Höfler C, Wedlich-Söldner R et al. (2014) Subcellular localization, interactions and dynamics of the phage-shock protein-like Lia response in *Bacillus subtilis*. Mol. Microbiol. 92 (4): 716–732.

50. Wolf D, Kalamorz F, Wecke T, Juszczak A, Mäder U et al. (2010) In-depth profiling of the LiaR response of *Bacillus subtilis*. J. Bacteriol. 192 (18): 4680–4693.
51. Wenzel M, Kohl B, Münch D, Raatschen N, Albada HB et al. (2012) Proteomic response of *Bacillus subtilis* to lantibiotics reflects differences in interaction with the cytoplasmic membrane. Antimicrob. Agents Chemother. 56 (11): 5749–5757.
52. Heidrich J, Thurotte A, Schneider D (2017) Specific interaction of IM30/Vipp1 with cyanobacterial and chloroplast membranes results in membrane remodeling and eventually in membrane fusion. Biochim. Biophys. Acta 1859 (4): 537–549.
53. Neuwald AF, Aravind L, Spouge JL, Koonin EV (1999) AAA+. A class of chaperone-like ATPases associated with the assembly, operation, and disassembly of protein complexes. Genome Res. 9 (1): 27–43.
54. Schumacher J, Zhang X, Jones S, Bordes P, Buck M (2004) ATP-dependent Transcriptional Activation by Bacterial PspF AAA+Protein. J. Mol. Biol. 338 (5): 863–875.
55. Joly N, Schumacher J, Buck M (2006) Heterogeneous nucleotide occupancy stimulates functionality of phage shock protein F, an AAA+ transcriptional activator. J. Biol. Chem. 281 (46): 34997–35007.
56. Joly N, Rappas M, Wigneshweraraj SR, Zhang X, Buck M (2007) Coupling nucleotide hydrolysis to transcription activation performance in a bacterial enhancer binding protein. Mol. Microbiol. 66 (3): 583–595.
57. Cannon WV, Austin S, Moore M, Buck M (1995) Identification of close contacts between the sigma N (sigma 54) protein and promoter DNA in closed promoter complexes. Nucleic Acids Res. 23 (3): 351–356.
58. Santero E, Hoover TR, North AK, Berger DK, Porter SC et al. (1992) Role of integration host factor in stimulating transcription from the σ54-dependent nifH promoter. J. Mol. Biol. 227 (3): 602–620.
59. Wang JT, Syed A, Hsieh M, Gralla JD (1995) Converting *Escherichia coli* RNA Polymerase into an Enhancer-Responsive Enzyme. Role of an NH2-Terminal Leucine Patch in sigma54. Science 270 (5238): 992–994.
60. Burrows PC, Joly N, Cannon WV, Cámara BP, Rappas M et al. (2009) Coupling sigma factor conformation to RNA polymerase reorganisation for DNA melting. J. Mol. Biol. 387 (2): 306–319.
61. Sharma A, Leach RN, Gell C, Zhang N, Burrows PC et al. (2014) Domain movements of the enhancer-dependent sigma factor drive DNA delivery into the

RNA polymerase active site. Insights from single molecule studies. Nucleic Acids Res. 42 (8): 5177–5190.

62. Joly N, Buck M (2011) Single chain forms of the enhancer binding protein PspF provide insights into geometric requirements for gene activation. J. Biol. Chem. 286 (14): 12734–12742.
63. Joly N, Burrows PC, Buck M (2008) An intramolecular route for coupling ATPase activity in AAA+ proteins for transcription activation. J. Biol. Chem. 283 (20): 13725–13735.
64. Rappas M, Schumacher J, Niwa H, Buck M, Zhang X (2006) Structural basis of the nucleotide driven conformational changes in the AAA+ domain of transcription activator PspF. J. Mol. Biol. 357 (2): 481–492.
65. Bordes P, Wigneshweraraj SR, Zhang X, Buck M (2004) Sigma54-dependent transcription activator phage shock protein F of *Escherichia coli*. A fragmentation approach to identify sequences that contribute to self-association. Biochem. J. 378 (Pt 3): 735–744.
66. Bordes P, Wigneshweraraj SR, Schumacher J, Zhang X, Chaney M et al. (2003) The ATP hydrolyzing transcription activator phage shock protein F of *Escherichia coli*. Identifying a surface that binds sigma 54. Proc. Natl. Acad. Sci. U S A 100 (5): 2278–2283.
67. Dworkin J, Jovanovic G, Model P (2000) The PspA Protein of *Escherichia coli* Is a Negative Regulator of σ54-Dependent Transcription. J. Bacteriol. 182 (2): 311–319.
68. Elderkin SL, Jones S, Schumacher J, Studholme D, Buck M (2002) Mechanism of Action of the *Escherichia coli* Phage Shock Protein PspA in Repression of the AAA Family Transcription Factor PspF. J. Mol. Biol. 320 (1): 23–37.
69. Joly N, Burrows PC, Engl C, Jovanovic G, Buck M (2009) A lower-order oligomer form of phage shock protein A (PspA) stably associates with the hexameric AAA(+) transcription activator protein PspF for negative regulation. J. Mol. Biol. 394 (4): 764–775.
70. Osadnik H, Schöpfel M, Heidrich ES, Mehner D, Lilie H et al. (2015) PspF-binding domain PspA1-144 and the PspA·F complex: New insights into the coiled-coil-dependent regulation of AAA+ proteins. Mol. Microbiol. 98 (4): 743–759.

71. McDonald C, Jovanovic G, Wallace BA, Ces O, Buck M (2017) Structure and function of PspA and Vipp1 N-terminal peptides. Insights into the membrane stress sensing and mitigation. Biochim. Biophys. Acta 1859 (1): 28–39.
72. Hankamer BD, Elderkin SL, Buck M, Nield J (2004) Organization of the AAA+ Adaptor Protein PspA Is an Oligomeric Ring. J. Biol. Chem. 279 (10): 8862–8866.
73. Kobayashi R, Suzuki T, Yoshida M (2007) *Escherichia coli* phage-shock protein A (PspA) binds to membrane phospholipids and repairs proton leakage of the damaged membranes. Mol. Microbiol. 66 (1): 100–109.
74. Thurotte A, Brüser T, Mascher T, Schneider D (2017) Membrane chaperoning by members of the PspA/IM30 protein family. Integr. Biol. 10 (1): e1264546.
75. Osadnik H (2014) Funktionelle und strukturelle Charakterisierung des *phage shock protein* A aus *Escherichia coli*. Dissertation. Leibniz Universität Hannover
76. Hennig R, Heidrich J, Saur M, Schmüser L, Roeters SJ et al. (2015) IM30 triggers membrane fusion in cyanobacteria and chloroplasts. Nat. Commun. 6: 7018.
77. McDonald C, Jovanovic G, Ces O, Buck M (2015) Membrane Stored Curvature Elastic Stress Modulates Recruitment of Maintenance Proteins PspA and Vipp1. mBio 6 (5): e01188-15.
78. Heidrich J, Wulf V, Hennig R, Saur M, Markl J et al. (2016) Organization into Higher Ordered Ring Structures Counteracts Membrane Binding of IM30, a Protein Associated with Inner Membranes in Chloroplasts and Cyanobacteria. J. Biol. Chem. 291 (29): 14954–14962.
79. Otters S, Braun P, Hubner J, Wanner G, Vothknecht UC et al. (2013) The first α-helical domain of the vesicle-inducing protein in plastids 1 promotes oligomerization and lipid binding. Planta 237 (2): 529–540.
80. Jones S, Lloyd LJ, Tan KK, Buck M (2003) Secretion Defects That Activate the Phage Shock Response of *Escherichia coli*. J. Bacteriol. 185 (22): 6707–6711.
81. Jovanovic G, Engl C, Mayhew AJ, Burrows PC, Buck M (2010) Properties of the phage-shock-protein (Psp) regulatory complex that govern signal transduction and induction of the Psp response in *Escherichia coli*. Microbiology 156 (10): 2920–2932.
82. Gueguen E, Flores-Kim J, Darwin AJ (2011) The *Yersinia enterocolitica* Phage Shock Proteins B and C Can Form Homodimers and Heterodimers In Vivo with the Possibility of Close Association between Multiple Domains. J. Bacteriol. 193 (20): 5747–5758.

83. Yamaguchi S, Gueguen E, Horstman NK, Darwin AJ (2010) Membrane association of PspA depends on activation of the phage-shock-protein response in *Yersinia enterocolitica*. Mol. Microbiol. 78 (2): 429–443.
84. Adams H, Teertstra W, Demmers J, Boesten R, Tommassen J (2003) Interactions between Phage-Shock Proteins in *Escherichia coli*. J. Bacteriol. 185 (4): 1174–1180.
85. Singh S, Darwin AJ (2011) FtsH-Dependent Degradation of Phage Shock Protein C in *Yersinia enterocolitica* and *Escherichia coli*. J. Bacteriol. 193 (23): 6436–6442.
86. Engl C, Jovanovic G, Lloyd LJ, Murray H, Spitaler M et al. (2009) *In vivo* localizations of membrane stress controllers PspA and PspG in *Escherichia coli*. Mol. Microbiol. 73 (3): 382–396.
87. Mehta P, Jovanovic G, Lenn T, Bruckbauer A, Engl C et al. (2013) Dynamics and stoichiometry of a regulated enhancer-binding protein in live *Escherichia coli* cells. Nat. Commun. 4: 1997.
88. Jovanovic G, Mehta P, McDonald C, Davidson AC, Uzdavinys P et al. (2014) The N-Terminal Amphipathic Helices Determine Regulatory and Effector Functions of Phage Shock Protein A (PspA) in *Escherichia coli*. J. Mol. Biol. 426 (7): 1498–1511.
89. Jovanovic G, Engl C, Buck M (2009) Physical, functional and conditional interactions between ArcAB and phage shock proteins upon secretin-induced stress in *Escherichia coli*. Mol. Microbiol. 74 (1): 16–28.
90. Engl C, Beek AT, Bekker M, Mattos JT de, Jovanovic G et al. (2011) Dissipation of proton motive force is not sufficient to induce the phage shock protein response in *Escherichia coli.* Curr. Microbiol. 62 (5): 1374–1385.
91. Wang P, Kuhn A, Dalbey RE (2010) Global change of gene expression and cell physiology in YidC-depleted *Escherichia coli*. J. Bacteriol. 192 (8): 2193–2209.
92. Jovanovic G, Lloyd LJ, Stumpf MPH, Mayhew AJ, Buck M (2006) Induction and Function of the Phage Shock Protein Extracytoplasmic Stress Response in *Escherichia coli*. J. Biol. Chem. 281 (30): 21147–21161.
93. Seo J, Savitzky DC, Ford E, Darwin AJ (2007) Global analysis of tolerance to secretin-induced stress in *Yersinia enterocolitica* suggests that the phage-shock-protein system may be a remarkably self-contained stress response. Mol. Microbiol. 65 (3): 714–727.

94. Mehner D, Osadnik H, Lünsdorf H, Brüser T (2012) The Tat System for Membrane Translocation of Folded Proteins Recruits the Membrane-stabilizing Psp Machinery in *Escherichia coli*. J. Biol. Chem. 287 (33): 27834–27842.
95. Vega NM, Allison KR, Khalil AS, Collins JJ (2012) Signaling-mediated bacterial persister formation. Nat. Chem. Biol. 8 (5): 431–433.
96. Berks BC (1996) A common export pathway for proteins binding complex redox cofactors. Mol. Microbiol. 22 (3): 393–404.
97. Bogsch EG, Sargent F, Stanley NR, Berks BC, Robinson C et al. (1998) An essential component of a novel bacterial protein export system with homologues in plastids and mitochondria. J. Biol. Chem. 273 (29): 18003–18006.
98. Sargent F, Stanley NR, Berks BC, Palmer T (1999) Sec-independent protein translocation in *Escherichia coli*. A distinct and pivotal role for the TatB protein. J. Biol. Chem. 274 (51): 36073–36082.
99. Mori H, Cline K (2002) A twin arginine signal peptide and the pH gradient trigger reversible assembly of the thylakoid DeltapH/Tat translocase. J. Cell Biol. 157 (2): 205–210.
100. Rodrigue A, Chanal A, Beck K, Müller M, Wu LF (1999) Co-translocation of a periplasmic enzyme complex by a hitchhiker mechanism through the bacterial tat pathway. J. Biol. Chem. 274 (19): 13223–13228.
101. Ize B, Stanley NR, Buchanan G, Palmer T (2003) Role of the *Escherichia coli* Tat pathway in outer membrane integrity. Mol. Microbiol. 48 (5): 1183–1193.
102. Berks BC, Palmer T, Sargent F (2005) Protein targeting by the bacterial twin-arginine translocation (Tat) pathway. Current opinion in microbiology 8 (2): 174–181.
103. Sargent F, Bogsch EG, Stanley NR, Wexler M, Robinson C et al. (1998) Overlapping functions of components of a bacterial Sec-independent protein export pathway. EMBO J. 17 (13): 3640–3650.
104. Weiner JH, Bilous PT, Shaw GM, Lubitz SP, Frost L et al. (1998) A novel and ubiquitous system for membrane targeting and secretion of cofactor-containing proteins. Cell 93 (1): 93–101.
105. Yen M-R, Tseng Y-H, Nguyen EH, Wu L-F, Saier MH (2002) Sequence and phylogenetic analyses of the twin-arginine targeting (Tat) protein export system. Arch. Microbiol. 177 (6): 441–450.

106. Chanal A, Santini C, Wu L (1998) Potential receptor function of three homologous components, TatA, TatB and TatE, of the twin-arginine signal sequence-dependent metalloenzyme translocation pathway in *Escherichia coli*. Mol. Microbiol. 30 (3): 674–676.

107. Koch S, Fritsch MJ, Buchanan G, Palmer T (2012) *Escherichia coli* TatA and TatB proteins have N-out, C-in topology in intact cells. J. Biol. Chem. 287 (18): 14420–14431.

108. Leeuw E de, Porcelli I, Sargent F, Palmer T, Berks BC (2001) Membrane interactions and self-association of the TatA and TatB components of the twin-arginine translocation pathway. FEBS Lett. 506 (2): 143–148.

109. Walther TH, Grage SL, Roth N, Ulrich AS (2010) Membrane alignment of the pore-forming component TatA(d) of the twin-arginine translocase from *Bacillus subtilis* resolved by solid-state NMR spectroscopy. J. Am. Chem. Soc. 132 (45): 15945–15956.

110. Rodriguez F, Rouse SL, Tait CE, Harmer J, Riso A de et al. (2013) Structural model for the protein-translocating element of the twin-arginine transport system. Proc. Natl. Acad. Sci. U S A 110 (12): E1092-101.

111. Zhang Y, Hu Y, Li H, Jin C (2014) Structural basis for TatA oligomerization. An NMR study of *Escherichia coli* TatA dimeric structure. PLoS ONE 9 (8): e103157.

112. Zhang Y, Wang L, Hu Y, Jin C (2014) Solution structure of the TatB component of the twin-arginine translocation system. Biochim. Biophys. Acta 1838 (7): 1881–1888.

113. Ramasamy S, Abrol R, Suloway CJM, Clemons WM (2013) The glove-like structure of the conserved membrane protein TatC provides insight into signal sequence recognition in twin-arginine translocation. Structure (London, England : 1993) 21 (5): 777–788.

114. Rollauer SE, Tarry MJ, Graham JE, Jääskeläinen M, Jäger F et al. (2012) Structure of the TatC core of the twin-arginine protein transport system. Nature 492 (7428): 210–214.

115. Oates J, Barrett CML, Barnett JP, Byrne KG, Bolhuis A et al. (2005) The *Escherichia coli* twin-arginine translocation apparatus incorporates a distinct form of TatABC complex, spectrum of modular TatA complexes and minor TatAB complex. J. Mol. Biol. 346 (1): 295–305.

116. Gohlke U, Pullan L, McDevitt CA, Porcelli I, Leeuw E de et al. (2005) The TatA component of the twin-arginine protein transport system forms channel complexes of variable diameter. Proc. Natl. Acad. Sci. U S A 102 (30): 10482–10486.

117. Leeuw E de, Granjon T, Porcelli I, Alami M, Carr SB et al. (2002) Oligomeric properties and signal peptide binding by *Escherichia coli* Tat protein transport complexes. J. Mol. Biol. 322 (5): 1135–1146.

118. Dabney-Smith C, Mori H, Cline K (2006) Oligomers of Tha4 organize at the thylakoid Tat translocase during protein transport. J. Biol. Chem. 281 (9): 5476–5483.

119. Richter S, Brüser T (2005) Targeting of unfolded PhoA to the TAT translocon of *Escherichia coli*. J. Biol. Chem. 280 (52): 42723–42730.

120. Greene NP, Porcelli I, Buchanan G, Hicks MG, Schermann SM et al. (2007) Cysteine Scanning Mutagenesis and Disulfide Mapping Studies of the TatA Component of the Bacterial Twin Arginine Translocase. J. Biol. Chem. 282 (33): 23937–23945.

121. Rathmann C, Hannover LU (2016) Determinanten für die Membranpassage von Tat-abhängig transportierten Proteinen in *Escherichia coli*. Dissertation. Leibniz Universität Hannover.

122. Bolhuis A, Mathers JE, Thomas JD, Barrett CML, Robinson C (2001) TatB and TatC form a functional and structural unit of the twin-arginine translocase from *Escherichia coli*. J. Biol. Chem. 276 (23): 20213–20219.

123. Behrendt J, Lindenstrauss U, Brüser T (2007) The TatBC complex formation suppresses a modular TatB-multimerization in *Escherichia coli*. FEBS Lett. 581 (21): 4085–4090.

124. Orriss GL, Tarry MJ, Ize B, Sargent F, Lea SM et al. (2007) TatBC, TatB, and TatC form structurally autonomous units within the twin arginine protein transport system of *Escherichia coli*. FEBS Lett. 581 (21): 4091–4097.

125. Tarry MJ, Schäfer E, Chen S, Buchanan G, Greene NP et al. (2009) Structural analysis of substrate binding by the TatBC component of the twin-arginine protein transport system. Proc. Natl. Acad. Sci. U S A 106 (32): 13284–13289.

126. McDevitt CA, Buchanan G, Sargent F, Palmer T, Berks BC (2006) Subunit composition and in vivo substrate-binding characteristics of *Escherichia coli* Tat protein complexes expressed at native levels. FEBS J. 273 (24): 5656–5668.

127. Alami M, Lüke I, Deitermann S, Eisner G, Koch H-G et al. (2003) Differential interactions between a twin-arginine signal peptide and its translocase in *Escherichia coli*. Mol. Cell. 12 (4): 937–946.

128. Gérard F, Cline K (2006) Efficient twin arginine translocation (Tat) pathway transport of a precursor protein covalently anchored to its initial cpTatC binding site. J. Biol. Chem. 281 (10): 6130–6135.

129. Gérard F, Cline K (2007) The thylakoid proton gradient promotes an advanced stage of signal peptide binding deep within the Tat pathway receptor complex. J. Biol. Chem. 282 (8): 5263–5272.

130. Zoufaly S, Fröbel J, Rose P, Flecken T, Maurer C et al. (2012) Mapping precursor-binding site on TatC subunit of twin arginine-specific protein translocase by site-specific photo cross-linking. J. Biol. Chem. 287 (16): 13430–13441.

131. Lausberg F, Fleckenstein S, Kreutzenbeck P, Fröbel J, Rose P et al. (2012) Genetic evidence for a tight cooperation of TatB and TatC during productive recognition of twin-arginine (Tat) signal peptides in *Escherichia coli*. PLoS ONE 7 (6): e39867.

132. Holzapfel E, Eisner G, Alami M, Barrett CML, Buchanan G et al. (2007) The entire N-terminal half of TatC is involved in twin-arginine precursor binding. Biochemistry 46 (10): 2892–2898.

133. Kreutzenbeck P, Kröger C, Lausberg F, Blaudeck N, Sprenger GA et al. (2007) *Escherichia coli* twin arginine (Tat) mutant translocases possessing relaxed signal peptide recognition specificities. J. Biol. Chem. 282 (11): 7903–7911.

134. Blümmel A-S, Drepper F, Knapp B, Eimer E, Warscheid B et al. (2017) Structural features of the TatC membrane protein that determine docking and insertion of a twin-arginine signal peptide. J. Biol. Chem. 292 (52): 21320–21329.

135. Maurer C, Panahandeh S, Jungkamp A-C, Moser M, Müller M (2010) TatB functions as an oligomeric binding site for folded Tat precursor proteins. Mol. Biol. Cell 21 (23): 4151–4161.

136. Taubert J, Hou B, Risselada HJ, Mehner D, Lünsdorf H et al. (2015) TatBC-Independent TatA/Tat Substrate Interactions Contribute to Transport Efficiency. PLoS ONE 10 (3): e0119761.

137. Taubert J, Brüser T (2014) Twin-arginine translocation-arresting protein regions contact TatA and TatB. Biol. Chem. 395 (7-8): 827–836.

138. Bageshwar UK, Musser SM (2007) Two electrical potential-dependent steps are required for transport by the *Escherichia coli* Tat machinery. J. Cell Biol. 179 (1): 87–99.

139. Lüke I, Handford JI, Palmer T, Sargent F (2009) Proteolytic processing of *Escherichia coli* twin-arginine signal peptides by LepB. Arch. Microbiol. 191 (12): 919–925.

140. Brüser T, Sanders C (2003) An alternative model of the twin arginine translocation system. Microbiol. Res. 158 (1): 7–17.

141. Sargent F, Gohlke U, Leeuw E de, Stanley NR, Palmer T et al. (2001) Purified components of the *Escherichia coli* Tat protein transport system form a double-layered ring structure. Eur. J. Biochem. 268 (12): 3361–3367.

142. Porcelli I, Leeuw E de, Wallis R, van den Brink-van der Laan E, Kruijff B de et al. (2002) Characterization and membrane assembly of the TatA component of the *Escherichia coli* twin-arginine protein transport system. Biochemistry 41 (46): 13690–13697.

143. Sargent F, Berks BC, Palmer T (2006) Pathfinders and trailblazers. A prokaryotic targeting system for transport of folded proteins. FEMS Microbiol. Lett. 254 (2): 198–207.

144. Aldridge C, Storm A, Cline K, Dabney-Smith C (2012) The chloroplast twin arginine transport (Tat) component, Tha4, undergoes conformational changes leading to Tat protein transport. J. Biol. Chem. 287 (41): 34752–34763.

145. Pal D, Fite K, Dabney-Smith C (2013) Direct interaction between a precursor mature domain and transport component Tha4 during twin arginine transport of chloroplasts. Plant Physiol. 161 (2): 990–1001.

146. Fröbel J, Rose P, Müller M (2011) Early contacts between substrate proteins and TatA translocase component in twin-arginine translocation. J. Biol. Chem. 286 (51): 43679–43689.

147. Hou B, Brüser T (2011) The Tat-dependent protein translocation pathway. Biomol. Concepts 2 (6): 507–523.

148. Alder NN, Theg SM (2003) Energetics of Protein Transport across Biological Membranes. Cell 112 (2): 231–242.

149. Natale P, Brüser T, Driessen AJM (2008) Sec- and Tat-mediated protein secretion across the bacterial cytoplasmic membrane--distinct translocases and mechanisms. Biochim. Biophys. Acta 1778 (9): 1735–1756.

150. Mehner D (2011) Charakterisierung und Identifizierung eines Interaktionspartners des Tat-Translokons von *Escherichia coli*. Dissertation. Leibniz Universität Hannover
151. Shiba Y, Yokoyama Y, Aono Y, Kiuchi T, Kusaka J et al. (2004) Activation of the Rcs signal transduction system is responsible for the thermosensitive growth defect of an *Escherichia coli* mutant lacking phosphatidylglycerol and cardiolipin. J. Bacteriol. 186 (19): 6526–6535.
152. Saha SK, Nishijima S, Matsuzaki H, Shibuya I, Matsumoto K (1996) A regulatory mechanism for the balanced synthesis of membrane phospholipid species in *Escherichia coli*. Biosci. Biotechnol. Biochem. 60 (1): 111–116.
153. Mileykovskaya E, Ryan AC, Mo X, Lin C-C, Khalaf KI et al. (2009) Phosphatidic acid and N-acylphosphatidylethanolamine form membrane domains in *Escherichia coli* mutant lacking cardiolipin and phosphatidylglycerol. J. Biol. Chem. 284 (5): 2990–3000.
154. Bergler H, Abraham D, Aschauer H, Turnowsky F (1994) Inhibition of lipid biosynthesis induces the expression of the *pspA* gene. Microbiology 140 (8): 1937–1944.
155. Miller JH (1972) Experiments in molecular genetics. Cold Spring Harbor: Cold Spring Harbor Laboratory. 466 p.
156. Wilms B, Hauck A, Reuss M, Syldatk C, Mattes R et al. (2001) High-cell-density fermentation for production of L-N-carbamoylase using an expression system based on the *Escherichia coli* rhaBAD promoter. Biotechnology and bioengineering 73 (2): 95–103.
157. Chung CT, Niemela SL, Miller RH (1989) One-step preparation of competent *Escherichia coli*. Transformation and storage of bacterial cells in the same solution. Proc. Natl. Acad. Sci. U S A 86 (7): 2172–2175.
158. Laemmli UK (1970) Cleavage of structural proteins during the assembly of the head of bacteriophage T4. Nature 227 (5259): 680–685.
159. Towbin H, Staehelin T, Gordon J (1979) Electrophoretic transfer of proteins from polyacrylamide gels to nitrocellulose sheets. Procedure and some applications. Proc. Natl. Acad. Sci. U S A 76 (9): 4350–4354.
160. Brüser T, Deutzmann R, Dahl C (1998) Evidence against the double-arginine motif as the only determinant for protein translocation by a novel Sec-independent pathway in *Escherichia coli*. FEMS Microbiol. Lett. 164 (2): 329–336.

161. Ogata K, Arakawa M, Kasahara T, Shioiri-Nakano K, Hiraoka K (1983) Detection of toxoplasma membrane antigens transferred from SDS-polyacrylamide gel to nitrocellulose with monoclonal antibody and avidin-biotin, peroxidase anti-peroxidase and immunoperoxidase methods. Journal of immunological methods 65 (1-2): 75–82.

162. Elderkin SL, Bordes P, Jones S, Rappas M, Buck M (2005) Molecular determinants for PspA-mediated repression of the AAA transcriptional activator PspF. J. Bacteriol. 187 (9): 3238–3248.

163. Cullis PR, Kruijff B de (1979) Lipid polymorphism and the functional roles of lipids in biological membranes. Biochim. Biophys. Acta 559 (4): 399–420.

164. Hui SW, Sen A (1989) Effects of lipid packing on polymorphic phase behavior and membrane properties. Proc. Natl. Acad. Sci. U S A 86 (15): 5825–5829.

165. Kinnunen PKJ (1996) On the molecular-level mechanisms of peripheral protein-membrane interactions induced by lipids forming inverted non-lamellar phases. Chemistry and Physics of Lipids 81 (2): 151–166.

166. DeChavigny A, Heacock PN, Dowhan W (1991) Sequence and inactivation of the *pss* gene of *Escherichia coli*. Phosphatidylethanolamine may not be essential for cell viability. J. Biol. Chem. 266 (8): 5323–5332.

167. Rand RP, Sengupta S (1972) Cardiolipin forms hexagonal structures with divalent cations. Biochim. Biophys. Acta 255 (2): 484–492.

168. Rietveld AG, Chupin VV, Koorengevel MC, Wienk HL, Dowhan W et al. (1994) Regulation of lipid polymorphism is essential for the viability of phosphatidylethanolamine-deficient *Escherichia coli* cells. J. Biol. Chem. 269 (46): 28670–28675.

169. Rietveld AG, Killian JA, Dowhan W, Kruijff B de (1993) Polymorphic regulation of membrane phospholipid composition in *Escherichia coli*. J. Biol. Chem. 268 (17): 12427–12433.

170. Rietveld AG, Koorengevel MC, Kruijff B de (1995) Non-bilayer lipids are required for efficient protein transport across the plasma membrane of *Escherichia coli*. EMBO J. 14 (22): 5506–5513.

171. Hildebrand PW, Preissner R, Frömmel C (2004) Structural features of transmembrane helices. FEBS Lett. 559 (1-3): 145–151.

172. Mouritsen OG, Bloom M (1984) Mattress model of lipid-protein interactions in membranes. Biophys. J. 46 (2): 141–153.

173. Killian JA, Salemink I, Planque MR de, Lindblom G, Koeppe RE et al. (1996) Induction of nonbilayer structures in diacylphosphatidylcholine model membranes by transmembrane alpha-helical peptides. Importance of hydrophobic mismatch and proposed role of tryptophans. Biochemistry 35 (3): 1037–1045.
174. Flores-Kim J, Darwin AJ (2016) The Phage Shock Protein Response. Annu. Rev. Microbiol. 70: 83–101.
175. Dombek KM, Ingram LO (1984) Effects of ethanol on the *Escherichia coli* plasma membrane. J. Bacteriol. 157 (1): 233–239.
176. Aguilar PS, Hernandez-Arriaga AM, Cybulski LE, Erazo AC, Mendoza D de (2001) Molecular basis of thermosensing. A two-component signal transduction thermometer in *Bacillus subtilis*. EMBO J. 20 (7): 1681–1691.
177. Cybulski LE, Martín M, Mansilla MC, Fernández A, Mendoza D de (2010) Membrane thickness cue for cold sensing in a bacterium. Curr. Biol. 20 (17): 1539–1544.
178. Saita E, Abriata LA, Tsai YT, Trajtenberg F, Lemmin T et al. (2015) A coiled coil switch mediates cold sensing by the thermosensory protein DesK. Mol. Microbiol. 98 (2): 258–271.
179. Inda ME, Oliveira RG, Mendoza D de, Cybulski LE (2016) The Single Transmembrane Segment of Minimal Sensor DesK Senses Temperature via a Membrane-Thickness Caliper. J. Bacteriol. 198 (21): 2945–2954.
180. Abriata LA, Albanesi D, Dal Peraro M, Mendoza D de (2017) Signal Sensing and Transduction by Histidine Kinases as Unveiled through Studies on a Temperature Sensor. Acc Chem Res 50 (6): 1359–1366.

Danksagung

Mein herzlicher Dank gilt Prof. Dr. Thomas Brüser für die Möglichkeit meine Dissertation am Institut für Mikrobiologie anzufertigen. Insbesondere auch dafür, dass er mir alle notwendigen Freiheiten ließ, mich an diesem, nicht ganz einfach zu verstehenden System, abzuarbeiten und eigene Ideen und Vorstellungen zu entwickeln. Du warst immer offen für meine Ideen, auch wenn diese nicht den etablierten Modellen entsprachen und hast mich stets ermutigt tiefer zu graben, danke dafür!

Prof. Dr. Kürsad Turgay danke ich ganz herzlich für die Übernahme des zweiten Gutachtens und die vielen Denkanstöße während meiner Seminarvorträge.

Prof. Dr. Edgar Maiss danke ich ebenfalls ganz herzlich für die Übernahme des Prüfungsvorsitzes.

Ganz besonderer Dank gilt natürlich auch allen aktuellen und ehemaligen Mitarbeitern des Instituts für Mikrobiologie, insbesondere Inge und Sybille, ohne deren stetige technische Hilfe dieses Projekt so nicht hätte durchgeführt werden können. Ihr seid die besten! Insbesondere Inge und natürlich auch Hendrik und Kathrin danke ich für wunderbare Pausen an der frischen Luft, die auch häufig dringend notwendig waren.

Claudia und Denise gilt ebenfalls mein größter Dank! Angefangen bei der Betreuung meiner Bachelorarbeit, über unzählige experimentelle Kochabende bis hin zur Fertigstellung meiner Promotion seid ihr immer für mich da gewesen, in allen Lebenslagen – vielen Dank dafür!

Mein allergrößter Dank gilt natürlich meiner Familie und insbesondere meinen Eltern und meinem Bruder, ohne deren fortwährende Unterstützung ich heute nicht an dem Punkt stehen würde! Danke.

LEBENSLAUF

Persönliche Daten

Name:	Eyleen Sabine Heidrich
Geburtsdatum:	11. Mai 1989
Geburtsort:	Bad Ems

Beruflicher Hintergrund

07/2018 – 10/2018	Wissenschaftliche Hilfskraft am Institut für Mikrobiologie, Leibniz Universität Hannover
01/2014 – 06/2018	Wissenschaftliche Mitarbeiterin am Institut für Mikrobiologie, Leibniz Universität Hannover
01/2011 – 03/2013	diverse Anstellungen als studentische Hilfskraft am Institut für Mikrobiologie, Leibniz Universität Hannover
11/2011 – 02/2012	studentische Hilfskraft am Institut für Lebensmittelchemie, Leibniz Universität Hannover

Ausbildung

04/2014 – heute	Leibniz Universität Hannover, Promotionsstudentin im Fach „Biologie“ in der Arbeitsgruppe Brüser am Institut für Mikrobiologie, Leibniz Universität Hannover
10/2011 – 01/2014	Leibniz Universität Hannover, Masterstudiengang „*Life Science*“, Abschluss: *Master of Science*
10/2008 – 10/2011	Leibniz Universität Hannover, Bachelorstudiengang „*Life Science*“, Abschluss: *Bachelor of Science*
08/1999 – 06/2008	Private Marienschule, Limburg (Lahn) Abschluss: Allgemeine Hochschulreife

Publikationsliste

1) Heidrich ES and Brüser T. Evidence for a second regulatory binding site on PspF that is occupied by the C-terminal domain of PspA. *PLoS One.* 2018 Jun 15;13(6):e0198564.

2) Hou B[1], Heidrich ES[1], Mehner-Breitfeld D, Brüser T. The TatA component of the twin-arginine translocation system locally weakens the cytoplasmic membrane of *Escherichia coli* upon protein substrate binding. *J. Biol. Chem*. 2018 293: 7592-3605.
[1]geteilte Erstautorenschaft

3) Osadnik H, Schöpfel M, Heidrich E, Mehner D, Lilie H, Parthier C, Risselada HJ, Grubmüller H, Stubbs MT, Brüser T. PspF-binding domain $PspA_{1-144}$ and the PspA·F complex: New insights into the coiled-coil-dependent regulation of AAA+ proteins. *Mol. Microbiol.* 2015 Nov;98(4):743-59.